Rationalising nanoparticle sizes measured by AFM, FlFFF and DLS: sample preparation, polydispersity and particle structure

MOHAMMED BAALOUSHA* AND JAMIE LEAD

1 School of Geography, Earth and Environmental Sciences, College of Life and Environmental Sciences, University of Birmingham, Birmingham, United Kingdom, m.a.baalousha@bham.ac.uk (* presenting author)

8e.Towards the fundamentals of nanoparticle interactions with the living world: a life cycle perspective.

This presentation will discuss the sources of variability in the measured nanomaterial (NM) size by different analytical tools including atomic force microscopy (AFM), dynamic light scattering (DLS) and flow-field flow fractionation (FlFFF). The results suggest that differences in NM size measurements between different analytical tools can be rationalised by taking into consideration (i) sample preparation, (ii) sample polydispersity and (iii) structural properties of the NMs.

Appropriate sample preparation is a key to obtain representative particle size distributions (PSDs), and this may vary on a case by case basis. For AFM analysis, an ultracentrifugation method is the optimal method to prepare samples from diluted suspensions of NMs (<1 mg L-1). For FlFFF, the overloading effect, particle-particle and particle-membrane interactions as well as nature of the calibration standards are important determinants of the quality of data. For DLS, the quality of the fitting of the autocorrelation function is a key issue in obtaining correct estimates of particle size. Conversion of intensity PSD to number or volume PSD is promising for determination of number and volume PSD, but hampered by uncertainties in solving and optimizing the autocorrelation function fit.

The differences between the z-average hydrodynamic diameter by DLS and the particle height by AFM can be accounted for by sample polydispersity. The ratio of z-average hydrodynamic diameter: AFM particle height approaches 1.0 for monodisperse samples and increases with sample polydispersity. A polydispersity index of 0.1 is suggested as a suitable limit above which DLS data no longer remains accurate. Conversion of the volume PSD by FlFFF-UV to number PSD helps to rationalise for some of the variability in the measured sizes. The remaining variability in the measured sizes can be attributed to structural variability in the particles and in this case is mainly attributed to the thickness and permeability of the particles/surface coating. For citrate coated NMs, the dFlFFF/dAFM approaches 1 and the particles are described as hard spheres, whereas for PVP coated NMs, the dFlFFF/dAFM deviates toward values greater than one, indicating that these particles are either permeable or non-spherical.

Yttrium mobility during weathering: implications for riverine Y/Ho

MICHAEL G. BABECHUK[1*], BALZ S. KAMBER[2], MIKE WIDDOWSON[3]

[1]Laurentian University, Sudbury, ON, Canada (* presenting author)
[2]Trinity College Dublin, Dublin, Ireland
[3]The Open University, Milton Keynes, United Kingdom

Yttrium has similar geochemical properties to the lanthanides and closely mirrors the behaviour of its geochemical twin, Ho, in anhydrous magmatic systems. In the hydrosphere, however, Y is noteably less particle reactive than the lanthanides [1] and is more mobile during chemical weathering as a result [e.g., 2]. Here, this behaviour is further explored using chemical transects through two basaltic weathering profiles in India that are preserved in different stages of alteration: the Bidar laterite profile (~50 m) and an incipient to intermediately weathered profile developed across two lava flows (~5 m) near Chhindwara. Both profiles were characterized using major element and high-precision trace element data to establish the progressive compositional changes during chemical weathering.

The parent rock Deccan Traps basalt of both profiles is chemically similar with an average Y/Ho ratio of 25.2 ± 1.1 in the least-weathered samples. In the Chhindwara weathering profile, the enhanced mobility of Y relative to the lanthanides is observed already at the incipient stages of weathering. The preferential loss of Y continues during increasing weathering intensity in the profile as demonstrated by a strong anti-correlation between the chemical index of alteration (CIA; ranging from 35-80) and the Y/Ho ratio (ranging from ~25-23). Yttrium mobility is evident at the scale of the profile as well as across a corestone-saprolite interface (< 1 m). The Bidar laterite profile (CIA>90) has highly subchondritic Y/Ho ratios (19.4-14.7) with the exception of one sample in the mottled zone with highly enriched REE abundances and a superchondritic Y/Ho ratio of 30.1.

River waters have superchondritic Y/Ho ratios prior to reaching the estuary (where additional, much more extreme Y/Ho fractionation occurs due to the higher particle reactivity of the HREE), indicating that the greater mobility of Y relative to the HREE during weathering may be sufficient to affect mass balance. Care must be taken to correctly identify the Y/Ho ratio of river water due to the possibility of marine chemical sedimentary rocks in the drainage area and/or contamination from phosphate fertilizers. Using previously published Y/Ho data from eastern Australia rivers [3,4] screened based on P content and salinity to minimize the influence of these complications, a net superchondritic Y/Ho ratio remains. Thus, the weathering behaviour of Y may be more important to the interpretation of riverine Y/Ho ratios than previously considered.

[1] Nozaki et al. (1997) *EPSL* **148**, 329-340.
[2] Hill et al. (2000) *Geology* **28**, 923-926.
[3] Lawrence et al. (2006) *Marine & Freshwater Research* **57**, 725-736.
[4] Lawrence et al. (2006) *Aquatic Geochemistry* **12**, 39-72.

Multi-laboratory Comparison of Sequential Metals Extractions

CAROL BABYAK [1*], JENNIFER N. GABLE [2], KWOK-CHOI PATRICK LEE [3], WILLIAM J. ROGERS [4], ROCK J. VITALE [5], AND NEIL E. CARRIKER [6]

[1] Appalachian State University, Boone, North Carolina, United States, babyakcm@appstate.edu (* presenting author)
[2] Environmental Standards, Inc., Valley Forge, Pennsylvania, United States, jgable@envstd.com
[3] Tennessee Valley Authority, Muscle Shoals, Alabama, United States, plee@tva.gov
[4] Tennessee Valley Authority, Muscle Shoals, Alabama, United States, wjrogers@tva.gov
[5] Environmental Standards, Inc., Valley Forge, Pennsylvania, United States, rvitale@envstd.com
[6] Tennessee Valley Authority, Chattanooga, Tennessee, United States, necarriker@tva.gov

Abstract

Following the December 2008 rupture of a coal fly ash retaining pond at the Tennessee Valley Authority (TVA) Kingston Fossil Plant near Harriman, Tennessee, a comprehensive monitoring effort was intiated to evaluate impact of the release on the surrounding aquatic environment. The sequential extraction procedure developed by Querol et. al [1] was utilized by TVA's contracted laboratory and by Appalachian State University (ASU) researchers to evaluate bioavailability of ash-related trace metals in sediments impacted by the release.

Sediment samples collected in 2009 were split and submitted to ASU and to TVA's contracted laboratory for sequential extraction and subsequent metals analysis. This paper presents a comparison of the laboratories' data using the same method.

In 2011, several of the 2009 sediment sampling locations were revisited; these 2011 sediment samples were subjected to sequential extraction by ASU following the same procedure as used for the 2009 samples. This paper also includes comparisons of the data for the 2009 and 2011 sediment samples collected at similar locations.

In 2011, TVA collected and homogenized surface sediment samples in bulk quantities at several locations for several purposes. Sub-samples were submitted to ASU for sequential extraction; these samples were air-dried prior to extraction and between extraction steps. TVA also submitted these surface sediment samples to TVA's contracted labroatory for sequential extraction; these samples were not dried prior to or during the extraction process. A third part of this paper compares sequential extraction data generated with and without drying prior to and during extraction.

Conclusion

This paper evaluates interlaboratory precision for the Querol et al. sequential extraction method; presents temporal trends in bioavailability for several locations; and evaluates the impact of the sampling, handling, and extraction environments on metals leaching during the sequential extraction process.

References

[1] Querol, X., Juan, R., Lopez-Soler, A., Fernandez-Turiel, J.L., Ruiz, C.R. (1996). Fuel **75**, 821-838.

Electron transfer and atom exchange among Fe and Mn phases

JONATHAN E. BACHMAN[1]*, DREW E. LATTA[2], MICHELLE M. SCHERER[1], AND KEVIN M. ROSSO[3]

[1]The University of Iowa, Civil and Environmental Engineering (*jonathan-bachman@uiowa.edu)
[2]Argonne National Laboratory, Biosciences (dlatta@anl.gov)
[3]Pacific Northwest National Laboratory, Chemical and Material Sciences (Kevin.Rosso@pnnl.gov)

Fe and Mn are both common redox-active metals in environmental systems, and Fe-Mn redox chemistry is an important consideration when predicting fate and transport of contaminants. Recent work has shown that electron transfer and atom exchange occurs between aqueous Fe(II) and Fe(III) oxides and results in extensive recrystallization both with and without secondary mineral formation [1]. It is unclear, however, whether similar redox processes occur among Fe and Mn phases that might result in incorporation and release of Fe in Mn oxides, or conversely, incorporation and release of Mn in Fe oxides. Furthermore, it appears unknown whether the reaction of aqueous Mn(II) with Mn oxides leads to similar atom exchange and recrystallization as has been observed for the reaction of aqueous Fe(II) with Fe(III) oxides [2].

We are exploring the mechanisms driving the redox reactions of Mn(II)/Fe-oxides, Fe(II)/Mn-oxides, and Mn(II)/Mn-oxides using 57Fe Mossbauer spectroscopy and isotope tracer approaches. We have found that Mn-incorporated in goethite is released in the presence of aqueous Fe(II), similar to what has recently been demonstrated for Ni in goethite [3]. These experiments will provide a more fundamental understanding of the reactivity at mineral-water interfaces, in addition to providing a model for trace metal incorporation and release in Mn and Fe oxides.

. [1] Gorski and Scherer (2011) Aquatic Redox Chemistry, **1071,** 315-343. [2] Handler *et al.* (2009) *Environmental Science & Technology* **43**. 1102-1107. [3] Friedrich *et al.* (2011) *Geology* **39**. 1083-1086

The Marmion Shear Zone: A kinematic study of Archean terrane boundaries

N. R. Backeberg[1*], C. D. Rowe[1]

[1] McGill University, Earth and Planetary Science, Montreal, Canada, nils.backeberg@mail.mcgill.ca (* presenting author)

Introduction

The Marmion Shear zone marks the Archean terrane boundary between the ~3.003 Ga Marmion tonalite-trondhjemite-granodiorite (TTG) gneisses and the 2.931 – 3.003 Ga Finlayson Lake greenstone belt [1]. The shear zone is intruded by younger undeformed granites. They have not been dated, but petrologically similar units in the Eye Dashwa pluton have been dated at 2.665 Ga [1]. The low-grade (< 1 g/t) Hammond Reef gold deposit is hosted within a network of fractures and alteration zones parallel to the Marmion Shear within the Marmion gneiss and *not* in a major fault or shear zone at the boundary nor within the mafic greenstone belts as seen in most Archean gold deposits, for example in Abitibi [2,3].

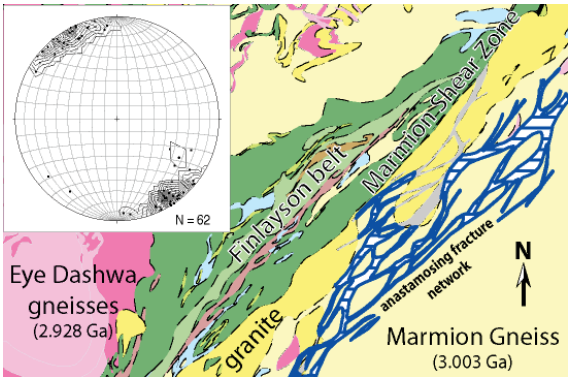

Figure 1: Geological map of the Marmion Shear area [1], showing the location of the anastamosing fracture and alteration zone (blue). The shear zone is intruded by a granite (yellow). Stereonet shows poles to flattening foliation (N = 62) across the Finlayson belt (green).

Preliminary Results and Observations

The Finlayson belt is divided into three parallel belts with different inherited ages (2.931 – 3.003 Ga [1]). At exposure level the belts are parallel to the northeast structural grain of the Marmion Shear (Figure 1). Penetrative flattening foliation is developed across the Finlayson belt (Figure 1). There are no spatial gradients in the strength of the foliation, which deforms all discontinuous lenticular lithologic units. Displaced lithologic unit boundaries demonstrate the presence of discrete faults.

The younger granite crosscuts the shear zone and ductile fabrics in the Marmion Gneiss, and has no penetrative deformation fabrics. It obscures the core of the shear zone. The deformation fabrics in both terranes bounding the Marmion Shear show a transition from ductile to discrete brittle structures, suggesting a common deformation path. The distinct anastamosing fracture network and zone of alteration which hosts the gold in the Marmion Gneiss is not seen in the Finlayson belt. This may be attributable to preferential fracturing and fluid migration within the gneiss during ore formation.

[1] Stone (2008) *Ontario Geological Survey Preliminary Map.* [2] Vearncombe (1998) *Geology* **26 (9)**, 855-858. [3] Wyman *et al.*, (1999) *Journal of Geology* **107**, 715-725

A cooling history for the Nicola Horst, British Columbia.

David Bacque[1*] and Bernard Guest[1]

[1]University of Calgary, Calgary, Canada, dpbacque@ucalgary.ca (* presenting author)

Introduction

The Nicola Horst (NH), is located in the Intermontane belt of British Columbia. It is bound along the east and west by steep post-Paleocene faults [1] (Fig 1). The faults are boundries between undeformed, low grade metamorphic rocks and deformed medium grade metamorphic rocks within the NH [2]. It has been suggested by some authors that the medium grade rocks are mid-crustal and are part of an antiformal thrust duplex [2,3]. The medium grade rocks, amphibolite facies, became exposed via unroofing along the steep post-Paleocene faults. This study aims to determine both the timing of the faults and model the isostatic response caused by the unroofing along the steep post-Paleocene faults using thermochronometry.

Thermochronology and geochronology

Most of the ages gathered in and around the NH have been for determining the absolute ages (geochronology) of the rocks. To understand how the NH formed, we are using thermochronometry, which records various closure temperatures depending on the mineral and system. Previous work done by Simon Fraser University produced four, unpublished, biotite Ar-Ar ages (50.3, 50.3, 56.5, 63.8 Ma, located in the northern, western, eastern, and southern areas respectively). Our samples (Fig 1) are located along a horizontal transect in the central area of the NH and along a vertical transect in the southern area of the NH. These samples are collected for purposes of producing a complete suite of ages, spanning temperatures from 900-60°C. By comparing cooling curves around the NH to ones within, we will determine a better age of the faults around the NH and model the response of the mid-crustal rocks exposed in the NH to the unroofing along the two post-Paleocene faults.

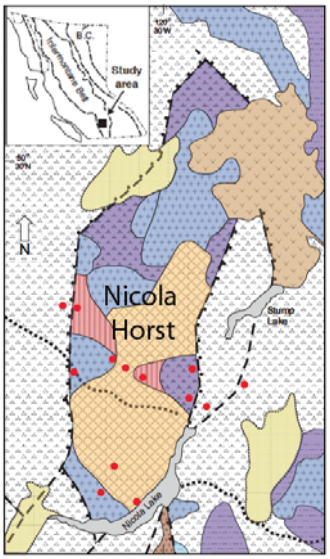

Figure 1: Nicola Horst is located in south central British Columbia. Blues, purples and red are Jurassic, Triassic and older, respectively. Browns, tans and yellows are Eocene, Tertiary and Quaternary, respectively. Red dots indicate locations of samples collected. Image modified from [2].

[1] Monger and McMillan (1989) *Geologic Survey of Canada* **Map 42-1989**. [2] Moore and Pettipas (1990a) *Ministry of Energy, Mines and Petroleum Resources* Open file **1990-29**, 3-13. [3] Erdmer, Moore, Heaman, Thompson, Daughtry, and Creaser (2001) *Canadian Journal of Earth Science* **39**, 1605-1623.

The importance of accurate and precise temperature reconstruction for alkenone paleobarometry

MARCUS P. S. BADGER[1*], RICH D. PANCOST[2]

[1]Department of Earth Sciences, University of Bristol, Wills Memorial Building, Queen's road, Bristol, BS8 1RJ, U.K., marcus.badger@bristol.ac.uk (* presenting author)
[2]Organic Geochemistry Unit, Bristol Biogeochemistry Research Centre, University of Bristol, Cantock's close, Bristol, BS8 1TS, U.K., r.d.pancost@bristol.ac.uk

By measuring the carbon isotope ratio of long chain ketones produced by haptophyte algae (alkenones) the isotope fractionation during photosynthesis (ε_p) can be determined. Fractionation is dependent on the concentration of carbon dioxide in surface waters, thus, past atmospheric CO_2 can be reconstructed. Recent studies have successfully applied this technique at across several intervals of rapid climatic change in the Cenozoic [1-4], and efforts have been made to use alkenone paleobarometry to constrain climate (or Earth system) sensitivity [2].

Several factors are important to the accurate and precise determination of atmospheric CO_2; for example, recent work has focussed on the effect of changes in algal cell size [5, 6]. However, reconstructions are also highly dependent on the accurate and precise determination of sea surface temperature (SST), as this effects both the determination of ε_p from alkenone $\delta^{13}C$ values, and the conversion of $[CO_2]_{(aq)}$ to atmospheric pCO_2. This has become of paticular importance given the multitude of proxies now applied to the reconstruction of SST, and uncertainty about exactly what each proxy represents.

Here we assess the sensitvity of alkenone pCO_2 estimates to innaccurate and/or inprecise SST reconstructions using new high resolution data from the Pliocene, and investigate the possible implications for previously published records. We highlight the importance of these results, especially the revised uncertainties of paleo-pCO_2 estimates, to understanding climates of the past and estimating climate sensitivity (or Earth system sensitivity) for models of the future.

[1] Bijl et al., (2010) *Science* **330,** 819-821. [2] Pagani et al., (2010) *Nature Geosciences* **3**, 27-30. [3] Seki et al., (2010) *EPSL* ***292,*** *201-211*. [4] Pagani et al., (2011) *Science* **334**, 1261-1264. [5] Henderiks and Pagani (2007) *Paleoceanography* **22**, PA3202. [6] Plancq et al., (2012) *Paleoceanography* **27,** PA1203.

The Major Element Composition of Earth's Core

JAMES BADRO[1*], JOHN BRODHOLT[2], ALEXANDER COTE[1,2]

[1]IPGP, Paris, France, badro@ipgp.fr (* presenting author)
[2]UCL, London, UK, j.brodholt@ucl.ac.uk

Earth's core formed as a results of a major chemical differentiation event; the melting of accretionary building blocks (meteorites, planetesimals, protoplanets) leads to a separation of the metal from the silicate, ensued by a gravitationally-driven segregation of a dense metal-rich core at the centre of the planet, with the lighter buoyant silicates remaining on top to form the mantle and crust. The bulk composition of the core depends on the path and conditions (pressure, temperature, redox) at which core formation took place; the process also leaves an imprint on the residual bulk silicate Earth, a record that is observable in present-day mantle rocks.

Constraining experimental and theoretical data with geophysical (core density and velocity profiles) observations provides a robust way to estimate the present day composition of the core, as well as the conditions under which it formed.

We will present results obtained from ab initio molecular dynamics calculations to estimate outer-core density and seismic velocity, and combine it with mineral physics on the inner core to define a range of possible compositions of the core that satisfies the observations. We will interpret these results and propose a consistent compositional model, and formulate plausible scenarios for core formation.

Lower crustal Archaean rocks in South-East Greenland

LEON BAGAS[1], TOMAS NÆRAA[2*], BARRY L. RENO[2,3], JOCHEN KOLB[2]

[1] Centre for Exploation Targeting, University of Western Australia Perth, Australia
[2] Geological Survey of Denmark and Greenland, Copenhagen, Denmark, tomn@geus.dk (*presenting author)
[3] Institute for Geography and Geology, University of Copenhagen, Denmark

The Skjoldungen region in South-East Greenland is characterised by felsic gneisses and granites that often contain abundant mafic and ultramafic inclusions (agmatitic) with only minor amounts of mainly mafic but also ultramafic gneisses occurring in narrow belts. The gneisses are commonly migmatitic and mafic gneisses often contain abundant intrusive felsic sheets. The gneissic basement is intruded by a ca. 2.7 Ga alkaline complex and preliminary age data suggest that regional migmatisation occurred during a period from 2.8 to 2.7 Ga [1].

The mafic gneisses group into calc-alkaline and tholeiitic suites, suggesting a heterogeneous mantle source. The felsic gneisses divide into a group with a adakite-like composition and a group characterised by large positive Eu anomalies and often depleted and fractionated HREE. Felsic gneisses formed during at least two stages: 1) an early phase of crustal differentiation of a mafic proto-crust possibly starting at ca. 2.86 Ga and, 2) a late stage related to crustal thickening and remelting which seems to relate to a prolonged stage of high grade metamorphism at ca. 2.8-2.7 Ga [1]. The regional crust is dominated by granites formed during the second stage. The early felsic gneisses have adakitic chemistry and aparrantly formed in the presence of residual garnet whereas the later felsic gneisses formed from an already differentiated lower crust with accumulated plagioclase. The tectonic setting during the early crust forming episode is envisaged to range from a magmatic-arc to the mid-ocean ridge setting. The later stage probably occurred during crustal thickening in a collision orogen involving the root zone of a magmatic arc at the base of the crust (Fig. 1).

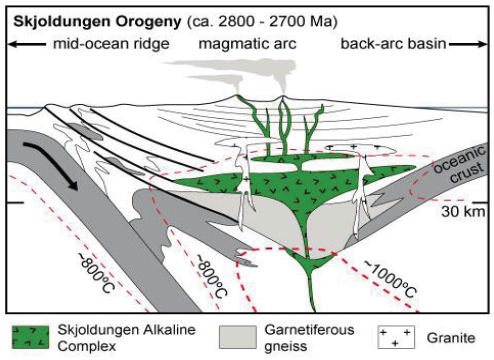

Figure 1: Model for the formation of the protoliths for gneisses in southeastern Greenland

[1] Kolb, J., Thane, K., Bagas, L., in review. Tectonometamorphic and magnetic evolution of high-grade Neo- to Mesoarcharan rocks of South-East Greenland. Gondwana Research.

Bacterial communities in drainage from waste-rock test piles

BRENDA L. BAILEY[1*], DAVID W. BLOWES[1], W. DOUGLAS GOULD[2], LESLIE SMITH[3] AND DAVID C. SEGO[4]

[1]University of Waterloo,Waterloo, Canada, blbailey@uwaterloo.ca
[2]Natural Resources Canada, Ottawa, Canada
[3]University of British Columbia, Vancouver, Canada
[4]University of Albert, Edmonton, Canada
(* presenting author)

Sulfide mineral oxidation is catalysed by microorganisms, increasing oxidation rates by orders of magnitude, releasing SO_4, Fe and H^+ [1]. Sulfide mineral oxidation rates decrease with decreasing temperature. Seasonal temperature fluctuations influence the rate of release of sulfide oxidation products from waste rock stockpiles over time [2]. Iron and sulfur oxidizing bacteria contribute to the oxidation of mine tailings in Arctic environments at temperatures as low as -11°C [2,3]. Yet, limited information exists on the importance of bacterially-catalysed oxidation of sulfide minerals in waste-rock stockpiles and their role in the generation of acid mine drainage in Arctic conditions.

Two large-scale waste-rock test piles, one with 0.035 wt. % S (Type I test pile) and another with 0.058 wt. % S (Type III test pile), located in the continuous permafrost region at the Diavik Diamond Mine were studied to examine the role of microoganisms in the biochemical evolution of test-pile drainage. Three groups of bacteria in test pile drainage were quantified using most probable number techniques [4] for neutrophilic and acidophilic sulfur oxidizers (SOBn and SOBa, respectively), and iron oxidizers (IOB). The media compositions, incubation conditions, and enumeration procedure are described in detail by Hulshof et al. [5]. The monitoring of populations present in test-pile drainage began in 2007 and a microbial succession was observed over time.

Drainage from the Type I test pile maintained a near neutral pH with low concentrations of SO_4 and Fe for the duration of this study. A population of SOBn was present from 2009 through 2010, with the exception of one sample in September 2010. Acidophilic sulfur oxidizers were only detected at very low numbers ($< 10^2$ bacteria/mL). IOB were detected in June 2009 and late 2010, but at low numbers ($< 10^3$ bacteria/mL).

Every year, the pH of the drainage from the Type III test pile decreased from near neutral in May to acidic conditions by October. Concentrations of SO_4 increased with decreasing pH. A population of SOBn were observed in the Type III test-pile drainage in 2008, however, population numbers decreased in late 2009 as the pH decreased. Acidophilic S oxidizers were only detected in 2009 after the drainage pH had decreased. In addition, the population of IOB increased with decreasing pH.

These results suggest bacteria populations evolved with changes in the drainage chemistry. Continued monitoring with more detailed analysis is required to better understand the biogeochemical evolution of these waste-rock test piles.

[1] Kirby et al. (1999) *Applied Geochemistry* **14**, 511-530.
[2] Elberling et al. (2000) *J. Contam. Hydrology* **41**, 225-238.
[3] Leduc et al. (1993) *FEMS Microbiology Letters* **108**, 189-194
[4] Cochran (1950) *Biometrics* **6**, 105-116.
[5] Hulshof (2006) *Water Research* **40**, 1816-1826.

Geodynamic regimes of intra-oceanic subduction: Thermomechanical modeling of geochemical signatures

B. BAITSCH GHIRARDELLO[1*], A. STRACKE[2], AND T.V. GERYA[1]

[1]ETHZ, Switzerland, Institut f. Geophysik (*), baitsch@erdw.ethz.ch

[2]Westfälische Wilhelms-Universität Münster, Institut f. Mineralogie, Germany, stracke.andreas@uni-muenster.de

The aim of this study is to investigate isotope signatures in different geodynamic regimes of intra-oceanic subduction processes with our 2D coupled geochemical-petrological-thermomechanical numerical model (I2ELVIS). We investigated systematically influences of fluid and melt weakening effects, which are responsible for the degree of plate coupling/decoupling and the mechanical strength of the overriding plate. Based on results of systematic experiments we distinguish the following three geodynamic regimes a) retreating regime, b) stable regime and c) advancing regime.

a) Retreating subduction regime is characterized by a strong rheological weakening of the overriding plate mantle by hydration/serpentinization and melt propagation processes. A necking of the (fore) arc causes the onset of decompression melting in the mantle wedge. Differently to the isotope signatures in the magmatic arc, decompression melting causes a MORB-like isotope signatures in the newly formed crust.

b) The volcanic rocks in a stable subduction regime are mainly produced from the subducted oceanic crust and molten hydrated mantle. Some of the stable subduction regimes are characterized by development of a broad area of subduction mélange in which subducted basaltic crust is strongly mechanically mixed with the serpentinized fore-arc mantle. These intense mixing is promoted by increased degree of fluid related weakening. The correspondent isotopic signature in the arc depends on the degree of fluid related weakening that controls intensity of flux melting.

c) Advancing subduction regime develops under condition of notably reduced fluid-related weakening that results in strong coupling between the plates in the fore-arc region. Strong coupling between plates produces large stresses that are able to overcome the mechanical resistance of the serpentinized fore-arc mantle that starts to subduct together with the plate. Large amount of new basaltic crust forms at the surface as the result of enhanced fluid-fluxed melting of the mantle wedge that coins the isotope signature of the arc.

Diffusion of water through quartz: a fluid inclusion study

RONALD J. BAKKER*, MIRIAM BAUMGARTNER, GERALD DOPPLER

Resource Mineralogy, University of Leoben, Austria, bakker@unileoben.ac.at (* presenting author)

Introduction

Diffusion of H_2O through minerals, such as quartz, that do not incorporate water at regular lattice positions is of major importance to understand fluid-rock interaction processes in deep rock, and to interpret fluid inclusion studies. The outcome of a variety of re-equilibration experiments with natural and synthetic fluid inclusions indicate that diffusion of H_2O plays an important role in these processes. Diffusion coefficients of H_2O in nominally anhydrous minerals were experimentally estimated from H_2O molecules (or part of these molecules) that replace oxygen at regular lattice positions in silicates, and which positions were detected in quenched samples after re-equilibration experiments.

Experiments

The properties of fluid inclusions in quartz can be relatively easily obtained from a variety of analytical techniques. Fluid inclusions can be regarded as constant volume containers inside a crystal lattice, which are more or less protected by the surrounding crystal from material exchange with rock pore volumes. Any change in fluid inclusion density and compositions is directly the result of diffusion processes. The exchange of fluid components in our experiments is provoked at high temperatures and pressures. Deoendent on experimental conditions, time, fluid inclusion size, and distance of fluid inclusions to the grain boundary, a variety of compositional changes are detected. similar effects are observed in assembalges of ynthetoc and natural fluid inclusions in quartz.

Conclusions

Concentration profiles based on fluid inclusion composition and density are not confirm diffusion coefficients obtained by altered isotopic compositions of quartz grains (i.e. the traditional technique to trace water in quartz). This illustrates that the mobility of H_2O in quartz must be a complex interaction of bulk diffusion and other processes suh as micro-crack enhanced or dislocation-enhanced diffusion. The reliability of natural fluid inclusions in metamorphic rock to determine rock-forming conditions can only be improved if these re-equilibration processes are fully understood.

Ice, but no fire: a new depositional age for the Rapitan Group, Canada

GEOFFREY J. BALDWIN[1*], ELIZABETH C. TURNER[1], AND BALZ S. KAMBER[2]

[1]Laurentian University, Department of Earth Sciences, Sudbury, ON, Canada, gj_baldwin@laurentian.ca (* presenting author), eturner@laurentian.ca

[2]Trinity College Dublin, Department of Geology, Dublin, Ireland, kamberbs@tcd.ie

The timing and causes of the glacial events associated with the 'Snowball Earth' hypothesis remain contentious. The earliest of these events, the Sturtian glaciation, has returned U-Pb zircon and Re-Os black shale ages from 740 Ma to as young as 660 Ma. Recently, strata correlated with the glaciogenic Rapitan Group of NW Canada have been dated at 716.47±0.24 Ma [1]. This supported a genetic correlation of the Sturtian glaciation and the Rapitan Group with the Franklin large igneous province (LIP), suggesting that the Sturtian glaciation may have been triggered by excessive CO_2 drawdown by weathering of this LIP – the 'fire and ice' model [1,2]. This model relies on penecontemporaneous emplacement of the LIP, its weathering, and Rapitan Group glacial onset at low latitudes. Here we present a new age for detrital zircon from the Rapitan Group itself. The sample was extracted from cross-bedded sandstone underlying the Rapitan iron formation by 75 m. A large number of zircon were pilot dated by LA-ICP-MS on double-sided tape and the youngest were then dated by high-precision ID-TIMS (see diagram). A coherent population of 8 grains defines a concordia age of 711.34±0.25 Ma. This is the new maximum age for deposition of the Rapitan Group and for the Sturtian glaciation in the region, and is consistent with Re-Os dates from shales overlying other Sturtian glacial deposits [3]. Significantly, it is a full 5 million years younger than the Franklin LIP, a span of time that is too long to support the 'fire and ice' model. The Rapitan Group may have been erroneously correlated with similar nearby strata. It is also possible that global 'Sturtian' glacial deposits were not the result of a single glacial episode.

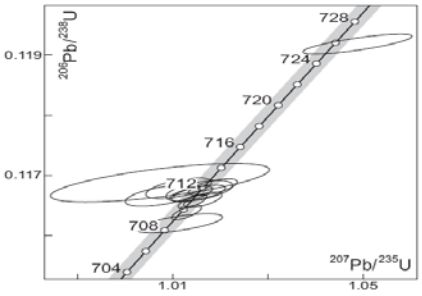

Figure 1: U-Pb concordia diagram for detrital zircon from the Rapitan Group, Canada. N=12, eight grains yielded a mean age of 711.34±0.25 Ma (MSWD = 2.0).

[1] Macdonald *et al.* (2010) *Science* **327**, 1241-1243. [2] Goddéris *et al.* (2003) *Earth Planet. Sci. Lett.* **211**, 1-12. [3] Rooney *et al.* (2011) *Precamb. Res.* **185**, 202-214.

Reconstruction of *P-T* paths in polymetamorphic rocks of the Clearwater core complex, northern Idaho

JULIA A. BALDWIN [1*] AND VICTOR E. GUEVARA[1]

[1]Dept. of Geosciences, University of Montana, Missoula, MT, 59812, USA, jbaldwin@mso.umt.edu (* presenting author), victor.guevara@umontana.edu

Understanding where, when, why, and how metamorphic core complexes form in settings of continental shortening is important because these features are part of the rock record of deformation. Moreover, core complexes provide the most direct observational information about the relationship between the middle and uppermost crust in the late stages of orogenesis, so offer a valuable opportunity to investigate crustal coupling and mass transfer within continental crust.

In the northern U.S. Rockies, core complexes show a prolonged metamorphic history, lie inboard of the $^{87}Sr/^{86}Sr$ 0.706 line, and are spatially associated with major Cordilleran batholiths. Peak metamorphic conditions are amphibolite facies, with maximum crustal depths of around 25-35 km in the most deeply exhumed complexes. Metamorphosed footwall rocks include units within Proterozoic crystalline basement as well as the sediments of the overlying Mesoproterozoic Belt Supergroup. Widespread extension occurred 59-40 Ma, with several core complexes recording an initial rapid phase of extension at *c.* 49-48 Ma followed by more protracted exhumation. The focus of this paper is on characterization of polymetamorphism in the Clearwater metamorphic core complex (CMCC) located in northern Idaho, which contains a history of both Proterozoic and Cretaceous-Eocene tectonometamophic events.

Metamorphic events in rocks within the CMCC range from Paleoproterozoic basement formation, Mesoproterozoic crustal thickening, and Cretaceous convergence, magmatism, and final exhumation in the Eocene. The samples focused on in this study are pelitic and unusual Mg-Al-rich schists from both within the high grade core of the complex, as well as schists that lie west and east of the bounding detachments. Previous work has indentified three major metamorphic events in the area [1]. The first has recently been correlated with Mesoproterozoic (1.3 Ga) crustal thickening based on Lu-Hf garnet dating [2]. Rocks also show evidence for a 1.1 Ga event. Zircon rims indicate Cretaceous to Eocene metamorphism in pulses from 82-80, 74-72, 64, and 59-55 Ma [3]. The younger dates likely correspond to fluid migration during exhumation of the complex. Here we present results of pseudosection modeling and garnet compositional isopleth thermometry to place contrainsts on the complex polymetamorphic history of these rocks. The Cretaceous to Eocene history is best preserved in multi-stage garnet microstructures with diffuse high Ca – low Mn rims, rutile converting to ilmenite, pre-kinematic staurolite, and abundant andalusite and sillimanite after kyanite, particularly in rocks within Eocene shear zones.

[1] Grover et al. (1992) *American Journal of Science*, **292**, 474-507. [2] Nesheim et al. (2012) *Lithos*, **134-135**, 91-107. [3] Doughty et al. (2007) *GSA Special Paper,* **434**, 211-241.

Coping with Oxygen: Peroxy defects in Rocks and the survival of bacteria

MELIKE BALK[1*], PAUL MASON[1], ALFONS J.M. STAMS[2], FRIEDEMANN FREUND[3,4], AND LYNN ROTHSCHILD[3]

[1] Department of Earth Sciences, Utrecht University, (m.balk@uu.nl, presenting author* and p.mason@uu.nl), [2]Laboratory of Microbiology, Wageningen University (fons.stams@wur.nl) [3]NASA Ames Research Center, Moffett Field, CA, (Lynn.J.Rothschild@nasa.gov), [4]SETI Institute, Mountain View, CA (friedemann.t.freund@nasa.gov).

An oxygen-rich atmosphere appears to have been a prerequisite for complex life to evolve on Earth and possibly elsewhere in the Universe. The question is still shrouded in uncertainty how free oxygen became available on the early Earth. Here we study processes that introduce peroxy defects into silicate minerals which, upon weathering, result in oxygen formation in an initially anoxic subsurface environment. Reactive Oxygen Species (ROS) are precursors to molecular oxygen during this process. Due to their toxicity they may have strongly influenced the evolution of life. ROS are generated during hydrolysis of peroxy defects, which consist of pairs of oxygen anions. A second pathway for formation occurs during (bio) transformations of iron sulphide minerals. ROS are produced and consumed by intracellular and extracellular reactions of Fe, Mn, C, N, and S species. We propose that despite an overall reducing or neutral oxidation state of the macroenvironment and the absence of free O_2 in the atmosphere, microorganisms on the early Earth had to cope with ROS in their microenvironments. They were thus under evolutionary pressure to develop enzymatic and other defences against the potentially dangerous, even lethal effects of ROS and oxygen.

We have investigated how oxygen might be released through weathering and test microorganisms in contact with rock surfaces and iron sulphides. Our results show how early Life might have adapted to oxygen. Early microorganisms must have "trained" to detoxify ROS prior to the evolution of aerobic metabolism and oxygenic photosynthesis. A possible way out of this dilemma comes from a study of igneous and high-grade metamorphic rocks, whose minerals contain a small but significant fraction of oxygen anions in the valence state 1- , forming peroxy links of the type $O_3Si\text{-}OO\text{-}SiO_3$ [1, 2]. As water hydrolyzes the peroxy links hydrogen peroxide, H_2O_2, forms. As a result, microorganisms attached to mineral grains will be exposed to a constant trickle of ROS from the H_2O_2 production. Many different groups of microorganisms are able to grow or survive in the presence of ROS.

[1] Balk et al. (2009) *Earth and Planetary Science Letters* **283,** 87-92. [2] Grant, R. A. *et al.* (2011) *Int. J. Environ. Res. Public Health* **8**, 1936-1956.

Impact of fungi and bacteria on the mobility of metals (Fe, Al) in podzolic soils

C. BALLAND-BOLOU-BI*, S. J. M. HOLMSTRÖM, N. G. HOLM

Stockholm University, Dept. of Geological Sciences, Stockholm, Sweden (*Clarissebolou-bi@geo.su.se)

Mineral weathering is a key process in soil leading to leaching and release of essential elements (Fe, Al), which sustain plant growth and determine the chemistry of soil solutions and exchange complex. Soil microorganisms (fungi and bacteria) play a major role in the availability of nutrients in soils. They participate in weathering of primary materials through the production of low-molecular organic molecules (siderophores and organic acids). Determination of their relative contribution and understanding their interaction with soil minerals through different mechanisms is a key step toward characterization of the mobility of metals and identification of the pedogenic processes in action.

Recent techniques of *in situ* dynamic sensor have been developed to assess bioavailable fractions of metal in soil according to different relevant time scales of environmental processes. Diffusive gradients in thin films (DGT) are one of these speciation analyses [1]. This technique allows to establish a permanent flux of labile metal through a gel and then to measure the labile concentration upon its deployment time (i.e. the labile fraction corresponds to free metals in solution and metals linked to inorganic and organic ligands). In order to identify different weathering agents implied on the mobility and speciation of metals (Fe and Al) in soil solutions both in field studies and laboratory experiments, we have deployed DGT and DET (Diffusive Equilibrium in Thin Film) in different horizons of a podzol (developed on granitic rocks) on Norunda Site (Sweden) in November 2011. In parallel, we lead several experiments of geological material (granite) bioweathering to investigate the impact of fungi and bacteria on the release of Fe and Al from granite. To characterize mechanisms of dissolution, we monitored low-molecular organic molecules produced by microorganisms, microbial biomass, pH, and free and labile iron and aluminium fraction released by combining DGT and DET techniques.

The comparison of the results between field studies and laboratory experiments will permit the improvement of our knowledge of the contribution of microorganisms on the bioavailability of metals in soils and also on the podzolisation process that remains still always debated.

[1] Zhang *et al.,* (2001) *Env. Sci. Technol.,* **35**, 2602-2607.

The oldest isolated life-bearing macrosystem on the planet?

C.J. BALLENTINE[1]*, G. HOLLAND[1,2], G.F. SLATER[3], L. LI[4], G. LACRAMPE-COULOUME[4] AND B. SHERWOOD LOLLAR[4]

[1]University of Manchester, UK, chris.ballentine@manchester.ac.uk
[2]University of Lancaster, UK, g.holland@lancaster.ac.uk
[3]McMaster University, Hamilton, Canada, gslater@mcmaster.ca
[4]University of Toronto, Toronto, Canada, bslollar@chem.utoronto.ca
(* presenting author)

Water bearing macrosystems that have been isolated from the surface, preserved on geological timescales (>10Ma) and capable of supporting life, are seemingly rare. The only study of its type is now established in the South African Precambrian Crystalline Shield [1, 2]. The Witwatersand Basin provides the case type study and a unique insight into the evolution of chemolithotrophic life, the ability of even the most nutrient poor environments to support life in extremis, and thus environments that may support life on other planets [2]. The stable isotopic composition of the water, showing a high degreee of water-rock interaction, allows the inference of isolation from surface waters and a long residence time. It is the in-situ buildup of radiogenic noble gases (e.g. ^{4}He, ^{21}Ne, ^{40}Ar, ^{136}Xe) that has provided the basis for quantifying how long this system may have been isolated from the surface [1]. An outstanding question is how rare are such systems?

We have determined the noble gas concentration and isotopic composition of 6 gas samples, co-produced with water, from deep exploratory boreholes in a producing mine in the Timmins region of the Canadian Precambrian Crystalline Shield. Neon isotopic compositions are similar to the Witwatersand study and used to validate the closed system assumption for the radiogenic noble gases [1]. Using a similar model to [1], modified for local conditions (2.8ppm U, 10.6ppm Th, 3.4% K and 1% porosity and 100% release efficiency), we calculate closed system noble gas ages of the free produced fluids to be between 650Ma to 1.5Ga. These are the oldest 'free water' yet found in a crustal system.

Multi-collector noble gas mass spectrometry provides an order of magnitude more precision in the isotope determination of some free fluids [3]. We also resolve in all samples a clear ^{129}Xe signal in excess of atmospheric values. We can discount mass fractionation mechanisms and need to identify the source of the ^{129}Xe enrichment, only ever observed before in mantle-derived terrestrial fluids. ^{3}He/^{4}He allows us to discount a significant magmatic fluid source. Similarly, U-fission Xe (e.g. $^{132\text{-}136}$Xe) are produced at a known rate with fission ^{129}I (^{129}I → ^{129}Xe, t½=15.7Ma). The excess U-fission ^{136}Xe precludes a simple U-fission source for the ^{129}I → ^{129}Xe.

The ^{129}Xe excess observed is nevertheless most likely due to a local source of ^{129}I. We are collecting data to resolve two possible sources: i) U-fission ^{129}I released at steady state into the porewater through an extreme CFF (Chemical Fractionation of Fission products) process. CFF is required to prevent the associated fission Xe products reaching the porefluid and in turn would impact our previous assumption of 100% release efficiency and require older ages yet; or ii) the possibility of organic rich sediments associated with the formation lithologies supplying either the ^{129}I or its decay product (^{129}Xe). The latter would require a fluid closure date related to the last major mineralising event at 2.670Ga.

While the age determinations undgergo refinement with the new Xe information, our results nevertheless suggest that ancient and isolated macrosystems that have the potential to support life [2] may yet be found in a substantial portion of the Earth's Precambrian Crystalline Shields.

[1] Lippmann-Pipke et al. (2011) *Chemical Geology* **283,** 287-296.
[2] Lin et al. (2006) *Science* **314,** 479-482.
[3] Holland et al. (2009) *Science* **326,** 1522-1525.

Biotite Weathering in Watersheds of the Slavkov Forest, Czech Republic

Z. BALOGH-BRUNSTAD[1,2*], L. SACCONE[3,4], M.M. SMITS[5], C. BERNER[6], H. WALLANDER[6], T.J. MCMASTER[4], S.L.S. STIPP[1]

[1]NanoGeoScience, University of Copenhagen, Denmark (*correspondence: balogh_brunz@hartwick.edu)
[2]Hartwick College, Oneonta, NY, USA
[3]Institute for Forest Products Research, Edinburgh Napier University, Scotland, UK
[4]H.H. Wills Physics Laboratory, University of Bristol, UK
[5]Environmental Biology, Hasselt University, Belgium
[6]Microbial Ecology, Lund University, Sweden

Introduction and Methods

Biotite is one of the primary sources of potassium and magnesium in soils and is easily weathered by microbes and plants to access these nutrients. It is shown that ectomycorrhizal fungi play a significant role in mineral dissolution and nutrient translocation to their host plant. Numerous controlled laboratory experiments have demonstrated physical and chemical interactions of ectomycorrhizal fungi with biotite, ranging in scale from individual grains to artificial mineral soils. However, whether ectomycorrhizal fungi have a significant contribution to soil mineral weathering under natural forest conditions, remains controversial.

In our study, mesh bags containing 1 wt% small biotite flakes and one large freshly cleaved flake in quartz sand, were buried in spruce forest soils for two years at three sites where the bedrocks were serpentinite (K limited), leucogranite (Mg limited) and amphibolite (no limitations). The 60 µm mesh size allowed fungal hyphae to grow in the bags, but excluded direct plant root contact with the minerals, allowing us to test the direct contribution of ectomycorrhizal fungi on biotite weathering under naturally occuring K and Mg limitations. Mineral surfaces were examined with scanning electron microscopy (SEM) and atomic force microscopy (AFM). The total ectomycorrhizal biomass was determined by Ergosterol analyses.

Results and Discussion

Microscopy documented 5% or less direct fungal attachment to basal planes of biotite from all sites, with the lowest occurrence found at the low Mg site. The ergosterol results support these observations, with the lowest colonization of the bags at the low Mg site. Potassium limitation does not influence ectomycorrhizal colonizations. Shallow etched channels, similar to hyphae in size and branching pattern, are seen by AFM and SEM. These channels show short, segmented sections, i.e. a pulsive growth pattern and at each "pulse," the channel deepens in the direction of growth. We propose that this morphology reflects both chemical dissolution and physical force at the hyphal-mineral interface. However, abiotic processes, such as wear from sand grains rolling over biotite surfaces can produce similar patterns that are nearly indistinguishable from channels formed by hyphal activity.

Our observations from these field experiments support laboratory results, i.e., that fungal hyphae exercise both chemical dissolution and physical force at the hyphal-mineral interface, but abiotic processes cannot be excluded as an explanation for the formation of shallow channels on the soft biotite surfaces.

Aragonite – calcite seas and the evolution of biocalcification

UWE BALTHASAR[1*] AND MAGGIE CUSACK[1]

[1]University of Glasgow, School of Geographical and Earth Sciences, Glasgow, UK, uwe.balthasar@glasgow.ac.uk (* presenting author), maggie.cusack@glasgow.ac.uk

The influence of aragonite-calcite sea conditions on the evolution of biocalcification remain poorly understood. While selection for the polymorph favored by the aragonite-calcite sea status is relatively strong for organisms that evolved shells for the first time [1], there is no statistically significant correlation between shifts in the aragonitic/calcitic proportions in calcareous skeletons through time and sea chemistry [2]. However, case studies suggest that changes in aragonite/calcite sea conditions can influence the mineralogy of individual calcifying lineages [3].

A particularly intriguing group in this context is trimerellids, the only known group of aragonitic brachiopods [4]. With shells up to 20cm wide, trimerellids were also the most prolific calcifiers amongst brachiopods of the Ordovician/Silurian calcite seas. The success of trimerellids as measured by their large shell size and cosmopolitan distribution in the Ordovician/Silurian palaeo-tropics suggests that the innovation of aragonite during a calcite sea interval was advantageous for this group.

This success is best explained by considering the role of temperature on $CaCO_3$ polymorph formation. While the switch between aragonite and calcite sea conditions is commonly attributed to the ratio of Mg/Ca or pCO_2 [5, 6], it is often ignored that Mg/Ca controls the formation of aragonite and calcite as a function of temperature [7], with warmer temperatures favoring aragonite. When combining the values of marine Mg/Ca through time [5] with the Mg/Ca – temperature curve that separates aragonite from calcite precipitation fields [7] it becomes apparent that aragonite was the favored polymorph in warm tropical surface waters even during calcite sea intervals (Fig. 1).

Based on the available data [5, 7], water temperatures above 25° C favored the formation of aragonite even during calcite sea intervals (Fig. 1). The conventional view of aragonite/calcite sea conditions as a globally homogenous model needs to be reconsidered in the light of latitudinal surface water temperature differences.

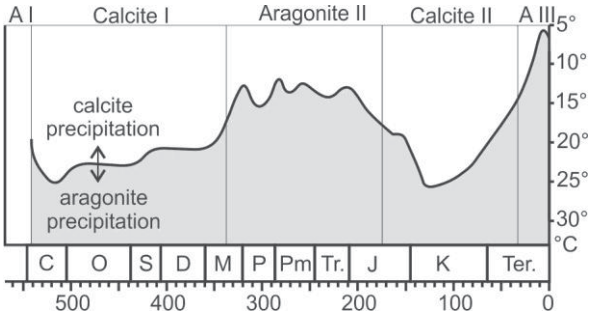

Figure 1: temperature separating the marine aragonite/calcite precipitation fields through time (from [4]; based on [5] and [7]).

[1] Porter (2010) *Geobiology* **8**, 256-277. [2] Kiessling et al (2008) *Nature Geoscience* **1**, 527-530. [3] Harper et al. (1997) *Geological Magazine* **134**, 403-407. [4] Balthasar et al. (2011) *Geology* **39**, 967–970. [5] Stanley & Hardy (1998) *Palaeogeography, Palaeoclimatology, Palaeoecology* **144**, 3-19. [6] Zhuravlev & Wood (2009) *Geology* **37**, 1123-1126. [7] Morse et al. (1997) *Geology* **25**, 85-87.

A transferable classical polarizable model for the water molecule

ANDRÁS BARANYAI[1*] AND PÉTER T. KISS[2]

[1]Eötvös University, Institute of Chemistry, Budapest, Hungary bajtony@chem.elte.hu (* presenting author)

[2]Eötvös University, Institute of Chemistry, Budapest, Hungary peter.kiss.20@gmail.com

The model

We developed a new model for the water molecule, which contains only three Gaussian charges. Using the gas-phase geometry, the dipole moment of the molecule matches, the quadrupole moment closely approximates the experimental values. Two positive charges are on the hydrogen atoms, while the negative charge is connected by a harmonic spring to its gas-phase position. This position is on the main axis of the molecule between the oxygen and the hydrogen atoms. The polarized state is established by the equality of the electrostatic forces and the spring force of the negative charge. In each time step the position of the massless negative charge is determined by iteration.Using the technique of Ewald summation, we derived expression for the energy, the forces, and the pressure for Gaussian charges. The dispersion interactions were fitted [1].

Tests of the new model

The model was tested and provided good results for the properties of gas-phase clusters up to 6 molecules, ambient water and hexagonal ice [1]. We calculated the properties of ice polymorphs under high pressure as well. In moderatly dense phases the closest O-O distances are very close to the same distances in hexagonal ice. In compressed phases, however, the number of neighboring molecules in the second shell is larger than in hexagonal ice. To use a repulsion suitable for hexagonal ice gives low density for the compressed ice phases. We calculated the "compressing force" for each particle and connected a variable "size" to this force. With this approach we obtained agreement from water clusters to ice VII up to 25 GPa [2]. Relying on earlier studies, we devised a reasonable form for an electric field dependent polarizability of the molecules. At low fields the polarizability starts from the experimental gas-phase value towards a treshold at high fields. The decline of this function was determined by the calculated dielectric constant of ambient water [3]. The model was tested for liquid-vapor behavior. The surface structure of the model was analysed. Its surface tension provides superior estimates of the experimental value than nonpolarizable models [4]. The algorithm of the program code is given for the model. Due to different numerical speeding up methods, it is only 2.6 times slower than the code of the well-known TIP4P nonpolarizable model [5].

[1] A. Baranyai, P.T. Kiss, J.Chem.Phys.,**133**, 144109 (2010)
[2] P.T. Kiss, A. Baranyai, J.Chem.Phys., **134**, 214111 (2011)
[3] A. Baranyai, P.T. Kiss, J.Chem. Phys.,**135**, 234110 (2011)
[4] P.T. Kiss, M. Darvas, A. Baranyai, and P. Jedlovszky, J.Chem.Phys., submitted
[5] P.T. Kiss, A. Baranyai, and A.A. Chialvo, J.Comput.Chem., submitted

Acknowledgement: Support for AB during this work was given by OTKA fund K84382..

Probing iron oxide interactions with organic matter by X-ray spectroscopy.

ANDREW BARBER[1*], ALESSANDRA LERI[2], KARINE LALONDE[3] AND YVES GÉLINAS[4]

[1]Concordia University, Montréal, Canada, andrew.jack.barber@gmail.com (* presenting author)
[2]Marymount Manhattan College, New York, USA , alessandra.leri@gmail.com
[3]Concordia University, Montréal, Canada, k_lalonde@hotmail.com
[4]Concordia University, Montréal, Canada, ygelinas@alcor.concordia.ca

Abstract

Iron oxides have been shown to promote the preservation of 1/5th of the total organic carbon pool in marine sediments (1). These iron-organic matter phases are formed within the oxic layer of marine sediments through oxidation of dissolved iron(II) produced during weathering and diagenetic recycling (2). However, it remains unclear what type of interaction (adsorption of organic matter onto the surface of oxides or co-precipitation to form iron-organic complexes) is formed between iron and organic matter in these systems. In this work, iron oxides were synthesized by oxidizing a solution of Fe(II) in seawater at constant, near circumneutral pH to closely mimic natural environmental conditions. Synchrotron X-ray absorption techniques (XANES and EXAFS) were used to probe the local environment of iron using beamline X26A at the Brookhaven National Laboratory. We determined that iron oxides precipitated in the presence of organic matter have a shifted iron Kα edge with respect to organic free iron oxide minerals, demonstrating that iron-OM co-precipitates are likely a prevalent form of iron in sedimentary environments. Using this shift in Kα edge the approximate contribution from organic free iron oxides and organic rich mononuclear iron compounds of our synthetic Fe(III)-OM precipitates were determined using linear combination fitting.

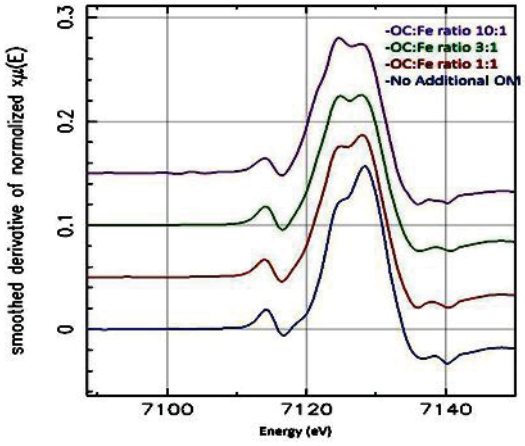

Figure 1: The first derivatives of stacked normalized iron Kα edge XANES spectra with OC:Fe ratios varying from 10:1 to 1:1.

[1] Lalonde et al. (in press) *Nature*. [2] Canfield, D. E. The geochemistry of river particulates from the continental USA: Major elements. (1997) *Geochim. Cosmochim. Acta* **61,** 3349–3365

Synchrotron radiation characterization of ferruginous bodies from human lung tissue

FABRIZIO BARDELLI[1*], ELENA BELLUSO[2], SILVANA CAPELLA[2], GIULIA VERONESI[3], AND LAURENT CHARLET[1]

[1]ISTerre, Grenoble, France, fabrizio.bardelli@gmail.com (* presenting author), charlet38@gmail.com
[2]Dipartimento di Scienze della Terra, Turin, Italy elena.belluso@unito.it silvana.capella@unito.it
[3]ESRF, Grenoble, France giulia.veronesi@esrf.fr

Introduction

Exposure to asbestos fibers is well known to be associated with respiratory diseases such, mesotheliomas and lung cancer. *FB* (**Figure 1**) are the result of a coating process, taking place in the host organism, of a variety of fibers such as asbestos (crocidolite, amosite, chrysotile) and phyllosilicate fibers (talc, mica, kaolinite), coal dust, oxalate, and fiberglass. This coating was generally accepted to be a protective mechanism produced by macrophages to segregate the cytotoxic fibers from the organic tissues [1]. However, more recently, other authors suggested that the coating material may enhance the cytotoxic properties of the asbestos fibers by increasing the production of free radicals [2,3,4,5,6]. In spite of the large attention devoted to this subject, the exact nature of the coating, along with the biological effect of *FB*, is still not clear. This is mainly due to the difficulty of sampling large enough amounts of *FB* using reliable isolation procedures, and to their microscopic dimensions (2-5 μm diameter, 20-90 μm length). The use of state of the art synchrotron radiation microprobe techniques gave the first direct characterization of single *FB*.

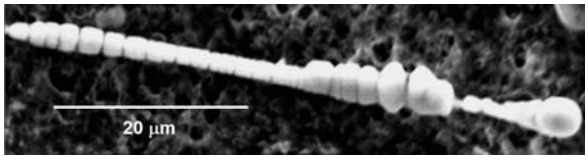

Figure 1: SEM image of a *FB* collected from human lung tissue.

Results and Conclusion

Human lung tissue rich in *FB*, owing to professional exposure, were collected from two subjects who were affected by lung cancer. μXRF high resolution elemental maps of *FB* (2 μm pixel size) were acquired on ID18F at ESRF, and μXANES spectra were recorded at selected points at the Fe edge on ID21. μXRF revealed that the external coating is mainly composed of Fe, Cu, Zn, and As (plus Ge and Ba in one subject) distributed in different areas of the *FB*, while μXANES gave the first direct confirmation that iron is mainly present as ferritine.

[1] Mace *et al.* (1980) *Cancer. Lett.*, **9**, 95. [2] Ghio *et al.* (2004) *Toxicologic Pathology*, **32**, 643. [3] Hardy *et al.* (1995) *Aust. Chem. Rev*, **90**, 97. [4] Lund *et al.* (1994) *Aust. Occup. Environ. Med.*, **51**, 200. [5] Pooley (1972) *Environ. Res.*, **5**, 363. [6] Pascolo *et al.* (2011) *Particle and Fibre Toxicology* **8**, 7.

Fe atom exchange between aqueous Fe^{2+} and hematite

MICHELLE BARGER[1*], KEVIN ROSSO[2], AND MICHELLE SCHERER[1]

[1]Civil and Environmental Engineering, University of Iowa, Iowa City, IA 52242(*correspondence: michelle-barger@uiowa.edu)
[2]Chemical and Materials Science Division, Pacific Northwest National Laboratory, Richland, Washington 99352

Recent work has revealed that Fe oxides are dynamic phases that will undergo significant Fe cycling in the presence of aqueous Fe(II) [1]. Complete exchange of Fe atoms between aqueous Fe(II) and goethite has been shown [2] and extensive exchange has also been observed for ferrihydrite and lepidocrocite [3]. Bulk electrical conduction linking oxidative adsorption of Fe(II) and reductive dissolution of the Fe(III) oxide at spatially separated sites has been suggested as a potential mechanism to explain the extensive exchange observed in the presence of Fe(II) [2; 4]. Interestingly, bulk electrical conduction linked to growth and dissolution has only been directly demonstrated in hematite, yet, ^{55}Fe isotope data indicate little exchange occurred between aqueous Fe(II) and hematite [3].

Here we are investigating atom exchange between aqueous isotope specific ^{57}Fe(II) and isotopically normal hematite to determine if exchange occurs between aqueous Fe(II) and hematite. Our working hypothesis is that the reaction of aqueous Fe(II) with hematite will result in significant Fe atom exchange and recyrstallization of hematite particles and that the rate of exchange will be influenced by particle size.

[1] Gorski and Scherer (2011) *Aquatic Redox Chemistry* **1071**, 315-343. [2] Handler *et al.* (2009) *Environ. Sci. Technol.* **43**, 1102-1107. [3] Pedersen *et al.* (2004)) *GCA* **43**, 3967-3977. [4] Yanina and Rosso (2008) *Science* **320**, 218-222. [5] Williams and Scherer (2004) *Environ. Sci. Technol.* **38**, 4782-4790.

Unravelling the crustal architecture of Cape Verde; the xenolith record

ABIGAIL K. BARKER[1*], DAVID NILSSON[1], VALENTIN R. TROLL[1], THOR H. HANSTEEN[2] AND ANDREAS KLÜGEL[3]

[1]CEMPEG, Department of Earth Sciences, Uppsala University, Uppsala, Sweden abigail.barker@geo.uu.se (* presenting author)
[2]IFM-GEOMAR, Dynamik des Ozeanbodens, Kiel, Germany
[3]Department of Earth Sciences, University of Bremen, Bremen, Germany

The Cape Verde submarine plateau was extensively sampled during the Meteor M80/3 research cruise in January 2010. The suite of sampled lavas are found to host a range of xenoliths. These xenoliths provide a spectrum of lithologies available to interact with magmas during transport through the lithospheric mantle and crust. Exploring the depths of origin of such xenoliths will complement the information we derive from the host lavas and thus the 3-D geochemical framework of magma-crust interaction in the Cape Verde magmatic plumbing systems. This will allow the development of a model for the crustal architecture beneath the Cape Verde oceanic plateau.

The host lavas are nephelinites containing clinopyroxene, nosean, nepheline, ± apatite, ± sanidine phenocrysts. The crustal xenoliths are mostly mafic plutonic assemblages with one sedimentary xenolith occurring. The mafic plutonic xenoliths are holocrystalline, and fine to medium grained. They contain plagioclase, clinopyroxene, olivine and/or amphibole. The sedimentary xenolith contains rounded grains of quartz, together with minor clay minerals, biotite and alkali feldspar.

Mafic plutonic xenoliths have developed reaction zones on contact with the host magma. The reaction zones are approximatley 50 to 100 microns and are observed petrographically by crystallisation of fine grained sericite, epidote and chlorite. Element mapping highlights the increase of Na and K and decrease in Ca and Al in the reaction zone compared to plagioclase of the xenolith.

REE profiles of clinopyroxenes in the host lavas are LREE enriched whereas clinopyoxenes from the plutonic xenoliths are LREE depleted. Modelling of REE melt compositions indicates the plutonic xenoliths are derived from MORB ocean crust opposed to intrusives of the Cape Verde plateau.

Mineral chemistry of the clinopyroxenes in the host lavas and xenoliths have been used to determine crystallization pressures. Thermobarometry indicates that clinopyroxenes in the host lavas formed at depths of 17 to 46 km[1], whereas those in the xenoliths formed at 5 to 15 km. This places the depth of origin of the plutonic xenoliths above the Cape Verde Moho and in the oceanic crust.

The xenoliths thus trace magma-crust interaction to the MORB oceanic crust and overlying sediments located beneath the Cape Verde submarine plateau. The spatial distribution and vertical representation provided by crustal xenoliths will help to develop a better idea of the 3-D architecture of the oceanic crust beneath the Cape Verde plateau.

[1] Barker et al., (2011) *Contrib. Mineral. Petrol.* doi: 10.1007/s00410-011-0708-2.

Laboratory CO_2 flow experiments to model hydrochemical and mineralogical changes in the Arbuckle aquifer during CO_2 storage

ROBINSON BARKER[1*], LYNN WATNEY[2], SAIBAL BHATTACHARYA[3], BRIAN STRAZISAR[4], LOGAN KELLY[1], SOPHIA FORD[1], SAUGATA DATTA[1]

[1]Kansas State University, Department of Geology, Manhattan, Kansas rbarker@ksu.edu (* presenting author)
[2] Kansas Geologic Survey, Lawrence, Kansas lwatney@kgsu.ku.edu
[3]Chesapeake Energy Corporation, Oklahoma City, Oklahoma saibal.bhattacharya@chk.com

[4]National Energy Technology Laboratory, Pittsburg, PA brian.strazisar@netl.doe.gov

The saline Arbuckle aquifer in south-central Kansas has been proposed for a pilot scale injection of CO_2 [1]. This paper presents characterization of Arbuckle mineralogy and hydrogeochemistry along with experimental flow cell data and geochemical modelling of CO_2 injection. Two wells (KGS 1-32 and 1-28) have been drilled to the basement to provide rock core and brine data for a site specific determination of the storage potential of the Arbuckle. Thin section and XRD data reveal dominant mineralogy in the injection zone to be dolomite with sporadic cherty nodules. Chert appears to replace dolomicrite and euhedral dolomite as well as infilling porosity. Porosity values range between 1.2 and 11.8% within the injection zone. Drill stem test water samples were collected from 8 depths (3677, 4182, 4335, 4520, 4876, 4927, 5036, 5183 ft) to describe the changing brine chemistry with depth. Sulfate peaks at 4876' and 4927' may be indicative of microbial action at these depths. Chemical analysis show a hyper saline brine (~50,000 - 190,000 TDS) dominated by Cl, Na and Ca. Elemental ratios of Cl:Br, Na:Cl and Ca:Sr are what is expected of a typical saline aquifer system [2]. Major and trace elemental chemistry suggest the brine originated from evaporated seawater that has been affected by digenetic processes.

Laboratory flow experiments carried out at the National Energy Technology Laboratory show increases in Ca, Mg, Na and Cl while Fe, S, P and SO_4 decrease within the first 15 hours while hours 15 through 24 show a reverse trend for these elements. Flow experiments at supercritical temperatures and pressures allow determination of the extent of mineral carbonation, mineral dissolution reactions and help constrain reaction rates determined through geochemical modelling [3].

[1] Carr *et al.* (2005) *AAPG Bulletin*. **89** 1607-1627. [2] Barker *et al.* (2011) Abstract, *American Geophysical Union*. [3] Kharaka *et al.* (2006) *J. Geochem. Explor.* **89** 183-183

A textural and mineralogical assessment of NWA 3118

G. C. BARLET [1*], D. W. DAVIS[1], D. MOSER[2], K. TAIT[1,3], I. BARKER[2] AND B. C. HYDE[3]

[1]Department of Geology, University of Toronto, Toronto, Canada barlet@geology.utoronto.ca
[2]Department of Earth Sciences, University of Western Ontario, London, Canada
[3]Department of Natural History, Royal Ontario Museum, Toronto, Canada

Northwest Africa (NWA) 3118 is a reduced CV3 chondrite, with large, irregularly shaped Calcium-Aluminum-rich Inclusions (CAIs) and Amoeboid Olivine Aggregates (AOAs) as well as dark inclusions [1]. Previous work by Ivanova [2,3,4] on NWA 3118 showed remarkable features such as compound CAIs with variable degrees of internal melting as well as unusual Zr-Y-Sc-rich mineral inclusion. NWA 3118, a relatively new addition to the list of chondrites, still contains numerous evidences about the early solar system. Initial textural observations were made by optical microscopy. EDS mapping and BSE imaging of uncoated slabs was carried out in variable pressure mode by FEG-SEM. In complement, we investigated the mineralogy of CAIs and AOAs using Raman Spectroscopy.

The surface distribution of chondritic components appears heterogeneous on our slabs where some areas are overpopulated by large inclusions, while other areas are composed of widespread small inclusions, and the rest is a mixture of both. Amorphous (fluffy) CAIs and AOAs are relatively common in NWA 3118 and appear very similar when observed optically. In some cases their shapes are controlled by compression between adjacent chondrules, although there does not seem to be any consistent axis of strain. Silicate chondrules themselves are rarely spherical and some of them appear to have responded to local strain, suggesting that they were partially molten when NWA 3118 was accreted.

Our specimen contains singular assemblages of fine-grained and coarse-grained amorphous CAIs. We also report the presence of compact (spherical) CAIs surrounded by Wark-Lovering rims embedded in fluffy CAIs. The largest compact CAI (400 micron) is associated with two significantly smaller distorted compact CAIs (50 micron) near the edge of its amorphous host.

Because amorphous CAIs and AOAs are nearly indistinguishable in texture, we presume that they were produced by similar physical processes in different reservoirs, or in the same reservoir with an evolving bulk chemistry. The presence of amorphous CAIs with different grain sizes supports the idea that the heat transfer and/or other factors that control crystal size (e.g. degree of undercooling) in the forming region were not uniform. In particular, the presence of compact CAIs included in amorphous CAIs suggests a variable non-uniform heat source where dusty CAI material may have been melted to form compact CAIs which subsequently accreted more dust in a process similar to that suggested for chondrules [5].

[1] Russell et al. (2005) *Meteoritical Bulletin* **89**, *MAPS* **40**, A201-A263. [2] Ivanova et al. (2010) *LPSC* **41**,1670. [3] Ivanova et al. (2011) *LPSC* **42**,1728. [4] Ivanova et al. (2011) *LPSC* **42**,1738. [5] Rubin (2010) *GCA* **74**, 4807–4828.

Links between tectonics and life, 4.0 to 2.3 Ga and the rise of oxygen

M.E. BARLEY[1*],

[1] School of Earth and Environment, The University of Western Australia, Crawley, Western Australia, 6009, Australia (correspondence: mark.barley@uwa.edu.au)

Earth is the only planet in our solar system with a bimodal topographic distribution crucial for the evolution of complex life. The tectonic records of the Archean to Paleoproterozoic (4.0 to 2.3 Ga) terranes indicate a link between evolving global tectonics with the formation of stable continents, increased subaerial volcanism and increased orogenic mountain building and the rise of atmospheric oxygen on Earth ~2.4 billion years ago. The first 2 stable cratons formed between 3.0 and 2.9 Ga after the first unambiguous evidence for plate tectonics. The Neoarchean record started at 2.8 Ga involving the possible break of a single pre-existing continent and the most prodigious period of generation and preservation of juvenile continental crust during a period of mantle plume breakout (2.72 to 2.65 Ga). During this period many cratons formed and aggregated into larger cratons and continents. Lower sea levels between 2.65 and 2.55 Ga were followed by a second (~2.51 to 2.45 Ga) period of plume breakout. Although oxygenic photosynthetic bacteria are thought to have evolved by 2.7 Ga or 2.5 Ga, the irreversible rise of atmospheric oxygen appears to have occured between 2.48 and 2.32 Ga suggesting a dynamic linkage and interaction of both sources and sinks of oxygen. Increased subaerial volcanism [1] and reduced temperature of magmatism (less komatiites) after 2.65 Ga helped cyanobacteria and also resulted in a decline of methane helping oxygen strat to rise [2]. There is growing evidence the long time the rise took involves interaction between cyanobacteria and oxygen using acid rock drainage bacteria from 2.48 Ga [3] as well as the rise of iron in the ocean using oxygen to form the bigest banded iron formations (BIFs). The 2.4 Ga break in tectonics and decline of BIFs helped the cyanobacteria and volcanic gasses with the rise of oxygen.

References.

[1] Kump and Barley (2007) Nature 448, 1033-1036.

[2] Konhauser at al. (2009) Nature 458, 750-753.

[3] Konhauser at al (2011) Nature 478, 369-373.

Chlorine isotope geochemistry of Icelandic geothermal waters

JAIME D. BARNES[1] AND ANDRI STEFÁNSSON[2]

[1]Department of Geological Sciences, University of Texas, Austin, Texas, USA jdbarnes@jsg.utexas.edu (* presenting author)

[2]Institute of Earth Sciences, University of Iceland, Reykajavik, Iceland, as@hi.is

The chlorine isotope composition of several geothermal systems in Iceland were determined in order to evaluate possible chlorine stable isotope fractionation in geothermal systems. The geothermal systems studied exhibit a range of temperatures (~38°C to >300°C) and pH (6 to 9.5). Chlorine concentrations range from ~5 to ~200 ppm. $\delta^{37}Cl$ values for all samples are near 0‰ (range = -0.3 to +0.3‰; error = +/- 0.2‰).

The source for the chlorine in the analyzed systems is commonly hypothesized to be from magmatic degassing or from leaching of host basalt during water-rock interaction. The $\delta^{37}Cl$ values are consistent with either of these hypotheses based on the near 0‰ value for the upper mantle and MORB glasses [1].

No large isotopic shifts due to fractionation are observed in these samples. These results are in agreement with previous experimental work on chlorine isotope fractionation between coexisting vapor and liquid in the system H2O–NaCl at 400°C and 450°C which show $\Delta^{37}Cl_{vapor-liquid}$ = 0 +/- 0.2‰ [2]. However, large Cl isotope fractionation has been observed in a few high-temperature (>100°C) and highly acidic volcanic fumaroles in Central America. ^{37}Cl preferentially partitions into the vapor phase as HCl resulting in extreme positive $\delta^{37}Cl$ values (~ +4 to +12‰) in acidic geothermal systems [3]. Further work will focus on acidic Icelandic geothermal systems in which Cl^- is hosted as HCl in order to explore the full range of $\delta^{37}Cl$ values in geothermal systems.

These results show that Cl stable isotopes act as a conservative tracer in neutral to slightly basic geothermal sytems regardless of phase separation; thereby, making Cl isotopes an excellent tracer of chloride sources in neutral systems.

[1] Sharp *et al.* (2007) *Nature* **446**, 1062-1065. [2] Liebscher *et al.* (2006) *Chemical Geology* **234**, 340-345. [3] Sharp *et al.* (2010) *GCA* **74**, 264-273.

The Composition of the Stillwater and Bushveld Parental Magmas.

SARAH-JANE BARNES [1]* AND PHILIPPE PAGE[2]

[1] Universite du Quebec a Chicoutimi, Canada sjbarnes@uqac.ca
[2] Universite du Quebec a Chicoutimi, Canada ppage@uqac.ca

The Bushveld and Stillwater Complexes contain most of the world's platinum-group element resources and it has long been recognized that their cumulate stratigraphies show similarities, which suggests that the magmas they formed from were similar with respect to major element compositions. At both localities a magma rich in SiO_2 and MgO is needed to produced the orthopyroxene rich lower parts of the intrusions. Chill margins with the composition of Mg-rich basaltic andesite are present at both localities (the B-1 and Gp-3 chills). To produce the gabbroic middle zones of the intrusions, melts close to tholetiitic basalt composition are required. Chills with these compositions are found at both intrusions (B-2 and Gp-1 chills). Recent studies on Bushveld have provided information on the trace element content of the Bushveld magmas and cumulates indicating that the magmas were strongly enriched in LILE and LREE (Fig. 1). We have determined the trace element content of the equivalent magmas from Stillwater and they are poorer in LILE and LREE. The Mg-rich andesite (Gp-3) are closer to boninite compositions than the Busheld B-1 rocks. The tholeiitic basalt (Gp-1) show some similarities to arc tholeiites.

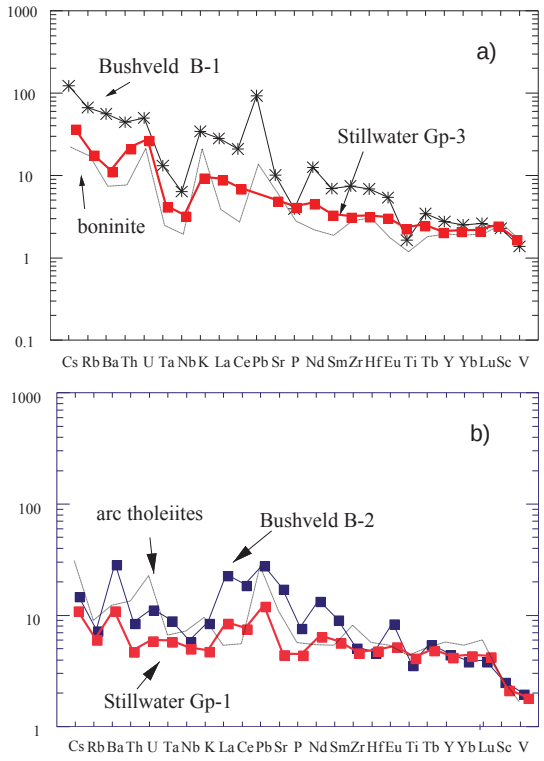

Fig. 1 Mantle normalized incompatible element plot of the marginal rocks of the Bushveld and Stillwater compared with modern magmas

Lead Isotopic bias during the *Chaîne Opératoire* of Non Ferrous metal: Implications for Provenance Studies

S. BARON[1*], C.G. TAMAS[2] AND B. CAUUET[3]

[1]CNRS, Toulouse, France, sbaron@univ-tlse2.fr (* presenting author)
[2]University Babes-Bolyai, calingtamas@yahoo.fr
[3]CNRS, Toulouse, France, cauuetb@aol.com

Introduction

The rise of the high resolution mass spectrometers (MC-ICP-MS) during the last ten years allows the analyses of traditional and non traditional isotopes to be more accurate, precise, relevant and consequently subtly interpretable [*e.g.* 1, 2]. The lead isotopic tracing, from mines/ore bodies to archaeological materials, constitutes the main tool of metal provenance studies. Despite the use of high-resolution isotopic measurements, the identification of the geographical ores source is difficult because of several factors. The most important factor is inherent to the ores themselves: *i)* the ores could have lead isotopic heterogeneity in a same ore body and *ii)* numerous different geographical mining districts could have same lead isotopic compositions. Furthermore, the ores are disconnected of any geological, archaeological and historical significance in respect with the metal provenance study. When the archaeological materials are well documented by mining archaeology and history, the provenance studies (coupled with high resolution measurements) are improved [3]. Another factor, rarely taken into account, is the possible lead isotopic bias during the metallurgical processes. Because the isotopic tracing is directly operated from ores to object at global scale, the consequence is that the *chaîne opératoire* is not taken into account. But, during the *chaîne opératoire*, numerous human operations occurred. Some archaeological experiments conducted on ores reduction have measured isotopic bias between ores / metal of slags and metal of slags / slags silicated matrix at furnace scale [4]. Through two regional studies, conducted on materials well documented by mining archaeology and history, we found isotopic bias due to the local *chaîne opératoire*. These results corroborate the previous experimental ones.

Results and discussions

We will present here the results from two *chaîne opératoire* well documented by mining archaeology: *i)* the lead-silver one in France for medieval time and ii) the gold-silver one in Romania for roman time. We will demonstrate here that the addings during the metallurgical processes produce lead isotopic bias. According the high-resolution isotopic measurement available today, it is necessary to take into account these biases in order to refine the tracing and understand the *chaîne opératoire* in its historical context. This approach will allow the understanding of regional management of ore sources in ancient times. It constitutes the first step before the beginning of a metal diffusion at global scale.

[1] Klein et al. (2010) *Archaeol. Anthropol. Sci.* **2**, 45-56. [2] Desaulty et al., (2011) PNAS **108**, 9002-9007. [3] Baron et al., **submitted** in *Archaeometry*. [4] Baron et al. (2009) *Appl. Geochem.* **24**, 2093-2101.

Mercury stable isotopes in fish tissue as indicators of photochemical transformations

GIDEON BARTOV[1*], THOMAS M. JOHNSON[1]

[1]University of Illinois Urbana-Champaign, Urbana, USA, (*gbartov2@illinois.edu)

During the 1950s and 1960s, the U.S Department of Energy (DOE) plant Y-12, near Oak Ridge, TN, was using Hg in the production of thermonuclear weapons. During normal plant operations, large amounts of Hg were discharged into the East Fork Poplar Creek (EFPC) and its floodplain [1]. Current research aims to better understand Hg transformations that control its mobility and bioavailability.

Hg isotopes have the potential to identify and perhaps quantify certain biogeochemical reactions. Photo-reduction and -demethylation have been shown to fractionate the odd isotopes of Hg (^{199}Hg and ^{201}Hg), independent of their mass, due to the magnetic isotope effect [2]. Fish are assumed to be good integrators of bioavailable Hg over space and time and do not change the mass independent fractionation signature of the odd Hg isotopes. As a result, it is possible to use fish as indicators of photochemical reactions occurring in the water column. According to Bergquist and Blum [2], photoreduction of $Hg(II)_{(aq)}$ creates a slope, on a Δ^{199}Hg vs. Δ^{201}Hg graph, of 1.00±0.02, methyl-Hg (MeHg) photoreduction has a slope of 1.36±0.02, and fish tissue plots on a 1.28±0.03.

Our study aims to detect and quantify Hg chemical transformations in the EFPC. Frozen fish tissues received from Oak Ridge National Laboratory were digested and analyzed on a Nu Instruments MC-ICP-MS using the Mead and Johnson [3] double-spike technique. The ^{202}Hg/^{198}Hg ratio (reported as δ^{202}Hg) was measured with a precision of ~0.11‰ relative to the NIST SRM 3133 Hg standard. Odd isotope deviations were measured with a precision of ~0.04‰ and are reported as Δ^{199}Hg and Δ^{201}Hg deviations from theoretical mass dependent fractionation values.

The δ^{202}Hg of the fish shows a weak increase increasing distance downstream from Y-12, from -0.57±0.08‰ (n=4) upstream to -0.29±0.15‰ (n=4) downstream. The odd isotope deviations also show a slight positive trend with increasing distance downstream from Y-12 (shifting Δ^{201}Hg from -0.05±0.04‰ to 0.05±0.04‰ and Δ^{199}Hg from -0.04±0.07‰ to 0.09±0.05‰). The slope of the data is 1.3, consistent with the slope obtained for photochemical demethylation by Bergquist and Blum [2]. Based on equations given by Bergquist and Blum [2], we can calculate, to first order, the amount of photoreduction of MeHg in the water between 4-11% using the Δ^{201}Hg values.

Fish are a good proxy for the extent of photoreduction of Hg in the water column; however, it would be beneficial to look directly at the Hg present in the water, the reactant pool. Therefore, water samples from the EFPC have been obtained and will be analyzed.

[1] Southworth *et al.* (2000) *Environmental Monitoring and Assessment* **63**, 481-494. [2] Bergquist and Blum (2007) *Science* **318**, 417-420. [3] Mead and Johnson (2010) *Analytical Bioanalytical Chemistry* **397**, 1529-1538.

Bottom Water Changes in the South Pacific Over the Last 30 ka Documented by Nd Isotopes

CHANDRANATH BASAK[1, 2]*, KATHARINA PAHNKE [1,2]

[1]Max Planck Institute for Marine Microbiology, Bremen, Germany *(cbasak@mpi-bremen.de)

[2]Institute for Chemistry and Biology of the Marine Environment (ICBM), Oldenburg, Germany

North Atlantic Deep water (NADW) and the Antarctic Bottom water (AABW) are the two central supporting pillars that control deep ocean ventilation and influence atmoshperic CO_2 concentrations on glacial-interglacial timescales. While much is known about past NADW changes, very little is known about variations in AABW formation and export from the Southern Ocean. Available paleo-records point at enhanced northward advection of southern sourced deep water during times of reduced NADW formation [1]. It is, however, not clear whether the observed presence of AABW in the North Atlantic is due to increased southern sourced deep water production or related to reduced NADW formation. In this study we used paleo seawater Nd isotope ratios to address the AABW formation history in the Pacific Southern Ocean for the last 30 ka.

Our study site is located in the eastern Pacific sector of the Southern Ocean [PS58/271-1; 61.24°S, 116.05°W, 5214m water depth; [2]]. Currently this site is bathed by AABW with contributions from Circumpolar Deep Water and Pacific Deep Water, and is located at the Polar Front. The Ross Sea is the nearest deep water formation area and the prsent-day northern limit of 'pure' Ross Sea bottom water (RSBW; defined by high salinity and density) reaches just south of our site. Thus, during times of enhanced deep water formation in the Ross Sea, RSBW would be expected to have reached the study site. Since RSBW carries the characteristic Nd isotope signal of Ross Sea sediments (ε_{Nd} = -7; [3]), any northward expansion of RSBW should be recorded in the sediments at our core site. The Late Holocene ε_{Nd} value (ε_{Nd} = - 6.2) at our study site is consistent with the influence of RSBW and CDW/PDW at the core site. The downcore ε_{Nd} record shows that the study site was bathed by a water mass with an Nd isotopic composition of (ε_{Nd} =) ~ -5.5 during the last glacial maximum (LGM). The ε_{Nd} value of the water mass gradaully started to change towards more Pacific deep water-like values (ε_{Nd} = -3) with the initiation of deglaciation around 18 ka BP. Strong Pacific deep water influence is observed at around 15.3 ka, followed by a gradaul decrease to the Late Holocene value (ε_{Nd} = -6.2). The time of maximum ε_{Nd} around 15.3 ka coincides with warming in the Southern Hemisphere and corresponding cooling and shut down of NADW in the Northern Hemispere. Our data do not support increased RSBW/AABW formation at this time, rather, we observe enhanced influence of Pacific deep water. If this holds true for the entire Southern Ocean, the observed presence of AABW in the deep North Atlantic has to be explained by reduced NADW production.

[1] Lynch-Stieglitz *et al.* (2007) *Science* **316**, 66-69. [2] Jacot Des Combes *et al.* (2008) *Paleoceanography* **23**, PA4209. [3] Pahnke *et al.* (2011) *Geophysical Research Abstracts*, 13, EGU General Assembly.

Toward an understanding of metal uptake in a methanogenic archaeon isolated from the Rancho La Brea Tar Pits

JENNA L. BASS[1], ELIZABETH L. EDWARDS[1], ALEXIS LLOYD[1], SARA J. WEAVER[1] AND JOHN S. MAGYAR[1*]

[1]Department of Chemistry, Barnard College, New York, NY 10027, USA jmagyar@barnard.edu (* presenting author)

Recalcitrant petroleum sources, such as heavy oil, oil sands, and asphalts, are an increasingly important part of the global petroleum supply. In situ conversion of these materials to methane would have significant environmental and economic advantages over current mining and extraction methods, but significant fundamental research on anaerobic methanogenic petroleum degradation is required before such approaches will become practical. Understanding the bioinorganic chemistry of such processes is essential to an overall understanding of methanogenesis, which requires a series of metallocofactors. Of these, several key proteins are nickel-binding proteins, including the hydrogenases. We are investigating mechanisms of nickel uptake in *Methanocorpusculum labreanum*, a methanogen isolated from natural asphalt sediments in the La Brea Tar Pits, Los Angeles. We have isolated a gene for a putative metalloregulatory protein from genomic DNA, cloned it into *E. coli*, and overexpressed and purified the resulting protein. Using a variety of spectroscopic methods, including UV-vis-NIR absorption, fluorescence, and circular dichroism spectroscopies, we are characterizing the coordination chemistry and structure of this protein. We have identified the presence of both flavins and iron-sulfur clusters, and work is currently underway to elucidate the structure and binding of these cofactors and the role they may play in regulating cellular nickel uptake.

Microbial uranium reduction monitoring: Linking isotopic fractionation factors with microbial metabolism

ANIRBAN BASU*, THOMAS M. JOHNSON, ROBERT SANFORD, AND CRAIG C. LUNDSTROM

Department of Geology, University of Illinois at Urbana-Champaign, Urbana, IL, USA, abasu3@illinois.edu (* presenting author), tmjohnsn@illinois.edu, rsanford@illinois.edu, lundstro@illinois.edu

Microbial reduction of soluble and mobile U(VI) to sparingly soluble U(IV) is a promising remediation strategy for uranium-contaminated aquifers. A wide range of microorganisms with diverse metabolic pathways can reduce U(VI) to U(IV). Microbial U(VI) reduction fractionates U isotopes; heavier isotopes partition in the solid U(IV) products. The remaining U(VI) pool becomes isotopically lighter with progressive reaction. The isotopic enrichment is quantified by measuring $^{238}U/^{235}U$ ratio in the remaining unreacted pool of U(VI) and the magnitude of the isotopic enrichment is expressed by the isotopic fractionation factor ε ($\varepsilon=1000*(\alpha-1)$; $\alpha = (^{238}U/^{235}U)_{Product}/(^{238}U/^{235}U)_{Reactant}$). The isotopic enrichment is related to the extent of reduction by the fractionation factor ε. $^{238}U/^{235}U$ ratios can be used to detect and possibly quantify U(VI) reduction, if the ε for the relevant microbial reductions are known.

Here we report ε values for U(VI) reduction by two strains of *Geobacter sulfurreducens* (PCA and Criddle), *Anaeromyxobacter dehalogenans* strain FRCW, *A. dehalogenans* strain FRC-R5, and *Desulfitobacterium* Viet1. For each bacterial species, we measured the ε values in duplicate batch incubation experiments with U(VI) and 0.5 mM electron-donor at 30 °C.

All strains tested in this study induced significant isotopic fractionation during U(VI) reduction. The ε yielded by *Geobacter sulfurreducens* strains PCA and Criddle were 0.68‰ and 0.95‰, respectively. The ε values for *A. dehalogenans* strain FRCW, *A. dehalogenans* strain FRC-R5, and *Desulfitobacterium* Viet1 were 0.75‰, 0.98‰, and 0.84‰, respectively. The results of this study indicate that the ε does vary with microbial metabolism. We observed an increasing trend in ε with decreasing cell-specific reduction rate. Our results suggest that cell-specific reduction rates are good indicators of the magnitude of microbial U isotopic fractionation. The ε tends to reach highest values (~1‰) under nutrient limited electron-donor poor conditions. Our results shed light on the fundamental relationship between metabolism and isotopic fractionation and will be useful to detect and possibly quantify U(VI) reductions in the sites undergoing active bioremediation.

Progress in detrital garnet Sm-Nd geochronology: the second point on the isochron

E.F. BAXTER , K.A. ECCLES, N.C. SULLIVAN

Boston University, Department of Earth Sciences, Boston, MA, 02215 U.S.A, (*correspondence: efb@bu.edu)

Detrital minerals in the sedimentary record provide valuable information about the tectonic evolution of the Earth. Detrital garnets also preserve a chemical record of tectonometamorphic processes, conditions and provenance [1] that may not necessarily be recorded by other commonly dated detrital minerals. Detrital garnets could therefore form a valuable and complimentary tool in detrital analysis of ancient tectonic processes and provenance. Here, we describe recent advances beyond previous attempts to date detrital garnets [2,3] and illuminate the current possibilities and limitations.

Two challenges must be overcome. First, is the sample size limitation which is solved through use of NdO^+ TIMS analysis with Ta_2O_5 activator [3,4]. This small sample capability provides an opportunity for geochronology on single >500 um grains or equivalent multi-grain separates. Second, a detrital garnet grain is no longer associated with the parent rock from which it crystallized. Thus there is no obvious second point to constrain an isochron. Here, detrital garnets may be crushed and treated with acids (including HF) to partially dissolve and analyze mineral inclusions which should in most cases adequately represent the original garnet host assemblage. But, well established methods for conventional garnet geochronology demonstrate that the garnet's inclusions often fall off the garnet-matrix isochron [5], and thus these inclusions are typically removed and discarded. Fortunately, in the detrital garnet application, the magnitude of the "age effect" related to the use of inclusions as the second point on the isochron (rather than the matrix) is small; generally less than a few million years which is an acceptable tolerance for most detrital geochronologic studies. Only if inherited zircons, which themselves can have high Sm/Nd ratios, represent a dominant part of the inclusion population could the detrital garnet age be skewed more significantly.

Test garnets extracted from New England (USA) sediments have been dated with this approach, yielding Acadian ages (as expected) with age uncertainty as low as ±4 Myrs on single grains as small as 3mg (or about 1.5mm diameter). $^{147}Sm/^{144}Nd$ ratios as high as 2.4 in cleansed garnet reflect success in separating inclusions from garnet via partial dissolution. Our data show a correlation with apparent isochron age and spread in $^{147}Sm/^{144}Nd$. The larger the spread between the two points in the isochron, the younger and more accurate the age. With our test samples, we have found that $^{147}Sm/^{144}Nd$ spread greater than 0.5 is necessary to produce accurate ages. Samples which yield less spread are too old, reflecting incomplete separation of garnet from inherited inclusions.

[1] Hutchinson AR & Oliver GJH 1998. J. Geol. Soc. Lond. 155, 541-550; [2] Oliver GJH et al. 2000. Geology, 28, 459-462; [3] Baxter EF et al. 2010. Goldschmidt; [4] Harvey J & Baxter EF 2009. Chem. Geol. 258, 251-257; [5] Pollington AD & Baxter EF 2011. Chem. Geol. 281, 270-282.

Hydrochemical and multiple isotopic approach to delineate the contamination of urban groundwater in Ulaanbaatar, Mongolia

BATSAIKHAN BAYARTUNGALAG[1*], SEONG-TAEK YUN[1], KYOUNG-HO KIM[1], BERNHARD MAYER[2], SANG-TAE KIM[3], BUYANKHISHIG NEMER[4], YOUNG-JOON LEE[5], AND EUN-SEON JANG[1]

[1]Korea University, Green School and the Department of Earth and Environmental Sciences, South Korea, bayartungalag@korea.ac.kr (* presenting author)
[2]University of Calgary, Geoscience, Canada
[3]McMaster University, Geography and Earth Sciences, Canada
[4]Mongolian University of Science and Technology, Hydrogeology and Environmental Geology, Mongolia
[5]Korea Environment Institute, South Korea

In Ulaanbaatar City (UB), Mongolia, significant population growth (currently, ~1.2 million) and rapid industrialization over the last two decades resulted in diverse environmental problems including a shortage and contamination of the water supply. Municipal water supply in UB depends on groundwater withdrawn from an alluvial aquifer located along the Tuul River. There are also many private wells completed in variable depths. Groundwater in UB has become increasingly polluted because of a deficient municipal sewer system, illegal waste dumping, air and soil pollution, and deforestation of surrounding areas. To our knowledge, there is no detailed survey that has assessed the status of groundwater quality in UB. Therefore, we have performed a hydrogeochemical survey including hydrochemical and multiple isotopic (i.e., $\delta^{13}C$ of dissolved inorganic carbon, $\delta^{15}N$ and $\delta^{18}O$ of nitrate, and $\delta^{34}S$ and $\delta^{18}O$ of sulfate) measurements on 45 groundwater, 4 surface water and 2 spring water samples collected in July 2011. The obtained data were interpreted in relation to land use patterns, which include the urban center, peripheral residential areas with dense traditional homes, grasslands, and forests.

Our results show the occurrence of three major hydrochemical types: 1) Ca-HCO_3 type, 2) Ca(-Na)-HCO_3-Cl(-NO_3) type, and 3) Ca-Na-HCO_3 type. The spatial distribution of different water types is controlled by land use. Types 1 and 3 occur under forest and grassland areas and are representative of unpolluted or less-contaminated groundwater. On the other hand, type 2 occurs predominantly in urbanized areas and shows progressive enrichments of groundwater with Cl+NO_3 (and NO_2)+SO_4 with increasing TDS, due to anthropogenic impact from latrines and domestic sewage. Nitrate contamination especially in the city center and peripheral residential areas is pervasive and severe resulting in NO_3^- concentrations of up to ~290 mg/L. The $\delta^{15}N$ and $\delta^{18}O$ values of nitrate suggest that in the city center and peripheral residential areas, latrines and domestic sewage are major sources of the severe nitrate contamination. Therefore, better management of latrines and sewage systems is urgently needed in UB. Our study also shows that groundwater contamination in UB is linked to the progressive population growth and city expansion.

Intensifying weathering and land-use in Iron Age Central Africa

GERMAIN BAYON[1]*, BERNARD DENNIELOU[1], JOËL ETOUBLEAU[1], EMMANUEL PONZEVERA[1], SAMUEL TOUCANNE[1], SYLVAIN BERMELL[1]

[1]IFREMER, Géosciences Marines, Plouzané, France
gbayon@ifremer.fr (* presenting author)

A major vegetation change occurred in Central Africa during the third millennium before present, when mature evergreen trees were abruptly replaced by savannas and secondary grasslands [1-3]. The consensus is that the forest disturbance was caused by a regional climate change [1-3]. However, this episode of forest clearance occurred contemporaneously with the migration of Bantu-speaking peoples from near the modern Nigeria-Cameroon border [4-7]. The so-called Bantu expansion led to diffusion of agriculture and iron smelting technology across Central Africa, with potential impacts on the environment [10]. Whether the Bantu farmers played an active role in the Central African deforestation event remains an open question.

Here we present major element (Al/K ratios) and radiogenic isotope (Nd, Hf) records from a marine sediment core recovered in the Gulf of Guinea, that permit the reconstruction of chemical weathering intensity in Central Africa for about the last 40,000 years. The data indicate a pulse of intensified weathering centered around 2,500 years ago, contemporaneous with the rainforest crisis. Evidence that this weathering event departs significantly from the long-term weathering fluctuations related to the Late Quaternary climate suggests that it was not triggered by natural climatic factors solely. Instead, we propose that the settlement of Bantu-speaking farmers in Central Africa at that time had a more pronounced environmental impact than initially thought.

[1] Vincens *et al.* (1999) *J. Biogeog.* **26**, 879-885. [2] Maley & Brenac (1998) *Rev. Palaeobot. Palynol.* **99**, 157-187. [3] Ngomanda *et al.* (2009) *Quat. Res.* **71**, 307-318. [4] Diamond & Bellwood (2003) *Science* **300**, 597-603. [5] Huffman (1982) *A. Rev. Anthropol.* **11**, 133–150. [6] Vansisa (1984) *J. Afr. Hist.* **25**, 129–145. [7] Holden (2002) *Proc. R. Soc. Lond. B* **269**, 793-799. [10] Willis *et al.* (2004) *Science* **304**, 402-403.

Rock micro-structure controls regolith thickness

E. BAZILEVSKAYA[1]*, M. LEBEDEVA[1], G. ROTHER[2], M. PAVICH[3], D. PARKINSON[4], D. COLE[5] AND S.L. BRANTLEY[1]

[1]The Pennsylvania State University, University Park, PA 16802 USA (*correspondence: eab204@psu.edu)
[2]Oak Ridge National Laboratory, Oak Ridge, TN 37831 USA
[3]U.S. Geological Survey, Reston, VA 20192 USA
[4] Lawrence Berkeley National Laboratory, Berkeley, CA 94720, USA
[5] School of Earth Science, Ohio State University, Columbus, Ohio, 43219

As feldspar transforms to clay, a zone of residual weathered material, regolith, forms on ridges of diabase and granite in the Piedmont Province, Virginia. In spite of similar erosion rates and the fact that Ca-rich plagioclase in diabase is expected to dissolve 10x faster, weathering has advanced 20x deeper into the granite compared to the diabase. This result runs counter to conventional wisdom that would predict a deeper weathering profile on the diabase. We explained this enigma by studying the nano- to micro-structural features of these two rocks in plagioclase reaction zone. Nano-pores (1 nm < d < ~5 μm) and micro-pores (> 3 μm) were studied by neutron scattering (NS) and micro-computed tomography (μ-CT), respectively. We found that granite has a larger connected micron-sized pore network than diabase as well as abundant micro-fractures around oxidizing biotite. In contrast, the plagioclase reaction zone in diabase has some regions of low porosity due to smectite and calcite precipitation. Therefore, we concluded that the regolith is 20x thinner on diabase because it supports only minimal fluid advection, while advective transport in granite is significant.

We explored this hypothesis with numerical modelling of plagioclase dissolution in diabase and granite. For diabase, the diffusion-only model yields shallow regolith with a thin reaction front -- as observed in the field. However, we could not model a deeper and thicker reaction front in granite with diffusion only. With advection in the numerical model, the reaction front in granite is wide and the regolith is deep, as observed.

Our results show that the difference in regolith thicknesses in the Piedmont is largely explained by different regimes of reactive fluid transport. Minimal advection creates shallow regolith and a thin reaction front in the more massive diabase. In contrast, significant advection occurred in the relatively fractured granite, producing deep regolith and a thick reaction front. At the grain-scale, infiltration of advecting fluid is controlled by texture (e.g., grain size distribution, porosity) and reaction-induced permeability. The parent lithology is an important factor in this latter permeability because oxidation of biotite at depth apparently accelerated pervasive fluid infiltration into the granite. If micro-structure is important in controlling the factor of 20x, then it is possible that felsic rocks such as granites generally develop thicker regolith profiles than diabase, regardless of age or location, under comparable geomorphological regimes. Such observations may help predict and explain regolith thickness in localities in many places around the globe.

.

Identifying Key Controls on the Behavior of an Acidic-U(VI) Plume at the Savannah River Site using Reactive Transport Modeling

S.A. BEA[1*], H. WAINWRIGHT[1], N. SPYCHER[1], S. HUBBARD[1], AND J. DAVIS[1]

[1]Lawrence Berkeley National Lab., Berkeley, CA, 94720 USA, sabea@lbl.gov (*presenting author)

Acidic waste solutions containing low level radioactivity from numerous isotopes were discharged to a series of unlined seepage basins at the F-Area of the Savannah River Site, South Carolina, from 1955 through 1989. Although the site has gone through many years of active remediation, the groundwater remains acidic, and the concentrations of U(VI) and other radionuclides are still significant. Monitored Natural Attenuation (MNA) is a desired closure strategy for the site, based on the premise that clean background groundwater will eventually neutralize the groundwater acidity, causing an increase in pH and driving natural immobilization of U(VI) through sorption. The development of the understanding of the long-term pH and U(VI) sorption behavior at the site is critical to assess MNA and in-situ treatment over the long term.

We use reactive transport (RT) models and uncertainty quantification (UQ) to explore key controls on the U(VI)-plume evolution and long-term mobility at this site through considering U(VI) adsorption by sediments and key hydrodynamic processes. Two-dimensional RT simulations through the saturated and vadose zones were conducted by considering the dissolution and precipitation of Al and Fe minerals, as well as H^+ and U(VI) surface complexation. Simulations indicate that mineral dissolution and precipitation together with sorption reactions on goethite and kaolinite (primary minerals present with quartz) could buffer pH at the site for long periods of time.

UQ techniques were applied with RT modeling in order to: (1) identify the complex physical and geochemical processes that control the migration of the acidic-U(VI) plume in the pH range where it is highly mobile, (2) evaluate those physical and geochemical parameters that are most controlling, and 3) attempt to predict the future plume evolution constrained by historical chemical and hydrological data. UQ-RT results show that model results are most sensitive to the reactive surface area available for sorption, discharge rates, the relative rates of H^+ influx and kaolinite dissolution. The plume behaviour also appears to be sensitive to parameters controlling the amount of residual U(VI) in the vadose zone, which acts as a buffering zone in the modeled system.

Iron isotope fractionation during femtosecond laser ablation of magnetite determined by aerosol size sorting experiments

BRIAN L. BEARD[1,2*], ANDREW D. CZAJA[1,2], WEIQIANG LI[1,2], JAMES J. SCHAUER[3], MICHAEL OLSON[3], CLARK M. JOHNSON[1,2]

[1]Univ. Wisconsin, Dept. of Geoscicence, Madison WI, USA beardb@geology.wisc.edu (* presenting author)

[2]NASA Astrobiology Institute

[3] Univ. Wisconsin, Dept. of Civil and Environmental Engineering, Madison WI, USA, jjschauer@wisc.edu

Aerosol particles generated from femtosecond laser ablation (fs-LA; 198nm laser manufactured by Photon Machines) of natural magnetite were size sorted using a Micro-Orifice Uniform-Deposit Impactor (MOUDI). The MOUDI separates particles by size based on aerodynamic properites using 10 stages. Aerosols were collected using fluences of 1, 2, and 4 J/cm^2 and there is a positive correlation between total Fe collected per laser shot; 25, 50, and 100 picograms of Fe per laser shot were harvested from the impactor, respectively. The aerosol size distribution of the fs-LA generated particles were determined by analyzing Fe concentration for each stage of the impactor using ^{57}Fe isotope dilition mass spectrometry (~10^5 laser shots) or spectroscopically via the ferrozine technique (~10^6 laser shots). The size distribution of aerosol particles done at different fluences are the same; all are unimodal with a peak at an aerodynamic size between 180 to 320 nm.

Sized aerosol particles have been analyzed for their Fe isotope composition. The smallest sized particles have δ^{56}Fe values that are less than the magnetite substrate by 0.5‰, whereas larger sized particles (≥180–320 nm stage) have δ^{56}Fe values that were up to +0.7‰ greater than the magnetite substrate. There are no differences in isotope compositions as a function of fluence. In all experiments, the integrated Fe isotope composition of all the stages matches that of the magnetite substrate. This isotopic mass balance highlights that although the process of fs-LA produces Fe isotope fractionation, if the generated aerosol is quantitatively delivered and ionized, one can obtain accurate Fe isotope measurements. Indeed, for sample-standard comparisons, accuracy of Fe isotope compositions will hinge on having similar transport efficiencies spatially in the ablation cell. For example, if 12% of the particles ≥ 180–320 nm in aerodynamic size are not transported to the ICP source, and these particles consist of 70% of the total Fe mass with δ^{56}Fe values that are 0.7‰ greater than the bulk substrate, the measured Fe isotope composition would be inaccurate by -0.1‰. This can easily be monitored, however, by comparing Fe yields derived by total ion signal. Using the above example, there would be a ~9% decrease in the total Fe ion signal.

The correlation between Fe isotope composition and particle size may result from condensation wherein the first condensed particles from fs-LA generated vapor have low δ^{56}Fe values. As condensation continued and some particles coarsened, they inherited higher δ^{56}Fe values from the isotopically heavy vapor.

Clay-rock alteration experiments at 80°C in closed and open conditions: application to the waste storage

CATHERINE BEAUCAIRE[1*], EMMANUEL TERTRE[2], ERIC FERRAGE[2], BERNARD GRENUT[1], STEPHANE PRONIER[2] AND BENOIT MADÉ[3]

[1]CEA, DEN/DANS/DPC/SECR/L3MR, Gif-sur-Yvette, France, catherine.beaucaire@cea.fr

[2]Université de Poitiers-CNRS, IC2MP UMR 7285, Poitiers, France, emmanuel.tertre@univ-poitiers.fr

[3]ANDRA, Chatenay-Malabry, France, benoit.made@andra.fr

In the framework of radioactive waste storage in geological formations, many investigations were carried out to characterize chemical properties of pore water at the field temperature (*e.g.*, 20°C). However, few studies were devoted to the modifications that temperature could induce on the chemical composition of pore water in the host-rock. Among the chemical parameters which are sensitive to temperature, the pH and $CO_{2(g)}$ partial pressure (*i.e.*, $p_{CO2(g)}$) are likely the most sensitive. These latter parameters could also strongly impact the mobility of radionuclides in geosphere. Under thermal gradient, many reactions would occur such as minerals dissolution-recrystallisation or organic matter degradation. The knowledge of geothermal systems in sedimentary contexts tends to prove that whatever the mineral or/and organic contribution, $p_{CO2(g)}$ is likely constrained by a mineralogical buffer combining carbonate mineral (calcite, dolomite), quartz or chalcedony and alumina-silicate phases (kaolinite, illite or Mg-chlorite) [1]. Hydrothermal alteration experiments were carried out with Callovo-Oxfordian clay-rock with the aim of characterizing the ultimate step of thermal alteration at 80°C, which is the temperature expected in the waste storage.

The experiments were performed in both open and closed systems where initial $p_{CO2(g)}$ values were fixed (*e.g.*, $p_{CO2(g)}$=0.4 atm.). High solid/solution ratios (1 to 3 kg/L) are chosen in order to favour neoformation of secondary mineral phases. Aqueous and gas phases were regularly extracted at temperature and fully analyzed. The evolution of clay mineralogy was also characterized using X-ray diffraction profile modeling of experimental patterns and Transmission Electron Microscopy. Then, results obtained for solution as well as for solids were interpreted and discussed in term of thermodynamic equilibrium achievement.

After 15 months of alteration in closed conditions at 80°C, the $p_{CO2(g)}$ is stabilized at 1 atm. and final solution is equilibrated with respect to quartz, kaolinite, calcite and ordered-dolomite. Modeling of experimental X-ray diffraction patterns [2] evidenced a slight increase of the illitic layers content in mixed-layer minerals (*i.e.*, 5%). However, it is not possible to conclude to illite neoformation. Consequently, in absence of equilibrium with a secondary Al-Si mineral phase which would participate to the complete mineralogical buffer, the constrain on $CO_{2(g)}$ is not evidenced in these experimental conditions. Other experiments devoted for determining reaction pathways are currently in progress.

[1] Coudrain-Ribstein, Gouze & De Marsily (1998) *Chem. Geol.,* **145**, *73-89*. [2] Ferrage, Vidal, Mosser-Rück, Cathelineau & Cuadros (2011) *Am. Min.* **96,** 207-223.

Can submarine groundwater discharge balance the oceanic strontium isotope budget?

AARON J. BECK[1*], MATTHEW A. CHARETTE[2], J. KIRK COCHRAN[3], MEAGAN E. GONNEEA[2] AND BERNHARD PEUCKER-EHRENBRINK[2]

[1]Virginia Institute of Marine Science, College of William & Mary, Gloucester Point, VA, USA
abeck@vims.edu (* presenting author)

[2]Department of Marine Chemistry and Geochemistry, Woods Hole Oceanographic Institution, Woods Hole, MA, USA
mcharette@whoi.edu
mgonneea@whoi.edu
bpeucker@whoi.edu

[3]School of Marine and Atmospheric Sciences, Stony Brook University, Stony Brook, NY, USA
kcochran@notes.cc.sunysb.edu

It is not clear if the strontium (Sr) isotope budget of the modern ocean is at steady state [1]. It has been hypothesized that submarine groundwater discharge (SGD) is an important Sr source to the ocean [2], but few data exist for Sr in coastal groundwater or in the geochemically-dynamic subterranean estuary (STE). We examined Sr concentrations and isotope ratios from 9 globally-distributed coastal sites, and examined the behavior of Sr in the STE.

Dissolved Sr generally exhibited conservative mixing behavior in the STE, although large differences were observed in the meteoric groundwater endmember among sites (0.1 – 24 μM Sr). Differences in groundwater Sr concentrations and isotope ratios ($^{87/86}Sr$ = 0.707-0.710) reflected aquifer lithology characteristics. In part, because groundwater Sr concentrations are orders of magnitude higher in less-radiogenic carbonate and volcanic island aquifers, the SGD endmember Sr ratio must be lower than modern seawater (i.e., less than 0.70916). A simple lithological model was used to estimate a global average groundwater endmember of 2.9 μM Sr with $^{87/86}Sr$ = 0.7089, representing a meteoric-SGD-driven Sr input to the ocean of 0.7-2.8 × 10^{10} mol Sr a^{-1}. Meteoric SGD therefore accounts for 2-8% of the oceanic Sr isotope budget, comparable to other known source terms, but insufficient to balance the remaining budget.

Sr isotope exchange was observed in the STE at five of the sites studied, invariably favored the meteoric groundwater endmember signature, and reached up to 40% exchange at salinity 10. Using reported estimates for brackish SGD, the estimated volume discharge at salinity 10 (7-11 × 10^{15} L a^{-1}) was used to evaluate the impact of isotope exchange in the STE on the brackish SGD Sr flux. A moderate estimate of 25% isotope exchange in the STE gives a resultant SGD Sr endmember isotope composition of 0.7091. The brackish SGD Sr flux accounts for 12-25% of the marine Sr isotope budget, and does not appear sufficient to balance some 40% of the remainder.

Substantial uncertainties remain for estimating the SGD source of Sr to the global ocean, such as the volume flux of meteoric SGD, and lacking measurements of groundwater Sr isotope composition in major SGD regions such as Papua New Guinea, the South America west coast, and West Africa. Nevertheless, the combined sources of meteoric SGD and isotope exchange in the STE are a major component of the modern oceanic Sr isotope budget, and represent a Sr source to the ocean that may have contributed to documented fluctuations in the oceanic $^{87/86}Sr$ ratio over geologic time.

[1] Davis *et al.* (2003) *EPSL* **211**, 173-187.
[2] Allègre *et al.* (2010) *EPSL* **292**, 51-56.

Primary origin *vs.* redistribution of trace elements by fluid flow in slope facies Ediacaran carbonate rocks from the Yangtze Platform (South China)

HARRY BECKER[1*], WIEBKE BAERO[1], MANUEL QUIRING[1], KONRAD HAMMERSCHMIDT[1], UWE WIECHERT[1] AND DOROTHEE HIPPLER[2]

[1]Freie Universitaet Berlin, Institut fuer Geologische Wissenschaften, Germany, hbecker@zedat.fu-berlin.de (* presenting author)

[2]Technische Universitaet Berlin, Institut fuer Angewandte Geowissenschaften, Germany

A major problem for the interpretation of the composition of ancient marine carbonates is the variable response of different elements to diagenesis and post-depositional fluid flow. We have studied this issue in Ediacaran dolostones, limestones and marlstones from members D1, D3 and D4 of the Doushantuo Formation (635-551 Ma) from the slope facies Panmen section (Songtao, Guizhou) on the Yangtze Platform. The carbonate rocks display a strong, but variable influence of secondary processes as indicated by $\delta^{18}O$ (-5 to -14) and $^{87}Sr/^{86}Sr$ (0.723 to 0.710) data in comparison to data of stratigraphically correlated samples from shallow platform settings [1]. Decreasing $^{87}Sr/^{86}Sr$ from bottom to top of the section and very low abundances of feldspar, illite and chlorite in some of these samples suggest that the radiogenic Sr in the carbonates was not introduced by closed-system diagenetic redistribution from silicates within the rock, but by open-system fluid flow and associated recrystallization of carbonates. In the D3 member, the overprint by fluid flow is indicated by a weak correlation of $\delta^{18}O$ with $^{87}Sr/^{86}Sr$ and correlation of $\delta^{18}O$ with $\delta^{13}C_{carb}$. Modeling of fluid-rock interaction shows that high and variable Sr abundances in water rich fluids (low-C/O) are consistent with the data trends in the D3 member, and may account for 1 to 2 ‰ of the variation in $\delta^{13}C_{carb}$. In spite of these secondary modifications, some carbonate rocks at different positions in the section display seawater signals in their acetic acid leachates, such as high Y/Ho and positive or negative Ce anomalies. Relatively high abundances of Th, REE and Pb in the acetic acid leachates and correlations of Th with Fe abundances, suggest that these elements were redistributed by fluid flow. They may have been originally hosted in Fe oxyhydroxide phases in the rock, released upon reduction and dissolution of Fe phases and incorporated into recrystallized carbonates. Further constraints were obtained from leaching experiments on cap dolostones of the section using stepwise digestion in 10% HAc, 6 M HCl and conc. HF-HNO_3. These results indicate the presence of HCl soluble Fe rich phases, presumably oxides or oxyhydroxides. The REE patterns of the HCl fraction are bell shaped and differ considerably from the patterns of acetic acid leachates. The data suggest that in many samples, fluid mobile elements, but also REE, Th and Fe have been redistributed into recrystallized carbonates. This is raising questions about the scale of postdepositional element redistribution in such sections.

[1] Sawaki *et al.* (2010) *Precambrian Research* **176**, 46-64.

Quantum-mechanical calculations on actinide sorption and reduction of sulfides and oxides

U. BECKER[1]* AND D. RENOCK[2]

[1] Dept. of Earth and Environmental Sciences, University of Michigan, Ann Arbor, MI., USA, ubecker@umich.edu (* presenting author)

[2] Dept. of Earth Sciences, Dartmouth College, Hanover, NH., USA, Devon.J.Renock@Dartmouth.edu

The results of several recent studies are challenging the way actinide geochemists consider redox processes in the near surface environment. Such studies include: the complex chemistry of electron and spin transitions between $U^{6+} \leftrightarrow U^{5+} \leftrightarrow U^{4+}$ aqueous complexes and solids, spatially separated redox processes linked over millimeter distances by complex networks of bacterial nanowires combined with pyrite, simultaneous oxidative growth and reductive dissolution on a single hematite crystal driven by potential differences between crystal faces, sulfide oxidation mechanisms that are rate-limited by the transition from high spin O_2 to low spin O.

In order to shed light on the electron transfer between reductants (*e.g.*, hydrogen sulfides, Fe^{2+}, hydroquinones as an organic/microbial analogue), oxidants (different actinyl complexes), catalytic mineral surfaces (periodic slabs and nano-clusters of hematite, pyrite, and mackinawite, and galena), and polarizing anions (*e.g.*, carbonate, sulfate).

An example calculation is the co-adsorption of a uranyl cation and a hydroquinone on the opposite sides of a pyrite nano-cube. The interaction of the hydroquinone with the uranyl complex through the pyrite nanoparticle can be quantified/visualized in different ways: (i) by the synergistic energy of the co-adsorption of uranyl and hydroquinone on pyrite, (ii) by the amount of electron transfer to the uranyl, and (iii) by visualization of the charge distribution in different adsorbate configurations.

During the co-adsorption/reduction process, the hydroquinone becomes positive (sum of Mulliken charges = 1.12) and the uranyl with an initial charge of +2 becomes almost neutral (+0.08), indicating electron transfer of about two elemental charges towards the uranyl. This is an indication that a neutral UO_2 unit is formed, which can serve as a nucleus of UO_2 formation. In contrast, if no hydroquinone is present, only about half an elemental charge is transferred from the pyrite nanoparticle. This is an example how the hydroquinone can be used as an analogue for electron shuttling by metal-reducing bacteria through the pyrite towards the uranyl.

Another example is the co-adsorption of hydroquinone and uranyl on a mackinawite nanoparticle. While the π orbitals of the quinone interact with the postitive Fe cations, the uranyl-O comes within bond distance with the Fe on the right. Electrons can be transferred within the same orbital of the entire system (e.g, the HOMO stretches over the entire system). Interestingly, even though mackinawite is a low-spin system as a bulk mineral, the co-attack by quinone and uranyl spin-polarizes the Fe atoms along the path in a down-up-up-down pattern. This is kinetically important to accommodate the spin transition on the right from U^{6+} (no spin) to U^{4+} (two unpaired spins).

Archaean cratonic mobilism and growth on a subductionless, stagnant lid Earth

BÉDARD, J.H.[1*], Harris, L.B.[2], THURSTON, P.[3]

[1]Geological Survey of Canada, Québec, Canada, jbedard@nrcan.gc.ca (*presenting author)

[2]Institut national de la recherche scientifique, Québec, Canada

[3]Laurentian University, Sudbury, Canada

Igneous rocks with geochemical signatures similar to those of Phanerozoic continental or oceanic arcs are rare in the Archaean and proposed Archaean ophiolites, Atlantic-style passive margins, overprinting thrust and fold belts, blueschists, ultra high-pressure rocks, paired metamorphic belts, orogenic andesites, and subduction-zone mélanges that typify Phanerozoic orogens are rare to absent. The archetypal Archaean granite-greenstone dome-and-keel architecture has no modern analogue. Most Archaean lavas have geochemical signatures that imply evolution by assimilation-fractional crystallization, rather than the source-metasomatic signatures of Phanerozoic arcs; and trace element models imply that the felsic contaminants were generated by anatexis of typical Archaean tholeiites. Mass balance calculations imply that melting of subducted crust or fractionation of basalt cannot generate requisite volumes of TTG in the available time, and a basal/delaminated oceanic plateau melting model is preferred.

Despite the absence of evidence for Archaean subduction, many Archaean cratons have shortening fabrics and cratons contain terranes with contrasting histories that were somehow assembled. What could be a plausible driving force for compression and terrane accretion on a subductionless Earth? Cratonic mobilism in response to mantle convection currents offers a possible solution to this paradox. Once a proto-craton develops a stiff mantle keel, it would become subject to pressure from mantle currents and would drift. Immature cratons or oceanic plateaux lack deep keels and so would be static. So, contrary to conventional wisdom, we consider that Archaean cratons are not immobile nucleii along whose margins 'mobile belts' form by subduction-zone accretion. Instead, we propose that Archaean cratons were active tectonic agents, accreting basaltic plateaux, other proto-cratons, and heterogeneous mantle domains as they migrated. Overridden oceanic plateau lithosphere would form subcretion complexes where the underthrust basalt would melt to generate syntectonic pulses of tonalite-trondhjemite-granodiorite (TTG), so contributing to craton growth and stabilisation. Garnet pyroxenite restites from anatexis would founder into the mantle and trigger new pulses of tholeiitic magmatism. The non-cratonic Earth would have been covered by a mosaic of shield volcanoes, with eruption and basal attrition being in a quasi steady-state in a stagnant lid régime, suggesting that mantle convection may have been layered in the Archaean.

The Neoproterozoic Franklin Large Igneous Province, geochemical and isotopic evidence for changing sources, and linkages between intrusive and extrusive components

BÉDARD, J.H.[1*], DELL'ORO, T.[2], WEIS, D.[2], SCOATES, J.S.[2], WILLIAMSON, N.[3], COUSENS, B.[3], NASLUND, H.R.[4], HAYES, B.[5], HRYCIUK, M.[6], WING, B.[6], BEARD, C.[2,7]

[1]Geol. Survey of Canada, Québec, Canada, jbedard@nrcan.gc.ca (* presenting author)

[2]PCIGR University of British Columbia, Vancouver, Canada

[3]Carleton University, Ottawa, Canada

[4]SUNY Binghamton, USA

[5]Cardiff University, UK

[6]McGill University, Montreal, Canada

[7]University of Bristol, UK

The Neoproterozoic (ca.716 Ma) Franklin Large Igneous Province formed during the breakup of Rodinia. The Natkusiak continental flood basalts (≤1 km thick, preserved as 2 lobes in a syncline) are the extrusive phase of the Franklin event, and erupted onto a shallow-water continental platform. An underlying fluvial sandstone, the Kuujjua Fm., pinches out towards the NE, suggesting pre-eruptive thermal doming, possibly associated with arrival of a mantle plume. The lowermost extrusive unit (ca 50-100 m thick) is a primitive basalt (7-11 wt% MgO), and is tentatively interpreted as agglutinate (welded fire fountain deposits) erupted from multiple vents. The unit is characterized by LREE-LILE-enrichment, high L/HREE, high $^{87/86}Sr_i$ (up to 0.70791), intermediate εNd (4.0-8.1) and εHf (0.03-6.7), high $^{208/204}Pb$ (up to 39.136), high $^{207/204}Pb$ (up to 15.686), and high $^{206/204}Pb$ (up to18.978) ratios; indicating either an enriched source, extensive crustal contamination, or influx of enriched fluids from the footwall. A hiatus in eruptive activity is marked by deposition of red-weathering volcaniclastic rocks that contain matrix-supported conglomerates (lahars or damburst deposits?) that fill palaeovalleys. Two differentiation cycles of laterally extensive basaltic (10-6% MgO) sheet flows were then deposited above the basal lavas and volcaniclastics. Both cycles show upward shifts in phenocryst populations, decreases in Mg#, Cr and Ni, and increases in incompatible element concentrations, consistent with up-section fractional crystallization. Only cycle 1 sheet flow basalts are exposed in the SW. These have higher εNd (7.7-9.6), lower $^{87/86}Sr_i$ (0.70251-0.70605), higher εHf (4.1-9.7), lower $^{208/204}Pb$ (36.196-37.623), lower $^{206/204}Pb$ (16.147-17. 787), and lower $^{207/204}Pb$ (15.383-15.605) than basal basalts. The cycle 1 sheet flow basalts in the NE have trace element and isotopic trends that differ from those in the SW (c.150km separation), indicating regional-scale isotopic heterogeneity in the source and/or contaminants of these lavas. Alternatively, isotopic heterogeneities may have been enhanced during ascent through the crust in a compartmentalized feeder system.

The plumbing system that fed the lavas is dominated by sills, with localized fault-guided dykes. Two magma populations have been identified: Younger diabasic sills with trace element signatures matching the sheet flow lavas, and older sills (based on cross-cutting relationships), commonly with olivine-enriched bases, that match the basal basalts. Field, geochemical and isotopic evidence imply that steep, dyke-like feeders were sites of preferential wall rock assimilation and allowed melt to ascend between sills. On the scale of the entire magmatic system, the secular decrease in incompatible trace element concentrations, L/HREE ratios, and radiogenic isotope signatures could be interpreted as a decrease in the degree of host contamination with time. Changing magma composition could also reflect a shift from a fertile mantle source to a less enriched source, possibly associated with upwelling of asthenospheric mantle during the separation of Siberia from Laurentia.

Reference materials mapping: spatial geochemical heterogeneity characterization

L.PAUL BÉDARD[1*], GABRIELLE ROCHEFORT[2], ALEXANDRE NÉRON[3], AND KIM H. ESBENSEN[4]

[1]Sciences de la Terre, Université du Québec à Chicoutimi, Chicoutimi, QC, Canada PBedard@uqac.ca (* presenting author)

[2]Sciences de la Terre, Université du Québec à Chicoutimi, Chicoutimi, QC, Canada gabrielle.rochefort@uqac.ca

[3]Sciences de la Terre, Université du Québec à Chicoutimi, Chicoutimi, QC, Canada alexandre.neron@uqac.ca

[4]Geological Survey of Denmark and Greenland, Copenhagen, Denmark, ke@geus.dk

Reference materials (RM) are mandatory to produce high quality analytical results, and therefore must be well characterized with respect to heterogeneity. Microbeam techniques use very small sample masses, which can make representativity a difficult goal to achieve. Characterization of RM has mainly been done by computing statistics on numerous replicate determinations (microbeam and bulk samples; mg to g). Such studies do not take into account the systematic spatial relationships between determinations and may hence not necesarily arrive at a representative heterogeneity estimate. In the case of glasses (NIST-600s, GSD-1, etc.) and some pressed pellets (MASS-1, MACS-1 and MASS-3), anomalous "hot pots" can sometimes be larger than beam size, and can be clustered or segregated along a spatial trend. Such information is critical to determine optimal beam size or for locating optimal transects for calibration. Improved heterogeneity characterisations will lead to improved constraints on precision and accuracy of RM in general and specifically for microbeam RM.

A set of systematic experiments has been carried out to map RM with LA-ICP-MS and microXRF, to determine concentration variations in the widest possible field of view regimen. The first step is instrumental optimization of mapping to control instrumental drift. MicroXRF mapping of pulverized RM (precious metal bearing: WMS-1, CHR-Pt+, MASS-1 and MASS-3) were used to delineate precious metals nuggets, which are indeed present in many instances. This has been used to demonstrate that large sample masses are often necessary for many sulfide RM. Precipitated materials (such as MASS-1) are devoid of nuggets while most powdered RM showed nuggets. LA-ICP-MS mapping of glasses typically used to calibrate analysis, e.g. NIST-600 series, also show heterogeneities, especially for precious metals. Elemental maps have been computed to show visually heterogeneities and their locations. Variographic analysis has been undertaken to visualize variability as a function of the spatial scales.

Spatial information is an important contribution in characterizing many RM (glass and powders). Such information was previously difficult or expensive to acquire. Now spatially resolved geochemical data for RM are rapidly becomming easily accessible; this type of characterisation is the next step in RM characterization.

Volatile transfer from magma sources in the Taupo Volcanic Zone

FLORENCE BÉGUÉ[1], CHAD DEERING[2*], DARREN GRAVLEY[1], BEN KENNEDY[1] AND ISABELLE CHAMBEFORT[3]

[1]University of Canterbury, Christchurch, New Zealand, florence.begue@pg.canterbury.ac.nz darren.gravley@canterbury.ac.nz ben.kennedy@canterbury.ac.nz

[2]University of Wisconsin-Oshkosh, Oshkosh, USA, deeringc@uwosh.edu (* presenting author)

[3]GNS Sciences, Wairakei Research Centre, Taupo, New Zealand, i.chambefort@gns.cri.nz

The Taupo Volcanic Zone (TVZ) is a rifted arc where dominantly silicic magmatism and volcanism has evolved intimately with tectonic. Two distinct rhyolite magma types (dry-reducing and wet-oxidizing) have erupted from the central TVZ over the past ~550kyrs [1]. We measured major, trace, and volatile element concentrations (including B isotopes) in quartz-hosted melt inclusions from several large, rhyolitic eruptions representing these distinct types in an effort to: 1) determine if the magma was vapour saturated, and 2) identify disparities in the volatile contributions to the overlying hydrothermal systems. Dry magma in the upper crust may not be volatile saturated and, therefore, would contribute very little to the overlying hydrothermal system.

Melt inclusions from the dry type Ohakuri and Mamaku eruptions (~240 ka) have high chlorine values ranging from 0.25 to 0.36wt%, and show a positive correlation between chlorine, fluorine, Rb/Sr ratio and other incompatible elements, suggesting that no vapour phase was exsolved prior to eruption. In comparison, volatile data from the wet type Kaharoa eruption (~1314AD) show vapour saturation and exsolution of a volatile phase during crystallisation [2].

The combination of boron and boron isotopes is an effective tracer of the volatile contribution from slab-derived fluids. Measured B and $\delta^{11}B$ in these two different types of systems, reveal distinct signatures. The isotopic composition of the Kaharoa is homogeneous, with $\delta^{11}B$ of + 4‰, and boron contents range from 20-30 ppm. Because the Kaharoa was saturated, the boron preferentially partitions into the fluid phase ($D_B^{fluid/melt} >> 1$), which requires that a much higher bulk content of boron existed prior to eruption. The Mamaku and Ohakuri melts, on the other hand, have homogeneous boron contents around 15 ppm, but isotopic ratios ranging from – 3 to + 3‰. These two different signatures can be linked to variable contributions of fluid from the subducting slab, and we attribute this to a decrease in slab-derived fluid flux across the TVZ.

Geochemical heterogeneities and the generation of wet vs. dry rhyolites in the TVZ can be directly linked to the input of slab-derived fluids. As such, boron could potentially be a very useful tracer for volatile transfer processes where magmas are saturated. Our methodology can determine if a magmatic system is volatile saturated, and hence, could help identify areas in the upper crust where there is a maximum potential for heat transfer to the overlying geothermal system.

[1] Deering (2008*) Journal of Petrology* **49**, 2245-2276. [2] Johnson (2011) *Geology* **39**, 311-314.

Great Oxidation Event: How quickly did it come and go?

A. BEKKER[1*], N. PLANAVSKY[2], C. SCOTT[3], C. PARTIN[1], B. RASMUSSEN[4]

[1]Department of Geological Sciences, University of Manitoba, Winnipeg, MB, R3T 2N2 Canada, bekker@cc.umanitoba.ca (* presenting author)

[2]Department of Earth Sciences, University of California, Riverside, CA 92521, USA, planavsky@gmail.com

[3]Department of Earth and Planetary Sciences, McGill University, Montreal, Canada, clinton.scott@mcgill.ca

[4]Department of Applied Geology, Curtin University, Kent Street, Bentley WA 6102, Australia, B.Rasmussen@curtin.edu.au

The loss of mass-independent fractionation of sulfur isotopes (MIF-S) defining the first appearance of oxygen in the atmosphere as a stable component, the so-called Great Oxidation Event (GOE), has been recently constrained between ~2.4 and 2.32 Ga. However, the texture of the pO_2 secular changes in the Late Archean to the Paleoproterozoic remains controversial and highly debated. Some authors favor a gradual rise in atmospheric oxygen starting at ca. 2.7 or 2.5 Ga and a peak at 2.1-2.0 Ga at the end of the Lomagundi positive carbon isotope excursion in seawater composition. Combining geological and geochemical constraints, we will discuss the history of atmospheric and oceanic redox conditions in the early Paleoproterozoic.

Detrital pyrite and uraninite in shallow-marine and terrestrial deposits persists until the loss of MIF-S at ca. 2.32 Ga, when sulfate evaporites first appear in the shallow-water marine record. This change indicates a rapid increase in the seawater sulfate content, at least 10 fold, to >>2 millimole level, associated with oxidation of the atmosphere-ocean system. Consistent with this rapid change, concentrations of redox-sensitive elements (e.g., Mo, Re, and U) in the ca. 2.32 Ga and younger GOE black shales are dramatically higher from those in the pre-GOE black shales. Although surface oxidation likely continued during the Lomagundi excursion, which was tied to high burial rates of organic carbon and high flux of oxygen to surface environments, evidence for this progressive rise is currently unrecognized, with the potential exception of the concentration of redox-sensitive elements in black shales.

The end of the Lomagundi excursion is associated with a sharp collapse in the surface oxidation state as reflected by an abrupt fall in seawater sulfate content, disappearance of sulfate evaporites from the rock record, and drop in concentrations of redox-sensitive elements in black shales. The surface oxidation state returned to the intermediate state between those before and during the GOE. In association with this collapse, methane flux from the ocean to the atmopshere and atmospheric methane concentrations increased, contributing to climatic stability during the Boring Billion. The end of the Lomagundi excursion at ca. 2.1-2.0 Ga and associated negative excursion in carbon isotope values of organic carbon in shales, the so-called Francevillian Event, thus reflects the collapse rather than a peak in the oxidation state of the atmosphere-ocean system.

Land use changes and mercury transfers to aquatic systems in the Brazilian Amazon

Bélanger[1*], Emilie; Lucotte[1], Marc; Oestreicher[1], Jordan; Moingt[1], Matthieu; Rozon, Christine[1]; Davidson[1,2], Robert; Grégoire[1], Benjamin,.

[1]Université du Québec à Montréal, GEOTOP
emilie.belan@gmail.com

[2]Biodôme de Montréal, Canada
robertdavids@gmail.com

In the Tapajos River region of the Brazilian Amazon, mercury (Hg) contamination has become a problem to human health trough fish consumption. Hg present in the water system rises into the trophic chain and affects riparian communities. Studies have shown that recent deforestation contributes to soil mercury release trough terrigenous organic matter fluxes to the aquatic environment. Changes in sedimentation patterns have also been observed, suggesting a large-scale modification of the natural organic matter dynamics in the drainage basins. Local small-scale farmers use slash-and-burn agricultural practices, which consist in slashing and burning a patch of forest to benefit from the soil fertility enrichment caused by fire. After one or two years, soil fertility drops and another patch is slashed and burned. This dynamics creates a mosaic of different land uses: agricultural lands, pastures, secondary forest fallows and forested areas. The aim of this study was to investigate the movements of organic matter and its associated Hg in the watershed and to relate it to land use characteristics. Three watersheds were characterized by geographical system analysis and sampled for vegetation (20 species), soils (33 cores), suspended particulate matter (6 stations) and sediment cores (3, one in each aquatic system). All samples were analyzed for total Hg, lignin biomarkers, C, N and Pb^{210} datation was performed on sediment cores. TOM signatures were elaborated for the different land uses and followed from the terrestrial environments to the aquatic systems. Our results show an increase of TOM and mercury concentrations in recent sediments, with maximum values ranging up to 310 ng/g, concomitant to land use changes and altered watershed characteristics. These findings on the newly colonized watersheds of the Amazon can help to establish the dynamic portrait of Hg movements, leading to the development of conservation measures adapted to this environment.

Influence of afforestation on soil : The case of mineral weathering

NICOLAS BÉLANGER[1*], BENOIT LAFLEUR[2], YVES CLAVEAU[2] AND DAVID PARÉ[3*]

[1]Université du Québec, Centre d'étude de la forêt
belanger.nicolas@teluq.ca (* presenting author)
[2]UQAM, Centre d'étude de la forêt
benoit.lafleur@uqat.ca
[2]UQAM, Centre d'étude de la forêt
y_claveau@sympatico.ca
[3]Canadian forest service, Laurentian forestry centre
david.pare@rncan-nrcan.gc.ca

Introduction

Planting fast growing trees on abandoned agricultural land (afforestation) is done all over the world as a means to satisfy increasing wood demand. However, similar to modern agriculture, increased nutrient uptake due to fast growth and nutrient export from harvest could lead to a decrease in soil nutrient availability and the increased use of fertilizer to maintain soil productivity. Recent research suggests that some tree species, notably late succession conifers, release acid exudates from their roots which attack the crystal lattice of minerals. This releases substantial amounts of base nutrients (Ca, Mg, K) which could sustain productivity over several rotations without fertilization. A sequential extraction/leaching procedure with diluted salt and weak acid solutions was therefore used to evaluate if available and structural base nutrients and other major cations (Na, Al, Fe) in soils were being depleted along a soil productivity (and age) gradient of hybrid *Populus*, a fast growing early succession deciduous tree genera used worldwide in an intensive plantation context, relative to abandoned agricultural fields.

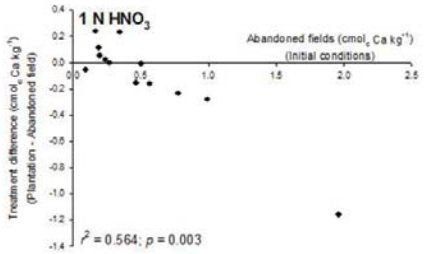

Figure 1. Relationship between abandoned fields and treatment difference for soil Ca following 1 N HNO_3 extraction.

Results and Conclusion

Soil structural Ca and Mg were lower under *Populus* at about half of the sites. The results suggest a greater capacity of the trees to promote soil mineral weathering than plants in abandoned fields. However, this ability appears to be linked to the initial chemical and mineralogical composition of the soils: the divergence between land use types was larger at sites with greater soil cation exchange capacity (more clay) and (or) structural Ca and Mg (more easily weathered Ca and Mg containing minerals) (Fig. 1). This means that fast growing *Populus* may only be capable of augmenting soil mineral weathering where soils are vulnerable to acid exudates. Hybrid *Populus* are not able to promote base nutrient release from minerals on coarse textured acidic soils where soil productivity is a real concern.

High-iron chamosite in bituminous coals in Xuanwei County, China: a possible contributing factor to a high lung cancer rate

HARVEY E. BELKIN[1*], AND JAMES C. HOWER[2]

[1]U.S. Geological Survey, Reston, USA, hbelkin@usgs.gov (* presenting author)
[2]University of Kentucky Center for Applied Energy Research, Lexington, USA, james.hower@uky.edu

Certain communes in Xuanwei County, eastern Yunnan Province, have some of the highest rates of lung cancer mortality in China. Nationwide, age-adjusted mortality rates (per 100,000) are 6.8 and 3.2 for Chinese males and females, respectively [1]. With rates for Yunnan Province 4.3 and 1.5. In Xuanwei County, the rates are 27.7 for males and 25.3 for females and in the three communes with the highest mortality, the rates are males 118.0 and females 125.6 [1]. This exceptionally high rate and the similarity between the male and female rates is unusual as the females in this locality are essentially non-smokers. Previous workers attributed the high incidence of Xuanwei County lung cancer to domestic combustion of locally mined coal in houses with non-vented stoves [2]; however, this practice occurs in many Provinces without the effect of a high lung cancer rate. Generation of polycyclic aromatic hydrocarbons (PAHs) by coal combustion was first thought to be the disease etiology [1]. Additional work on coal mineralogy and combustion models suggested that small (<10 μm) to nanometer-sized quartz played a significant role in the disease etiology and that the combined influence of silica-volatile (PAHs) interaction was more hazardous and causal than either component alone [3].

We have examined 12 smoky bituminous coals from mines in communes with various degrees of age-adjusted lung cancer death rate as well as smokeless anthracite coals from mines southwest of Xuanwei City. We find no significant relationship between overall coal characteristics and the lung cancer rate with the exception of the iron content of the coal (expressed as Fe_2O_3 on an ash-basis). The abundance of very iron-rich chamosite [(Fe/(Fe+Mg)) > 0.85] is the source of this iron enrichment (iron sulfides and oxides are rare).

Although iron is critical for normal cell function, because of its ability to reduce oxygen, iron is the most potent inducer of free radicals in most biological systems. Recent work on the cause of coal workers' pneumoconiosis suggests a strong correlation with the bioavailable iron content of coal [4]. We suggest that during domestic coal combustion, chamosite is thermally decomposed and may supply minute iron oxides to the coal smoke. Although our statistical basis is small (n = 12) the presence of this high-iron phase may add to the combined influence of PAHs and silica and should be considered as a potential contributing factor to the high lung cancer rate.

[1] Mumford *et al.* (1987) *Science*, **235,** 217-220. [2] Chapman *et al.* (1988) *Arch. Environ. Health*, **43**, 180-185. [3] Large *et al.* (2009) *Environ. Science & Tech*. **43**, 9016-9021. [4] Xi *et al.* (2005) *Environ. Health Persp*. **113**, 964-968.

The Effects of Dissolved Chloride on the $Fe^{3+}/\sum Fe$ of Rhyodacitic Melt

AARON S. BELL*[1], JAMES WEBSTER[2], & M. DARBY DYAR[3]

[1]American Museum of Natural History, New York, NY, USA, abell@amnh.org
[2]American Museum of Natural History, New York, NY, USA, jdw@amnh.org
[3]Mount Holyoke College South Hadley, MA, USA , mdyar@mounthoyoke.edu

We have conducted a series of experiments designed to evaluate intrinsic effects of the dissolved chlorine on the equilibrium $Fe^{3+}/\sum Fe$ in hydrous, chloride-rich rhyodacite liquids. Experiments were conducted at series of controlled fO_2 in an IHPV at 950°C and 130 MPa. The $Fe^{3+}/\sum Fe$ values of the run-product glasses were measured with synchrotron μ-XANES spectroscopy on beamline 13ID-D at the Advanced Photon Source, Argonne National Laboratory.

Data from experiments indicate that the addition of dissolved chloride increases the equilibrium $Fe^{3+}/\sum Fe$ of the melt relative to values predicted by several popular algorithms that equate $Fe^{3+}/\sum Fe$ with fO_2 and bulk melt composition. The deviation of the observed $Fe^{3+}/\sum Fe$ values from their predicted "equilibrium" values suggests that the interaction of dissolved chloride with Fe in the melt alters the activity-composition relationships for FeO and $FeO_{1.5}$ in the melt. Calculated G^{ex} associated with the $FeO_{1.5}$ and FeO components of the melt systematically vary as a function of the imposed experimental fO_2.

Data from these experiments imply that hydrous Fe-poor melts with intermediate silica and fairly modest chloride contents (i.e., ≤ 0.75 wt%) may display rather oxidized $Fe^{3+}/\sum Fe$ values despite possessing a relatively reduced equilibrium fO_2. The data further suggest that any empirical or thermodynamic model of the $Fe^{3+}/\sum Fe$ in silicate liquids must include terms to account for the non-ideal behaviour of $\gamma FeO_{1.5}/\gamma FeO$ that is associated with the presence of dissolved chlorine in the melt.

Jack Hills zircons record a thermal event coincident with the hypothesized Late Heavy Bombardment

*E. A. BELL, T. M. HARRISON

Dept. of Earth and Space Sciences, University of California Los Angeles, Los Angeles, CA, USA, ebell21@ucla.edu (* presenting author)

Introduction

The Late Heavy Bombardment (LHB) is a hypothesized period of intense bombardment of the inner solar system at ca. 3.9 Ga, inferred from disturbed lunar ages. Major thermal effects to the Earth's crust are expected from LHB-impact scenarios, but unambiguous terrestrial evidence of this event is unknown, probably owing to the sparse geologic record from this period. However, detrital zircons from Jack Hills, Western Australia span the period 4.3-3.0 Ga, including the time period of the LHB, and may record evidence for this event.

Results and Discussion

We investigated the trace element chemistry of the Jack Hills detrital zircon record for the period 4.0 – 3.8 Ga in search of apparent changes in thermal conditions consistent with the LHB. The Ti-in-zircon temperature (T^{xlln}) distribution is well established for Hadean detrital grains, clustering about an average value of ~680°C – likely indicating near water-saturated granitic melting conditions. The average T^{xlln} does not change appreciably through the period 4.0-3.8 Ga, but between 3.91-3.84 Ga, there is a notable group of low-Ti zircons with apparent T^{xlln} extending well below the granite solidus. Further investigation revealed that this period contains two groups of zircons with clearly distinguishable trace element signatures. Group I resembles the Hadean Jack Hills zircons in Ti, Hf, Ce, U, and Th/U, whereas Group II contains lower Ti, Ce, and Th/U along with higher Hf and U. Group II also displays a high degree of U-Pb concordance compared to the 4.0-3.8 Ga Jack Hills zircons as a whole, despite their high U contents. We interpret Group II as originating from the solid-state recrystallization of originally magmatic (perhaps even Group I-like) zircon during a thermal event ca. 3.9 Ga. This thermal excursion is also seen in epitaxial growths on Hadean zircon cores found in previous studies.

Conclusion

A group of Jack Hills zircons at ca. 3.9 Ga appear recrystallized, and likely record a significant thermal event in the source terrane. Although an endogenic cause for this thermal event cannot be definitively ruled out, these observations may constitute the first terrestrial evidence for the LHB.

Genome-enabled studies of anaerobic, nitrate-dependent U(IV) oxidation

HARRY R. BELLER[1]*, TINA C. LEGLER[2], STACI R. KANE[2], PEGGY O'DAY[3], PENG ZHOU[1,3]

[1]Lawrence Berkeley National Laboratory, HRBeller@lbl.gov (* presenting author)
[2] Lawrence Livermore National Laboratory
[3] University of California, Merced

Anaerobic, nitrate-dependent U(IV) oxidation has considerable relevance to the bioremediation of uranium-contaminated aquifers and also represents a novel bacterial metabolic capability of fundamental scientific interest. A favored process for U bioremediation is *in situ* reductive immobilization, a process by which anaerobic bacteria reduce water-soluble U(VI) complexes to poorly soluble U(IV) phases. The discovery that *Thiobacillus denitrificans* [1] and other bacteria can anaerobically re-oxidize, and thus, re-mobilize, uranium in groundwater highlights a process that could compromise the efficiency of this bioremediation approach. While microbial U(VI) reduction has been the subject of extensive research, far less is known about anaerobic U(IV) re-oxidation.

We will discuss our efforts to identify the genes/proteins that are key to nitrate-dependent U(IV) oxidation in *T. denitrificans*. These efforts included: (a) detailed analysis of the *T. denitrificans* genome [2], (b) whole-genome transcriptional analyses of *T. denitrificans* with high-density, oligonucleotide microarrays [3], (c) proteomic studies of membrane-associated, *c*-type cytochromes in *T. denitrificans* [4], and (d) development of a genetic system in *T. denitrificans* [5].

We identified two diheme, *c*-type cytochromes critical to anaerobic U(IV) oxidation in *T. denitrificans* (putatively c_4 and c_5 cytochromes, Tbd_0187 and Tbd_0146, respectively). Insertion mutations in each of the two genes encoding these cytochromes resulted in a greater than 50% decrease in nitrate-dependent U(IV) oxidation activity, and complementation *in trans* restored activity to wild-type levels. Sucrose-density-gradient ultracentrifugation confirmed that both cytochromes are membrane associated. Sequence-based evidence links the Tbd_0187 protein to the high midpoint reduction potentials that would be required to catalyze U(IV) oxidation. Insertion mutations in other membrane-associated *c*-type cytochromes in *T. denitrificans* did not diminish U(IV) oxidation. To date, Tbd_0146 and Tbd_0187 are the only genes identified as being associated with anaerobic U(IV) oxidation.

We are also investigating nitrate-dependent Fe(II) oxidation in *T. denitrificans*, a process that we observed to accelerate U(IV) oxidation. Notably, the two cytochromes involved in U(IV) oxidation in *T. denitrificans* do not appear to be involved in Fe(II) oxidation. Random transposon mutagenesis studies to further investigate Fe(II) oxidation in *T. denitrificans* are ongoing.

[1] Beller (2005) *Applied and Environmental Microbiology* **71**, 2170-2174. [2] Beller *et al.* (2006) *Journal of Bacteriology* **188**, 1473-1488. [3] Beller *et al.* (2006) *Journal of Bacteriology* **188**, 7005-7015. [4] Beller *et al.* (2009) *Biodegradation* **20**, 45-53. [5] Letain *et al.* (2007) *Applied and Environmental Microbiology* **73**, 3265-3271.

Stable Isotope and Isotopomeric Constraints on N_2O Production in Wastewater Treatment Plants

F. BELLUCCI[1*], M. GONZALEZ-MELER[2], N.C. STURCHIO[2], J.K. BÖHLKE[3], N. E. OSTROM[4], AND J. KOZAK[5]

[1]Argonne National Laboratory, Argonne, IL, USA, fbellucci@anl.gov (* presenting author)
[2]University of Illinois at Chicago, Chicago, IL, USA, mmeler@uic.edu; sturchio@uic.edu
[3]U.S. Geological Survey, Reston, VA, USA, jkbohlke@usgs.gov
[4]Michigan State University, E. Lansing, MI, USA ostromn@msu.edu
[5]Metropolitan Water Reclamation District of Greater Chicago, Chicago, IL, USA, joseph.kozak@mwrd.org

Wastewater treatment plants (WWTPs) constitute a substantial source of N_2O to the atmosphere, with a wide range of estimated emission factors, varying from 0.3 to 140 g N_2O/person/yr [1]. The majority of N_2O emissions occur in the aerobic reactors, where both incomplete nitrification and denitrification might contribute to the overall N_2O emissions. To better constrain production mechanisms and overall N_2O fluxes, we measured N and O isotope ratios of NH_4^+, NO_2^-/NO_3^-, and N_2O, and isotopomer ratios (N isotope site preference) of N_2O at two large-scale activated-sludge WWTPs in Chicago.

The average N2O concentration in the off-gas from the aerobic reactors was 34 and 56 ppmv for plants 1 and 2, respectively. At both plants the isotopic distribution of the major aqueous N-species (NO_3^- and NH_4^+) within the aerobic reactor can be approximated with a Rayleigh-type fractionation model determined by nitrification of ammonium along the wastewater flow path, accompanied by denitrification of about 5 % of the NO_3^- produced, with constant fractionation factors of about -15 ‰ and -20 ‰ for NH_4^+ nitrification and NO_3^- denitrification, respectively. The N isotope site preference in N_2O, averaging +2.7 ‰ and +3.9 ‰ at the two plants, suggests that N_2O was mainly produced by incomplete denitrification [2] in the portions of the tanks where dissolved oxygen was between 0.2 and 2.5 mg/L (fig. 1).

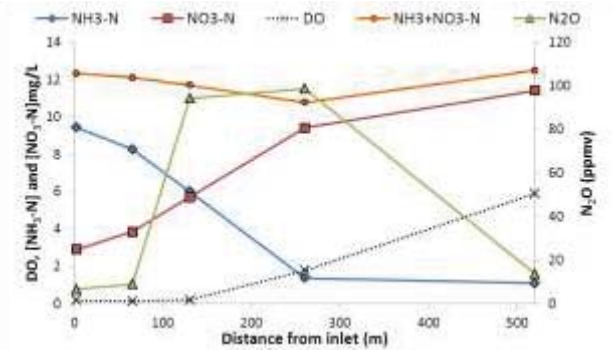

Figure 1. Average concentrations of dissolved oxygen (DO), N aqueous species, and off-gas N_2O along the wastewater flow path in a single tank of the aerobic reactor at plant 1.

[1] Ahn *et al.* (2010) *Environ. Sci. Technol.* **44**, 4505-4511.
[2] Sutka *et al.* (2006) *Appl. Environ. Microbiol.* **72**, 638-644.

The early formation of the continental crust: constraints from zircon Hf-isotope data

E.A. BELOUSOVA[1], W.L. GRIFFIN[1], Y.A. KOSTITSYN[2], N.J. PEARSON[1], G. BEGG[3] AND S.Y. O'REILLY[1]

[1]ARC Centre of Excellence for Core to Crust Fluid Systems, Department of Earth and Planetary Sciences, Macquarie University, Sydney, NSW 2109, Australia elena.belousova@mq.edu.au (*presenting author); bill.griffin@mq.edu.au; norman.pearson@mq.edu.au; sue.oreilly@mq.edu.au

[2]GEOKHI RAS, Moscow, Russia, kostitsyn@geokhi.ru

[3]Minerals Targeting Intl., West Perth WA, 6005, Australia, graham@mineralstargeting.com

A worldwide database of >16,000 U–Pb and Hf-isotope analyses of zircon, largely from detrital sources, has been interogated to analyse the processes of crustal evolution on a global scale, and to test existing models for the growth of continental crust through time. At any timeslice, most zircons have ε_{Hf} well below the Depleted Mantle (DM) growth curve, reflecting later reworking of originally juvenile material. To quantitatively estimate the proportion of juvenile material added to the crust at any given time during its evolution, it is necessary to correct for this effect. "Crustal" model ages are calculated assuming the zircon-bearing magmas were generated from the average continental crust ($^{176}Lu/^{177}Hf = 0.015$); zircons with non-juvenile Hf are projected back to the DM growth curve using this ratio. Juvenile magmas are defined as having $\varepsilon_{Hf} \geq 0.75$ times the ε_{Hf} of the DM at the time of genesis. The distribution of corrected model ages can then be used to model the true crustal growth rate over the 4.56 Ga of Earth's history. The modelling shows that there was little episodicity in the production of new crust, as opposed to peaks in magmatic ages. The distribution of age-Hf isotope data from zircons worldwide implies that at least 60% of the existing continental crust separated from the mantle before 2.5 Ga, and has been variably reworked since then. However, taking into consideration new evidence coming from geophysical data, and correcting for the geographical biases in database, the formation of most continental crust still earlier in Earth's history (at least 70% before 2.5 Ga) is even more probable. Thus, crustal reworking has dominated over net juvenile additions to the continental crust, at least since the end of the Archean. Moreover, the juvenile proportion of newly formed crust in any timeslice decreases stepwise through time: it is about 70% in the 4.0–2.2 Ga time interval, about 50% in the 1.8–0.6 Ga time interval, and possibly less than 50% after 0.6 Ga. These changes may be related to the formation of supercontinents.

Applications of the Arctic sea ice proxy IP_{25}: Quantitative versus qualitative considerations

SIMON BELT[1*], PATRICIA CABEDO SANZ[1], ALBA NAVARRO RODRIGUEZ[1], JOCHEN KNIES[2], KATRINE HUSUM[3], AND JACQUES GIRAUDEAU[4]

[1]Plymouth University, Plymouth, UK, sbelt@plymouth.ac.uk (* presenting author)

[2]Geological Survey of Norway, Trondheim, Norway, Jochen.Knies@NGO.NO

[3]University of Tromsø, Tromsø, Norway, katrine.husum@uit.no

[4]Université Bordeaux, Bordeaux, France, J.Giraudeau@epoc.u-bordeaux.fr

Background

The presence of the sea ice diatom biomarker IP_{25} in Arctic marine sediments has been used in previous studies as a proxy for past spring sea ice occurrence and as an indicator of wider palaeoenvironmental conditions for different regions of the Arctic over various timescales [e.g. 1, 2]. Recent attempts have also been made to make the interpretations of the IP_{25} data more quantitative by comparison of IP_{25} (and other biomarker) concentrations with known sea ice conditions (3). However, the extent to which such calibrations can be extrapolated for longer timescales and for different Arctic regions remains unclear.

Current work

This presentation will focus on recent results, with particular emphasis on the importance of accurate analytical methods for the quantification of IP_{25} in marine sedments and a consideration of the factors that likely influence whether IP_{25}-based interpretations can be considered as qualitative or quantitative. Recent case studies to illustrate these points will be taken from different geological epochs (including modern times, the Holocene and the Younger Dryas) and from a diverse range of Arctic and sub-Arctic regions including the Canadian Arctic and the Nordic Seas. The outcomes of these analyses not only provide important information on past Arctic sea ice conditions, but also help identify areas of research that still require attention.

[1] Belt et al. (2007) *Org. Geochem.* **38**, 16-27. [2] Vare et al. (2009) *QSR* **28**, 1354-1366. [3] Müller et al. (2011) *EPSL* **306**, 137-148.

Geochemical proxies for changes in dust sources in Negev desert loess

MICHAL BEN-ISRAEL[1,2*], YIGAL EREL[1], YEHOUDA ENZEL[1], RIVKA AMIT[2]

[1]Hebrew University of Jerusalem, Institute of Earth Sciences, Israel, michal.benisrael@mail.huji.ac.il (* presenting author)
[2]Geological Survey of Israel, Jerusalem, Israel

The loess of the Negev desert of Israel, was deposited mainly during the late Pleistocene [1, 2]. It is characterized by a bimodal grain-size distribution with modes between 2-8 micrometer (fine silt) and 50-60 micrometer (coarse silt) that represent two different sources of dust, one distal and one proximal [3].

Here we investigate the carbonate-free samples of the two size fractions and search for a geochemical signature of the distal and proximal sources of the loess in three OSL-dated primary loess sequences along a climatic transect: Hura village (~250 mm/yr) and Ramat Beka (~150 mm/yr) in the northern Negev and Mt. Harif (~100 mm/yr) in the central Negev. The fractions are separated and analyzed for major and trace elements and for Sr and Nd isotopic composition. Preliminary results show differences between the fine and coarse fractions that agree with the observation of two different sources contributing to loess in the Negev. Sr-Nd isotopic ratios of both silt fractions suggest contribution from several distal (e.g. Sahara, Arabia) and local proximal sources (e.g. Sinai deserts, Nile delta sediments, and the Sinai-Negev sand dunes). Moreover, changes in loess sources over time were detected in shifts in Sr and Nd isotopic values of the fine fractions, these shifts acure at ~60-70 kyr in Mt. Harif and Ramat Beka sites and at ~20 kyr at Hura site.

These results support the formation model of primary desert loess by eolian abrasion of sand dunes and suggest that the loess chemical and isotopic composition reflect changes of dust sources over time.

[1] Crouvi *et al.* (2009) *Journal of Geophysical Research* **114 (F02017)**, 1-16.
[2] Amit *et al.* (2011) *Geological Society of America Bulletin* **123**, 873-889.
[3] Yaalon and Dan (1974), *Zeitschrift fur Geomorphologie Supplementband* **20**, 91–105.

CHARACTERIZATION OF HUMIC ACID REACTIVITY MODIFICATIONS DUE TO ADSORPTION ONTO α-AL_2O_3

M. F. BENEDETTI[1*], N. JANOT[1,2], X. ZHENG[3], J.P. CROUE[3], P. E. REILLER[2]

[1] Université Paris Diderot, Sorbonne Paris Cité, Institut de Physique du Globe de Paris, UMR 7154 CNRS, F-75013 Paris, France, benedetti@ipgp.fr (* presenting author)
[2] CEA/DEN/DANS/DPC/SECR, Laboratoire de Spéciation des Radionucléides et des Molécules, F-91191 Gif-sur-Yvette, France, Pascal.REILLER@cea.fr
[3] King Abdullah University of Science and Technology Thuwal, Water Desalination and Reuse Research Center, Kingdom of Saudi Arabia, jp.croue@kaust.edu.sa

Adsorption of purified Aldrich humic acid (PAHA) onto α-Al_2O_3 is studied by batch experiments at different pH, ionic strength and coverage ratios R (mg of PAHA by m² of mineral surface). After equilibration, samples are centrifuged and the concentration of PAHA in the supernatants is measured. The amount of adsorbed PAHA per m² of mineral surface is decreasing with increasing pH. At constant pH value, the amount of adsorbed PAHA increases with initial PAHA concentration until a constant pH-dependant value is reached.

UV/Visible specific parameters such as specific absorbance $SUVA_{254}$, ratio of absorbance values E_2/E_3 and width of the electron-transfer absorbance band Δ_{ET} are calculated for supernatant PAHA fractions of adsorption experiments at pH 6.8, to have an insight on the evolution of PAHA characteristics with varying coverage ratio. No modification is observed compared to original compound for $R \geq 20$ mg_{PAHA}/g. Below this ratio, aromaticity decreases with initial PAHA concentration. Size-exclusion chromatography - organic carbon detection measurements on these supernatants also show a preferential adsorption of more aromatic and higher size fractions.

Spectrophotometric titrations were done to estimate changes of reactivity of supernatants from adsorption experiments made at $pH \approx 6.8$ and different PAHA concentrations. Evolutions of UV/Visible spectra with varying pH were treated to obtain titration curves that are interpreted within the NICA-Donnan framework. Protonation parameters of non-sorbed PAHA fractions are compared to those obtained for the PAHA before contact with the oxide. The amount of low-affinity type of sites and the value of their median affinity constant decrease after adsorption. From PAHA concentration in the supernatant and mass balance calculations, "titration curves" are obtained and fitted for the adsorbed fractions for the first time. These changes in reactivity to our opinion could explain the difficulty to model the behavior of ternary systems composed of pollutants/HS/mineral since additivity is not respected.

Figure 1: LC-OCD chromatograms of PAHA and of supernatants from adsorption experiments at 0.1M and $pH \approx 6.8$ (R in mgPAHA/g α-Al_2O_3).

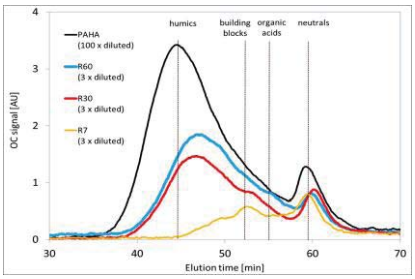

Stabilization and Assembly of Mineral Clusters Guided by Enamel Proteins.

PING-AN FANG[1], HENRY C. MARGOLIS[2], JAMES F. CONWAY[1], JAMES P. SIMMER[3], ELIA BENIASH[1*]

[1]University of Pittsburgh, Pittsburgh, PA, USA;
[2]The Forsyth Institute, Cambridge, MA, USA;
[3]University of Michigan, Ann Arbor, MI, USA;
*-presenting author ebeniash@pitt.edu

Dental enamel, being the most mineralized vertebrate tissue, is extremely well preserved in the paleontological record and thus a favorite subject for studies of vertebrate evolution, archeology and paleoclimate. Enamel is a structurally complex hierarchical nanomaterial. Although, mature enamel is 95% carbonate apaptite it starts as a network of nanocrystaline arrays suspended in a protein matrix, with the mineral phase comprising only 10% of its volume. Despite these differences in composition, the mineral organization in nascient and mature enamel is identical. While the organic matrix is believed to regulate mineral formation, the basic mechanisms of enamel mineralization are poorly understood. Here we present our recent studies of calcium phosphate mineralization *in vitro* in the presence of the major enamel matrix protein, amelogenin. These experiments were carried out on carbon-coated electron microscopy (EM) grids, and studied in conventional and cryo-EM. We found that amelogenin induces formation of parallel arrays of apatitic crystallites that are structurally similar to the basic building blocks of enamel, enamel rods. Importantly, these structures only formed when monomeric, rather than preassembled, amelogenin was introduced to the mineralization solutions. These results suggest that the mineralization occurs not on the preformed organic matrix as in other systems but instead via cooperative interactions between forming crystals and assembling proteins.[*1*] Our cryo-EM studies show that amelogeinin undergoes stepwise assembly via oligomers that then organize into higher order structures. Our results indicate that amelogenin oligomers stabilize calcium phosphate prenucleation clusters and organize them into linear chains. Subsequently, the clusters fuse together to form needle-shaped mineral particles which further organize into parallel arrays.[*2*] We find that the mechanism of enamel formation is very different from the templated mineralization that is observed in other biomineralization systems. Specifically our results indicate that amelogenin oligomers can stabilize prenucleation clusters and organize them into mesostructures prior to their crystallization. This mechanism in which protein assemblies fully control organization of the initial mineral phase enables formation of intricate structures that cannot be obtained via classical crystallization from supersaturated solutions. These studies supported by NIH grants R01DE016376 (to H.C.M.), R01DE016703 (to E.B.) and PA grant SAP 4100031302 (to J.F.C.)

[1] E. Beniash, J. P. Simmer, H. C. Margolis, (2005) *J. Struct. Biol.* **149**, 182. [2] P. A. Fang, J. F. Conway, H. C. Margolis, J. P. Simmer, E. Beniash, (2011) *PNAS* **108**, 14097.

Fluid inclusions give chemical, physical, biological, and climatic insights into acid saline lake and groundwater systems

KATHLEEN COUNTER BENISON
Dept. of Earth and Atmospheric Sciences, Central Michigan University, Mt. Pleasant, Michigan, 48859 USA, benis1kc@cmich.edu

Acid saline lakes and associated shallow groundwaters represent amongst the Earth's most extreme aqueous chemistries. Modern lakes and groundwaters in Western Australia and Chile have pHs as low as 1.5, total dissolved solids as high as 32%, unusually high concentrations of Al, Si, and Fe, and many other atypical chemical characteristics. Permian lake environments in the U.S. midcontinent had even more extreme water compositions.

Fluid inclusions in halite and gypsum from modern and Permian acid saline lakes record specific physical, chemical, and biological conditions of these environments. Primary inclusions in these chemical sediments trap shallow lake water, air bubbles, crystals of other minerals, and microorganisms. Isolated fluid inclusions in early diagenetic phases of halite are remnants of shallow groundwaters and yield their chemical compositions.

A variety of traditional methods, including petrography, freezing/melting microthermometry and laser Raman spectroscopy, and innovative variations, such as homogenization of artificially-nucleated vapor bubbles and UV-vis petrography, produce data detailing environmental conditions. Other traditionally used methods, such as laser ablation ICP-MS, are not effective due to the nature of the inclusions. Making synthetic solutions that match the complexity of natural acid saline inclusions is another challenge. Ongoing efforts include the analyses of modern and Permian air and documentation of microorganisms and organic compounds within these fluid inclusions (Fig. 1).

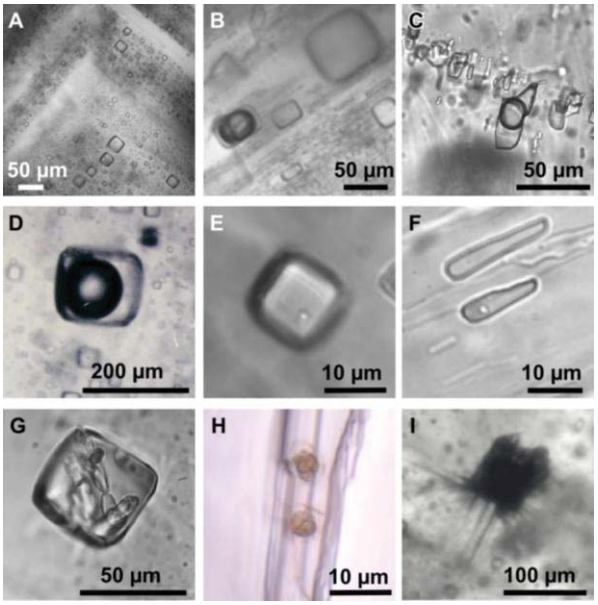

Figure 1: Primary fluid inclusions in acid saline halite and gypsum. A. Fluid inclusions along growth bands in Permian Nippewalla Group halite, Kansas. B. Air in inclusion in modern halite, Western Australia. C. Air in inclusion in modern gypsum, Western Australia. D. Air in inclusion in Permian halite, Nippewalla Group, Kansas. E. Cocci-shaped bacterium/archaeon suspect in Permian halite, Nippewalla Group, Kansas. F. Cocci-shaped bacterium/archaeon suspect in modern gypsum, Western Australia. G. Organic compounds and crystals in fluid inclusion, Permian Nippewalla Group halite, Kansas. H. Algal or pollen suspects in modern gypsum, Western Australia. I. Microbial community in inclusion, Permian Opeche Shale halite, North Dakota.

Equilibrium core formation loses it's lustre: High pressure & temperature partitioning of gold

NEIL BENNETT[1*] & JAMES BRENAN[1]

[1]The University of Toronto, Toronto, Canada, bennett@geology.utoronto.ca (* presenting author)

Experiments to determine the distribution of highly siderophile elements (HSE) between core-forming metal and the magma ocean suggest that the primitive upper mantle (PUM) should be highly depleted in most of these constituents relative to what is observed. This is not the case for Au. We have measured Au solubility at 2GPa and 1800-2315°C, at ~IW-IW+2.5, under both C-bearing and C-free conditions. Metal-silicate partition coefficients ($D_{Met/Sil}$) were then calculated using the relation of [1]. After combination with the low temperature results of [2], the following temperature dependence for $D_{Met/Sil}$ was found:

$$D_{Met/Sil} = 1.14(0.07)*10^4/T\,(\mathrm{K}) - 1.41(0.34)$$

$D_{Met/Sil}$ is essentially independent of fO_2 and the results from previous studies at 0.1MPa-23GPa [2], [3] agree well with our 2GPa data. Temperature therefore appears to be the primary factor controlling the affinity of Au for Fe-metal. Os isotope systematics and concentrations of the other HSEs in the PUM are best explained by a late veneer of LL-chondrite, comprising 0.5% of the bulk silicate earth [4]. $D_{Met/Sil}$ values for Au limit metal-silicate equilibration to ~2450°C if an over-abundance of Au in the PUM is to be avoided, placing the base of the magma ocean at ~400km. This is much shallower than the >800km depth required by the convergence of Ni-Co partitioning [5]. Low $D_{Met/Sil}$ values at high temperature also predict Au/Ir ratios much greater than estimated for the PUM. Metal-silicate equilibrium therefore appears unable to account for the Au content of the PUM. One solution to this discrepancy may be incomplete equilibration between the magma-ocean and the accreting cores of large, differentiated planetesimals [6]. In this scenario, Au may be transported to the Earth's proto-core deprived of communication with molten-silicate, thus imbuing the core with a Au content greater than predicted by metal-silicate partitioning.

[1] Borisov *et al* (1994) *GCA* **58**, 705-716. [2] Borisov & Palme (1996) *Min. & Pet.* **56**, 297-312. [3] Danielson *et al* (2005) *LPSC XXXVI*, 1955. [4] Brenan & McDonough (2009) *Nature* **2**, 798-801 [5] Bouhifd & Jephcoat (2011) *EPSL* **307**, 341-348. [6] Dahl & Stevenson (2010) *EPSL* **295**, 177-186.

Expanding early Earth frontiers: A new Eoarchean-Hadean(?) terrane in Southwestern Greenland

VICKIE C. BENNETT[1*], ALLEN P. NUTMAN[2], JOE HIESS[3] AND CLARK R.L. FRIEND[4]

[1]Australian National University, Canberra, Australia, vickie.bennett@anu.edu.au. (* presenting author)
[2]Universisty of Wollongong, allen.nutman@gmail.com
[3]NIGL, British Geological Survey, jies@bgs.ac.uk
[4]45 Stanway Road, Headington, Oxford, UK

The strongest controls on early Earth processes and environments are obtained through direct study of the rock record, which currently, with few exceptions, terminates at ca. 3.9 Ga. Although rare >4.0 Ga zircons and their inclusion suites preserved in Western Australian Mesoarchean metasediments provide a wealth of information about early Earth history and conditions, they are an incomplete and likely restricted record of early processes.

Here we present new geochemical observations from metagabbros and associated felsic rocks from a previously unstudied region of SW Greenland. Minimum age constraints on the metagabbros are provided by U-Pb zircon (SHRIMP) ages of cross-cutting granitoids; a dated tonalite has a dominant population of euhedral, oscillatory-zoned magmatic zircons with an age of 3889±5 Ma. Two adjacent relatively older gabbros yielded populations of small, oval zircons with only ca. 2.97 Ga ages, which are interpreted to have formed in a recognized regional metamorphic event. This event is not recorded at either Isua or on Akilia, demonstrating that this is a distinct block of ancient crust, rather than contiguous with previously documented Eoarchean domains. Initial εHf values of the ca. 3.89 Ga zircons are within error of estimated chondritic compositions, with no evidence for early Lu/Hf fractionation. This is in accord with Lu-Hf data from zircon populations extracted from >3.7 rocks worldwide.

Measured Hf isotopic compositions of the metagabbro Mesoarchean metamorphic zircons determined by LA-MC-ICPMS range from εHf= -79 to -83; initial compositions calculated at the metamorphic age are highly negative (-13 to -16). Two-stage chondritic mantle model ages calculated using plausible $^{176}Lu/^{177}Hf$ ratios for the pre-zircon first stage are >4.0 Ga. For example, using $^{176}Lu/^{177}Hf$ =0.018 as typifies Isua metabasaltic rocks, yields chondritic model ages of ca. 4.3 Ga. In contrast, similar-aged metamorphic zircons from a nearby Mesoarchean metasedimentary rock have positive initial εHf values =+8 with DM model ages equal to zircon crystallization age. The ancient Hf model ages combined with the minimum 3.89 Ga age provided by cross-cutting tonalites point to a ≥4.0 Ga age for the metagabbros. Continued investigations of these potential Hadean rocks are in progress.

The majority of rocks analysed from SW Greenland Eoarchean terranes have ^{142}Nd isotopic anomalies when compared with modern terrestrial rocks, with the magnitude of ^{142}Nd generally increasing with crystallization age as shown by Bennett et al, (*Science*, 2007). In the absence of igneous zircons in the ≥3.89 Ga metagabbros, ^{142}Nd compositions may provide confirmation of the Hadean age suggested by Hf isotopic modelling. These recently recognised earliest Eoarchean and possibly Hadean suites are a significant new laboratory for testing models of early Earth formation and evolution.

3D visualisation of core-forming melts

M. BERG*[1], I.BUTLER[1,2], S.REDFERN[3], G.D. BROMILEY[1,4]

[1]School of Geosciences, Grant Institute, University of Edinburgh, Edinburgh, UK M.Berg@sms.ed.ac.uk (*presenting author)
[2]ECOSSE (Edinburgh Collaborative of Subsurface and Engineering) Joint Research Institute of the Edinburgh Research Partnership in Engineering and Mathematics, UK
[3]Dept. Earth Sciences, University of Cambridge, Cambridge, UK
[4]Centre for Science at Extreme Conditions, Erskine Williamson Building, University of Edinburgh, Edinburgh, UK

The mechanism of metal-silicate segregation is key to constraining core formation processes in the early Earth. Experiments performed at conditions of core formation in terrestrial planets have generally found metallic melts to be immobile in a solid silicate matrix. This implies that a liquid silicate 'Magma Ocean' was required for efficient differentiation to occur. There is some doubt as to the applicability of this model to other planetary bodies, particularly those with smaller radii, which may not have been heated to silicate melting temperatures. Recent experimental work has found that deformation can enhance permeability of melt through a solid silicate system without the need to melt the surrounding silicate. We have conducted a series of deformation experiments in the rotational Paris-Edinburgh Cell (roPEC), which allows controlled deformation at simultaneous high pressures and temperatures over a large range of strain rates. Textural analysis confirms melt is interconnected at a grain scale. This implies core formation could have taken place earlier and more rapidly than previously believed, affecting inferred geochemistry of the core and mantle. We use 3D reconstructions of the sample interior from Computed Axial Tomography scans to characterise melt network geometry in order to constrain melt migration rates and permeability.

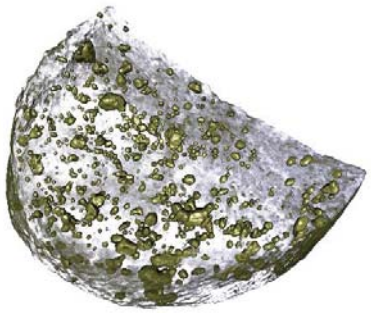

Figure 1: Preliminary tomographic reconstruction of undeformed sample. Sample diameter is 2mm. High density Fe_3S shown in gold, grey-transparent areas are olivine.

Petrogenesis of voluminous silicic magma in northeast Iceland

SYLVIA E. BERG[1, 2*], VALENTIN R. TROLL[2], MORTEN S. RIISHUUS[1] AND STEFFI BURCHARDT[2]

[1]Nordic Volcanological Center, Reykjavik, Iceland sylvia@hi.is (*presenting author)
[2]Dept. of Earth Science, CEMPEG, Uppsala University, Sweden

Neogene silicic volcanic complexes in the greater Borgarfjörður eystri area, NE-Iceland, are the focus of a petrological and geochemical investigation. The region contains the second-most voluminous occurrence of silicic rocks in Iceland, including caldera structures, inclined sheet swarms, extensive ignimbrite sheets, sub-volcanic rhyolites and silicic lava flows. Despite the relevance of these rocks to understand the generation of evolved magmas in Iceland, the area is geologically poorly studied [c.f. 1, 2, 3].

The voluminous occurrence of evolved rocks in Iceland (10-12 %) is very unusual for an ocean island or a mid-oceanic ridge, with a typical signal of magmatic bimodality, often called "Bunsen-Daly" compositional gap [e.g. 4, 5, 6]. The Bunsen-Daly Gap is a long-standing and fundamental issue in petrology and difficult to reconcile with continuous fractional crystallization as a dominant process in magmatic differentiation [7]. This implies that partial melting of hydrothermally altered crust may play a significant role. Our aim is to contribute to a solution to this issue by unravelling the origin, timing and evolution of voluminous evolved rhyolites in NE-Iceland.

We use a combined petrological, textural, experimental and in-situ isotope approach on a comprehensive sample suite of intrusive and extrusive rocks, ranging from basaltic to silicic compositions. We are performing major, trace element and Sr-Nd-Hf-Pb-He-O isotope geochemistry, as well as U-Pb geochronology and Ar/Ar geochronology on rocks and mineral separates. Zircon oxygen isotope analysis will be performed in conjuction with zircon U-Pb geochronology for further assessment of the role of processes such as partial melting of hydrated country rock and/or fractional crystallization in generating Icelandic rhyolites. In addition, high pressure-temperature partial melting experiments aim to reproduce and further constrain natural processes. Using the combined data set we intend to produce a comprehensive and quantitative analysis of rhyolite petrogenesis, and of the temporal, structural and geochemical evolution of silicic volcanism in NE-Iceland. The chosen field area serves as a good analogue for active central volcanoes in Iceland, such as Askja and Krafla, where interaction of basaltic and more evolved magma has led to explosive eruptions.

[1] Gústafsson (1992) PhD dissertation, Berlin University. [2] Martin & Sigmarsson (2010) Lithos **116**, 129–144. [3] Burchardt, Tanner, Troll, Krumbholz & Gustafsson (2011) G^3 **12** (7), Q0AB09. [4] Bunsen (1851) Annalen der Physik und Chemie **159** (6), 197-272. [5] Daly (1925) Proceedings of the American Academy of Arts and Sciences **60** (1), 3-80. [6] Barth, Correns & Eskola (1939) Die Entstehung der Gesteine. Springer Verlag, Berlin. [7] Bowen (1928) The evolution of the igneous rocks. Princeton University Press.

Petrology of two pre-orogenic granites, Damara Orogen, Namibia

CHRISTIAN BERGEMANN[1*], STEFAN JUNG[1], JASPER BERNDT[2] AND ANDREAS STRACKE[2]

[1] Mineralogisch-Petrographisches Institut, Universität Hamburg, Germany (*), christian_bergemann@yahoo.de

[2] Institut für Mineralogie, Universität Münster, Germany

The Damara Orogen sensu strictu of Namibia was formed during the late Archean/early Proterozoic Pan-African orogenic event. It is characterised by medium p/high T regional metamorphism and large-scale granitoid intrusion. The two plutons investigated in this study are part of the Damaran Northern Central Zone within the Okombahe district and can readily be distinguished by field criteria. LA-ICP-MS U-Pb geochronology on zircon yielded similar ages of 576±6 Ma and 571±5 Ma. This is the earliest date of granite intrusion discovered in the Central Damara Orogen. Both plutons consist of granodiorite and granite that are metaluminous to slightly peraluminous. Both rock types have high calculated zircon saturation temperatures up to 890°C, show only limited fractionation and exhibit no signs of shallow crustal contamination. Chemical and isotope data overlap almost completely in which the granodiorites and granites are characterized by a range in K_2O (3.1-5.9 wt.%) and moderate to high HFSE and LREE abundances (up to 620 ppm Zr and 250 ppm Ce) and a strong enrichment of LREE over HREE (La/Yb: 19-49) with variable negative Eu anomalies (Eu/Eu*: 0.82-0.19). Initial Sr and Nd isotopic compositions vary over a narrow range (init $^{87}Sr/^{86}Sr$: 0.704 - 0.706; init. ε Nd: -1.9 to -3.9). Relatively young Nd model ages (T_{DM}: 1.2-1.4 Ga) and 1.7 Ga-old restitic zircon suggest a derivation from a juvenile source rock of probably meta-igneous composition. As the intrusion ages precede the minimum age of high-grade regional metamorphism, crustal heating as the cause of granite formation can be ruled out. Previous studies have shown that the meta-igneous basement of the Damara orogen has an average heat production of 6.8 HGU (1 HGU=10^{-13} cal/cm^3*sec; Haack et al. 1983). This value is significantly higher than that of average continental crust (2.14 HGU; Rudnick & Gao 2004) hence, a major contribution from pre-existing continental crust is possible. In addition, intrusion of large scale mafic bodies in the lower crust could also potentially provide some extra heat for crustal melting, however, seismic refraction studies gave no evidence for the existence of large volumes of mafic rocks in the lower crust (Green 1983). We therefore suggest that emplacement of numerous sill-like intrusions (Petford & Gallagher 2001) may have provided the necessary heat for melt generation.

[1] Haack, Gohn & Hartmann (1983) Spec. Publ. geol. Soc. S. Afr. 11, 225-231. [2] Rudnick & Gao (2004) In: Treatise on Geochemistry, Elsevier. 3, 1-64. [3] Green (1983) Spec. Publ. geol. Soc. S. Afr. 11, 355-367. [4] Petford & Gallagher (2001) Earth and Planetary Science Letters 193, 483-499.

Mercury Isotopes in the Precambrian

BERGQUIST, B.A.[1]*, GHOSH, S.[2], ONO, S.[3], HAZEN, R.M.[4], SVERJENSKY, D.[5], PAPINEAU, D.[6], KAH, L.C.[7], BLUM, J.D.[8]

[1]University of Toronto, Toronto, Canada, bergquist@geology.utoronto.ca*

[2]Unveristy of Toronto, Toronto, Canada, sanghamitra.ghosh@utoronto.ca

[3]MIT, Boston, USA, sono@mit.edu

[4]CIW Geophysical Laboratory, Washington, DC, USA, rhazen@ciw.edu

[5]Johns Hopkins University, Baltimore, USA, sver@jhu.edu

[6]Boston College, Chestnut Hill, USA, dominic.papineau@bc.edu

[7]University of Tennessee, Knoxville, USA, lckah@utk.edu

[8]University of Michigan, Ann Arbor, USA, jdblum@umich.edu

Mercury (Hg) is an active redox-sensitive metal with a complex biogeochemical cycle that displays a wide range of stable Hg isotopic fractionation. In addition to mass-dependent fractionation (MDF), Hg isotopes also display large (up to 10‰) mass-independent fractionation (MIF). The large MIF in Hg isotopes is commonly expressed only for the odd isotopes (^{199}Hg, ^{201}Hg). To date, the large MIF in the odd Hg isotopes is thought to occur during kinetic photochemical reactions due to the magnetic isotope effect. In the first photochemical experiments (Bergquist and Blum, 2007), Hg(II) species were photo-reduced to Hg(0) in the presence of fulvic acid. It was found that the odd isotopes were preferentially enriched in the reactant in the aqueous reservoir. In these experiments, the Hg/DOM ratios were such that Hg was likely bound to carboxylic ligands. However, subsequent experiments show that the sign and ratio of MIF can be changed during photo-reduction in the presence of different organic ligands or in presence of UVC. In particular, Zheng et al. (2010) demonstrated that photoreduction of Hg bound to reduced S containing ligands results in the odd isotopes being depleted in the reactant in the aqueous phase.

The chemistry of the atmosphere and ocean changed drastically in the Precambrian due to the evolution of life and rise of oxygen. The large changes in the redox conditions and the sulfur cycle of the surface Earth along with changes in UV penenetration likely had large impacts on the biogeochemical cycle of Hg and on the Hg isotope system. It is also likely that the nature of the organic ligands binding Hg changed dramatically in response to evolution of different groups of organisms. The goal of this research was to study Hg isotopes preserved in the sedimentary and metasedimentary geologic record where major changes in either UV shielding or major changes in the nature of DOC may have occurred. Preliminary Hg isotope analyses show that the younger samples mostly show negative MIF with $\Delta^{199}Hg/\Delta^{201}Hg$ close to 1 whereas the older samples have positive MIF with $\Delta^{199}Hg/\Delta^{201}Hg$ greater than 2. The timing of the shift is consistent with the first major glaciation and suggestion of an organic fractal haze, which would have blocked higher energy UV. The timing is also consistant with a change in S isotopes that is thought to occur because of an increase in sulfate and sulfate reducing bacteria. Both possible explanations will be discussed in the context of experimental constraints. These are preliminary results, but they reveal the potential of Hg isotopes to add to our understanding of the eveolution of life and chemistry of the early Earth.

CO_2-rich fluids in the mantle: a comparative fluid inclusion study

MÁRTA BERKESI[1], CSABA SZABÓ[1*], TIBOR GUZMICS[1], ZSANETT PINTÉR[1], RÉKA KÁLDOS[1], JEAN DUBESSY[2], MUNJAE PARK[3] AND GYÖRGY CZUPPON[4]

[1]Lithosphere Fluid Research Lab, Eötvös University, Budapest, Hungary (*martaberkesi@caesar.elte.hu)
[2]G2R, Université de Lorraine, CNRS, CREGU, Nancy, France (jean.dubessy@g2r.uhp-nancy.fr)
[3]School of Earth and Environmental Sciences, Seoul National University, Seoul, Republic of Korea
[4]Institute for Geological and Geochemical Research, Budapest, Hungary

Negative crystal shaped fluid inclusions enclosed in spinel lherzolites from five different locations all around the world were the subject of a detailed fluid inclusion study. Samples were studied from: the Central Pannonian Basin (Hungary), Cameroon Volcanic Line (Cameroon), Jeju Island (S-Korea), Rio Grande Rift (New-Mexico, USA) and from Mt. Quincan (Australia). As a result, CO_2-rich fluids within the fluid inclusions could be studied and compared.

High resolution Raman spectroscopy at different temperatures revealed that fluids in inclusions are heterogeneous and contain small amounts of other species. We show that nitrogen (N_2) can be present in the dense fluid and is more common than was previously thought. H_2O is present in almost all of the inclusions, and was identified by the combination of stepwise heating experiments and Raman spectroscopy [1]. Our results show that, although H_2O is a minor component in mantle fluids, its relative amount varies between different locations, which has not been previously recognized.

Sulfur in the fluid at room temperature can be present either as H_2S or as SO_2, however these species never occur together at the same location. In addition, following fluid inclusion exposure by the FIB-SEM (Focused Ion Beam-Scanning Electron Microscopy) technique, a complexity of S-bearing solid phases has also been identified: sulfides and sulfates were also found within the fluid inclusion cavity. OH-bearing solids are also found in some cases within the fluid inclusions.

Combination of Raman spectroscopy and the FIB-SEM technique proved the presence of carbonates and quartz that are interpreted to be a reaction product of the trapped CO_2 and the host pyroxene. In addition, a common feature found on the inclusion walls is a thin glass film at a submicron scale that documents the ability of mantle fluids to dissolve and transport trace elements and cause cryptic metasomatism as has previously been inferred [2].

We can conclude that, similar to the solid phases involved in the construction of the subcontinental lithospheric mantle, the coexisting fluid can also be heterogeneous in the mantle, although the dominant component in each case is CO_2.

[1] Berkesi *et al.* (2009) *J. Raman Spectrosc.* **40**, 1461-1463.
[2] Hidas *et al.* (2010) *Chem. Geol.* **274**, 1-18.

Investigating the role of microbial processes in the weathering of rock-derived graphitic carbons

SABRINA BERLENDIS [1 *], OLIVIER BEYSSAC[1], KARIM BENZERARA[1], FERIEL SKOURI-PANET[1], CELINE FERARD[1]

[1] IMPMC, CNRS & Université Pierre et Marie Curie, Paris, France , sabrina.berlendis@impmc.upmc.fr, (* presenting author)
olivier.beyssac@impmc.upmc.fr,
karim.benzerara@impmc.upmc.fr

During erosion and chemical weathering, organic carbon contained in (meta)sedimentary rocks may be oxidized or recycled. Recent studies in the Himalaya[1] and Andes[2] orogenic systems have demonstrated that the fate of these carbonaceous phases is highly dependent on their graphitization degree: in such large-scale systems only graphite is finally preserved whereas poorly graphitic compounds are oxidized. This oxidation which happens in the bedrock or during fluvial transport is assisted, and most likely driven, by microbial processes. The present study investigates the effect of inorganic compounds commonly found in shale and coal (metals, sulphur and nitrogen compounds) on the bio-alteration of carbonaceous material by microbial populations. For that purpose, we sampled several carbon-bearing rocks which experienced varying metamorphic grades and have therefore various structural organizations for carbons (from kerogen/coal to graphite) following a strict protocol to minimize contamination. The sample set includes carboniferous coals (Graissessac and Briançon basins, France) and black shales as well as graphitic schists (Western Alps, France). The mineralogy and structure of organic carbon have been characterized by various techniques (XRD, Raman and IR, SEM). The high-grade metamorphic rocks contain highly crystalline carbonaceous phases (graphite) and a low mineral diversity (chlorite, muscovite and quartz). In addition, sulfate minerals such as jarosite and gypsum were detected in slightly less graphitized schist rock. By contrast, the coals contain turbostratic carbons and a wide variety of minerals (montmorillonite, feldspar, illite and kaolinite). Back to the lab, enrichment cultures were set up under both oxic and anoxic conditions using the rock-derived carbonaceous material as the sole carbon source. The effect of various inorganic electron donors and acceptors added in combination are tested. Microscopy and biomolecular studies show a low biomass content in microbial enrichments, but we have detected in some of them thin filamentous bacteria and short rod cells that are embedded in a biofilm deeply-incrusted inside carbonaceous particles and other minerals. The metabolic functions of enriched microbial populations are currently assessed by microscopy, hybridization techniques and spectroscopy techniques. Their possible influences on the alteration of rock-derived graphitic carbons will be discussed.

[1] Galy (2008) *Science* **322**, 943-945.
[2] Bouchez (2010) *Geology* , **38**, 255-258.

The halogen composition of hydrothermal fluids in the Taupo Volcanic Zone, New Zealand.

NELSON F. BERNAL[1*], SARAH A. GLEESON[1], PAUL HOSKIN[2]

[1]University of Alberta, Department of Earth and Atmospheric Sciences, Edmonton, Canada, T6G 2E3.
bernal@ualberta.ca (* presenting author)
sgleeson@ualberta.ca
[2]The University of Auckland, Geology, School of Environment, Auckland, New Zealand.
p.hoskin@auckland.ac.nz

9f. Innovative geochemical approaches to understanding geothermal systems

The halogen composition of seven geothermal fields and eight hot spring areas in the Taupo Volcanic Zone (TVZ), North Island New Zealand, were studied in order to constrain the origin of the geothermal fluids and to identify the effect of physico-chemical processes on the isotopic composition of these fluids. A set of 74 samples from well brines and hot springs were analyzed for Cl, Br, Li, δ^{37}Cl, δ^{18}O and δD. In particular, this study offers a first approach to the application of the Cl/Br systematics in geothermal fluids to constrain the behaviour of stable chlorine isotopes.

The determination of the Cl/Br ratios in the set of samples analyzed, allowed the initial characterization of geothermal fields and hot spring areas in the TVZ. The highest Cl/Br ratios were found at Mokai (1,664), Orakeikorako (1,611), Rotokawa (1,478) and White Island (1,373). The chlorine isotopic composition of all the samples ranged from -0.97 to 0.67‰. With the exception of some samples from Orakeikorako and Rotokawa, most samples with high Cl/Br ratios had positive δ^{37}Cl values, the geothermal field Mokai was the most enriched in δ^{37}Cl (0.03 to 0.38‰). The sample from Broadlands Ohaaki had a negative δ^{37}Cl value (-0.57‰) and a Cl/Br ratio of 870. In the hot springs the Cl/Br ratios also correlate well with the δ^{37}Cl values. Waikite has the highest δ^{37}Cl values (0.47 to 0.67‰), followed by Taupo, White Island, Tokaanu and Waimangu.

The data suggest that in the central part of the TVZ, there is a deep fluid of magmatic origin with a Cl/Br ratio of at least 1,200, a positive δ^{37}Cl signature around 0.5‰, a Cl concentration above 3,200 ppm and a Li content of more than 29 ppm. Fluids with similar characteristics were found at Tokaanu, White Island, Mokai, Wairakei, Tauhara and Ngatamariki. A second fluid is characterized by negative δ^{37}Cl values (-0.02 to -0.97‰), Cl/Br ratios below 1,200 and Li concentrations around 10 ppm. The influence of this second fluid is more dominant towards the E and NE of the TVZ in hot spring areas and geothermal systems like Rotorua, Waiotapu, Rotokawa and Kawerau.

How citrate slows magnesite growth: a high temperature AFM study

ULF-NIKLAS BERNINGER[1*], QUENTIN GAUTIER[2], GUNTRAM JORDAN[1] AND JACQUES SCHOTT[2]

[1] Ludwig-Maximilians-Universität, Department für Geo- und Umweltwissenschaften, Munich, Germany,
ulf-niklas.berninger@campus.lmu.de (*presenting author)
[2]CNRS, Géosciences et Enviroment Toulouse, Toulouse, France,
quentin.gautier@get.obs-mip.fr

Preliminary work and experimental methods

Magnesite shows a high stability in natural enviroments and hence is of scientific interest due to its potential for long-term CO_2 sequestration. In a recent study we were investigating the inhibition of carboxylic ligands on magnesite growth and found out that among the investigated ligands citrate caused the highest degree of inhibition [1]. Besides the effect of complexation of Mg^{2+} in aqueous solution, a prominent surface effect of citrate was detected. This surface effect of citrate on magnesite growth at elevated temperatures, however, is still insufficiently understood.

In the present study, hydrothermal atomic force microscopy (HAFM) was used to investigate magnesite growth on the (104) surface as a function of citrate concentrations (0.1-10 mmol/kgw) and saturation state. Experiments were conducted at pressures up to 4 bars, temperatures of 100 °C and 120 °C and alkaline conditions (pH 7.5-8.5).

Results and outlook

HAFM experiments showed that spiral growth is the dominant growth mechanism over a wide range of saturation state in ligand-free solutions as well as in the presence of citrate. Accordingly, the determined growth rates follow an exponential dependency on supersaturation and are in close agreement with previous mixed-flow reactor experiments [1][2]. Furthermore, HAFM observations revealed that citrate interacts with steps on the (104) surface of magnesite producing growth islands elongated along the trajectory of the c-axis. This pronounced morphological change was taking place without an effect on obtuse step kinematics but with a reduced advancement rate of acute steps. These observations indicate specific blocking of acute kinks by citrate. For the rotation frequence of spirals and thus the growth rate, acute step advancement is essential. The rate of step generation via spiral growth in the presence of 1 mmol/kgw citrate was thereby decreased by a factor of more than 3.

Overall, this study confirms the control exerted by acute steps on magnesite growth rates. Therefore, numerical molecular simulations should preferentially focus on stereochemical effects between organic molecules and acute steps and kinks. This could help to better understand and predict the role of organic additives on magnesite growth.

[1] Gautier *et al.* (2012) in prep. [2] Saldi *et al.* (2009) *Geochim. Cosmochim. Acta* **73**, 5646-5657.

Controls on the Carbonation of Steel Slag

ELEANOR J. BERRYMAN[1*], ANTHONY E. WILLIAMS-JONES[1], ARTASCHES A. MIGDISOV[1], SIEGER VAN DER LAAN[2]

[1]McGill University, Montreal, Canada, berryman.eleanor@gmail.com(* presenting author)
[2]Tata Steel RD&T, IJmuiden, The Netherlands

Goals and Methodology

Mineral carbonation provides a robust method for permanent sequestration of CO_2 that is environmentally inert. Larnite (Ca_2SiO_4), the major constituent of steel slag, reacts readily with aqueous CO_2 [1]. Consequently, its carbonation offers an exciting opportunity to reduce CO_2 emissions at source [2]. A potential added benefit is that this treatment may render steel slag suitable for recycling. This study investigates the impact of temperature, fluid flux and reaction gradient on the dissolution and carbonation of steel slag, and is part of a larger study designed to determine the conditions under which conversion of larnite, and other calcium silicates, to calcite is optimized.

The experiments were conducted on 2 – 3 mm diameter steel slag grains supplied by Tata Steel RD&T. A CO_2-saturated aqueous fluid was pumped through a steel flow-through reactor containing these grains at a temperature between 120°C to 200°C; the fluid pressure was 250 bar. Fluid flux was varied between 0.8 and 6 mL/min/cm^2. The duration of experiments ranged from 3 to 7 days.

Results

The steel slag grains reacted with the CO_2-saturated aqueous fluid to form phosphorus-bearing Ca-carbonate phases. At high fluid flux, these phases dissolved at the edges of grains, leaving behind a porous aluminium and iron oxide rind. Increasing temperature increased the rate of this reaction. At low fluid flux, carbonates precipitated on the slag grain surface inhibiting further reaction. In contrast, at intermediate fluid flux, dissolution of the primary Ca-bearing minerals was balanced by precipitation of carbonate phases, thereby optimising carbonation of the steel slag.

Conclusions

These results of this study show that carbonation of steel slag by aqueous CO_2 is feasible using relatively large grains and that it can be optimised by varying fluid flux. Experiments of the type described above will contribute to the eventual global reduction of industrial CO_2 emissions.

[1] Santos et al. (2009) *Journal of Hazardous Materials* **168**, 1397-1403.
[2] Berryman et al. (2011) *Mineralogical Magazine* **73(3)**, 522.

CO_2 attack of a caprock-type argillite: From lab experiments to modeling

GUILLAUME BERTHE[1,2*], SEBASTIEN SAVOYE[3], CHARLESWITTEBROODT[1], JEAN-LUC MICHELOT[2]

[1]IRSN, DEI/SARG/LR2S,92260 Fontenay-aux-Roses, France
[2]IDES,CNRS-Université Paris-Sud F-91405 Orsay, France
[3]CEA, DEN/DANS/L3MR, F-91191 Gif-sur-Yvette, France
guillaume.berthe@cea.fr (*presenting author)

Introduction

In the case of a CO_2 storage in geological media, the understanding of the behavior of the caprock encountering an acid fluid is crucial. A set of twenty "dynamic" through-diffusion experiments was performed to investigate the changes in chemical and physical properties of a caprock-type argillite.

Methods

The "dynamic" through-diffusion setup enables, during the CO_2 attack, (i) a monitoring of the ion concentrations in the upstream and the downstream reservoirs and, (ii) an estimate of the transport property change, using HTO, HDO, ^{36}Cl and Br^- as tracers [1]. The impact of several parameters on the caprock behavior was studied, such as the amount of carbonate minerals, the sample thickness, the upstream volume, the presence or not of calcite-filled fracture and the bedding plane orientation regarding the diffusion.

Results and Discussion

The results showed that the extent of the reaction front, lowering the caprock confinement properties, would be more related to the initial rock transport properties and the calcite texture than the amount of carbonate minerals.

This large set of experimental data acquired, allowed us to identify from the chemistry-transport modeling some key parameters, such as the kinetic rate equations used for describing the dissolution/precipitation reactions (Figure 1).

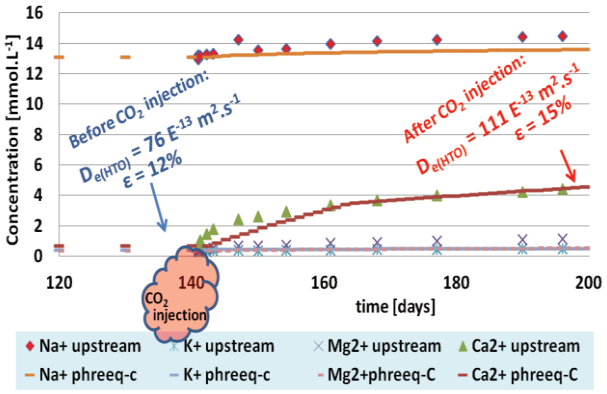

Figure 1: Comparison of experimental concentrations measured in the upstream reservoir with the simulated ones obtained by means of PHREEQC using rate equations from [2].

[1] Savoye *et.al.* (2010) *Environ. Sci. Techn.* **44**, 3698-3704.
[2] Palandri *et al* (2004) USGS, open file report 2004-1068, 64 pp.

Can we use ice sheet reconstructions to constrain meltwater for deglacial simulations?

INGO BETHKE[12]*, CAMILLE LI[12] AND KERIM H. NISANCIOGLU[12]

[1]Bjerknes Centre for Climate Research, Bergen, Norway, ingo.bethke@bjerknes.uib.no (* presenting author)
[2]Uni Research, Bergen, Norway

Abstract

Freshwater pulses from melting ice sheets are thought to be important for driving climate variability. This study investigates challenges in simulating and understanding deglacial climate evolution within this framework, with emphasis on uncertainties in the ocean overturning sensitivity to meltwater inputs. The response of the model used in this study to a single Northern Hemisphere (NH) meltwater pulse is familiar: a weakening of the overturning circulation, an expansion of NH sea ice cover and a meridional temperature seesaw. Nonlinear processes are vital in shaping this response, and are found to have a decisive influence when more complex scenarios with a history of pulses are involved. For this study, a meltwater history for the last deglaciation (21-9 ka) was computed from the ICE-5G ice sheet reconstruction, and the meltwater was routed into the ocean through idealized ice sheet drainages. Forced with this meltwater history, model configurations with different freshwater sensitivities produce a range of outcomes for the deglaciation. Theses outcomes are determined by the thresholds for collapse and resumption of the overturning circulation, as well as the dependence of the sensitivity on the changing background climate. For all sensitivity configurations, there is a mismatch between the simulated deglaciation and proxy records, indicating that uncertainties in the meltwater scenario play an important role as well. This study illustrates that current uncertainties in model sensitivity to freshwater and meltwater reconstructions are limiting in efforts to forward-model deglacial climate variability using data-constrained meltwater forcing scenarios.

Strata-specific bacterial diversity in aquifers of the Thuringian Basin/Germany

A. BEYER[1;2*], M. LONSCHINSKI[2], E. KOTHE[1], G. BÜCHEL[2],

[1] Friedrich Schiller University, Institute of Microbiology-Microbial Phytopathology, Jena, Germany
andrea-beyer@uni-jena.de (*presenting author)
erika.kothe@rz.uni-jena.de
[2] Friedrich Schiller University, Institute of Applied Geology, Jena, Germany
georg.buechel@uni-jena.de
martin.lonschinski@uni-jena.de

The INFLUINS (Integrated fluid dynamics in sedimentary basins) project investigates coupled dynamics of near surface and deep flow patterns of fluids, transported materials and component substances in the Thuringian Basin. The extensive basin landscape is located in eastern Germany and belongs to the Triassic period of Bunter sandstone (Buntsandstein), shell limestone (Muschelkalk) and Keuper, which crop out at the surface. Older sediments and Permian (Zechstein) can be found at the edges of the basin. With microbial investigations, we are analyzing the bacterial diversity of ground- and mineral water at different locations to see whether there are special patterns in bacterial distributions originating from the different rock strata. This will facilitate understanding fluid movement in the Thuringian Basin. We determined bacterial diversity from water samples out of two natural springs and ten groundwater wells by cultivation and subsequent morphological, physiological and molecular identification. To elucidate differences to other rock strata, we compared these samples to two brine springs (4.62 M and 1.03 M salt content), located in Permian aquifers. First results show that the largest proportions were found to be members of Bacilli and γ- proteobacteria, including the genera *Pseudomonas* and *Bacillus*. Next steps will be a comparison of cultivation-dependent and cultivation-independent methods to gain further information on bacterial strains which where uncultivable or suppressed by other bacteria strains.

Trends in Solute fluxes across a 3.8 km elevation transection from Narayani river system in central Himalaya

M.P. BHATT, J. HARTMANN

KlimaCampus, University of Hamburg, Hamburg, Germany, maya.bhatt@zmaw.de

Chemical weathering is an integral part of the rock and carbon cycles and rates vary largely. To study the variability of chemical weathering rates and controls within a mountainuous system, the hydrochemistry along the Narayani basin in central Himalaya region has been sampled including glacial meltwater samples of the upstream Langtang glacier.

Cation composition of the water was dominated by carbonate and silicate dissolution. Preliminary results based on samples of the first months show that concentration of measured chemical parameters such as the sum of base cations, dissolved silica and alkalinity decreased exponentially with elevation (from 169 m to 3989 m). Contribution of sea-salt appeared negligible to the total mass of solute along the drainage network except for the lowermost elevation site. The export of sea-salt corrected sulfate at the outlet point of the Narayani river suggests pyrite dissolution as its main source. Thus the oxidation of sulfide minerals might regulate significantly the dissolution of minerals within the basin. Export of nitrate from the Narayani basin appeared many fold higher than observed fluxes in the Langtang sub-basin, located upstream in the upper Himalaya.

First results suggest that area specific cationic and silica weathering fluxes were comparable with previous reports from the region but appeared to be increased at lower latitudes if compared to the upper Himalayan section of the basin and the world average. Human influence, primarily agricultural activities, may have increased the rate to some extent. Preliminary results of the weathering advance rate of the basin, at the terminus of the Himalaya, also appeared increased compared to large river systems of the world [1, 2, 3]. Influence of controlling factors like relief, physical erosion rates, temperature and precipitation will be discussed.

[1] Navarre-Sitchler & Brantley (2007) *EPSL* **261**, 321-334.
[2] Meybeck and Ragu (1997) *UNEP*, 245p.
[3] Gaillardet et al. (1999) *CG* **159**, 3-30.

Monitoring of Oxidation-Reduction Reactions between redox active Fe and Cysteine : Spectroscopic studies and Multiplet Calculations

AMRITA BHATTACHARYYA[1*], JOSEPH DVORAK[2], ELI STAVITSKI[2] AND CARMEN ENID MARTÍNEZ[1]

[1] The Pennsylvania State University, Department of Crop and Soil Sciences, University Park, USA, axb1000@psu.edu (* presenting author), cem17@psu.edu

[2] Brookhaven National Laboratory, National Synchrotron Light Source, Upton, USA, jdvorak@bnl.gov, istavitski@bnl.gov

Section Heading

Introduction This study aims to monitor the electron exchange interactions between the Fe(II,III) center and the different functional groups of cysteine (carboxylic, amine and thiol) with time using X-ray absorption spectroscopy. We present the XANES spectra of Fe(II,III)-cysteine complexes at all relevant absorption edges (Fe L-edge and C, N,O and S K-edges) collected at different times (0,2,10 and 12 months) after the initial synthesis of the complexes as well as the Fe K-edge EXAFS of Fe(II,III)-cysteine complexes, also as a function of time. The experimental results are compared with multiplet and quantum mechanical simulations, providing a detailed picture of the iron-ligand structure, co-ordination, and electron shuttling capabilities of the complex.

Results and Conclusion

The Fe L-edge XANES of Fe(III)-cysteine indicates an initial reduction of Fe(III) caused by an internal electron transfer reaction either from N of $–NH_2$ or S of -SH, both of which show oxidation in their respective spectral features. The N K-edge of Fe(II) cysteine at all time scales did not show much variation and is identical to the N spectrum of cysteine. The N of Fe(III) cysteine showed oxidation of N (to nitrate, a +5 oxidation state of N) at time scales 0, 10 and 12 months; however, at time=2 months the N spectral features resemble that of N in cysteine. The O K-edge spectra for Fe(II) cysteine shows a change in spectral pattern with passage of time whereas that for Fe(III) cysteine does not change much after the time of initial synthesis and had characteristics similar to that of O in cysteine. Oxidation of Fe(II) in Fe(II)-cysteine with time was accompanied by a simultaneous reduction of the C as revealed by the C K-edge features of Fe(II) cysteine. This is reflected in a reduction of the C which involves an electron exchange of the C within the unsaturated –COOH of cysteine. In contrast, the C K-edge features for Fe(III) cysteine show no variation with time. The S K-edge of Fe(II) cysteine show S oxidation states intermediate between sulfoxide and sulfate. Overall, spectral characteristics of Fe(II,III)-cysteine complexes suggest thiol/disulfide exchange, H-atom transfer, or electron transfer between Fe and cysteine. Our studies of the Fe(II,III)-cysteine system provide a mechanistic understanding of the electron shuttling that occurs between a redox active metal and a redox active ligand. In this particular case, cysteine represents an organic molecule with functionalities (O-, S-, N- functional groups) and a C backbone that may mimic the functional groups present in organic matter from terrestrial and aquatic environments.

High resolution rare earth element (REE) study on mussel shells, a proxy for the geochemical cycling at the coastal region?

NANXI BIAN[1*], PAMELA A. MARTIN [2], ALBERT COLMAN[1] AND CATHERINE PFISTER[3]

[1]Department of Geophysical Sciences, the University of Chicago, Chicago, IL, USA, nanxibian@uchicago.edu

[2]Department of Earth and Environmental Sciences, IUPUI, Indianapolis, IN, USA

[3]Department of Ecology and Evolution, University of Chicago, Chicago, IL, USA

Trace and minor element variations in biogenic calcium carbonate shells have been widely applied in reconstruction of past environmental conditions [1,2,3]. Successively deposited biogenic calcareous shells, such as mussel shells, may have the potential to provide high resolution records of temporally resolved variability to investigate changes in climatic configurations and/or geochemical cycling where instrumental records are non-existent. In our previous work, we developed a high precision analytical method, using laser ablation coupled with sector field inductively coupled plasma mass spectrometry (LA-ICP-MS), to obtain high resolution time series of a suite of element/Ca ratios for mussel shells [4]. Here, we investigate the potential of one species of mussels, *Mytilus californianus*, to provide high-resolution records of coastal geochemical changes.

Mussel shell samples used in this study are from Tatoosh Island, Washington, USA, a coastal upwelling region where 11 years of instrumental records are avaialble to calibrate shell chemistry on modern shells. Age models of the shells are anchored by stable isotope analysis on seasonally resolved micromilled shell material. An anti-correlated relationship between rare earth element (REE)/Ca and $\delta^{18}O$ is apparent upon comparison of the two records. A reliable shell age model is then constructed by combining both high resolution REE/Ca records and the seasonally resolved $\delta^{18}O$ records. Multi-Taper Method (MTM) spectral analysis was applied to identify significant quasi-periodic variability in shell REE/Ca records [5]. An intra-annual (3-5 cycles/year) periodic component has been identified in both modern and midden shells; similar periodic variability was also observed in the high resolution instrumental data for evironmental parameters, such as upwelling and temperature. Calculated Ce anormalies (Ce*), a proxy for redox state in the water column, show similar ranges of variations in modern and acient shells. Our results indicate REE/Ca ratios in mussel shells have the potential to serve as a proxy for the geochemical cycling at this coastal area and could possiblly offer hints for explaining the recent and dramatic pH declines at this location [6].

[1] Klein et al. (1996) *Geology* **24**, 415-418. [2] Lea et al. (1999) *GCA* **63**, 2369-2379. [3] Wyndham et al. (2004) *GCA* **68**, 2067-2080. [4] Bian et al. (2012) *GCA*, submitted. [5] Mann and Lees (1996) *Climate Change* ***33***, 409-445. [6] Wootton et al. (2008) *PNAS* ***105***, 18848-18853.

Molecular structure and acidity

BARRY BICKMORE[1]*, JOSHUA MAURER[1], AND KENDRICK SHEPHERD[1]

[1]Brigham Young University, Geological Sciences, Provo, UT, USA barry_bickmore@byu.edu (*presenting author), josh3996@gmail.com, kenear@gmail.com

Surface complexation models (SCMs) are often capable of fitting the same macroscopic data (e.g., titration data) by employing substantially different assumptions about molecular-scale reactions. This has been addressed by constraining SCMs with 1) more macroscopic data and information about molecular-scale processes obtained from 2) advanced spectroscopic techniques, 3) molecular modeling studies, and 4) quantitative structure-activity relationships (QSARs) like MUSIC [1]. All of these are reasonable, but even given the first three options, QSARs would still be necessary to provide a conceptual framework for interpreting the other types of results.

A problem with QSARs is that they assume only certain aspects of the molecular structure determine a particular type of reactivity. Sometimes, however, other structural features are important, but were roughly constant in the calibration set. E.g., MUSIC is calibrated on a certain set of (hydr)oxo-monomers, and assumes only the metal-oxygen bond valences and coordination numbers are important for determining functional group acidities. The model is then applied to the acidities of oxide surface functional groups, which are much more difficult to experimentally determine.

Are the MUSIC predictions always accurate for oxide surface functional group acidity, or are some important structural features missing from the model? Our previous work [2] used an expanded calibration set of solution monomers to show that in addition to bond valence and coordination number, the electronegativity of the metal atoms is also necessary to accurately predict acidity, but we provided no compelling structural explanation.

We are now assembling a complete potential energy model, based largely on the Bond-Valence Model (BVM), to guide development of QSARs based on the BVM. Our model combines the predictions of the VSEPR model of molecular geometry with the BVM, using the concept of bond valence vectors [3], along with van der Waals and electrostatic potentials to describe non-bonded interactions. So far, we have been able to show that changes in Me-H van der Waals potential energies due to structural relaxation are likely to be important for determining acidity in our calibration set of oxyacids, and that this effect is highly correlated with the electronegativity of the metal atoms. Thus, we have found a way to explain our previous results in structural terms, and a way to determine how an acidity QSAR based on bond valence, coordination number, and acidity might be successfully transferred to oxided surfaces. This kind of theoretical guidance for creating and transferring QSARs is essential for systems like mineral-water interfaces, where it is often difficult to check the veracity of model results at the molecular scale.

[1] Hiemstra *et al*. (1996) *J. Colloid Interface Sci*., **184,** 680–692. [2] Bickmore *et al.* (2006) *GCA* **70**, 4057-4071. [3] Harvey et al. (2006) *Acta Crstallographica*, B62, 1038-1042.

Very fast silicic magma genesis in caldera and rift environments based on isotope zoning in zircons, experiments, and thermal modeling

BINDEMAN IN[1]*, LUNDSTROM C.[2], SCHMITT AK[3], SIMAKIN[4] A., SELIGMAN A.[1] AND DREW D[1]

[1]Geol Sci, Univ of Oregon, Eugene, USA, bindeman@uoregon.edu (*presenting), [2]University of Illinois, Urbana-Champaign, IL, USA, [3]Earth Space Sci, UCLA, Los Angeles, CA, USA, [4]Inst Physics Earth, Moscow, Russia

Large-volume sub-liquidus silicic rocks are erupted in caldera environments with short repose time. Modern in situ isotopic methods have recently permitted analysis of isotopic and trace elemental abundances on micron to smaller scale and demonstrate strong crystalline heterogeneity. We review recent discoveries of isotopically (O, U-Pb) zircons in large volume ignimbrites (Snake River Plain, Kamchatka, and Iceland).

We report results from a long-duration isotope exchange experiment with natural zircon and rutile that was held for 4 months at 850°C and 0.3 kbars in a silica-rich solution doped with ^{18}O, ^{2}H, ^{7}Li and ^{10}B. The length-scales of in-diffusion were examined by depth profiling using time-of-flight (TOF) and Cameca 1270 high-sensitivity dynamic SIMS. Rutile and zircon developed ~2 μm and ≤0.13μm Fickian profiles, respectively, suggesting that rutile diffusion coefficients were at ~400 times greater than zircon's, and both are consistent with the wet diffusion coefficients for zircons and rutiles reported by Watson and Cherniak (1997) and Moore et al (1998). These results are relevant for interpreting timescales of magma evolution, in particular those related to controversial sharp intra-crystal zircon oxygen isotopic gradients. We instead consider sharp boundaries to be related to rapid episodes of solution-reprecipitation that outpace diffusive exchange, and generate concave-up zircon crystal size distributions (CSDs). Isotopic profiles in natural zircons will translate into 100-1000 yrs residence and characterize 100-1000 km^3 volumes of near-liquidus magmas.

Given diffusive-equilibration and recrystallization timescales, these new results call for very fast magma segregation from diverse in $\delta^{18}O$ hydrothermally-altered protoliths, occuring rapidly at shallow depths. As oxygen is a major component of silicates and oxides, isotopic variation of several permil reflect tens of percent of mass addition. Isotopic diversity in zircons spanning 2-7‰ $\delta^{18}O$ characterize near-liquidus magmas of 100-1000km^3 volume. Coexisting high, normal and low-$\delta^{18}O$ zircons indicate contributions from diverse protoliths, and convective mixing on 10^2-10^3 yr. timescales comparable to mineral-diffusive, solution-reprecipitation, and crystal size distribution timescales. Modeled convective rates of silicic magmas are fast enough to homogenize ~1000 km^3 magma over 10^4 yr. timescales.

Numerical experiments demonstrate the feasibility of rapid (10m/yr) convective melting rate which may translate into >10km^3/yr magma production rates over spatial dimensions of typical calderas. We suggest that neither conductive cooling nor hydrothermal refrigeration are capable of dissipating heat sufficiently fast to prevent catastrophic melting.

Evidence for a mid-crustal channel flow during the Sveconorwegian orogeny of Baltica ?

B. BINGEN [1*], G. VIOLA [1,2], K. YI [3] AND A.K. ENGVIK [1]

[1]Geological Survey of Norway, 7491 Trondheim, Norway, bernard.bingen@ngu.no (* presenting author)
[2]Norwegian University of Science and Technology, 7491 Trondheim, Norway, giulio.viola@ngu.no
[3]Korea Basic Science Institute, 363-883 Chungbuk, South Korea, kyi@kbsi.re.kr

New structural, petrological and SIMS U-Pb zircon data from SE Norway suggest that a mid-crustal channel flow may have developed during the main Sveconorwegian orogenic phase at the margin of Baltica. The 500 km wide Sveconorwegian orogen is interpreted as the product of a hot and long-lived, polyphase, bivergent orogeny, resulting from the collision of Baltica with another major plate (Amazonia, Laurentia) at the end of the Mesoproterozoic. The Sveconorwegian orogen is built on Mesoproterozoic crust that youngs toward the west. The orogeny followed a voluminous 1200-1130 Ma bimodal, within-plate magmatism in the west, more extensive than previously assumed. High-pressure (HP) metamorphic rocks are only recorded in the east of the orogen. These three observations suggest a warm lithosphere at the onset of orogeny, increasingly warmer toward the west. At around 1080 Ma, Bamble and Kongsberg were thrusted westwards on top of Telemark marking the onset of collisional tectonics. The main orogenic phase started at c. 1050 Ma. In the Idefjorden terrane, HP granulite-facies mafic boudins and kyanite gneisses locally record conditions of c. 930 °C - 1.3 GPa at c. 1050 Ma. This was followed by widespread LP amphibolite-facies partial melting. Leucosomes associated with top-to-the-west regional kinematics and resulting from muscovite-, biotite- and amphibole-dehydration melting of orthogneiss and paragneiss, range in age from 1039 ± 17 to 997 ± 16 Ma, as provided by low-U zircon rims. This partial melting episode was coeval with metamorphism along the Vardefjell shear zone bounding the Idefjorden terrane in the west, and coeval with widespread syn-collisional granitic plutonism and LP amphibolite- to granulite-facies metamorphism in the west of the orogen in Rogaland-Vest Agder. The reported long-lived high-grade conditions suggest development of a mid-crustal west-directed (?) channel flow activated after c. 1040 Ma, probably associated with a slowly eroding orogenic plateau. Lack of foreland basins to the east of the orogen is consistent with west directed flow. In this model, the low-grade Telemark supracrustals may belong to a shallow orogenic lid, covering a large area in the centre the orogen and characterized by deposition of immature sediments in grabens (Eidsborg Fm <1118 Ma, Kalhovde Fm <1065 Ma). At c. 980 Ma, the Sveconorwegian orogeny propagated eastwards in the footwall of the arcuate, southeast-verging, "Mylonite Zone" back-thrust, leading to eclogite-facies metamorphism in the Eastern Segment. Convergence was followed by gravitational collapse after c. 970 Ma. High-grade LP conditions were maintained in Rogaland-Vest Agder until c. 930 Ma and were associated with voluminous post-collisional plutonism, including anorthosites.

Isotopic fractionation between Cr^{3+} species in aqueous solutions

JEAN LOUIS BIRCK[1*], TU-HAN LUU[1,2], AND ROXANE JOURDAIN[1,3]

[1]IPGP, Paris, France, birck@ipgp.fr (*presenting author)
[2] luu@ipgp.fr
[3]roxanejourdain@gmail.com

When chromium is oxidized from the 3+ to the 6+ state, the 6+ species displays a δCr_{53-52} of up to 7 permil ($^{o}/_{oo}$) relative to the 3+ state [1-3]. Here we show that large fractionation predicted by theory [4] within the same oxidation state (3+) can also be evidenced. Cations are present in different species which result from the interaction with the anions present in the solution. Chromium has the property similar to only a few other elements (e.g. Os) that coexisting species do not re-equilibrate immediately when the medium changes (e.g. by dilution or by addition of an acid). In contrast to most cations which interact instantaneously with the aqueous solvent, Cr^{3+} requires several days at room temperature in HCl solution for the different species to reach equilibrium.

Procedure

This property which is usually a drawback for a clean separation of Cr from other elements [5] can be used for identification purposes as described in the following. A chromium III standard solution was made in HCl 6N to produce easily measurable amounts of chlorocomplexes and was left for several days to reach equilibrium. A chromatographic separation [5] was achieved in less than 30mn to avoid significant kinetic isotopic effects. The isotopic ratios of the different hydrated chlorocomplexes as well as the Cl free hydrated $[Cr(H_2O)_6]^{3+}$ cation were measured by high precicion MC-ICPMS at medium mass resolution (ca 4000) with a precision of $0.05^{o}/_{oo}$.

Results and conclusion

The $[Cr(H_2O)_6]^{3+}$ species shows an excess in δCr_{53-52} of 2.37 ± 0.05 $^{o}/_{oo}$ relative to the starting Cr solution. $[CrCl(H_2O)_5]^{2+}$ displays a deficit in δCr_{53-52} of -0.03 ± 0.05 $^{o}/_{oo}$. The higher complexes $[CrCl_x(H_2O)_{(6-x)}]^{(3-x)+}$ x>1 which have not yet been resolved in the chemical separation display alltogether a deficit of δCr_{53-52}: -0.39 ± 0.05 $^{o}/_{oo}$. HBr and H_2SO_4 media have also been investigated; they yield negative values for $[Cr(H_2O)_6]^{3+}$ which are interpreted as being dominated by kinetic effects during the hydrolysis of the anion-chromium complexes.

The results for the HCl media are in a first order agreement with the theoretical estimates of Schauble et al. [1]. Whether the significant fractionation that may occur in solutions within the Cr^{3+} oxidation state has an impact in natural samples has to be investigated.

[1] Johnson, Bullen (2004) Rev. Min. & Geochem. **55,** 289-319. [2] Ellis et al. (2002) Science 295, 2060-2062. [3] Frei *et al.* (2009) Nature **461**,250-253. [4] Schauble et *al.* (2004) Chem. Geol. **205**, 99-114. [5] Strelow (1973) in Ion exchange and solvent extraction Marcel Dekker. **5**, 121-206

The solubility of amorphous aluminous silica between 100 - 350°C: Implications for scaling in geothermal power stations

JULIA. K. BJÖRKE [1, 2*]; BRUCE. W. MOUNTAIN [2]; TERRY. M. SEWARD[1]

[1]Victoria University, Wellington, New Zealand, j.bjorke@gns.cri.nz (*presenting author), terry.seward@vuw.ac.nz
[2]GNS Science, Wairakei Research Centre, Taupo, New Zealand, b.mountain@gns.cri.nz

Scaling is a common problem in geothermal power plants. In particular it occurs from brines where minerals become saturated and precipitate. To prevent scaling, geochemists use thermodynamic modelling to apply treatment methods, such as adjusting temperature or pH. Amorphous aluminous silica scaling has been reported in many geothermal power plants such as in New Zealand, Philippines, Salton Sea, Japan and Iceland [1]. Currently, the sole study on the solubility of amorphous aluminous silica was carried out by Gallup 1998 [2]. These were simple batch experiments in which there was no control on pH or Al concentration. A general reaction can be written for the precipitation of this phase as:

$$xH_4SiO_4 + yAl(OH)_4^- + yH^+ = xSiO_2.yAlO_{1.5} + (2x + 2.5y)H_2O.$$

Unlike amorphous silica precipitation, this reaction is pH and Al concentration dependent over a wide region of pH. Unfortunately, there have been no well-controlled experiments to determine thermodynamic data for this reaction.

Preliminary calculations, using the data of Gallup 1998 [2], were used to estimate the solubility of amorphous aluminous silica and compare it with the solubility of pure silica. These show that scaling, caused by amorphous aluminous silica, can occur at temperatures up to 50°C higher than for pure silica, based on the chemistry of a cooling, flashed Ohaaki brine.

Four samples of amorphous aluminous silica scale were collected from Wairakei and Ohaaki geothermal power plants. XRD, XRF and SEM analyses were carried out on the samples and to verify that Al was not present as a distinct Al phase from the amorphous silica. Results from the XRD analyses showed amorphous material with quartz peaks in all samples. XRF results show concentrations of SiO_2 ranging from 73.89-76.70%, Al_2O_3 from 8.38-10.46%, K_2O from 2.13-3.05%, Na_2O from 1.72-2.15%, CaO from 1.08-2.13% and MgO from 0.06-1.99%. Other oxides were less than 1% of the total sample. XRD results and EDX mapping by SEM verified that Al is present within the silica and is not in a distinct phase. Al concentration is zoned and correlates with increases in alkali concentration.

Experiments are planned to investigate the solubility of amorphous aluminous silica in the temperature range 100 - 350°C. These will be conducted at saturated vapor pressure and with varying pH using a continuous flow-through system and batch reactors.

[1] Gallup (1997) *Geothermics* **26**, 483-499. [2] Gallup (1998) *Geothermics* **27**, 485-501.

Oxygen consumption by granite samples under sterile glacial melt water conditions

EVA BJÖRKMAN[1], DAQING CUI[1,2], AND IGNASI PUIGDOMENECH[3*]

[1]Mat. & Env. Chem., Stockholm University, Stockholm, Sweden, eva.bjorkman@mmk.su.se (* presenting author)
[2]Studsvik, Nyköping, Sweden, daqing.cui@studsvik.se
[3]Swedish Nuclear Fuel and Waste Management Co (SKB), Stockholm, Sweden, ignasi@skb.se

Background

During future glacial periods in Fennoscandia it may not be excluded that, at least temporarily, increased groundwater recharge and flows may occur. The glacial melt water may have large amounts of dissolved O_2, and this might affect the stability of spent nuclear fuel canisters in the repositories planned in Sweden and Finland [1]. Several processes are able to remove dissolved oxygen: reactions with Fe(II) and sulphide minerals in the rock matrix and in fracture fillings and microbial processes consuming CH_4 or DOC [2].

As the availability of microbial substrates might be substantially reduced during glacial periods, there is a need to confirm the consumption of O_2 by abiotic reactions with Fe(II) minerals. The relative importance of inorganic and microbial processes is difficult to obtain unless special precautions are taken [3,4]

Experimental details

Batch experiments were performed at ~22°C under sterile conditions in serum bottles filled with minerals, MQ sterilized water and a gas phase containing N_2 at ~1.3 bar to which a known amount of air was added. The O_2 in the head-space gas was analyzed for up to 727 days by GC, using the Ar in the injected air as reference.

Two different rock types were used: a quartz monzodiorite and a fine-grained granite with several size fractions ranging between 0.25 and 10 mm. A chlorite sample was used as a Fe(II)-rich reference mineral, and quartz and pure water as un-reactive controls. The materials were characterized by BET, pore size distribution, Mösbauer, and chemical analysis.

Results and Conclusions

The quartz and water samples showed stable O_2 concentration within ±500 ppm while oxygen decreased to different degrees in the rock samples and it was completely exhausted in the chlorite experiments demonstrating oxygen consumption by Fe(II) under sterile conditions. The importance of the surface area is evidenced from the reaction rates expressed as "moles O_2 day^{-1} m^{-2}" which overall vary between -2.7×10^{-8} and -1.3×10^{-8} independent on mineral type, iron content or size fraction used.

The rates obtained are comparable to previous laboratory studies and support the long-term safety evaluation [1] of spent nuclear fuel repositories during glacial periods.

[1] Sidborn *et al* (2010) *Report SKB-TR-10-57*. [2] MacQuarrie et al (2010) *J. Contaminant Hydrol.* **112**, 64-76. [3] Puigdomenech *et al* (2000) *Scient. Basis Nucl. Waste Manag. XXIII*. (Smith & Shoesmith eds) 179-184. [4]Trotignon *et al* (2002) *Geochim. Cosmochim. Acta* **66**, 2583-2601.

A thermal and erosional history of cratonic lithosphere over billion-year time scales

TERRENCE BLACKBURN[1*], SAMUEL BOWRING[1], TAYLOR PERRON[1], KEVIN MAHAN[2], FRANCIS DUDAS[1]

[1]EAPS, MIT, Cambridge, MA, USA (*correspondance: terrence@mit.edu)
[2] Dept of Geol. Sci., Univ. of CU Boulder, CO, USA

The continental lithosphere contains the oldest and most stable structures on Earth, where fragments of ancient material have withstood destruction by tectonic and surface processes operating over billions of years. Though present-day erosion of in these remnants is slow, a record of how they have uplifted, eroded and cooled over Earth's history can provide insight into the composition and density of the continents and forces operating to exhume them over geologic time. Because the exhumation or burial of the Earth's surface has a direct effect on the rate of heat loss within the lithosphere, a continuous record of lithosphere exhumation can be reconstructed through the use of a temperature-sensitive radiometric dating technique known as thermochronology. The combination of thermochronologic data with thermal models for heat transfer in the lithosphere can be used to measure the processes operating to cool or heat the lithosphere in the geologic past. Thermochronologic systems sensitive to cooling at high temperatures is insensitive to the "noise" associated with near-surface cooling and therefore provides a measure of the background rate of erosion or burial associated with the vertical motions of a craton. The U-Pb thermochronologic system is sensitive to cooling at temperatures of ~400-650 °C, corresponding to lower crustal depths in cratonic regions of ~20-50 km. Here we utilize this technique to reconstruct an ancient and long-lived thermal history of volcanically exhumed lower crustal fragments, samples that resided at depth for billions of years before recent volcanism transported them to the surface as xenoliths. A high fidelity reconstruction of time-temperature paths for these samples is produced using the U-Pb system's dual decay scheme, where parent isotopes 238U and 235U decay at different rates to daughter isotopes 206Pb and 207Pb, respectively. Coupling this dual isotopic system with diffusion's length scale dependency, which causes different crystal sizes to retain Pb over different absolute time scales, results in a set of daughter isotopic compositions for a range of crystal sizes that is unique to the time-temperature history of the sample. Combining these measurements with thermal and Pb-diffusion models constrains the range of possible erosion histories. Measured U-Pb data are consistent with near zero erosion rates persisting over time scales approaching the age of the continents themselves. This indicates that the isostatic balance observed in the present-day continents has been largely maintained over geologic time, extending back at least to the onset of cooling within each terrane. Since this stability was first meet, the craton has experienced a balance between erosion and burial, with a corollary balance between the lithosphere's internal buoyancy forces and near zero isostatic uplift, further indicating a minimal change in the relative densities of the lithosphere and mantle over intervals lasting billions of years.

DATING FLUID FLOW EVENTS IN A SHALLOW SEDIMENTARY BASIN: THE KEY CONTRIBUTION OF K-Ar GEOCHRONOLOGY OF AUTHIGENIC ILLITE

THOMAS BLAISE[1,2,*], NORBERT CLAUER[3], MICHEL CATHELINEAU[1], PHILIPPE BOULVAIS[4], MARIE-CHRISTINE BOIRON[1], ISABELLE TECHER[5], ALEXANDRE TARANTOLA[1], PHILIPPE LANDREIN[2]

[1]G2R, Univ. Lorraine, France ; * thomas.blaise@G2R.uhp-nancy.fr
[2]ANDRA, Chatenay-Malabry, France
[3]LHyGES, Univ. Strasbourg, France
[4]Geosciences Rennes, France
[5]GIS, Univ. Nîmes, France

In shallow parts of sedimentary basins, low-temperature diagenetic processes (<90-100°C) produce discrete mineralogical changes on both the carbonates and clays. These processes are somehow challenging to investigate as most of the geothermometers are at their application limits. Furthermore, the low concentrations of trace elements in the newly-formed minerals (e.g., REE in fluorite, U in calcite) complicate the dating attempts. In this context, this study presents petrographic and geochemical data acquired on secondary minerals filling the fractures, vugs and primary porosity of three aquifers of the Mesozoic sedimentary sequence from Paris Basin, France.

The Oxfordian and Middle Jurassic limestone aquifers located respectively above and below Callovian-Oxfordian claystones are essentially cemented by successive stages of blocky calcite. Isotopic tracing ($\delta^{18}O$, $\delta^{13}C$ and $^{87}Sr/^{86}Sr$) and data acquired on hosted fluid inclusions (salinity, δD of paleo-fluids) reveal that the physical-chemical properties of calcite-forming waters were rather different for each of the aquifers and from present-day groundwaters. The aquifer located in Lower Triassic siliciclastic sedimentary rocks is buried at a 2000m depth and evidences a diagenetic alteration, among which quartz overgrowth, adularia precipitation and widespread illitization. Illite nanometric particles (<0.02 and 0.02-0.05 µm fractions) were separated, analyzed (DRX, EDS microprobe, $\delta^{18}O$, $^{87}Sr/^{86}Sr$) and K-Ar dated. Two ranges of K-Ar ages were obtained: 183 ± 2 Ma (2 samples), 150 ± 2 Ma (7 samples) and an additional age at 116 ± 2Ma. All ages are consistently younger than the Triassic sedimentation. They further strongly suggest that at least two mineralizing fluid flows occurred before the maximal burial of the sediments (Upper Cretaceous). These ages fit with the identified episodes of successive opening stages of the central Atlantic Ocean where increasing heat flows and associated fluid circulations have induced: (i) several Pb-Zn-F-Ba mineralizations along the margin of the basin, and (ii) extensive illitization in Triassic and Permian sandstones in many locations of Western Europe.

The study shows also that each studied aquifer underwent an individual and specific diagenetic history that highlights the role of the Callovian-Oxfordian claystones as an efficient hydrological barrier between the limestone units. This effective isolation is of major engineering importance as these claystones represent the currently studied target for a long-term geological disposal of radioactive waste.

Complementarity of computational molecular modelling and experimental techniques to study trace elements geochemistry

MARC BLANCHARD[1*]

[1]IMPMC, UPMC, CNRS, 4 place Jussieu, 75252 Paris Cedex 05, France, marc.blanchard@impmc.upmc.fr (* presenting author)

Chemical reactions at the interfaces between soils components and water play an important role in numerous natural processes, like in particular the fate and behaviour of potentially toxic trace metals. One efficient approach has recently emerged to address this question. It consists in the combination of X-ray absorption spectroscopy (XAS) and isotopic techniques. Besides this experimental approach, computational molecular modelling can also contribute significantly to improve our understanding of the atomic-scale processes that control the biogeochemical cycles of trace elements. This presentation will expose the complementarity of both experimental and theoretical approaches. Within the same theoretical framework, it is now possible (i) to calculate the local structural and electronic properties of any atom in the studied system and compare these properties with XAS data, (ii) to model XANES spectra, which allows a better interpretation of spectral features, and (iii) to determine the equilibrium fractionation factors of traditional as well as non-traditional isotopes, associated with any structural site of the system. Several applications will be presented, including the arsenic adsorption complexes at the hematite surface [1], the calculated XANES spectra of 3d transition metal compounds [2], and the isotopic properties of Al- and OH-bearing hematite [3].

[1] Blanchard *et al*. (submitted) *GCA*. [2] Cabaret *et al*. (2010) *PCCP* **12**, 5619-5633. [3] Blanchard *et al*. (2010) *GCA* **74**, 3948-3962.

Time-resolved SAXS study of nucleation and growth of iron(III) oxyhydroxides

MARK W. BLIGH[1*], ANDREW L. ROSE[2], RICHARD N. COLLINS[1], AND T. DAVID WAITE[1]

[1]University of New South Wales, Sydney, Australia, m.bligh@unsw.edu.au (*presenting author), d.waite@unsw.edu.au, richard.collins@unsw.edu.au

[2]Southern Cross University, Lismore, Australia, andrew.rose@scu.edu.au

Introduction.The process of hydrolysis and polymerization of Fe(III) oxyhydroxides plays an important role in the chemistry of natural waters. However, these transformations are rapid and occur over timescales that are much smaller than those typically studied. Time-resolved SAXS studies provide the capacity to investigate nucleation and the evolution of particle size distribution on a sub-second timescale. Different mechanisms of particle production have previously been identified, for example, a nucleation burst followed by monomer addition [1] and, nucleation followed by aggregation [2]. In this study we use TR-SAXS to examine polymerization of Fe(III) oxyhydroxides following rapid mixing, such that mixing times are less than reaction times. In this initial study, at [Fe] = 1 mM, required to produce sufficient scattering intensity, reaction times were sufficiently long only at pH 3 and 4. Investigation of higher pHs will require the optimization of a micro-fluidic device.

Results and Conclusions. The SAXS curves were analysed, both directly and by fitting a pair distance function, to produce values for the invariant Q, zero-angle scattering intensity $I(0)$, and radius of gyration R_g. Q is a measure of the total scattering mass while $I(0)$ is sensitive to particle size and number. At pH 3, with $[NO_3]$ = 6 mM, R_g stabilized at ~25 nm after only 30 s while both Q and $I(0)$ continued to increase till ~300 s. At times >300 s, Q was relatively stable while $I(0)$ decreased. In the same system at pH 4, R_g followed the same pattern as for pH 3, however maximum values for Q and $I(0)$ were attained after ~77 s, and decreased thereafter. These results show that at early times, small but increasing numbers of maximum sized particles coexisted with monomers or oligomers that were too small to scatter significantly in the q-range used to calculate Q. Such a system evolution implies that slow nucleation and relatively rapid particle growth proceeded concurrently until the maximum scattering mass was achieved. Particle growth appears to have occurred via a monomer addition mechanism ('monomers' here may be oligomers) since the stable R_g implies that significant aggregation is not occurring. The more rapid development of the maximum scattering mass at pH 4, compared to pH 3, is consistent with a higher rate of polymerisation of Fe(III) hydrolysis species and therefore more rapid production of stable nuclei. Whether the observed decreases of Q and $I(0)$ following attainment of maximum values are due to sedimentation or further transformation via dissolution and reprecipitation remains unclear and will be the subject of further investigation.

[1] Liu *et al.* (2010) *Langmuir* **26**, 17405-17412. [2] Polte *et al.* (2010) *ACS Nano* **4**, 1076-1082.

Determining garnet crystallization kinetics from growth zoning and Mn-calibrated Sm-Nd ages at Townshend Dam, VT

ROSE A. BLOOM[1*], DAVID M. HIRSCH[1], BESIM DRAGOVICH[2], MATT GATEWOOD[3], ETHAN BAXTER[2], HAROLD STOWELL[3]

[1]Western Washington University, Bellingham, WA USA, bloomr3@students.wwu.edu (* presenting author), hirschd@geol.wwu.edu

[2]Boston University, Boston, MA USA, dragovic@bu.edu, efb@bu.edu

[3]The University of Alabama, Tuscaloosa, AL, USA, matthewpgatewood@gmail.com, hstowell@geo.ua.edu

Introduction

Essential to an understanding of metamorphic rocks are the rates at which a metamorphic reaction can occur. Kinetics of porphyroblast crystallization includes rates of both growth and nucleation. Though some studies have been able to quantify growth rates, direct measurements of nucleation rates have remained enigmatic. We present a method to indirectly measure nucleation as well as growth rates of chemically zoned porphyroblasts by linking chemical and age data.

This project examined a garnet + muscovite + paragonite + biotite + chlorite + quartz + plagioclase schist from the Pinney Hollow formation at Townshend Dam, VT. Biotite-quartz-rich layers alternate with muscovite-paragonite-rich layers on a millimeter scale and define the foliation. Garnets are sub- to euhedral, vary in size from 5 to 30 mm in diameter, and display curved quartz inclusion trails continuous with foliation at the rims.

Method

The specimen was imaged in 3D using high-resolution X-ray computed tomography. Garnet porphyroblasts were extracted and portions of them with quantified Mn content underwent Sm-Nd geochronology methods to produce a Mn-age curve for the rock [1]. A subvolume from the interior of the specimen was separated and disaggregated, allowing extraction of 62 garnets. Morphological centers of each were exposed, polished, and chemically mapped (via SEM-EDS). The EDS characterization facilitated location of peak-Mn regions, from which core-rim linescans were performed via EPMA for quantitative zoning determination. Mn data were converted to ages via reference to the Mn-age curve [1], allowing determination of nucleation and growth kinetics.

Results

Townshend Dam garnets show concentric, smooth Mn zoning curves. Microprobe analyses yield central garnet MnO content ranging from 2.3 to 11 wt%, depending on the size of the garnet. Rims of garnets are Mn-poor with ca. 0.1 to 0.2 wt% MnO. Data collection is ongoing, but preliminary EPMA results indicate that among the analyzed garnets, the range of core X(Mn) is 0.047-0.249, corresponding (via the curve in [1]) to an age range of 384.8-378.1 Ma. Given this duration of nucleation (6.7 m.y.), the number of garnets (62), and the subvolume size (1210 mm^3), we calculate a nucleation rate of approximately 0.0076 nuclei per m.y. per mm^3.

[1] Gatewood et al. (2011) AGU Fall Mtg., Abstract #V13G-05.

Influence of alkalinity on the magnesium composition of amorphous calcium carbonate

CHRISTINA BLUE[1*], NIZHOU HAN[1], AND PATRICIA DOVE[1]

[1]Virginia Tech, Department of Geosciences, Blacksburg, USA cblue@vt.edu (*presenting author)

An increasing number of studies are showing that many calcifying organisms form skeletons by nonclassical growth. This biomineralization process begins with the accumulation of an amorphous precursor phase that subsequently transforms to an organic-mineral composite. Little is known about mineralization by this pathway because the last 50 years of research have focused almost entirely on traditional, step-growth processes.

To investigate the factors that influence the composition of amorphous calcium carbonate (ACC) and quantify their effects, we have developed a procedure for synthesizing this phase under controlled chemical conditions. The method uses a flow through reactor and high precision syringe pumps to prepare ACC from solutions that maintain a constant supersaturation and a well-characterized solution chemistry. This approach confers significant advantages over previous approaches such as the "Koga" method [1], that uses very high pH solutions (11.2–13.5), and the "ammonium carbonate" method [2], that produces highly variable supersaturation conditions and introduces significant amounts of ammonium ion to the mineralizing solution.

Using the new flow-through method, we are investigating the effect of alkalinity on the magnesium content of calcite that forms via the ACC intermediate phase. Previous studies have suggested that the magnesium levels in biogenic calcite may be correlated with the alkalinity of local growth environment [3]. The first phase of this project determined the effect of alkalinity on the magnesium content of the ACC at 24–25°C. The experiments were conducted by preparing two sets of syringes that contained solutions of 1) variable alkalinity using 40mM–150mM $NaHCO_3$ and 2) a 5:1 ratio of Mg:Ca (modern seawater) using $MgCl_2 \bullet 6H_2O$ and $CaCl_2 \bullet 2H_2O$. For the range of alkalinities used in this study, the effluent pH was 9.0–9.3. After achieving steady state output conditions, the ACC products were collected on 0.20 micron nylon mesh filter and characterized using SEM, Raman Spectroscopy, and ICP-OES. Future work will also determine the effect of alkalinity on the composition and structure of calcite that forms by the ACC pathway.

[1] Koga et al. (1998) *Thermochimica Acta,* **318**, 239-244. [2] Han & Aizenberg (2008) *Chem. Mater.,* **20**, 1064-1068. [3] Boyle & Erez (2004) *Eos Trans. AGU, **84(52)**,* Ocean Sci. Meet. Suppl.

Magmatic vs crustal volatiles: a reconnaisance tool for geothermal energy exploration

LARA S. BLYTHE[1*], VALENTIN R. TROLL[1], DAVID R. HILTON[2], FRANCES M. DEEGAN[3], ESTER M. JOLIS[1] AND JAMES STIMAC[4]

[1]Dept. of Earth Sciences, Uppsala University, Uppsala, Sweden. lara.blythe@geo.uu.se (* presenting author).

[2]Geosciences Research Division, Scripps Institution of Oceanography, La Jolla, California, USA.

[3]Laboratory for Isotope Geology, Swedish Museum of Natural History, Stockhom, Sweden.

[4] Geoglobal Energy LLC, Santa Rosa, California, USA.

Volcanically-hosted geothermal energy is an important resource in Indonesia of which Salak Geothermal Field in W Java is the largest developed one [1]. All 5 power-producing plants on Java are located in the western and central crustal sectors [1] and there appears to be a correlation between the location of commercially-viable geothermal systems, such as Salak Geothermal Field, and the thickness of the local upper crust and/or the volume of sediment on the downgoing plate [2]. This implies that crustal input from the subducting slab or from upper crust is central to the development of productive geothermal resources in this part of the world. Java's upper crust can be divided into three lateral segments: thick crust of continental affinity in the west [3], grading into arc-type and oceanic crust in central Java into increasingly oceanic affinity eastwards [3; 4].

Here we combine He isotope data from gas, fluids, pyroxene separates and whole rock Sr and Nd isotope values from volcanoes along the Sunda Arc (from Anak Krakatau to Bali, East of Java) with literature data to further understand sources to the crustal contamination signals and their influence on geothermal systems.

Helium isotope values (in R/R_A notation) are lower in both crystal and geothermal samples (down to $3.4R_A$ in pyroxene at Gede volcano) in the central and western crustal sectors, when compared to the eastern sector (7.46 R_A from fumaroles at Kawah Ijen volcano). Equally, Sr (as demonstrated by [5]) and Nd vary systematically eastwards along the arc, with values showing a significant crustal influence in central and western Java. East of the Progo-Muria fault, which delineates the central and eastern crustal sectors, volcanic rocks and geothermal samples give a more mantle-like signal (i.e. in eastern Java and Bali). The correlation between upper crustal type and crustal contamination is present in all three isotope systems (He-Sr-Nd). Together with the location of all commercially productive geothermal plants in west and central Java we propose that regional crustal influences may be highly relevant in understanding the development of geothermal systems with exploitation potential in Indonesia.

[1] Bertani, R. (2005) *Geothermics* **34**, 651-690.
[2] Stimac, J. *et al*. (2008) *Geothermics* **37**, 300-331.
[3] Hamilton, W. (1979) *U.S.G.S: Professional Paper* **1078**, 1-345.
[4] Smyth, H.R. *et al*. (2007) *Earth Planet Sc Lett* **258**, 269-282.
[5] Whitford, D.J. (1975) *Geochim Cosmochim Ac* **342**, 1287-1302.

Reconstruction of the North Atlantic Circulation back to the Last Interglacial by a combined proxy approach

E. BÖHM[1]*, J. LIPPOLD[1], M. GUTJAHR[2], J.GRÜTZNER[3], A. MANGINI[1]

[1] Heidelberg Academy of Sciences, INF 229, Heidelberg, Germany
*correspondence: eboehm@iup.uni-heidelberg.de
jlippold@iup.uni-heidelberg.de, amangini@iup.uni-heidelberg.de
[2] National Oceanography Centre Southampton, UK
m.gutjahr@soton.ac.uk
[3] Alfred Wegener Institute, Bremerhaven, Germany
Jens.Gruetzner@awi.de

Studies of past variations of the Atlantic Meridional Overturning Circulation (AMOC) are essential for evaluating possible future developments. In order to asses such past variations two new proxies (Nd isotopes and $^{231}Pa/^{230}Th$) have been applied frequently in recent years, but only two combined data sets are available to date [1,2]. The combined use of Fe-Mn oxyhydroxide-derived Nd isotopes (ε_{Nd}), a sensitive chemical water mass tag, and $^{231}Pa/^{230}Th_{xs}$, a kinematic circulation proxy, from identical sediment core samples allows to obtain information about both the rate of overturning circulation and water mass provenance.

Here we present neodymium isotope compositions of past seawater and $^{231}Pa/^{230}Th$ extracted from sediments from a high sedimentation rate location (< 10 cm/ka) in the western North Atlantic (ODP Site 1063, Bermuda Rise), back to the Last Interglacial (Eemian).

First measurements of ε_{Nd} have been accomplished for the time range from 53 to 150 ka with a temporal resolution averaging 3 ka. The Nd isotopic record suggests the presence of Southern Source Water during MIS 6 to MIS 6.4 as well as active deep water formation in the North Atlantic at the beginning of the Eemian Interglacial (MIS 5.5). The transition between these two different modes in AMOC is marked by a distinct drop in the ε_{Nd} values (-11.5 to -14). This is consistent with ε_{Nd} results from [1] and [2] at the transition from MIS 2 to MIS 1.1 which implies recurring millenial-scaled identical processes converting the AMOC from a Glacial mode into an Interglacial mode.

Numerous measurements of Pa/Th have been performed in the time range from 65 to 143 ka with a high temporal resolution (1 ka or less). Results show that the Pa/Th method reaches its detecting limit at 125 ka due to the short half life of ^{231}Pa ($T_{1/2}$=33 ka). The interval between 95 and 125 ka displays strong fluctuations (Pa/Th=0.046 to 0.079) with one pronounced peak at 119 ka (Pa/Th=0.095) indicative of a slowdown of the AMOC (no corresponding peak in opal). This is consistent with [3] who found a short cold event with near-glacial surface ocean summer temperatures in MIS 5.5.

[1] Gutjahr, M. and J. Lippold, 2011. Paleoceanography. 26(PA2101). [2] Roberts, N., A. Piotrowski, J. McManus and L. Keigwin, 2010. Science. 327(75). [3] Bauch, H., E. Kandiano, J. Helmke, N. Andersen, A. Rosell-Mele, H. Erlenkeuser, 2011. Quaternary Science Reviews, 30(15-16): 1813-1818.

Fe(II)-mediated reduction of Cr(VI) and U(VI) in the presence of Fe(III) oxyhydroxides

DANIEL D. BOLAND[1*], RICHARD N. COLLINS[1], CHRIS J. GLOVER[2], TIMOTHY E. PAYNE[1,3] AND T. DAVID WAITE[1]

[1]School of Civil and Environmental Engineering, The University of New South Wales, Sydney, Australia, daniel.boland@student.unsw.edu.au. (* presenting author)
[2]Australian Synchrotron Company Ltd, Clayton, Australia.
[3]Institute for Environmental Research, Australian Nuclear Science and Technology Organisation, Lucas Heights, Sydney, Australia.

Reduction of both Cr(VI) and U(VI) generally leads to the precipitation of insoluble phases and, thus, decreases the mobility of these toxic metals. In this study we examined the reduction of Cr(VI) during the Fe(II)-catalysed transformation of ferrihydrite to goethite, and compared the results to our previous experiments examining U(VI) reduction in the same system [1].

Cr(VI) was sorbed to ferrihydrite, silica-coprecipitated ferrihydrite (Si-ferrihydrite) and goethite in pH 6.5 buffered solutions in the form of CrO_4^{2-}, and Fe(II) added at 1mM. Cr K-edge X-ray absorption spectroscopy (XAS) analyses of the resultant solids showed that there was an immediate reduction of Cr(VI) to Cr(III) under all treatments (Figure 1), preceding any changes to the Fe(III) oxyhydroxide initially present. This contrasts to U(VI) in the same system, whose reduction is dependent upon the presence of goethite. Ferrihydrite continued to transform to goethite as expected, which has implications for the reactivity of this now Cr-bearing substrate.

These results are consistent with what may predicted by the relative positions of Cr and U in the "redox ladder". They emphasise the validity of using localised thermodynamic calculations to predict the redox state of trace species present during Fe(II)-catalysed Fe(III) oxyhydroxide transformations.

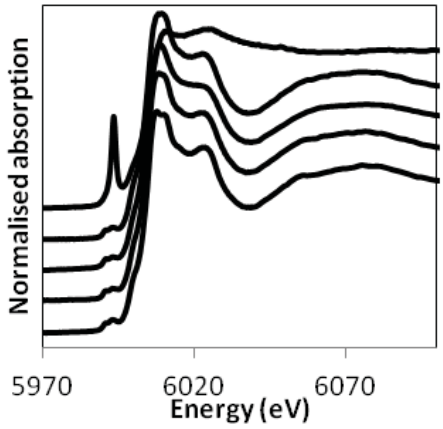

Figure 1: Cr K-edge XAS data. From top: Cr(VI) sorbed on ferrihydrite, following reaction with Fe(II) on ferrihydrite, Si-ferrihydrite and goethite, Cr (III)-substituted Fe(III) oxyhydroxide. Reduction is clear from the diminished pre-edge feature.

Chemistry of diatoms and coccoliths records carbon acquisition strategies during biomineralization

CLARA BOLTON[1], KIRSTEN ISENSEE[1],LUZ MARIA MEJIA-RAMIREZ[1], ANA MENDEZ-VICENTE[1], JORGE PISONERO[2], NOBUMICHI SHIMIZU[3], HEATHER STOLL[1]*

[1]Geology Dept., Univeristy of Oviedo, Oviedo, Spain , hstoll@geol.uniovi.es (* presenting author)

[2]Physics Dept., University of Oviedo, Oviedo, Spain

[3]Geology and Geophysis, Woods Hole Oceanographic Institute, Woods Hole, USA

Introduction

A strong biological control over trace element or stable isotopic composition of marine biominerals is frequently viewed as a liability in reconstructing past ocean chemistry and temperature, and the significance of reconstructing the biological processes themselves is often overlooked. We propose that the chemistry of opal, produced by diatoms, and calcite, produced by coccolithophorids, predominantly reflects key biological processes for cellular carbon acquisition. Reconstruction of these biological processes in the past will reveal how marine algae responded to changes in atmospheric CO2, key to both the past and future carbon cycle.

Biomineralization effects on stable isotopes in coccoliths

Coccolithophorids exhibit strong biological effects in carbon and oxygen isotopic composition. Previously we hypothesized that the size-correlated range of vital effects in carbonate liths produced by different coccolithophore species was due to variable significance of carbon concentrating mechanims in their C acquisition. Our new culture experiments with coccolithophorids reveal strong plasticity in the magnitude of stable carbon isotope vital effects in coccoliths of *Calcidiscus leptoporus* and *Emiliania huxleyi* with variable CO_2. At high CO_2 coccoliths of both species are more isotopically enriched, but the magnitude is greater in *C. leptoporus* leading to reduced interspecific offsets at high CO_2. In the case of *E. huxleyi*, higher CO_2 conditions resulted in significant reduction in the magnitude of DIC accumulation in the intracellular carbon pool, and more positive carbon isotopic values inside the particulate organic matter. A model of carbon acquisition incorporating both photosynthetic and carbonate production is used to assess mechanisms for these relationships. Stable isotope data from size-separated deep-sea sediments dominated by small, intermediate, and large coccoliths show a range of vital effects which is distinct during several major Cenozoic proxy-inferred climate-CO_2 transitions. Furthermore, where vital effects are significant their magnitude scales with coccolith size in the same sense as modern cultures.

Biomineralization effects on diatom B content

From two species of diatoms, *Thalassiosira weissflogii* and *T. pseudonana*, cultured at a range of pCO_2 from 200 to 2000 ppmv, B content of cleaned diatom opal was measured by Laser Ablation-ICP-MS and Secondary Ion Mass Spectrometry. Determination of growth rate, type of carbon acquired, and silicon and carbon quotas during diatom growth provides data on biomineralization process. B content in *T. pseudonana* is correlated with bicarbonate uptake rate and with normalized Si quotas. For *T. weissflogii*, which is a bicarbonate-restricted user at the pH studied, B content seems to be regulated primarily by the borate/bicarbonate seawater ratio, at pCO_2 <1000ppmv . We present a simple cellular model of B and Si uptake by diatoms to quantitatively explore the mechanisms for variable B content and its potential as a proxy.

Oceanic Material recycled within the Subpatagonian Lithospheric Mantle (Cerro del Fraile, Argentina)

B. FACCINI[1] , C. BONADIMAN[1*], M. COLTORTI[1], M. GREGOÌRE[2], AND F. SIENA [1]

[1] Department of Earth Sciences, Ferrara University, Ferrara, bdc@unife.it

[2] DTP, CNRS-UMR 5562 Observatoire Midi-Pyrenées, Toulouse, France

A detailed petrological study of mafic and ultramafic xenoliths from the Cerro del Fraile (Southern Patagonia, Argentina) was developed in order to highlight: I) the mineralogical and geochemical composition of the lithospheric mantle beneath the area, II) the nature of the metasomatising agents which infiltrate the mantle wedge above the Antarctic subducting Plate, III) the processes that allow the mantle to be refertilised and IV) the nature of the material dragged down in the subduction zone and recycled within the south patagonian sub-arc mantle.

Major and trace element analyses of clinopyroxene and orthopyroxene in peridotitic and pyroxenitic rocks suggest that a proto-adakite, deriving from the melting of the subducting Antarctic plate, was responsible for both the metasomatic features of the peridotitic rocks and the crystallisation of the pyroxenites. A few composite xenoliths bridge the two processes - peridotite enrichment and pyroxenite crystallization - indicating that the variously depleted mantle reacts with the incoming melt to generate a newly fertile mantle domain. HREE and Al2O3 and MgO contents in pyroxenes indicate a partial melting degree varying from 10 to 25 %. The peculiar enrichment in Zr (-Hf), Th and U of the pyroxenes speaks in favour of the melting of oceanic sediments, which are composed of a remarkable amount of manganese nodules and micronodules and, possibly, organic matter. Some geochemical analogies have been found between the calculated metasomatic melts and the Austral Volcanic Zone adakites. In this case, the amount of sediments involved in the genesis of the infiltrating melts is larger than that previously proposed for the genesis of the erupted Patagonian adakites. Chemical-physical conditions favouring the upward percolation through the mantle wedge of these SiO2-rich and viscous melts are also discussed.

U-Pb age zoning in titanite by SIMS: New criteria for preservation

CHLOË E. BONAMICI[1*], REINHARD KOZDON[1], C. MARK FANNING[2], JOHN W. VALLEY[1]

[1]WiscSIMS, University of Wisconsin-Madison, Madison, WI, 53706, USA, bonamici@wisc.edu (* presenting author)
[2]Research School of Earth Sciences, Australian National University, Canberra, Australia, Mark.Fanning@anu.edu.au

We report a set of thirty-two U-Pb SIMS ages measured in situ along two traverses of a single titanite porphyroclast from the Carthage-Colton mylonite zone in the Adirondack Mountains, New York, USA. Ages span ~140 m.y. from 1190 Ma to 1050 Ma and generally decrease from core to rim; however, ages within the interior of the grain fluctuate by as much as 50 m.y. over length scales < 100 μm. Electron microprobe element maps and Th/U spot analyses (SIMS) reveal distinct core and rim compositional domains. These do not correlate with the observed grain-interior age fluctuations and thus argue against trace element growth zoning as the source of U-Pb age variability. Light microscopy and EBSD mapping verify that the grain has not been recrystallized and show that more than 50% of the grain suffered deformation-related mechanical twinning. Ages in twinned areas of the grain are younger and more variable than ages in untwinned areas, suggesting that the presence of organized planar defects may have affected Pb mobility and abundance. SIMS $\delta^{18}O$ zoning along traverses parallel to U-Pb traverses, indicates volume diffusion of oxygen during cooling from peak T of 700°C. The strong positive correlation between $\delta^{18}O$ and U-Pb age (Figure) is consistent with the presence of first-order, core-to-rim age zonation similar in shape and extent to the zonation developed by diffusive exchange of oxygen, and it agrees with experimental studies that show similar diffusivities for oxygen and Pb in titanite over the temperature range 600-800°C.

We conclude that U-Pb age zoning within the Adirondack titanite grain reflects heterogeneous Pb redistribution by a combination of volume and intragrain fast-path diffusion. The oldest ages, preserved in untwinned areas, correlate with the 1164 ± 11 Ma intrusion age of the Diana metasyenite that hosts the grain. The youngest, ca. 1050 Ma ages near the grain rim are consistent with Pb loss and age resetting by volume diffusion during granulite-facies metamorphism accompanying the Ottawan phase (1090-1020 Ma) of the Grenville orogeny. We interpret the transitional and highly variable ages in twinned areas as reflecting segmentation of part of the grain into smaller diffusion domains between twin boundaries that behaved as diffusion fast paths. An integrated whole-grain age on this Adirondack grain would, at best, constrain the minimum age for syenite intrusion or the maximum age of high-T Ottawan metamorphism. Knowledge and careful characterization of the correlation between U-Pb age and $\delta^{18}O$ zoning in titanite will permit retrieval of more accurate ages for each event and may additionally allow for applications of coupled U-Pb-$\delta^{18}O$ titanite geospeedometry.

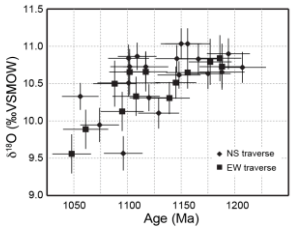

Microbial communities in low-permeability uranium mine tailings

V.F. BONDICI[1], J.E. HILL[2], N.H. KHAN[3], J.R. LAWRENCE[4], G.M. WOLFAARDT[5], T. KOTZER[6] D.R. KORBER[7*]

[1]Univ. of Saskatchewan, Saskatoon, Canada, vfb326@mail.usask.ca
[2]Univ. of Saskatchewan, Saskatoon, Canada, Janet.Hill@usask.ca
[3]Univ. of Saskatchewan, Saskatoon, Canada, mnk252@mail.usask.ca
[4]Environment Canada, Saskatoon, Canada, John.Lawrence@ec.gc.ca
[5]Ryerson Univ., Toronto, Canada, gwolfaar@ryerson.ca
[6]Cameco Corp., Saskatoon, Canada, Tom_Kotzer@cameco.com
[7]Univ. of Saskatchewan, Saskatoon, Canada, drk137@usask.ca
(*presenting author)

Uranium mine tailings management

The processing of uranium mine tailings at the Deilmann Tailings Management Facility (DTMF) at Key Lake was designed to stably co-precipitate ferrihydrite with various elements of concern (EOCs), such as As, Se, Ni, and Mo, present in the processed rock. During UO_2 extraction, tailings are milled to ≤100 μm diameter; on disposal in the DTMF, a saturated, diffusion-dominated matrix with restricted pore space (dry bulk density ~1.2 – 1.6 g/cm^3) results. The chemical stability of the DTMF relies upon maintenance of highly oxic, high pH conditions. However, microbes, given time and nutrients, have the potential to metabolically reduce the tailings which could result in the solubilization and subsequent mobilization of the EOCs. To date, the DTMF hasn't been studied from a microbiological perspective; it has been suggested that the high pH, radiation, and limiting nutrients in the DTMF would limit microbial growth and activity.

Characterization of the tailings microbial community

An in-depth analysis of microbial diversity, as well as their metabolic potential, within the tailings system has been undertaken using culture dependent and culture-independent analyses. A total of 60 tailings samples were obtained at 1 m intervals over a top 60 m of the tailings body and subjected to DNA extraction, as well as cultivation on a variety of microbiological media. A surprisingly high diversity (determined using 16s rRNA sequencing) of cultivatable bacteria under aerobic and anaerobic conditions were isolated over the tailings depth profile. These bacteria exhibited a range of characteristics reflective of being highly-adapated to life within the DTMF: of the 59 unique isolates, 69% were multiple metal resistant, 15% exhibited dual-metal hypertolerance, and a number were capable of reducing or oxidizing various metal elements.

Using extracted DNA from composited tailings samples from the upper, middle and lower 20 m layers of the DTMF profile, three *cpn60* clone libraries were assembled and sequenced. A total of 920, 952, and 693 sequences were generated for the upper, middle, and lower zones, respectively. Comparative phylogenetic analysis led to the classification of the different sequences from the three libraries into nine taxonomic groups: Gemmatimonadetes, Verrucomicrobia, Acidobacteria, Synergistetes, Planctomycetes, Actinobacteria, Bacteriodetes, Proteobacteria and Firmicutes. The prevalence of populations of metabolically-diverse, metal-resistant microorganisms capable of transforming metal elements suggests the potential for these organisms to influence the geochemical stability of the tailings. Integration of biological and geochemical data will aid in the construction of a predictive stability model that incorporates the role of organisms with unique metabolic activities.

Linking mackinawite (FeS) structure to redox activity

SHARON E. BONE[1*], KIDEOK KWON[2], JOHN R. BARGAR[3], GARRISON SPOSITO [1]

[1]Lawrence Berkeley National Laboratories, Berkeley, USA, SBone@lbl.gov (* presenting author), GSposito@lbl.gov
[2]Sandia National Laboratory, Albuquerque, USA, kkwon@sandia.gov
[3]Stanford Synchrotron Radiation Lightsource, Menlo Park, USA, bargar@slac.stanford.edu

The nanoparticulate tetragonal iron sulfide mineral mackinawite (FeS) is thought to be ubiquitous in wetlands, estuaries and groundwater where bacterially produced sulfide and ferrous iron mix. FeS has the potential to be used as a bioremediation tool because of its ability to reduce a range of contaminants including chlorinated organics, metals and metalloids.

The goal of our research is to link the molecular-scale structure of FeS to its reactivity towards environmental contaminants, in this case, the biomagnifying toxicant mercury. To this end, we have integrated X-ray spectroscopic, X-ray scattering, computational and wet chemical techniques to investigate FeS size and structure, and to identify which FeS moieties participate in reduction as well as what oxidized products result as a function of time, pH, and [Hg(II)] in batch reactors.

Using Hg L_{III}-edge extended X-ray absorption fine structure (EXAFS) spectroscopy we have found that Hg(II) forms a discrete Hg(0) phase after reaction with FeS. Density functional theory (DFT) computations show that surface Fe(II) in FeS preferentially binds Hg(II) relative to surface S(-II), suggesting a pathway by which electrons might be transferred to Hg(II) to produce Hg(0) and Fe(III). Using Fe K- and $L_{II,III}$-edge X-ray absorption spectroscopy, we have quantified Fe(III) formation in FeS suspensions. Fe(III) exists in octahedral coordination as a second, amorphous phase, possibly as a mixed Fe(II)-Fe(III) phase, which may be a pre-cursor to the Fe(II)-Fe(III) sulfide, greigite. Lastly, we used X-ray diffraction, electron microscopy and Fe K-edge EXAFS spectroscopy to derive a particle size distribution for FeS, and to determine FeS molecular-nanoscale structure before and after oxidation. We combined this information with thermodynamic modelling of equilibrium aqueous Fe(II) and S(-II) concentrations in order to identify the redox processes that occur in FeS suspensions.

Our research demonstrates that Fe(II) in FeS is key to FeS reactivity, dominating its surface chemistry and redox activity.

Timing the evolution of seawater chemistry during the Neoproterozoic: case study of the Svalbard succession.

P. BONNAND[1*], I. J. PARKINSON[1], I. J. FAIRCHILD[2], E. MCMILLAN[2], D. CONDON[3], G. P. HALVERSON[4].

[1]Department of Environment, Earth and Ecosystem, The Open University, Walton Hall, Milton Keynes, MK7 6AA, UK
[2]School of Geography, Earth and Environmental Sciences, University of Birmingham, Edgbaston, Birmingham, B15 2TT, UK.
[3]NERC Isotope Geosciences Laboratory, British Geological Survey, Keyworth, Nottinghamshire NG12 5GG, UK
[4]Department of Earth and Planetary Sciences, McGill University, 3450 University Street, Montreal, QC H3A 2A7, Canada
[*]p.bonnand@open.ac.uk

The Neoproterozoic Era (1000-542 Ma) is a key period in the evolution of the Earth system. This period is characterised by the widespread occurrence of glacigenic sediments and by large variations in carbon isotope compositions of seawater [1]. These excursions are among the largest described in the geological record, and together with global periods of glaciation, make the Neoproterozoic one of the most dramatic periods of change in surface processes on Earth. Another major change that occured during this period is a purported increase in oxygen concentration in the atmosphere and associated changes in ocean redox [2]. In order to unravel the global record of evolving Neoproterozoic ocean chemistry, several successions around the world have been studied [e. g. 3]. However, the lack of precise radiometric constraints on suitably preserved samples in most Neoproterozoic sedimentary successions hinders the interpretation and correlation of geochemical signals. The Polarisbreen Group in northeast Svalbard is one of the best preserved Neoproterozoic successions and has great potential to significantly improve the record of Neoproterozoic environmental evolution, but to date has yielded no direct radiometric age constraints

In this study, we investigate the potential of the Svalbard succession to represent a type succession to assess the climate and chemical variations that occured during the Neoproterozoic. The Svalbard succession is characterised by the presence of 2 distinct glaciation episods which have been correlated with the first and second Cryogenian glaciations [3, 4]. Here, we present new constraints on the depositional age of two discrete glacial intervals in the Polarisbreen Group based on U-Pb detrital zircon data from siliciclastic sediments. We also investigate Sr isotopes and REE concentration in well preserved carbonate rocks through the succession in order to correlate the variation in Sr isotopes to the proposed Neoproterozoic seawater Sr curve [3] and assess variation in marine redox conditions during this interval.

These new data will allow a better correlation of the Svalbard succession with other Neoproetrozoic successions and provide a framework to characterise the evolution of seawater during the Neorpoterozoic.

[1] Fairchild and Kennedy (2007) *Journal of the Geological Society.* [2] Holland (2006) *Philosophical Transactions of the royal Society.*[3] Halverson et al. (2010) *Precambrian Research*. [4] Fairchild and Hambrey *(1995) Precambrian Research.*

Assessing the use of $^{13}C\{^{1}H\}$ CPMAS NMR for comparisons of boreal watershed soil and dissolved organic matter compositions

JENNIFER BONNELL*, CELINE SCHNEIDER, CHRISTINA BOTTARO AND SUSAN ZIEGLER[1]

[1]Memorial University, St. John's, NL, Canada, jennifer.bonnell@mun.ca (*presenting author)

Understanding high latitude ecosystems and their links to global carbon cycling depends greatly on our study of the composition of both dissolved and soil organic matter (DOM and SOM, respectively) and their interactions. DOM plays a major role in aquatic carbon and nutrient cycling, but may also reveal changes in landscape biogeochemistry. Headwater streams are intimately connected to and strongly influenced by the terrestrial environment such that stream DOM likely provides important chemical clues relevant to change in the watershed.

^{13}C cross polarization magic angle spinning nuclear magnetic resonance spectroscopy (^{13}C $\{^{1}H\}$ CPMAS NMR, hereafter referred to as CP) has been used extensively in the study of both DOM and SOM. It allows assignment of types of carbon in relative proportions, which informs our understanding of the chemical composition, source, and diagenetic state. It is well known that CP introduces a matrix effect caused by the dependence of signal strength of different carbon groups on the hydrogen environment surrounding it, resulting in types of carbon being over- or underrepresented in terms of relative proportion. ^{13}C single pulse NMR (^{13}C SPMAS NMR, hereafter referred to as SP) can be performed to determine the actual proportions of carbon types. Samples from a boreal forest headwater stream were run using both CP and SP to determine if an average correction factor (CF) could be applied by carbon type across a larger suite of DOM samples taken from a large boreal watershed in western Newfoundland. Five carbon types (aliphatic, carbohydrate, aromatic, carboxylic, and carbonyl) were assessed across all samples. Amplification or under representation of carbon types via CP was consistent in both stream DOM samples, and CFs were calculated for each carbon type. CFs were tested and consistently predicted results within 5%, on average (ranging from 0.59% to 7.7%), of carbon type percentages obtained via SP. The greatest effect observed was the underrepresentation of aromatic carbon, while both carbohydrate and aliphatic carbon were the most amplified.

This same methodological comparison was applied to litter and organic and mineral horizon soils (from the same watershed), as well as DOM derived from these soil horizons (leachates) to determine if these corrections would be consistent across sample types. While some similar CP effects were observed across both soil and leachate samples, the magnitude of these differences was less than that observed in stream DOM samples, and varied between soil and leachate samples. The larger CFs required for stream DOM samples, perhaps due to the lower carbon abundance relative to other matrix components, are particularly important as we consider how the chemical composition of stream DOM relates to the landscape. Obtaining and applying CFs for a specific study area to enable comparisons of the chemical composition of DOM in both soil and aquatic environments should facilitate our understanding of terrestrial-aquatic biogeochemical linkages, allowing a more accurate comparison across sample types.

A model for copper isotopic fractionation during weathering and transport

DAVID M. BORROK[1*], JESICA U. NAVARRETE[1], FOTIOS CHRISTOS A. KAFANTARIS[1]

[1]University of Texas at El Paso, USA, dborrok@utep.edu (*presenting author), jnavarrete2@miners.utep.edu, fkafantaris@miners.utep.edu

A consensus appears to be forming that the fractionation of Cu isotopes in natural systems is underpinned by redox reactions (chiefly changes from Cu(I) to Cu(II) and vice-versa). The heavier Cu isotope, ^{65}Cu, is preferentially incorporated in the oxidizied Cu species relative to ^{63}Cu. This has been speculated for coexisting minerals, coexisting fluid/mineral systems, and for biological systems, including microorganisms, plants, and mammals. Although additional reactions such as adsorption, organic complexation, and diffusion add complexity, Cu isotopes may prove to be a powerful tool for understanding current and historical redox processes in nature. The problem, however, is that we don't yet have a full understanding of how this redox-related fractionation process is reflected in different environments and over different scales.

Using experimental and field data collected from new and previous Cu isotope investigations, we present a conceptual model for the fractionation of Cu isotopes during the aqueous and oxidative weathering of Cu(I) sulfide minerals. The model suggests that the Cu isotopic signature of the fluid phase (relative to the mineral) is controlled by the relative rates of oxidation and leaching/transport.

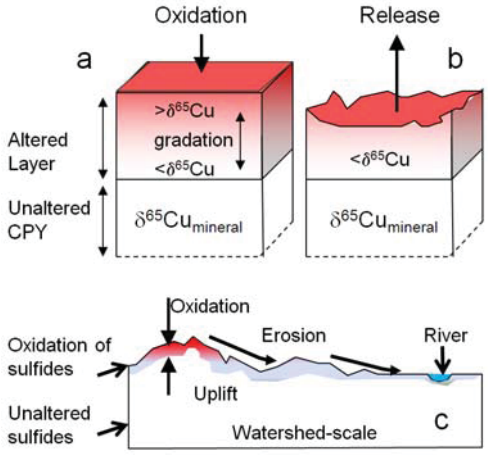

Figure 1: Conceptual model for Cu isotopic fractionation during chalcopyrite (CPY) oxidation, including (a) oxidation of Cu(I) to Cu(II) at the mineral surface followed by (b) the release of Cu into solution. Panel (c) is a cartoon watershed-scale version of this process.

We further examine how this model might be adapted from the molecular scale to watershed and continental scales, highlighting key knowledge gaps. Specifically, we address how Cu isotope controls might change from aqueous systems at low pH that are rich in dissolved Cu to higher pH systems where dissolved Cu is scarce and largely complexed by organic ligands.

The carbon dioxide mineral sequestration analogues: examples from Tuscany (Italy)

CHIARA BOSCHI[1*], LUIGI DALLAI[1], ANDREA DINI[1], ILARIA BANESCHI[1], ANTONIO LANGONE[2], ANDREA CAVALLO[3], GIOVANNI RUGGIERI[4],

[1]Institute of Geosciences and Earth Resources - CNR, Pisa, Italy, c.boschi@igg.cnr.it (* presenting author)
[2] Institute of Geosciences and Earth Resources - CNR, Pavia, Italy,
[3] Istituto Nazionale di Geofisica e Vulcanologia, Roma, Italy,
[4] Institute of Geosciences and Earth Resources - CNR, Firenze, Italy

The Southern area of Tuscany (Italy) provides clear examples of natural analogues of carbon dioxide mineral sequestration. Our studies focused on the geological and geochemical characterization of the different natural manifestations of CO_2-trapping processes. Widespread serpentinite-hosted magnesite deposits have been investigated in the Southern Tuscany (Monti Livornesi, Colline Metallifere, Elba Island), together with shallower deposits of hydromagnesite in Montecastelli area. The magnesite deposits are a consequence of a realtively shallow hydrothermal circulation of Si- and CO_2-rich fluids intensively affecting serpentinite lenses, hosted by argillites [1].

The hydromagnesite incrustations (Figure 1), with the typically white rounded shape and vein or fracture fillings, represent an ongoing carbonation process on a gangue materials dumped from a serpentinite-hosted copper mine, close to Pomarance (Tuscany, Italy).

The study of these natural analogues complements laboratory experiments and possibly provides opportunity to constrain the boundary conditions and the mechanisms for CO_2-bearing phases to form. Here, we report a review of our geological mapping, petrological observation, mineralogical and geochemical analyses together with isotopical studies (C, O, Sr) of different outcrops in order to address: 1) the carbon source (deep versus atmospheric); 2) the fluid path-way during the alteration in relationship with the induced/reactived fracturation; 3) the areal diffusion and the efficency of the carbonation process; and 4) the mass balance of major and trace element during the alteration.

Figure 1: Example of hydromagnesite incrustation at Montecastelli

[1] Boschi (2009) *Chemical Geology* **Volume 265**, 209–226.

Eating Iron and Loving it: Ferrous Iron Metabolism in *Rhodopseudomonas palustris* TIE-1

ARPITA BOSE[1*], DIANNE K. NEWMAN[2], AND PETER R. GIRGUIS[3]

[1]Harvard University, Department of Organismic and Evolutionary Biology, abose@fas.harvard.edu, (* presenting author)
[2]California Institute of Technology, Department of Biology, dkn@caltech.edu
[3]Harvard University, Department of Organismic and Evolutionary Biology, pgirguis@oeb.harvard.edu

Iron is an essential element in biological systems, and its transport is thus a prime concern to all life. Iron also serves as an electron donor and acceptor for microbial respiration. However, a lot remains to be understood about these processes and we believe that studying iron specialists will provide fresh insight. *Rhodopseudomonas palustris* TIE-1, is an α-proteobacterial iron specialist that uses energy from light and electrons from ferrous iron Fe(II) to support photoautotrophy (photoferrotrophy). *R. palustris* TIE-1 is the only genetically tractable photoferrotrophic microbe, and we are interested in employing molecular and geochemical analyses to better understand A) how it copes with high Fe(II) concentrations, and B) how electrons are transferred from Fe(II) to the photosynthetic reaction center.

Bioinformatics was used to interrogate the genome of *R. palustris* TIE-1 for putative Fe(II) transporters. The *pioABC* operon, the genetic locus essential for photoferrotrophy, was also included in this analysis. This locus might be responsible for both iron and electron transport. A combination of techniques such as heterologous complementation, mutant analysis, and immunofluorescence was used to confirm the role of the identified loci in Fe(II) transport. To assess the role of the Pio proteins in electron transfer from Fe(II) to the photosynthetic reaction center, novel bioelectrochemical reactors were devised. Our data indicate that *R. palustris* TIE-1 employs different membrane-bound Fe(II) transport systems under aerobic, anaerobic and photoferrotrophic conditions. Although the role of the Pio proteins in iron transport remains unclear, we demonstrate that they allow *R. palustris* TIE-1 to accept electrons from a poised electrode in the presence of light, supporting net carbon fixation and growth. We refer to this process as "photoelectrosynthesis" (PES).

This comprehensive study provides a better understanding of Fe(II) transport in α-proteobacteria. We also show that a pure phototrophic culture can perform PES, which has not been demonstrated previously. The role of the Pio proteins in PES brings to light the use of a common protein module to perform electron transfer reactions in unrelated bacteria. Ongoing studies are aimed at further understanding this process at the molecular level.

DISTRUBUTION OF FERRIHYDRITE IN SEDIMENTS AND ITS ROLE IN REGULATING GROUNDWATER ARSENIC EXPOSURE POTENTIAL

BENJAMIN BOSTICK[1*], JING SUN[2], IVAN MIHAJLOV[3], STEVE CHILLRUD[4] AND BRIAN MAILLOUX[5]

[1]Lamont-Doherty Earth Observatory of Columbia University, Palisades, U.S.A, chilli@ldeo.columbia.edu
[2]Columbia University, New York, U.S.A, jingsun@ldeo.columbia.edu
[3]Columbia University, New York, U.S.A, mihajlov@ldeo.columbia.edu
[4]Lamont-Doherty Earth Observatory, Palisades, U.S.A, chilli@ldeo.columbia.edu
[5]Barnard College, New York, U.S.A, bmaillou@barnard.edu

The environment plays a key role in regulating the concentation of environmental toxins such as arsenic. Minerals are the matrix on which contaminants are retained, affecting both their aqueous concentrations and the transport properties. In some cases, minerals serve as either electron acceptors and donors for a variety of biogeochemical processes that affect the mineral form, surface area, and reactivity of sediments. This critical role is well established, yet suprisingly little is known about the distribution of some of the most important minerals in regulating arsenic concentration. Here, we quantify the concentrations of ferrihydrite in a variety of settings, and study the relationship between its concentration and dissolved arsenic levels from a variety of arsenic-affected environments. Ferrihydrite is a metastable mineral that only somewhat crystalline, and is highly reactive for both adsorption and microbially-mediate reduction. Its presence is often controversial given this metastability, yet the retention of arsenic and other ions is often not easily modeled with low surface area Fe minerals. Using a combination of sequential extractions and X-ray absorption spectroscopy to identify these phases, we find that there is clear evidence for the persistence of ferrihyrite or other poorly crystalline Fe(III) phases even in tropical environments where rapid Fe cycling often is assumed to convert it to hematite and goethite. We attribute the stability of these nanoparticulate forms of Fe(III) to the presence of adsorbed silicate or phophate or other phases on the mineral surface in these environments. A critical factor in the identification of this phase involves the differentiation of crystalline minerals that have distinct, but variable spectral signatures depending on factors such as morphology and particle size. The distribution of ferrihydrite and Fe(III) in sediments also appears affect As speciation, possibly by affecting Fe reduction. While ferrihydrite is found, it often appears to be less effective at minimizing aqueous As levels than crystalline oxides.

A new look on the barium cycle: Stable barium isotope fractionation in ODP sediments and calibration experiments

BÖTTCHER M.E.[1,*], VON ALLMEN, K.[2], PAYTAN, A.[3], NEUBERT, N.[1,2], BRUMSACK, H.-J.[4], SAMANKASSOU, E.[5], AND NÄGLER, T.F.[2]

[1]Leibniz IOW, Warnemünde, FRG, michael.boettcher@io-warnemuende.de (* presenting author)
[2]University of Bern, Switzerland, naegler@geo.uibe.ch
[3]University of California, Santa Cruz, USA, apaytan@ucsc.edu
[4] ICBM, University of Oldenburg, FRG, brumsack@icbm.de
[5]University of Geneva,Switzerland, Elias.Samankassou@unige.ch
[6]Present address: University of Hannover, FRG

We show by the analysis of the stable barium isotope composition ($^{137}Ba/^{134}Ba$) of natural marine barite ($BaSO_4$), that significant isotope fractionation takes place in the marine biogeochemical barium cycle. We have combined previous measurements of the S and O isotopic composition with new Ba isotope ratio determinations. We find that biogenic marine barites separated from sediments collected in different parts of the world´s Ocean with ages up to about 55 million years fall within a close range and have isotope ratios comparable to recently reported value for continental barium-bearing minerals (von Allmen et al., 2010). Whereas, cold seep barites, show isotope values close to modern biogenic barite, marine hydrothermal samples are enriched in the lighter isotope. Highest ^{134}Ba-enrichments are found in authigenic barite minerals formed above black shales in the deep sediments of ODP Leg 207 that are depleted in sulfate due to AOM-triggered microbial sulfate reduction.

Laboratory experiments were conducted to investigate the potential of different low-temperature reactions to result in barium isotope discrimination. These reactions include adsorption of dissolved Ba on MnO_2 and kaolinite, and the precipitation of anhydrous $BaCO_3$ and $BaSO_4$ under different experimental conditions (reaction process and temperature). The Ba minerals were generally enriched in light Ba compared to the aqueous solution, to magnitudes depending on precipitation conditions.

As an important finding, we can conclude that diagenetic barites at ODP Leg 207 record coupled transport induced isotope discrimination, probably superimposed by desorption/adsorption processes in the sulfate-depleted part of the sediment column. Despite the relatively short residence time, the barium isotopic composition of primary barites seem to have been relatively constant through the past 55 m.y.

It should be noted that S and O measurements of a Cambrian barite sample from China showed the influence of microbial sulfate reduction and were accompanied by a depletion in the heavy Ba isotope comparable to our findings from ODP Leg 207.

[1] von Allmen et al. (2010) Chemical Geology **277**, 70-77.

Environmental impacts of nanomaterials: physico-chemical evolution, exposure mechanisms and mechanisms disturbing the biological activity in aqueous environment

JEAN-YVES BOTTERO[1,2*], MELANIE AUFFAN[1,2], JEROME LABILLE[1,2], ARMAND MASION[1,2], JEROME ROSE[1,2]

[1] CEREGE UMR 6635 CNRS-Université Aix-Marseille, France (bottero@cerege.fr)

[2] GDRI I-CEINT International Center for Enviromental Implications of Nanotechnology

The new properties of materials at the nanoscale are at the heart of current scientific advances such as drug vectorization, cancerous tumor targeting, replacement of silicon in microelectronics by carbon, or the manufacture of more resistant materials... The main cause for this change in properties is the very high surface to volume ratio of nanoparticles and stronger reactivity. It is therefore impossible to simply transfer the physical, chemical, and thermodynamic knowledges on reactions occurring at the solution/microparticles interface to those occurring at the solution/nanoparticles interface (<20-30 nm). Thanks to the unique properties of nanoparticles, nanotechnologies will considerably grow in the near future. However, this growth stirs up awareness that we cannot ignore. In particular, people wonder about the impact of mass-produced nanoparticles that could spread into the environment.

To date, scientists master the manufacture and use of nanomaterials, however we do not know what are the risks for humans and ecosystems. No database exists regarding the amounts released within the ecosystems. However, nanoparticles due to their reactivity, their surface atoms are labile, their redox states can change easily, they are highly reactive towards aqueous compounds and can change from hydrophobic to hydrophilic. Before contacting biota they interact with many objects such as natural organic matter, clays, oxides…. It is impossible to study and understand the environmental biological effects of nanomaterials without a good knowledge of the exposure, their physico-chemical properties changes. The properties of nanoparticles able to disturb the biological activity depend on their size, on their mineralogy, their crystallinity, and their surface reactivity. All these parameters affect the toxicity via their oxido-reductive potential, the generation of Reactive Oxygen Species (ROS), their dissolution into toxic or non ions (*e.g.* Cd^{2+}, Zn^{2+}, Ag^{+}), or also the retention of toxic molecules on their surface (*e.g.* As, Cd, Co). The exposure i.e interactions with components , transfer within the water column or/and sediments is a crucial problem which can be resolved through experiments in mesocosms, search and analysis of Nps in media and analysis of the transformation after alteration of "nano products".

Dating drinking water in eskers from Amos, Abitibi, Canada

CHRISTINE BOUCHER[1*], LAURELINE BERTHOT[2], MARIE LAROCQUE[3], MARTIN ROY[4], VINCENT CLOUTIER[5], DANIELE L. PINTI[6], MARIA CLARA CASTRO[7], CHRIS M. HALL[8]

[1,2,4,6] GEOTOP-UQAM, Montréal, QC, Canada
[1] christinebouc@hotmail.com (* presenting author)
[2] berthot.laureline@courrier.uqam.ca
[4] roy.martin@uqam.ca
[6] pinti.daniele@uqam.ca

[3] Département des Sciences de la Terre et de l'Atmosphère, UQAM, Montréal, QC, Canada
[3] larocque.marie@uqam.ca

[5] Groupe de recherche sur l'eau souterraine, UQAT, Amos QC, Canada
[5] vincent.cloutier@uqat.ca

[7,8] Dept. of Earth and Environmental Sciences, University of Michigan, Ann Arbor, MH, USA
[7] mccastro@umich.edu
[8] cmhall@umich.edu

In Abitibi-Témiscamingue (Québec), eskers, glaciofluvial landforms formed by accumulations of sand and gravel, were deposited during the last deglaciation. 8000 years BP, peatlands developed around the esker flanks by drainage of the Lake Barlow-Ojibway. The eskers are known to be aquifers containing drinking water of exceptional quality, yet little is known about their hydrologic regime. A better understanding of these systems is necessary to assess the vulnerability of these aquifers to potential contaminants and to implement a suitable management plan for water resources. With a such goal, a multi-isotopic study was initiated in eskers of Amos region (Saint-Mathieu-Berry, Baraute and Harricana Moraine) using stable noble gases and ^{222}Rn to date these waters and trace fluid flow within the eskers and into surrounding peatlands. $^{3}He/^{4}He$ ratios have been preliminarily used to identify water mixing and to estimate groundwater residence times through the ^{3}H-^{3}He method and, when possible, U-Th-^{4}He age model [1].

First results point to the occurrence of tritiogenic ^{3}He in groundwater flowing in the Saint-Mathieu-Berry esker that provide drinking water to the town of Amos and the bottled water Eska. Using tritium contents measured in 2004 [2] and in 2011, this study yields an age of 21-23 years. Groundwater from two deep wells (40 and 70 m) from the Harricana moraine gives ^{3}H-^{3}He ages of 7-9 yrs.

Interestingly, the Barraute esker, which is buried under Quaternary clay and the well of Landriennne which taps water at the interface with the Proterozoic basement show $^{3}He/^{4}He$ ratios (R) (normalized to that of atmosphere or Ra) of 0.930±0.022 Ra and 0.946±0.024 Ra, respectively. R/Ra below atmospheric ratio suggests a possible contribution of radiogenic ^{4}He and thus, older water ages. This finding is in agreement with the higher salinity measured in these two wells compared to the regional background.

Rocks samples from the Harricana Moraine were selected for measurements of U and Th contents and to estimate the ^{4}He release rate from the protoliths composing this aquifer [1] in order to calculate meaningful U-Th-^{4}He ages for Barraute and Landrienne groundwaters.

[1] Solomon (1996) *Water Resou. Res.* **32**, 1805-1813. [2] Riverin (2006) Msc Thesis, University Laval, pp.

Core differentiation of the IVA asteroid

R. A. BOUCHET[1*], J. BLICHERT-TOFT[1] AND F. ALBAREDE[1]

[1]ENS Lyon, LGLTPE, 69007 Lyon, FRANCE, romain.bouchet@ens-lyon.fr (* presenting author)

The group of IVA iron meteorites are regarded as magmatic cumulates that, together, have recorded most of the crystallization sequence of the core of a small planet (e.g. [1]). The main argument for a crystallization process rests on the chemical trends defined by the siderophile elements [2]. Using mathematical parameterization of element partition coefficients [3], we tested the hypothesis of fractional crystallization between a solid and a liquid by calculating the amount of sulfur in the liquid. Because the resulting sulfur concentrations did not follow a simple fractional crystallization law, we instead considered fractional crystallization between a solid and a mush. We calculated two key parameters from the trace element concentrations of the IVA irons [2]: the amount of sulfur in the liquid and the fraction of solid in the mush. The computed fraction of solid in the mush is very near unity during most of the differentiation history, implying that the underlying assumption of crystallization between a solid and a liquid suspension is invalid.

We therefore examined whether the chemical trends observed for siderophile elements in the IVA iron meteorites may record a compaction process rather than crystallization. Elements such as Au and Ni were progressively removed in the process, whereas compatible elements such as Ir and Pt became more concentrated in the residue. The correlation between cooling rates and Ni content in the IVA irons therefore signals a trend opposite to what is commonly admitted in the literature [4] and supports centrifugal solidification and cooling rates increasing as compaction proceeds. In addition, the calculated composition points to sulfur-saturated liquids. Upon compaction, these liquids rose in the solid metal where they were partially trapped as troilite inclusions, such as is observed in a number of IVA irons. The low Th/U ratio of these troilite inclusions [5] may reflect fractionation upon unmixing of minute amounts of silicate melts [6]. Although most of the silicates were subsequently lost, some occasionally survived as silicate inclusions [7].

[1] Chabot and Haack (2006) *Univ. of Arizona Press*, 741-771. [2] Wasson and Richardson (2001) *GCA* **65**, 951-970. [3] Chabot and Jones (2003) *MAPS* **38**, 1425-1436. [4] Rasmussen et al. (1995) *GCA* **59**, 3049-3059. [5] Blichert-Toft et al. (2010) *EPSL* **296**, 469-480. [6] Murrell and Burnett (1986) *JGR* **91**, 8126-8136. [7] Scott and Wasson (1975) *Rev. Geophys. Space Phys.* **13**, 527-546.

Modeling stable isotope ratios of metals in the weathering zone: mass-balance controls

J. BOUCHEZ[1*], F. VON BLANCKENBURG[1] AND J. A. SCHUESSLER[1]

[1]German Research Centre for Geosciences (GFZ), Potsdam, Germany (*presenting author; bouchez@gfz-potsdam.de)

During the last decade, the stable isotope composition of metals and metalloids (e.g. Li, B, Mg, Ca, Fe, Cu, Zn, Sr, Mo) in the weathering zone were mapped out. The overarching aim is to improve our understanding of the processes fractionating isotopes and generating elemental transfers between the main compartments (e.g. bedrock, soil, surface water and plants). However, a conceptual framework is still lacking for interpreting isotope data in terms of isotope fractionation factors, or in terms of elemental fluxes. Such a framework represents a prerequestite to identify biogeochemical processes from isotope ratios measured in river material or in the sedimentary record.

To this end, we design a simple steady-state model based on elemental mass-balance equations, and simulate, at first-order, a weathering system from the scale of a soil column to that of continents. The model links (1) isotope compositions of the main compartments of the weathering zone (expressed in the δ-unit) (2) isotope fractionation factors Δ_{prec} and Δ_{up} (associated with precipitation of secondary weathering products, and with plant uptake, respectively) (3) elemental fluxes to, within and out of the weathering zone. The fluxes are expressed relative to the supply rate of the considered element into the weathering zone which is, at steady-state, denudation rate times bedrock chemical composition.

Using this model, we show how soil water or river water isotope composition δ_{water} will be offset from the bedrock composition δ_{rock} by an amount that is not only (1) depending on the flux weighted-average of Δ_{prec} and Δ_{up}, but also (2) increasing with increasing elemental flux of combined net precipitation of secondary weathering products and net litter formation, and (3) increasing with decreasing elemental flux resulting from the dissolution of primary minerals. (2) and (3) represent strong mass balance effects that likely depend on the considered element (and on its biogeochemical properties such as solubility, affinity for clay minerals, or importance as a nutrient) and the geomorphic regime of the considered setting (e.g. supply versus kinetically limitated weathering). These mass-balance effects have to be taken into account when linking isotope ratios with isotope fractionation factors and biogeochemical processes in the weathering zone.

Furthermore, the model shows that δ_{water} will depend strongly on the intensity of biological uptake only if a significant proportion of the considered element is exported as plant litter, establishing a prerequisite to the use of metal stable isotope ratios in the sedimentary record as a tracer of terrestrial biological activity.

The model also has important implications in terms of sampling strategy: it can be shown in particular that the effects of Δ_{prec} and of Δ_{up} cannot be disentangled using isotope composition of river water or of bulk sediment alone. For this purpose, separates of organic and secondary phases from river particulate load or from topsoil, are needed.

No REE into the Earth's core

M.A. BOUHIFD[1*], M. BOYET[1], D. ANDRAULT[1], N. BOLFAN-CASANOVA[1] AND J.L. DEVIDAL[1]

[1]Laboratoire Magmas et Volcans, Université Blaise Pascal, CNRS UMR 6524, 5 Rue Kessler, 63000 Clermont-Ferrand, France

Introduction

The earliest history of the Earth was marked by accretion and core formation within about 100 Myr [1, for a review]. Short-lived radioisotope systems such as ^{146}Sm-^{142}Nd (composed by two refractory elements) are useful in determining how the silicate Earth, for example, evolved during and after accretion. Recent Sm-Nd data show that all terrestrial samples have on average 20 ppm ^{142}Nd excess relative to chondritic meteorites [2]. It is thus evident that an enriched Hadean reservoir has to exist, unless the bulk Earth accreted with a Sm/Nd ratio that was higher than the chondrite average. Within several hypothesis [3], the enriched Hadean reservoir maybe the core since rare earth elements (REE) are not strictly litophiles in more reducing conditions [4]. In order to test this hypothesis, experiments at core-forming conditions (P, T, f_{O2}, etc) are needed to assess whether or not the core plays an active role in the observed ^{142}Nd anomalies.

To simulate Earth's core formation under conditions of segregation from a deep magma ocean, we performed multi-anvil experiments between 3 and 8 GPa at various temperatures between 2073 and 2373 K, to determine the partition coefficients of REE between molten C1-chondrite model composition and various Fe-rich alloys (including $Fe_{90}Ni_{10}$, $Fe_{83}Si_{17}$, and $Fe_{80}Ni_{10}S_{10}$). The run products indicate that the oxygen fugacity (f_{O2}) ranges from 1.5 to 5 log units below the iron-wüstite (IW) buffer, and is in agreement with core-formation models in which metallic liquid equilibrates with molten silicate under reducing conditions. The chemical compositions of the run products were determined by laser ablation ICP-MS and electron microprobe. Our results show a low liquid metal-silicate melt partition coefficients of all REE that range between 10^{-3} and 10^{-5} (an increase of the partition coefficients with decreasing the f_{O2} is observed). More importantly, our experiments show that the metal-silicate partition coefficients of Sm and Nd are similar within the investigated conditions, meaning that the Sm/Nd ratio is not fractionated by metal-silicate segregation. Another line of support of this conclusion is found by an independent work on the cosmochemical and petrological study of enstatite chondrites [5].

Conclusion

If the bulk Earth has chondritic ^{142}Nd/^{144}Nd ratio, an enriched Hadean reservoir has to exist within the deep mantle. In contrast, if the bulk Earth has an Nd isotopic composition distinct from that of the chondrites, then there is no need to invoke a hidden reservoir. In any case the Earth's core is out of the equation concerning the ^{142}Nd anomalies.

[1] Kleine *et al*. (2009) *GCA* **73**, 5150-5188.
[2] Boyet and Carlson (2005) Science **309**, 576-581.
[3] Andreasen *et al*. (2008) *EPSL* **266**, 14-28.
[4] Lodders (1996) *Meteoritics & Planetary Science* **31**, 749-766.
[5] Gannoun *et al*. (2011) *GCA* **75**, 3269-3289.

Mg,Fe-rich carbonates stability at lower mantle conditions

E. BOULARD[1]*, W. MAO[1]

[1]Stanford University, Stanford, U.S.A., boulard@stanford.edu (*presenting author); wmao@stanford.edu

Only a small fraction of the total carbon budget of the Earth is found at the surface; with the mantle and core likely being the largest carbon (C) reservoirs in the planet [e.g. 1, 2]. Carbonates are the main C-bearing minerals that are recycled into the deep Earth. Previous studies, focusing on the stability of Ca and Mg rich carbonates in the upper mantle, demonstrated the possibility of C to be recycled into the lower part of the mantle [e.g. 3]. A few experimental studies have been conducted on the stability of magnesite ($MgCO_3$) in equilibrium with silicates at lower mantles pressure and temperature (P-T) conditions. The decarbonation reaction: $MgCO_3$(magnesite) + SiO_2 (stishovite) -> $MgSiO_3$ (perovskite) + CO_2 (solid) has been reported at lower mantle conditions limiting the carbon cycle to about the first 1200 km deep (about 45 GPa - 2200 K) [4]. On the other hand, Seto et al. [5] supports the possibility for a deeper recycling of carbon in the Earth in relatively cold slabs, as they observed decarbonation of magnesite in equilibrium with mid ocean ridge basalt (MORB) at higher temperature. However, several carbonate phase transitions have been reported at higher P-T [e.g. 6].

We conducted high P-T experiements on iron-bearing carbonates stability. We used both *in situ* and *ex situ* analyses including synchrotron based X-ray diffraction and transmission electron microscopy to characterize the structure and the chemistry of the different phases in the samples. Two new high P-T phases were observed for two compositions: (1) the $(Mg,Fe)CO_3$ system above 85 GPa – 2000 K [7] and (2) the $FeCO_3$ composition above 40 GPa – 1500 K [8]. In both of these new phases, the structures determined from *ex situ* analyses led us to propose a change in the C environment as the C formed $(CO_4)^{-4}$ tetrahedra instead of triangular $(CO_3)^{-2}$ groups as in carbonates. We will discuss the influence of such structural changes on carbonate stability and its solubility within mantle silicate phases.

[1] Javoy, M. et al. (1982) *Nature*, **300**, p. 171-173. [2] Dasgupta, R., and M.M. Hirschmann (2010) *Earth Planet. Sci. Lett.*, **298** (1-2), 1-13. [3] Poli et al. (2009) *Earth Planet. Sci. Lett.*, **278**(3-4), 350-360. [4] Takafuji et al. (2006) *Physics and Chemistry of Minerals*, **33**, p. 651-654. [5] Seto et al. (2008) *Physics and Chemistry of Minerals*, **35**, p. 223-229. [6] Isshiki et al. (2004) *Nature*, **427**, p. 60-63.[7] Boulard et al. (2011) *PNAS*, **108**, no 13, 5184-5187. [8] Boulard et al. (in press) *J. Geophys. Res.*

Upper crustal record of migmatites exhumation: the South Armorican Domain

PHILIPPE BOULVAIS[1*], ROMAIN TARTESE[1,2], MARIE-CHRISTINE BOIRON[3], MARC POUJOL[1], GILLES RUFFET[1],

[1]Université de Rennes 1,UMR CNRS 6118 Géosciences Rennes, 35042 Rennes, France - philippe.boulvais@univ-rennes1.fr (* presenting author)

[2]Open University, Planetary and Space Sciences, Milton Keynes, UK

[3]Université de Lorraine, UMR CNRS 7566 G2R, 54501 Vandoeuvre-lès-Nancy, France

The South Armorican Massif hosts a high-grade metamorphic domain mainly composed of medium to high-grade micaschists, migmatitic gneisses and anatectic granites [1]. At the end of the Carboniferous, these deep crustal units were exhumed rapidly during the extension associated with the collapse of the Hercynian chain [2]. To the North, this domain is limited by the listhospheric-scale South Armorican Shear Zone (SASZ). Giant quartz veins are associated with the SASZ and recorded important synmetamorphic fluid circulation [3]. Together with very low $\delta^{18}O$ values for some euhedral quartz, down to -2‰, low-salinity fluid inclusions argue for a contribution from meteoric fluids [3]. Corresponding $\delta^{18}O_{fluid}$ values estimated around -11‰ are probably related to the high palaeo-elevation of meteoric precipitation. Scarce, but significant, CO_2 fluid inclusions in euhedral quartz indicate also a metamorphic contribution. Metamorphic fluids were probably sourced from the exhumed metamorphic basement in the southern part of the Massif. Also, because of the synchronicity between the metamorphic event (exhumation) and the meteoric infiltration, it is proposed that the heat advected towards the surface by the exhumation of high-grade metamorphic rocks provided the driving force for meteoric fluid circulation on a regional scale.

The meteoric infiltration is recorded regionally by the mylonites which actually define the SASZ and by the syn-kinematic granites which emplaced along the SASZ. Low $\delta^{18}O$ values have been measured on some feldspar and zircon grains in the formers [4] while oxygen isotope disequilibirum was recorded by Qz-Fds pairs in the latters [5]. The muscovite Ar-Ar and monazite U-Th-Pb chronometers from these lithologies were highly disturbed [4,6]. In the Questembert granite, a classical example of a syn-kinematic granite, pervasive infiltration of oxydative meteoric water was facilitated by the penetrative character of the deformation (C/S planes are observed throughout the massif) and was probably responsible for the leaching of millions of tons of uranium while the granite was still at depth.

[1] Brown M. and Dallmeyer R.D. (1996) *Journal of metamorphic Geology* **14**, 361-379. [2] Gapais D. et al. (1993) *Comptes Rendus de l'Académie des Sciences* **316**, 1123-1129. [3] Lemarchand J. et al. (2012) *Journal of the Geological Society* **169**, 17-27. [4] Tartèse R. et al. (2012) *Journal of Geodynamics*, in press. [5] Tartèse R and Boulvais P (2010) *Lithos* **114**, 353-368. [6] Tartèse R. et al. (2011) *Terra Nova* **23**, 390-398.

Petrology, geochemistry and petrogenesis of the Beattie Syenite, Porcupine-Destor fault zone, Abitibi Subprovince, Québec

JULIE BOURDEAU[1]*, ANDRÉ E. LALONDE[1], JEAN GOUTIER[2]

[1]University of Ottawa, Ottawa, Canada, bourdeau.julie.e@gmail.com*, aelzr7@uottawa.ca

[2]Ministère des Ressources Naturelles et de la Faune, Rouyn-Noranda, Canada, jean.goutier@mrnf.gouv.qc.ca

Abstract

The Beattie Syenite is composed of five lenticular bodies of syenitic rocks that occur immediately north of the Porcupine-Destor fault zone in the town of Duparquet, approximately 32 km north of Rouyn-Noranda in the Abitibi Subprovince. The principal body is 3.3 km long and 425 m in width and is flanked by a series of smaller lenses to the south and northeast. The intrusion has yielded zircon ages of 2682 ±1 Ma and 2682.9 ±1.1 Ma and hosted the major part of the Au-mineralization of the now defunct Beattie mine; a major producer of gold in the area from 1933 to 1956 (9.66 Mt at 4.88 g/t Au). A total of 5 principal petrographic units are defined on the basis of field relationships, petrography, mineralogy, and textures:

1) The Beattie syenite porphyry unit is composed of 2-10% of tabular euhedral feldspar phenocrysts (2-10 mm) set in a red feldspathic and aphanitic matrix.

2) The unaltered syenite unit is composed of 2-10% of euhedral feldspar phenocrysts (2-10 mm) in a fine-grained matrix. It is characterized by unaltered phenocrysts of amphibole and titanite and is the only unit with relicts of pyroxene.

3) The Central Duparquet syenite porphyry containing between 2-25% of coarse equant euhedral feldspar phenocrysts (5-16 mm) in a red or sometimes grey aphanitic matrix.

4) The megaporphyritic syenite unit is composed of very coarse alkali feldspar phenocrysts, 1-6 cm across, in a red aphanitic matrix.

5) The feldspar lath dyke unit occurs as numerous thin dykes, on the order of a few meters in width, that cross-cut all other petrographic units. The lath dykes display a characteristic trachytoid texture defined by the preferential alignment of alkali feldspar laths (1-3 cm) in a grey or red aphanitic matrix.

From petrographic observations, there is evidence of a syenitic magma which is exhibited by the occurrence of syenite dykes with trachytoid flow textures. Detailed petrographical and mineralogical studies reveal a series of hydrothermal events including the precipitation of albite, sericite, chlorite and carbonate minerals. Initial geochemical results indicate that the Beattie Syenite is part of the alkaline series, as defined in the ($Na_2O + K_2O$) vs. SiO_2 diagram, and is feldspar normative. Whole-rock normalized REE patterns demonstrate that all the petrographic units are comagmatic. Furthermore, with selective trace elements, the tectonic setting of the syenite according to [1] would correspond to a volcanic-arc environment.

[1] Pearce, Harris and Tindle (1984) *Journal of Petrology* **25**, 956-983

Isotope fingerprints for the formation and the composition of the Earth

BERNARD BOURDON [1]*

[1]Laboratoire de Géologie de Lyon, ENS Lyon, UCBL and CNRS UMR 5276, Lyon France, bernard.bourdon@ens-lyon.fr

Building blocks

Most models for the formation and composition of the Earth usually focus on specific characteristics of its chemical or isotope composition. For example, since the formation of the Earth leads to substantial heating of planetary materials, volatile depletion and metal-silicate separation, it is sensible to consider only the refractory lithophile elements (RLE) to assess the potential building blocks of the Earth. In this context, the carbonaceous chondrites, notably the CI chondrites give the best match for RLE in the Earth's mantle and are often used as a starting material, although the processes mentioned above can affect the siderophile and volatile element concentrations in this starting material.

In contrast, when considering isotope observations, it appears that enstatite chondrites show an almost perfect match with many isotope systems, including oxygen, chromium, nickel and titanium. Then, if one considers the ^{146}Sm-^{142}Nd system, it appears that the terrestrial composition does not match with carbonaceous chondrites but could be better explained by ordinary or enstatite chondrites. However, the ^{146}Sm-^{142}Nd observations can also be explained by a non-chondritic Earth. Last, in the case of silicon isotopes, there is a clear offset between the terrestrial composition and that of chondrites. In summary, there seems to major issues in building the Earth from a single class of chondrites or from unprocessed chondritic material.

Processing of planetary materials

There are several processes that can modify the composition of the planetary materials that have formed the Earth, including thermal processing leading to volatile depletion (partial condensation or evaporation), grain sorting, impact-driven processes or metal segregation. In this presentation, I will examine the possible role of these processes in light of our recent isotope observations with a focus on Nd, Si, Mg, Mo and Sr isotopes and show how mixtures of various chondritic materials together with significant later processing is required to explain the composition of the Earth.

Molecular-scale basis of the ion exchange selectivity of clay minerals

IAN C. BOURG[1,*]

[1]Earth Sciences Division, Lawrence Berkeley National Laboratory, Berkeley, USA, icbourg@lbl.gov (* presenting author)

Ion exchange reactions on clay mineral surfaces play important roles in the aquatic geochemistry and mechanical properties of argillaceous media (soils, sediments, clayshales, engineered clay barriers). Despite more than a hundred years of investigation, fundamental aspects of the ion exchange selectivity of clay minerals, such as the activity coefficients of adsorbed species, the molecular-scale basis of ion exchange selectivity coefficients, and the structure of the electrical double layer (EDL), are poorly understood [1]. We report new molecular dynamics (MD) simulations elucidating the structure of the EDL on smectite surfaces contacting mixed NaCl-$CaCl_2$ electrolyte solutions at dilute concentrations ($\leq$ 0.1 mol_c dm^{-3}). Our simulations used methodologies known to correctly describe the structure and diffusion coefficients of water and solutes in smectite interlayer nanopores [2]. They complement our previous simulations of concentrated electrolyte solutions (0.34 to 1.83 mol_c dm^{-3}) on smectite surfaces [3]. Our results confirm the molecular-scale view of EDL stucture on phyllosilicate basal surfaces derived from X-ray reflectivity measurements of adsorption on mica surfaces [4]. They also provide insights into several fundamental aspects of the ion exchange selectivity of clays, such as the adequacy of the Gaines-Thomas or Vanselow conventions and the affinity of clay surfaces for $CaCl^+$ ion pairs [1].

[1] Bourg & Sposito (2011) *Ion-Exchange Phenomena*, In: *Handbook of Soil Science*, 2nd ed., Chapter 16. [2] Bourg & Sposito (2010) *Environ. Sci. Technol.* **44**, 2085. [3] Bourg & Sposito (2011) *J. Colloid Interface Sci.* **360**, 701. [4] Lee, Fenter, Park *et al.* (2010) *Langmuir* **26**, 16647.

Landscape-scale pedogenic relationships between soil carbon and secondary metal oxides in Hubbard Brook podzols, northeastern US

REBECCA R. BOURGAULT[1*], DONALD S. ROSS[1], SCOTT W. BAILEY[2], PATRICIA A. BROUSSEAU[3], JOHN P. GANNON[3], KEVIN J. MCGUIRE[3] AND THOMAS D. BULLEN[4]

[1]University of Vermont, Burlington, VT, USA, rbourgau@uvm.edu (* presenting author), dross@uvm.edu

[2]US Forest Service, North Woodstock, NH, USA, swbailey@fs.fed.us

[3]Virginia Tech, Blacksburg, VA, USA, patrb87@vt.edu, jpgannon@vt.edu, kevin.mcguire@vt.edu

[4]US Geological Survey, Menlo Park, CA, USA, tdbullen@usgs.gov

Abstract

Podzols are unique soils in which metals and carbon are intimately linked by the pedogenic process of podzolization. In this soil-forming process, organic matter (OM) chelated by Al, Fe and Mn leaches from the soil surface and accumulates in the subsurface spodic (B) horizon. Spodic materials (ill-defined associations of Al, Fe, Mn and C) in the B horizon are more resistant to decomposition than OM in the soil surface, in part due to the stabilizing effect of chelation and/ or sorption by Al, Fe and Mn. Podzols are found globally in a variety of environments, and therefore represent an important carbon sink. Research suggests that spatial variations in podzolization can result in part from hydrologic processes such as dominant flowpath direction, and reduction-oxidation processes driven by water table dynamics. These processes determine solubility, transport, and accumulation of Al, Fe, Mn and C. In this study, we document vertical and lateral distributions of total soil C in Watershed 3 (WS3), which is a forested, podzolized catchment in the Hubbard Brook Experimental Forest (HBEF), New Hampshire, in the Northeastern US. We will examine the relationships of C to total secondary Fe oxides and Mn oxides (extracted by citrate-dithionite), and poorly crystalline Al and Fe oxides (extracted by acid ammonium oxalate). Eighty pedons have been described, sampled, and extracted by horizon throughout WS3. In order to determine the role of hydrologic processes in determining soil chemistry in WS3, combined hydrometric monitoring and isotope tracers are used to document flowpaths, water table dynamics, and ground water chemistry and transport. Preliminary results indicate redistribution of spodic materials according to flowpaths. For example, where lateral flowpaths predominate, there is landscape-scale lateral podzolization: leaching/ loss of metals and C upslope, and accumulation of metals and C downslope. In contrast, pedon-scale vertical podzolization is more evident where flowpaths are dominantly vertical, such as on well-drained backslopes. As expected, the Mn:Fe ratio is higher in laterally deposited spodic materials as opposed to vertically deposited spodic materials, due to the fact that Mn is more sensitive to redox conditions and therefore more mobile than Fe. Understanding the spatial distributions of Al, Fe, Mn, and C at the landscape scale in WS3 may provide valuable information about the complex interactions between water and soils, metals and carbon in a forested, podzolized Northeastern US watershed.

An experimental study of the stability of the REE(III) in sulphate-bearing aqueous solutions

N. BOURQUE*, ART. MIGDISOV, AND A.E. WILLIAMS-JONES

McGill University, Earth & Planet. Sci., Montreal, QC, Canada (*correspondence: nicolas.bourque@mail.mcgill.ca)

During the past fifteen years, numerous studies of a variety of geological settings have demonstrated that the rare earth elements (REE) are mobilized by hydrothermal fluids [1, 2, 3]. As sulphate complexes of the REE are known to be among the most stable aqueous species at ambient temperature, it is therefore reasonable to propose that these species play an important role in REE transport in hydrothermal systems with high sulphate activity. However, published experimental data on the behaviour of REE sulphate species at elevated temperatures are limited to Nd, Sm, and Er [1] and therefore, evaluations of the mobility of the REE in hydrothermal sulphate-bearing solutions have been based mainly on the theoretical predictions of Haas et al. (1995). In view of this, we have systematically investigated the behaviour of the REE, including Y, in sulphate-bearing aqueous solutions and determined the properties of sulphate complexes of these elements at elevated temperature.

The technique employed in the experiments was identical to that described in Migdisov and Williams-Jones (2007). The experiments involved determining the solubility of REE oxides and fluorides in solutions with a range of sulphate concentrations, and were performed at temperatures up to 250 °C and saturated pressure of water vapour.

The data derived from the measured solubility of the REE solids show that the stability of REE sulphate species varies little with the atomic number of the REE. For example, the logarithm of the first formation constant of La (log β_1) at 200˚C differs from that of Yb by less than 1 log unit. The same observation was made in earlier spectroscopic studies of Nd, Sm, and Er sulphate species [1]. This observation suggests that the REE are unlikely to fractionate in nature, if they are transported as sulphate species.

[1] Migdisov, A.E. Williams-Jones (2008) *Geochimica et Cosmochimica Acta* **72**, 5291–5303

[2] Migdisov, A.E. Williams-Jones (2007) *Geochimica et Cosmochimica Acta* **71**, 3056–3069.

[3] Haas et al. (2005), *Geochimica et Cosmochimima*. Acta **59**, 4329–4350.

Minor and trace element composition of iron oxides from IOCG deposits worldwide and its application to mineral exploration

EMILIE BOUTROY[1*], GEORGES BEAUDOIN[1], SARAH-JANE BARNES[2] AND LOUISE CORRIVEAU[3]

[1]Université Laval, Département de géologie et de génie géologique, emilie.boutroy.1@ulaval.ca (* presenting author)
Georges.Beaudoin@ggl.ulaval.ca
[2]Université du Québec à Chicoutimi (UQAC), Sciences de la Terre, sjbarnes@uqac.ca
[3]Geological Survey of Canada, Natural Resources Canada louise.corriveau@rncan-nrcan.gc.ca

There are significant variations in the concentration of trace elements in magnetite and hematite depending on the metallogenic environment at the time of formation of the deposit. This makes iron oxides useful as indicator minerals for mineral exploration.

Iron oxides are a major component of Iron Oxide Copper-Gold deposits (IOCG) and of Iron Oxide-Apatite deposits (IOA). Magnetite and hematite in IOCG (n= 84 samples) and IOA deposits (n= 6), representative of 8 major IOCG and IOA deposits, worldwide, representing a range of geological environments and ages of formation, were analyzed by electron microprobe analysis (EMPA). A subset of IOCG (n = 30 samples) and IOA (n= 6) was analysed by LA-ICP-MS. The IOCG deposits samples are divided based on the principal iron oxide present: (1) Hematite (n = 10), (2) Magnetite (n = 37) and (3) Hematite ± Magnetite (n =8). Similarly, IOA deposits are divided: (1) Magnetite (n = 3) and (2) Magnetite ± Hematite. In these types of deposits, iron oxides are in mineralization and in host rock alteration assemblages, and there are typically multiple generations of iron oxides. Iron oxides are studied according to their paragenetic stage: (1) ore stage and (2) hydrothermal alteration of host rocks. Hydrothermal alteration iron oxides are grouped according to the type of alteration: (1) Ca-Fe alteration (Am-Ap-Mag), (2) Na(Fe) alteration (Ab-Scp-Mag/Hem), (3) High temperature K-Fe alteration (Bt-Kfs-Mag) and (4) Low temperature K-Fe (Ser-Kfs±Chl±Cb-Hem). Preliminary results show hematite in Hematite-group IOCG deposits is depleted in Zn, Ni, Mn, V and enriched in K, Ti, Al, Si compared to magnetite in Magnetite-group IOCG deposits. In Magnetite-IOA deposits, magnetite is enriched in V, Al and Mg compared to Magnetite-Hematite-IOA deposits, which is enriched in Ca.

Compared to primary magnetite in Ni-Cu-PGE deposits, ore-stage magnetite in IOCG deposits are depleted in Ni, Cu and Cr and enriched in Ti, Al and Si.

Functional gene pyrosequencing sheds light on the distribution and diversity of a key nitrogen cycle gene (*nirS*) in marine systems

JENNIFER L. BOWEN[*1], DAVID WEISMAN[1], AMAL JAYAKUMAR[2], MICHIE YASUDA[1] AND BESS B. WARD[2]

[1]University of Massachusetts Boston, MA, USA Department of Biology, jennifer.bowen@umb.edu (*presenting author), weisman@lydon.com, michie.yasuda@umb.edu

[2]Princeton University, Princeton, NJ, USA Department of Geosciences, ajayakum@princeton.edu, bbw@princeton.edu

Introduction

Denitrification, a critical pathway in the nitrogen cycle that converts dissolved inorganic nitrogen to its gaseous form, plays a central role in removing nitrogen from the environment. Denitrification in estuaries, continental shelves, and oxygen minimum zones accounts for nearly 60% of the global fixed nitrogen loss [1]. There are two genes, *nirS* and *nirK* that encode functionally similar nitrite reductase enzymes that facilitate the denitrification process. The two genes do not appear to co-occur within a given microorganism but both genes are present in most environments. In the marine environment *nirS* tends to be more abundant than *nirK* [2]. Examining the structure and abundance of denitrifiers represented by the *nirS* gene in a variety of marine environments will shed new light on biogeochemical ecology of this critically important ecosystem service.

Results and Conclusions

We used functional gene pyrosequencing to examine the abundance and diversity of denitrifying bacteria in all three major oceanic oxygen minimum zones as well as in coastal sediments from Chesapeake Bay and a New England salt marsh. To assess the role of sequencing error in inflating our diversity estimates we sequenced amplicons of four clones and show that our data analysis pipeline successfully identifies and removes the overwhelming majority of spurious sequences (Fig. 1). The data indicate an astonishing degree of diversity in the *nirS* gene, with over 3500 taxa (defined operationally as sharing 95% sequence identity), found in salt marsh sediments alone. Pyrosequencing detects distinct differences in the composition of nirS assemblages in water column and sediment environments.

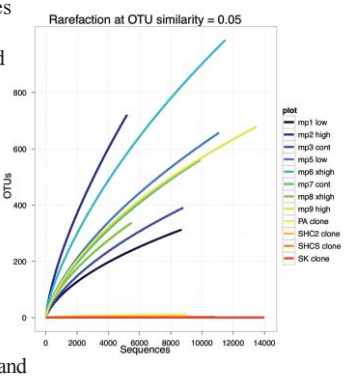

Figure 1: Rarefaction curves resulting from pyrosequencing of the nirS gene in salt marsh sediments and in control sequenced

[1] Seitzinger (2004) *Ecol. Appl.* **52**, 47-59. [2] Jones and Hallin (2010) *ISME J* **4**, 633-641.

Role of hydration energy on near-surface H_2O and ion molecular-scale dynamics: Comparing Na- and Ca-hectorites with NMR spectroscopy

GEOFFREY M. BOWERS[1,3*], R. JAMES KIRKPATRICK[2], JARED WESLEY SINGER[3]

[1]Alfred University, Division of Chemistry, Alfred, NY, USA, bowers@alfred.edu (* presenting author)
[2]Michigan State University, College of Natural Science, East Lansing, MI, USA, rjkirk@cns.msu.edu
[3]Alfred University, Kazuo Inamori School of Engineering, Alfred, NY, USA, jws4@alfred.edu

Solid-state NMR spectroscopy is uniquely equipped to study behavior at interfaces and in confinement within complex geochemical systems. The primary advantage of this technique is that it can simultaneously provide information on the molecular-scale structure and dynamic behavior over a broad range of rate scales difficult to probe via other methods (kHz to MHz) and on a site-specific basis. In this work, we share recent results from our ongoing variable temperature NMR studies of phyllosilicate/H_2O interfaces [1-4] by focusing on the influence that metal charge and hydration energy have on H_2O and metal ion structure and dynamics in the interlayer of Na- and Ca-hectorites between -120°C and 50°C. We find that near-surface ^2H_2O in 2-layer hydrates of Na- and Ca-hectorites are well modeled by simultaneous C2/C3 reorientation of a slightly compressed or extended hydration shell (with respect to an ideal octahedral hydration shell) at a rate in excess of 200 kHz between -50°C and 40°C [1]. Though our model and ^2H VT NMR show the hydration shell compression/extension varies slightly over the temperature range in each type of hectorite, the Ca^{2+} hydration shell geometry deviates less from the ideal case at all temperatures, consistent with the higher hydration energy of Ca^{2+} vs. Na^+. Associated ^2H T_1 relaxation experiments at several temperatures shows nearly identical reductions in T_1 with respect to temperature, though the ^2H nuclei in Ca-hectorite relax more quickly at all temperatures, suggesting a higher intensity of motion in the power spectrum at 45.6 MHz and that the power spectrum intensity increases with decreasing temperature for Na- and Ca-hectorite. With respect to the associated metal dynamics, both Na^+ and Ca^{2+} in 2-layer hectorite hydrates are dominated by rapid diffusion in 2 or 3 dimensions, though comparison of the ^{23}Na and ^{43}Ca VT NMR shows that Ca^{2+} experiences very rapid diffusion at much lower temperatures than Na^+ (-120°C vs. -20°C, respectively). These results are consistent with our recently published general principle that rapid diffusion becomes the dominant mode of metal cation motion for near-surface water and ions in smectites at lower temperatures as the metal hydration energy increases if the ionic radii are similar [1].

[1] Bowers et al. (2011) *Journal of Physical Chemistry C* **115**, 23395-23407. [2] Bowers et al. (2008) *Journal of Physical Chemistry C* **112**, 6430-6438. [3] Weiss et al. (1990) *Geochimica et Cosmochimica Acta* **54**, 1655-1669. [4] Bowers et al. (2012) in preparation.

Characterization of naphthenic acids in oil sands tailings ponds by two-dimensional gas chromatography time-of-flight mass spectrometry (GCxGC-TOF-MS)

DAVID BOWMAN*, B. E. MCCARRY

[1]McMaster University, Department of Chemistry and Chemical Biology, Hamilton, Ontario
bowmand@mcmaster.ca (* presenting author)
mccarry@mcmaster.ca

Naphthenic acids are a complex mixture of aliphatic and polyalicyclic organic acids found naturally in hydrocarbon deposits. Oilsand ore is refined using the Clark hot water extraction procedure; naphthenic acids are extracted and end up in the process water. These waters are sent to large tailing ponds where particulate materials settle out slowly. Naphthenic acids are of environmental concern due to their toxicities in various mammals and fish; these concerns have lead to a zero discharge policy for oil sands tailings.[1] Naphthenic acids are known to be utilized by plants.[2] We have proposed that these compounds may be utilized by soil bacteria in the tailings ponds which may serve as a source for the generation of H_2S.

In this study, we are using two-dimensional gas chromatography time-of-flight mass spectrometry (GCxGC-TOF-MS) to provide profiles of complex mixtures of naphthenic acids (see Figure 1). Using this method it is possible to resolve over 8000 components in this sample. We hypothesize that the profiles of naphthenic acids will be altered by bacterial biodegradation and that these changes will be detectable using GCxGC. The extraordinary peak capacity and resolving power of two-dimensional gas chromatography makes it a suitable tool for the comparison of profiles of naphthenic acid mixtures.

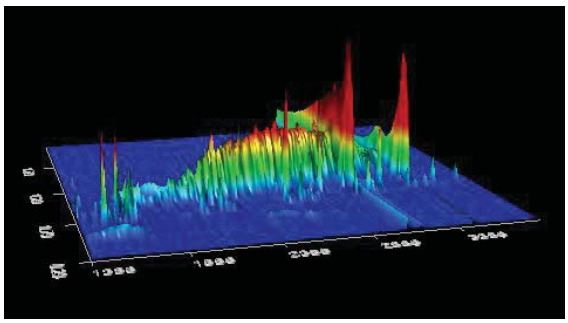

Figure 1: Two-dimensional total ion chromatogram (TIC) plot of naphthenic acids in oil sand process water sample (sample provided by Syncrude).

[1] Hao, C.; Headley, J.; Peru, K.; Frank, R.; Yang, P.; Solomon, K. (2005) *Journal of Chromatography A* **1067**, 277-284.
[2] Headley, J. V.; Armstrong, S. A.; Han, X.; Martin, J. W.; Mapolelo, M. M.; Smith, D. F.; Rogers, R. P.; Marshall, A. G (2009) *Rapid Communications in Mass Spectrometry* **4**, 515-522.

Mercury species and thiols from GEOTRACES cruises in the North and South Atlantic Ocean

K.M. BOWMAN[1], T. KADING[2], G.S. SWARR[2], C.H. LAMBORG[2]*, C.R. HAMMERSCHMIDT[1] AND M. RIJKENBERG[3]

[1]Wright State University, Earth and Environmental Science, Dayton OH USA (correspondence: bowman.49@wright.edu)
[2]Woods Hole Oceanographic Institution, Marine Chemistry and Geochemistry, Woods Hole, MA USA (*presenting: clamborg@whoi.edu)
[3]Royal Netherlands Institute for Sea Research, Marine Geology, The Netherlands

As part of GEOTRACES research activities, we have measured dissolved and particulate mercury (Hg) species, aerosol and rainwater total Hg and dissolved thiols from a US zonal transect in the North Atlantic Ocean as well as total Hg from a meridional transect in the South Atlantic Ocean from a Dutch/UK sponsored cruise. This is currently the largest database of its kind. Findings include: 1) total Hg profiles are nutrient-like in the upper 1000 m, but show a mixture of qualities in deep water that appeared to be controlled by water mass transport; 2) surface total Hg concentrations were strongly affected by rain inputs, productivity and the Amazon River plume; 3) dissolved elemental Hg frequently followed nitrate distributions; 4) monomethyl- and dimethyl-Hg showed distinctive peaks in the oxygen minimum zones; 5) methylated Hg concentrations showed a lower response to organic carbon remineralization rates than those recently reported for the Pacific and Indian Oceans; 6) thiols appear to be important complexing agents for Hg (and other metals) in surface waters; 7) thiol concentration distributions are similar to chlorophyll, and therefore do not predict methylated Hg concentrations well.

Transformations of aqueous U(VI) during redox cycling of Fe phases

MAXIM I. BOYANOV[1]*, DREW E. LATTA[1], MICHELLE M. SCHERER[2], EDWARD J. O'LOUGHLIN[1], AND KENNETH M.. KEMNER[1]

[1]Argonne National Laboratory, Argonne, IL, USA, mboyanov@anl.gov (* presenting author)
[2]The University of Iowa, Iowa City, IA, USA

The activity of dissimilatory iron-reducing bacteria or the corrosion of waste containers often result in the presence of Fe^{II} and Fe^{III} species in subsurface environments. Recent work has shown that dissolved Fe^{II} exchanges atoms with Fe^{III}-containing solids in a dissolution-reprecipitation equilibrium, which likely proceeds via formation of minor but highly reactive Fe^{II}/Fe^{III} species at the surface. The fate of dissolved or adsorbed U^{VI} during such transformations will depend on the reactivity and transformations of both major and minor Fe phases, with possible outcomes including reduction and precipitation of $U^{IV}O_2$ (uraninite), reduction and incorporation of U^{IV} atoms in other phases, and non-reductive solid-phase incorporation of U^{VI}. We examined the reaction of dissolved U^{VI} with a host of Fe^{II}-containing phases, including dissolved and carboxyl-adsorbed Fe^{II}, green rusts with different interlayer anions, magnetite, and NAu-2 nontronite clay, as well as with oxidized analogues such as maghemite and pyroaurite. The goal was to establish the uptake mechanisms and to characterize the molecular structure of the solid-associated U species.

Experimental Methodology

We used x-ray absorption fine-structure spectroscopy (EXAFS and XANES) at the U L_{III}- and Fe K-edge to probe the speciation of U and Fe in the hydrated solid phases after reaction. Samples were reacted under geochemical conditions relevant to the subsurface, including the presence of carbonate and/or phosphate.

Discussion of Results

U^{VI} was reduced to U^{IV} by sulfate, chloride, and carbonate green rusts; the speciation of reduced U^{IV} varied between that in uraninite and a non-uraninite, adsorbed/incorporated U^{IV} species. Pyroaurite sequestered U^{VI} as a U^{VI}-carbonate complex, presumably by interlayer ion exchange. Magnetite reduced U^{VI} to nanoparticulate uraninite when its Fe^{II}/Fe^{III} content exceeded 0.38. Reactions with more oxidized magnetite ($Fe^{II}/Fe^{III}<0.38$) resulted in oxidized U species. The latter had less uranyl character than U^{VI} adsorbed to maghemite, suggesting U uptake in a distinct phase. Reactions between U^{VI}, nontronite, and Fe^{II} also resulted in oxidized, non-uranyl U species that were distinct from nontronite-adsorbed U^{VI}. Carboxyl-adsorbed U^{VI} and Fe^{II} reacted only when Fe^{II}-OH-Fe^{II} bonds formed, resulting in a combination of uraninite and U^{IV} atoms coordinated to Fe atoms in the nucleated mineral. The presence of dissolved phosphate (U:P=1:1) in the same system inhibited uraninite formation and resulted in U^{IV} atoms in phosphate-coordinated sites. The diversity of U incorporation modes in these model systems highlights the complexity in predicting U fate in subsurface environments — non-uraninite U^{IV} and non-uranyl oxidized U were also significant species in biostiumulated sediments from a contaminated field site (Oak Ridge, TN), and in naturally reduced soil from Hedrick, IA, reacted with U^{VI}.

Nucleosynthetic Nd isotope anomalies in primitive enstatite chondrites

M. BOYET[1]* AND A. GANNOUN[1]

[1] Laboratoire Magmas et Volcans, Université Blaise Pascal, CNRS UMR 6524, 5 rue Kessler, 63038 Clermont-Ferrand, France Boyet@opgc.univ-bpclermont.fr

Introduction

The first high precision measurements of $^{142}Nd/^{144}Nd$ ratios in chondrites have revealed that different groups of chondrites are characterized by different ratios [1, 2]. In order to interpret properly the deviation of $^{142}Nd/^{144}Nd$ ratio measured between terrestrial samples and chondrite material, it is crucial to understand the cause of the ^{142}Nd deviation in the different groups of chondrites. Enstatite chondrites (EC) present similar isotope compositions to terrestrial samples for a large number of elements (O, N, Mo, Cr, Ti) and have also the smallest ^{142}Nd offset (-10±12 ppm, [3]). We have selected primitive EC belonging to the EH subgroup for further Sm-Nd isotope investigations using a step-wise acid disolution method. The goal of this study is to better characterize the carrier phase of Nd nucleosynthetic anomalies and define their isotope composition.

Methods and Results

Sample powders were subjected to the following sequential leaching procedure: (1) H_2O then acetic acid, (2) EDTA, (3) 6M HCl, (4) Aqua regia and concentrated HF-HNO_3 mixture.. The major and trace element compositions of each fraction have been measured by ICP-AES and ICP-MS, respectively. Sm and Nd were separated using a 3 steps chemistry procedure and isotopes were measured on the Thermo-Fischer thermal ionization mass spectrometer at Laboratoire Magmas et Volcan, Clermont-Ferrand.

Most of the REE (50 to 80%) are contained in the first two leachate fractions mostly derived from the dissolution of oldhamite and ninigerite as deduced from the major element compositions. The last fraction have small REE contents (5-20%) which is mostly derived from the dissolution of enstatite and djerfisherite. Nd isotopes anomalies (ratios normalized to $^{146}Nd/^{144}Nd=0.7219$) are always positive for ^{145}Nd, ^{148}Nd and ^{150}Nd and negative in ^{142}Nd in fraction (1) to (3). The largest isotope anomalies are always measured in the last fraction (residu) with ^{142}Nd excess ranging from +200 to +600 ppm. The largest effects are measured in ALH77295, which is the most primitive EC analysed in this study.

Discussion

The residues obtained after leaching treatment are strongly enriched in s-process nuclides. The different Nd isotopes plot along the same correlation lines defined for leachates and residues of carbonaceous and odinary chondrites [4] suggesting that all residues contain s-process rich presolar grains. The amount of Sm in each fraction was too small to allow precise measurement of the $^{144}Sm/^{152}Sm$ ratios, however the p-process variability seems to be relatively small.

[1] Boyet and Carlson M. (2005) Science 309, 576-581. [2] Carlson et al. (2007) Science 316, 1175-1178. [3] Gannoun et al. (2011) PNAS 108, 7693-7697. [4] Qin et al. (2011) GCA 75, 7806-7828.

Aerosol release of Fe into the ocean: the extreme cases

EDWARD BOYLE[1]* AND JESSICA FITZSIMMONS[1,2]

[1]Massachusetts Institute of Technology, Cambridge MA 02139 USA, eaboyle@mit.edu

[2]MIT/WHOI Joint Program in Oceanography, jessfitz@mit.edu

By now it is well-known that partial dissolution of Fe from atmospheric aerosols is a major source of iron for oceanic phytoplankton and nitrogen fixers. But many of the details of the process are only partially understood: (1) What regulates the degree of Fe dissolution? (mineralogy of the source and chemical processing within the atmosphere are believed to be important, with anthropogenic aerosols releasing more Fe either because of the source or processing from anthropogenic acidity and photochemical processing), (2) What determines the form that iron takes upon release into seawater? (it appears that most of the aerosol-released Fe is converted into organic or inorganic colloidal form in high-dust regions, although there is an expectation that soluble organic complexes should also be important), (3) How does the dust flux influence the biota? (both phytoplankton and nitrogen fixers).

In order to learn more about these issues, we will discuss the contrasting oceanic iron distributions under a high-dust region (tropical North Atlantic) and a low-dust region (southeast Pacific between Chile and Easter Island). Under the high-dust region, most of the surface water Fe is colloidal and is removed to low concentrations near the chlorophyll maximum. Phosphorus is depleted to extremely low concentrations, as any excess over Redfield N:P ratios is compensated by nitrogen fixation. Below that, iron increases in step with increasing AOU, and the C:Fe ratio is low (~100,000). Under the low-dust environment, Fe is relatively low (0.10-0.15 nM) and uniform in the upper few hundred meters (despite increasing AOU below the chlorophyll maximum) and then increases to much higher C:Fe ratios (~500,000). Dissolved inorganic phosphorus remains at fairly high concentrations (~0.20 uM) because insufficient Fe prevents nitrogen fixers from compensating for the low N:P ratio in the upwelling deep waters.

Evolution of bioturbation buffered Neoproterozoic oxygenation

RICHARD A. BOYLE[1*] & TIMOTHY M. LENTON [1]

[1]University of Exeter, UK, r.a.boyle@exeter.ac.uk (*presenting author)

A range of geochemical evidence suggests a major oxygenation of the ocean (and by implication atmosphere) at the end of the Neoproterozoic – a change that may well have been necessary (although not sufficient) for the proliferation of the earliest animal life. However, indications of a localised reversion to more anoxic (and sulphidic) ocean conditions during the Cambrian raise the possibility of a subsequent drop in atmospheric oxygen. Furthermore, an explanation for why oxygen stopped rising during the Neoproterozoic remains elusive. Here we hypothesize that the efficiency of phosphorous removal from the ocean was significantly increased by the onset of large-scale sediment bioturbation and resultant ventilation - caused by the proliferation of macroscopic animals. This was due to (a) increased microbial P sequestration under oxic sedimentary conditions, and (b) greater net organic carbon oxidation reducing the C:P burial ratio[1,2]. The resulting reduction in the concentration of phosphorus in the ocean suppressed new production and organic carbon burial, reducing the long-term source of atmospheric oxygen and thereby buffering its concentration on a multi-million year timescale. We suggest that a plausible scenario for the integrated evolution of the Earth system at the end of the Neoproterozoic is therefore "increased marine P concentration via weathering of the land surface following terrestrial colonisation $\longrightarrow$ increased marine production and organic carbon burial $\longrightarrow$ increased atmospheric oxygen $\longrightarrow$ drastic increase in biomass and motility of the (already multi-cellular and differentiated) animal biosphere $\longrightarrow$ increased bioturbation $\longrightarrow$ reduction in marine P reservoir size and stabilisation of global phosphate and oxygen cycles"[3,4]. We argue that these feedbacks and a trajectory along these lines can help explain why atmospheric O_2 and marine PO_4 fluctuations have been well buffered during the Phanerozoic.

References

[1] Ingall, Bustin & Van Capellen. 1993. Geochim Cosmochim Act.**57**(2). 303-316.

[2] Krom & Berner. 1980. Limnol. Oceanog.**25**(5). 797-806.

[3] Lenton & Watson 2004. Geophy. Res. Lett. **31**(5) L05202.1-L05202.5.

[4] Boyle, 2008. Phd Thesis. University of East Anglia.

Lead-isotope geochemistry of the Bagirkacdere lead– zinc deposit, Biga Peninsula, NW Turkey

BOZKAYA, GULCAN

Cumhuriyet University, Department of Geological Engineering, Sivas, Turkey, gbozkaya@cumhuriyet.edu.tr

The Biga Peninsula contains several base-metal skarn deposits associated with Oligo-Miocene age granitic intrusions. The Bagirkacdere lead-zinc deposit is a typical example of the skarn-type deposits occurring in the northern section of the Biga Peninsula (5.2 Mt at 3.8 % Pb, 2.18 % Zn). The mineralization developed within the Paleozoic meta-sedimentary (Torasan metamorphics) and meta-granitic rocks (Camlik meta-granitoids) as stratabound disseminations and thin veins in schists, marble and meta-granitoids of the skarn zone. Pyrite, sphalerite and galena are the main sulphide minerals and they are accompained by minor amounts of chalcopyrite, arsenopyrite and hematite. Limonite, malachite, smithsonite, anglesite and cerrusite are secondary alteration products. The skarn is dominated by garnet, calc-silicates, epidote, actinolite, diopsite, feldspar and quartz.

Lead isotope ratios for galena have mean values of $^{206}Pb/^{204}Pb$ 18.758, $^{207}Pb/^{204}Pb$ 15.698, and $^{208}Pb/^{204}Pb$ 38.958. . When the data are plotted on the model curves for average crustal Pb-isotope evolution [1], $^{207}Pb/^{204}Pb$ and $^{208}Pb/^{204}Pb$ ratios are close to or above the evolution curves and clearly indicate a crustal source. Possible Pb sources have been investigated using the plumbo-tectonic diagrams [2] and the $^{208}Pb/^{204}Pb$ vs. $^{206}Pb/^{204}Pb$ data points are distributed along a trend between the representative curves for the Lower and Upper Crust, but they are closer to the Orogenic and Upper Crustal curves. The isotope data has higher $^{206}Pb/^{204}Pb$ ratios that are close to the 0-age suggesting young (Cenozoic) Pb-model ages [1]. The Pb data for Bagirkacdere is similar to mineralization at Arapucandere and Koru, which are close to Bagirkacdere in the north part of peninsula, indicating that similar processes were operatring over a wide area.

The $\delta^{34}S$ values of galena and sphalerite from the Bagirkacdere deposit, which are close to 0 ‰, are consistant with dominantly magmatic sulphur reservoir [3]. The combined lead and sulfur isotope data indicate that the source of lead and other metals in the skarn is primarily derived from Tertiary granites.

[1] Stacey and Kramers (1975) Earth Planetary Science Letters **26**, 207–221. [2] Zartman and Haines (1988) Geochimica et Cosmochimica Acta **52**, 1327–1339. [3] Bozkaya (2011) Goldschmidt, Abstract Volume, 571.

Source, transport, and matrix controls on metal bioavailability in floodplain soils

DANIEL J. BRABANDER[1,2*], EMILY R. ESTES[1], YONGMEI SHEN[1], AND JAMES P. SHINE[1]

[1]Harvard School of Public Health, Boston, USA, , eestes@fas.harvard.edu, yshen@hsph.harvard.edu, jshine@hsph.harvard.edu

[2]Wellesley College, Wellesley, USA dbraband@wellesley.edu (*presenting author)

With the deposition of metal-bearing sediments from upstream sources, floodplains have the potential to serve as an exposure vector for heavy metals. Not only are floodplains frequently located proximate to population centers, transported metals may also be present in more bioavailable forms (adsorbed or in secondary mineral phases) than in source material. Thus, a complex set of transport and biogeochemical transformation processes determines the spatio-temporal distribution of metal-bearing phases. Given that complexity, which variables (source, transport, matrix, aging) control metal speciation and the fraction of metals that are bioavailable by ingestion and inhalation pathways?

We examine this question for lead-, zinc-, and cadmium-bearing soils in the Neosho-Tar Creek floodplain system in Miami, Oklahoma, USA. To identify the source of metals within floodplain soils we have combined major and trace element geochemistry with multivariable statistical analysis (PCA) to develop fingerprints for distinct metal sources (Figure 1). By combining this approach with X-ray diffraction (XRD) to broadly characterize soil mineralogy we have developed endmembers for mixing models that apportion the relative contribution of various metal-bearing phases (detrital primary ore minerals versus secondary iron oxides and hydroxides (FeOx) minerals).

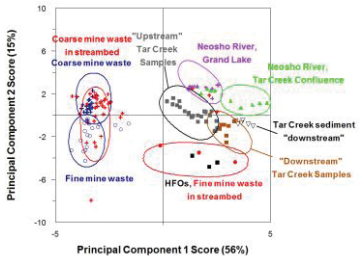

Figure 1: PCA of bulk element concentrations from floodplain soil and river sediment samples that demonstrate endmember sources and mixing relationships

Floodplain soil and sediment coring additionally allow us to reconstruct historic flood events and the temporal changes in metal flux, distribution, and speciation. We examine the role that shallow burial plays on the aging and in-situ weathering processes that result in FeOx mineral transformations. This combined approach will aid in estimating current and future risks associated with this evolving pool of bioavailable metals.

Calcite ($CaCO_3$) growth as a function of calcium-to-carbonate ratio in the presence of strontium: implications for the mechanism of inhibition

JACQUELYN N. BRACCO[1*], MEG C. GRANTHAM[1], ANDREW G. STACK[2]

[1]Georgia Institute of Technology, Earth and Atmospheric Sciences, Atlanta, USA, jbracco3@mail.gatech.edu (* presenting author)

[2]Oak Ridge National Laboratory, Chemical Sciences Division, Oak Ridge, USA, stackag@ornl.gov

One potential remediation method for toxic contaminants that has been proposed is to sequester the contaminant as an impurity in the crystal lattice of a mineral which incorporates the impurity. For example, radioactive strontium is present as a contaminant in a number of U.S. DOE sites and it may be possible to sequester it *in situ* through the engineered growth of calcium carbonate.[1] To enable targeted precipitation without porosity clogging and scale formation, separate injection wells of calcium and carbonate containing solutions have been proposed.

To understand this phenomenon, here we use atomic force microscopy (AFM) to examine the effect of strontium on calcite growth rates under solutions containing variable ratios of aqueous calcium-to-carbonate. Growth rates of the obtuse and acute step orientations on calcite were measured at two saturation indices as a function of the aqueous calcium-to-carbonate ratio and various aqueous strontium concentrations ranging from $0 - 9 \times 10^{-3}$ M. It was found that the amount of strontium necessary to inhibit growth correlated with the aqueous calcium concentration, but no correlation or inverse correlation was observed for carbonate. This suggests strontium is inhibiting attachment of calcium but not carbonate attachment or detachment.

At an average strontium-to-calcium ratio of 1.1 for the obtuse step orienation and 1.4 for the acute step orientation, the average step velcocity decreases to half of the maximum step velocity, which corresponds to the ratio where the concentration of strontium and calcium on the step at kink propagation sites is the same.[2] We propose that this corresponds to the cation exchange coefficent for calcium and strontium bound to precursor sites on the step.

The implications of this study are two-fold. Firstly, to ensure calcite growth is not inhibited by strontium, the concentration of calcium should be kept approximately higher than the cation exchange coefficient. Secondly, extensions of existing analytical models are unable to capture all the salient features of observed growth rates, indicating that improvement in analytical expressions can still be made.

This research was sponsored by the Division of Chemical Sciences, Geosciences, and Biosciences, Office of Basic Energy Sciences, U.S. Department of Energy.

[1] Tartakovsky, A. M. et al. (2008) *Wat. Resour. Res.*, **44**, W06S04.
[2] De Yoreo, J. J. et al. (2009) *Cryst. Growth Des.* **9**, 5135-5144.

Volcanogenic massive sulfide deposits host the evidence for sulfate-rich Archean oceans

JAMIE BRAINARD[1], ANDREW CHORNEY[1], AND HIROSHI OHMOTO[1]

[1]Penn State Astrobiology Center and Department of Geosciences, Penn State University, University Park, USA, JLB5156@psu.edu; APC5060@psu.edu; HQO@psu.edu

Recent researchers have suggested that the Archean oceans were sulfate poor (<0.1 mM SO_4^{2-}, compared to 28 mM today), because the atmosphere was supposedly poor in O_2 ($pO_2 < 10^{-6}$ atm) to completely oxidize the sulfur-bearing volcanic gases (H_2S and SO_2) and sulfide minerals in soils to SO_4^{2-}. However, such a scenario cannot explain the abundance of pyrite of Archean ages, much like those of younger ages, because these pyrites most likely formed by bacterial (or thermochemical) reduction of seawater SO_4^{2-}-.

One of the strongest lines of evidence for SO_4^{2-} rich Archean oceans comes from volcanogenic massive sulfide (VMS) deposits and alteration zones in their host rocks. VMS deposits, such as the black smoker deposits on MORs, formed on and beneath the seafloor by reactions between submarine hydrothermal fluids (typically ~50° to ~450°C) and the local seawater. The hydrothermal fluids evolved mostly through reactions between the underlying volcanic rocks and deep-circulating seawater, rather than derived directly from magmas. Therefore, the mineralogy and geochemistry of VMS deposits and their alteration zones reflect the chemistry of the contemporaneous ocean water. Phanerozoic VMS deposits are characterized by the abundance of pyrite and sulfate minerals, and by increased Fe^{3+}/Fe^{2+} ratios in the alteration zones due to the involvement of sulfate-rich seawater: some of the H_2S used to form the pyrite was generated by reduction of seawater sulfate by FeO components in rocks, resulting in the increases of Fe^{3+}/Fe^{2+} ratios. The ~3.2 Ga Panorama Formation of Western Australia hosts many VMS deposits with mineralogy, geochemistry, and associated alteration zones that are essentially identical to those of Phanerozoic ages, suggesting that the processes of submarine mineralization and the sulfate content of the seawater at 3.2 Ga were essentially the same as today.

Many other Archean VMS deposits and their alteration zones host barite ($BaSO_4$), such as the ~3.46 Ga Big Stubby deposits in Western Australia, the 3.26 Ga Fig Tree deposite in South Africa, the 2.6 Ga Geco deposit in Canada, and the 2.7 Ga Hemlo deposits in Ontario, Canada, suggesting that the Archean oceans remained sulfate-rich. The only major difference between the sulfate in the Archean oceans and that in the Phanerozoic oceans was the $\delta^{34}S$ values, between +2 and +5‰ during the Archean, but between +10 and +35‰ for the Phanerozoic. This difference has caused the $\delta^{34}S$ values of sulfides in Archean VMS deposits to be less than +5‰, where as those of Phanerozoic ages could be higher than +5‰, because the H_2S in the hydrothermal solutions came from the leaching of sulfides in igneous rocks ($\delta^{34}S \approx 0$‰) and from the partial reduction of seawater sulfate. These data suggest that the Archean oceans were as sulfate-rich as today's oceans due to the weathering of pyrite in rocks under an O_2-rich atmosphere.

Oxygen isotopes & Mg content in brachiopod calcite: equilibrium fractionation and a new paleotemperature equation

UWE BRAND[1*], K. AZMY[2], A. LOGAN[3], A. M. BITNER[4], B. DURZI[5], T. DURZI[6], M. ZUSCHIN[7]

[1]Department of Earth Sciences, Brock University, St. Catharines, Canada, uwe.brand@brocku.ca (* presenting author)
[2]Memorial University, St. Johns, Canada, kazmy@mun.ca
[3]University of New Brunswick, Saint John, Canada, logan@unbsi.ca
[4]Polish Academy of Sciences, Warsaw, Poland, bitner@twarda.pan.pl
[5]18 Paradise Close, Grand Harbour, Cayman Islands
[6]University of Guelph, Guelph, Canada, tdurzi@uoguelph.ca
[7]University of Vienna, Vienna, Austria, martin.zuschin@univie.at

Modern brachiopods and ambient seawater were collected at fourteen localities from the Arctic to the Antarctic. The brachiopods were analysesd for Mg, $\delta^{13}C$ and $\delta^{18}O$, and their ambient seawater was measured for temperature, salinity and $\delta^{18}O$. Our materials were supplemented by those of Lowenstam [1]. $\delta^{18}O$ values of marine carbonates increase by about 0.06 or 0.17 ‰ per mol% $MgCO_3$ [2,3], and failing to adjustment for this 'Mg-effect" has a profound impact on water temperatures determined with standard paleotemperature equations. This Mg-effect on $\delta^{18}O$ values applies to all marine invertebrates secreting shells or tests made of calcite with variable amounts of $MgCO_3$, such as articulated brachiopods, foraminifera and enchinoderms. The Mg content of our brachiopods varies from a low of 250 to a high of 30,660 ppm, which needs to be accounted for by the oxygen isotope impact of the Mg-effect. We propose a new paleotemperature equation that considers the pristine biogenic calcite (δc) and accounts for both the Mg-effect as well as the established seawater oxygen isotope (δw) correction:

$$T°C=14.5-3.5((\delta c\text{-Mg effect})-\delta w)+0.13((\delta c\text{-Mg effect})-\delta w)^2$$

The 'Mg effect' is defined as the $MgCO_3$ content of brachiopod calcite*0.17 ‰ (per mol% $MgCO_3$, accepting the latest study results [3]). Without adjustment for the Mg-effect, paleo seawater temperatures and compositions may be different than actual ones.

Without considering the effect of $MgCO_3$ on the oxygen isotopic composition, most modern brachiopods were found to precipitate shell carbonate in equilibrium with ambient seawater [4,5]. To re-evaluate the exceptions, *Thecidellina* and *Hemithiris* were collected from several localities. After making allowance for the Mg-effect on their $\delta^{18}O$ compositions and water-$\delta^{18}O$ corrected, calculated seawater temperatures were significantly similar to measured ones. $\delta^{18}O$ values of other modern brachiopods deemed problematic, after adjustment for the Mg-effect also offered up equilibrium water temperatures. Thus, we can state that modern, calcitic, articulated brachiopods incorporate oxygen isotopes into shell calcite in equilibrium with ambient seawater, and this will be of critical importance to other modern and fossil calcitic carbonates.

[1] Lowenstam (1961) *Journal of Geology* **69**, 241-260.
[2] Tarutani et al. (1969) *GCA* **33**, 987-996.
[3] Jiménez-López et al. (2004) *GCA* **68**, 3367-3377.
[4] Brand et al. (2003) *Chemical Geology* **198**, 305-334.
[5] Parkinson et al. (2005) *Chemical Geology* **219**, 193-235.

X-ray Spectromicroscopy: Illuminating the biogeochemical cycles of elements in the marine environment

JAY A. BRANDES[1*], ELLERY D. INGALL[2], AND JULIA M. DIAZ[3],

[11]Skidaway Institute of Oceanography, 10 Ocean Science Circle, Savannah, GA 31411 USA,jay.brandes@skio.usg.edu (* presenting author)

[2]Georgia Tech, Atlanta, GA, USA, ellery.ingall@eas.gatech.edu

[3]Harvard University, Cambridge, MA, USA, jdiaz@seas.harvard.edu

The geochemical cycling of elements on Earth's surface is intrinsically linked to biological processes. These links include biologically-mediated formation/solution of minerals, sorption/desorption onto surfaces modified by organic matter, and biological activity. All such processes begin at the nanoscale. Therefore the ability to examine biologically generated or modified sediments, soils and other particulates at nanoscales provides a fundamental view into the cycling of elements. Unexpected insights are often generated using instruments capable of examining the nanoscale composition, speciation, redox state and co-association of elements within particulates. For example, in the marine environment, one can consider the generation and sequestration of carbon by phytoplankton as being limited by the availability of necessary nutrients, such as phosphorus (P) and iron (Fe). X-ray spectromicroscopy of P within planktonic organisms, sinking particulates, and underlying sediments has revealed a wide array of P types, including organic P compounds, polyphosphates, apatites and other P-containing minerals. Further examination of the associations of P, Fe and other elements also shows a variety of nutrient removal mechanisms. The results begin to show how P is sequestered in the environment, first through the preservation and burial of poorly organized but relatively pure biogenic polyphosphates and calcium phosphates, then through transformation into more ordered, and substituted mineral phases. Overall the picture of P chemistry at sub-micron scales reveals a complex system interacting both with biologically produced particulate P and terrestrially- or aeolian-derived P mineral phases.

Mesozoic MORB

P. A. BRANDL[1*], M. REGELOUS[1], C. BEIER[1] AND K. M. HAASE[1]

[1]GeoZentrum Nordbayern, Friedrich-Alexander Universiät Erlangen-Nürnberg, Erlangen, Germany, philipp.brandl@gzn.uni-erlangen.de (* presenting author)

Formation of the oceanic crust at mid-ocean ridge spreading centres and its subsequent evolution has an important influence on sea-level, the carbon cycle and seawater chemistry over timescales of 10-100 Ma. Previous geochemical studies of ancient MORB (e.g. [1, 2, 3]) reported chemical differences between Mesozoic and young mid-ocean ridge basalt (MORB) that were interpreted as the result of a 50-60°C higher upper mantle temperature [1, 2]. Higher mantle temperature on average would cause shallower depth of mid-ocean ridges, rising sea-levels and global warming by increased CO_2 emission.

We present new major and trace element data, measured using electron microprobe and LA-ICPMS techniques, for more than 360 glasses from 30 DSDP-ODP-IODP drill sites. The age of the oceanic crust at these sites ranges from 6 Ma up to 160-170 Ma, and all sites were drilled into normal oceanic crust far from hotspots. We have analysed exclusively fresh volcanic glasses, since whole-rock samples may be compromised by alteration and accumulation of phenocrysts.

We find that there are small but significant differences between fractionation corrected major element compositions of old (drilled) and zero-age (dredged) samples, e.g. for Na_{72}, Fe_{72}, Ca_{72}, and Al_{72}. We can exclude any analytical bias, alteration effects or uncertainties in fractionation correction for these differences. For both, Pacific and Atlantic, there is no clear systematic change in fractionation corrected major element composition of drilled MORB with time, as would be expected for a change in mantle temperature [1]. Some of these differences between zero-age and drilled MORB samples could arise if the oceanic crust is compositionally layered. MORB drilled from off-axis represent younger flows erupted further from the ridge axis. In contrast, most samples in the zero-age MORB dataset were dredged from the ridge axis, which eventually make up the lowermost section of the oceanic crust [4].

Lavas erupted off-axis may sample different parts of the melting region and/or undergo different fractional crystallisation histories to lavas erupted at the ridge axis. This effect could mean that average MORB compositions calculated using only samples dredged from the ridge axis are not completely representative of the extrusive section of the oceanic crust.

[1] Humler et al. (1999) *Earth Planet. Sci. Lett.* **173**, 7-23. [2] Fisk and Kelley (2002) *Earth Planet. Sci. Lett.* **202**, 741-752. [3] Janney and Castillo (2001) *Earth Planet. Sci. Lett.* **192**, 291-302. [4] Hooft et al. (1996) *Earth Planet. Sci. Lett.* **142**, 289-309.

The Shergottite Chronology Debate: In Support of Young Igneous Crystallization Ages

ALAN BRANDON[1]*

[1]University of Houston, Department of Earth and Atmospheric Sciences, Houston, TX, 77204, USA, abrandon@uh.edu

The shergottite meteorites provide powerful constraints on early differentiation in Mars ([1,2] and references therein). These constraints depend on having well determined igneous crystallization ages for the rocks, from which initial ratios for radiogenic isotope systems are calculated. Shergottite ages interpreted to be igneous, ranging from 474 to 166 Ma have been obtained from internal isochrons using the Lu-Hf, Sm-Nd, and Rb-Sr systems (e.g. [1,3]). Recently, these young igneous crystallization ages have been called into question [4,5,6]. Secondary Pb-Pb isochrons for different shergottites give purportedly circa 4.1 Ga ages and have been interpreted to be the true igneous ages while the younger ages represent resetting from shock or fluid-rock interaction [4,5,6].

This issue is examined here by first presenting the petrological, mineralogical, and lithophile isotope evidence that supports the young ages as being igneous. Second, these relationships are evaluated using Re-Os isotopes [7]. One strong piece of supporting evidence for young ages is the EETA 79001 Re-Os isochron (Figure 1). The two lithologies sampled come from portions of the meteorite several centimeters apart, give an isochron age of 164±12

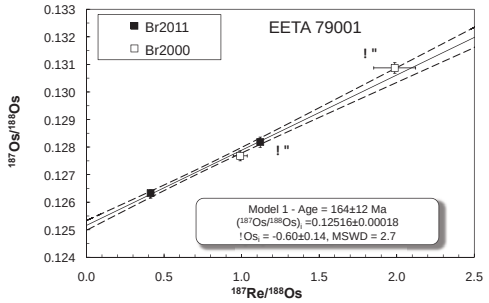

Figure 1: Re-Os isotope systematics of EETA 79001, modified from [7]. A and B designate fractions analyzed from litholigies A and B, respectively. Data from [7] – Br2011, from [8] – Br2000.

Ma (±2σ), concordant to internal mineral isochron ages for ^{87}Rb-^{87}Sr of 173±10, 177±12, and 174±3 Ma, for ^{147}Sm-^{143}Nd of 169±23 Ma, for ^{238}U- ^{206}Pb of 150±15 Ma, and for ^{232}Th-^{208}Pb of 170±36 Ma [9,10,11]. It is not likely possible to generate such systematics from shock unless diffusion rates are orders of magnitude faster than expected. Additional evidence will be presented that examines this issue.

[1] Nyquist et al. 2001, *Rev. Chronol. Evolut. Mars* **96**, 105–164. [2] Debaille et al. 2007, *Nature* **450**, 525-528. [3] Shafer et al. 2010, *GCA* **74**, 7307–7328. [4] Bouvier et al. 2005, *EPSL* **240**, 221-233. [5] Bouvier et al. 2008, *EPSL* **266**, 105-124. [6] Bouvier et al. 2009, *EPSL* **280**, 285-295. [7] Brandon et al., 2011. [8] Brandon et al. 2000, *GCA* **64**, 4083-4095. [9] Chen & Wasserburg 1986, *GCA* **50**, 955-968. [10] Nyquist et al. 2001, *LPS* **XXXII**, #1407. [11] Wooden et al., 1982, *LPS* **XIII**, 879-880.

Replacement of Barite by Radiobarite at close to equilibrium conditions and room temperature

FELIX BRANDT[1*], MARTINA KLINKENBERG[1], KONSTANTIN ROZOV[1], GUISEPPE MODOLO[1], DIRK BOSBACH[1]

[1]Forschungszentrum Juelich, IEK-6, Juelich, Germany, f.brandt@fz-juelich.de (*presenting author); m.klinkenberg@fz-juelich.de; k.rozov@fz-juelich.de, g.modolo@fz-juelich.de, d.bosbach@fz-juelich.de

The solubility control of Ra by coprecipitation of a $Ra_xBa_{1-x}SO_4$ solid solution has been demonstrated in many cases and can be modeled reliably (Doerner & Hoskins, 1925). However, an open question is whether a Ra containing solution will equilibrate with solid $BaSO_4$ under repository relevant conditions. Here, Radium enters a system in which barite is in equilibrium with the aqueous solution. Previous studies have indicated that Ra uptake is not limited by pure adsorption but involves a significant fraction of the bulk solid, i.e. barite partially or fully recrystallizes to radiobarite (Bosbach et al., 2010; Curti et al., 2010). Here, we present experimental data from batch recrystallization experiments at room temperature in which a pure barite solid was put into contact with an aqueous solution with an initial Ra/Ba ratio of 0.3 ($5 \cdot 10^{-6}$ mol/L Ra) at neutral pH. Two barites of different morphology and surface area were used during the recrystallization experiments at close to equilibrium conditions and with variation of solid to liquid ratio.

The experimental results show a decrease of the Ra concentration to $3.5 \cdot 10^{-9}$ to $7 \cdot 10^{-9}$ mol/L within the first 70 days of the experiment at a solid/liquid ratio of 5 g/L. At a solid/liquid ratio of 0.5 g/L a slower decrease of the Ra concentration to $2 \cdot 10^{-8}$ mol/L is observed after 180 days. The decrease of the Ra concentration is apparently not related to the specific surface area of the barite crystals. The final radium concentrations are in the range as can be expected from thermodynamic calculations assuming full reequilibration of the barite to a $Ra_xBa_{1-x}SO_4$ solid. Different thermodynamic models describing the mechanism of Ra incorporation into barite are discussed: (1) Ba – Ra exchange into the crystal volume, combining the Ra – Ba exchange with the Ba – Ba recrystallization rate at equilibrium conditions (Curti et al, 2010);

(2) the formation of a Ra-Ba-Phase on barite surfaces. The formation of a Ra-Ba phase on the barite surfaces could be possible because all experiments are already slightly supersaturated with regard to $Ra_xBa_{1-x}SO_4$ after about one day. Crystallization rates calculated according to this model are in a similar range for all experiments when normalized to the barite surface area.

The results of this study will provide the basis for further spectroscopic and microscopic investigations in order to obtain a molecular-level understanding of the Ra incorporation into barite.

[1] Doerner, H. A. & Hoskins, W. M. (1925) *Journal of the American Chemical Society*, **47**, 662-675
[2] Bosbach, D.; Böttle, M. & Metz, V. (2010) *Waste Management, Svensk Kärnbränslehantering AB*
[3] Curti, E.; Fujiwara, K.; Iijima, K.; Tits, J.; Cuesta, C.; Kitamura, A.; Glaus, M. & Müller, W. (2010) *Geochimica et Cosmochimica Acta*, **74**, 3553-3570

Back to the Future: The Art of Weathering

SUSAN BRANTLEY[1*] HEATHER BUSS[2] MARJORIE SCHULZ[3]

[1]The Pennsylvania State University, Earth and Environmental Systems Institute, University Park, PA, USA, sxb7@psu.edu (*presenting author)

[2]University of Bristol, School of Earth Sciences, Bristol, UK, h.buss@bristol.ac.uk

[3]U.S. Geological Survey, 345 Middlefield Road, Menlo Park, CA, USA, mschulz@usgs.gov

Geologists and soil scientists attempt to go back to the future to read the geochemical record written in regolith. If we could do this, we could use earthcasting models to project the surface earth in the future just as we use forecasting models to project the weather. But going back into geological time to read the record in soil profiles is both a science and an art due to the interdependence of chemistry, physics, and biology at the earth's surface. The art of earthcasting is also hard because such models must have the capacity to span timescales ranging from seconds for hydrogeochemical effects up to tens of millions of years or longer for tectonic processes.

We discuss the contributions of one scientist, Art White (recently retired from the U.S. Geological Survey, Menlo Park, CA, USA), who spent a career investigating geochemical processes and how they affect mineral-water reactions in pursuit of understanding the surface Earth. Art recognized that soil profiles are records of biogeochemistry that can be interpreted using kinetics and thermodynamics. With the use of geochemical, physical, hydrological and biological measurements, regolith formation rates can be constrained and geochemical descriptions can be made quantitative. Art's work in the laboratory – including a 16 year experiment – and at several field sites as part of the USGS WEBB program, including Panola, Georgia; the Luquillo Mountains, Puerto Rico; and the Santa Cruz terraces, CA; resulted in a series of papers that have greatly influenced our understanding of the earth's surface. Today, much of this work is termed Critical Zone science: Art was one of the originators of the Critical Zone Exploration Network and is therefore one of the original CZEN masters. His contributions helped lead to the big programs in Critical Zone science in the U.S.A. and elsewhere. Art and the many scientists before him (back to even the 16th century when soil profiles were first studied) set the stage for today's "artists of weathering". Now, new field opportunities, theoretical models, analytical tools, microbiological observations and sensors are elucidating the beauty and art of the Critical Zone.

Low temperature alkaline pH hydrolysis of oxygen-free Titan tholins

CORALIE BRASSE[1]*, FRANCOIS RAULIN[2], PATRICE COLL[3], OLIVIER POCH[4], AND ARNAUD BUCH[5]

[1] Laboratoire Inter-universitaire des Systèmes Atmosphériques, Créteil, France, coralie.brasse@lisa.u-pec.fr (* presenting author)

[1] Laboratoire Inter-universitaire des Systèmes Atmosphériques, Créteil, France, francois.raulin@lisa.u-pec.fr

[3] Laboratoire Inter-universitaire des Systèmes Atmosphériques, Créteil, France, patrice.coll@lisa.u-pec.fr

[4] Laboratoire Inter-universitaire des Systèmes Atmosphériques, Créteil, France, olivier.poch@lisa.u-pec.fr

[5] Centro de Investigaciones Quimicas, Cuernavaca, Mexico, ramirez_sandra@ciq.uaem.mx

[6]Ecole Centrale Paris, Laboratoire de Génie des Procédés et Matériaux, bucha@ecp.fr

The largest moon of Saturn, Titan, is known for its dense, nitrogen-rich atmosphere. The organic aerosols which are produced in Titan's atmosphere are of great astrobiological interest. particularly because of their potential evolution when they reach the surface and may interact with putative ammonia-water cryomagma[1].

In this context we have followed the evolution of alkaline pH hydrolysis (13wt% ammonia-water) of Titan tholins (produced by an experimental setup using a plasma DC discharge named PLASMA) at low temperature. Our group identified urea as the main product of tholins hydrolysis along with several amino acids (alanine, glycine and aspartic acid). However, those molecules have also been detected in non-hydrolyzed tholins meaning that oxygen gets in the PLASMA reactor during the tholins synthesis[2]. So the synthesis system has been improved by isolating the whole device in a specially designed glove box which protects the PLASMA experiment from the terrestrial atmosphere.

After confirming the non-presence of oxygen in tholins produced with this new experimental setup, it is necessary to perform alkaline pH hydrolysis in oxygen-free tholins in order to verify that organic molecules cited above are still produced or not... Moreover, a recent study shows that the subsurface ocean may contain lower fraction of ammonia (about 5wt% or lower[3]), than previously used. Thus new hydrolysis experiments will take this lower value into account. Additionally, a new report [4] provides upper and lower limits for the bulk content of Titan's interior for various gas species. It also shows that most of them are likely stored and dissolved in the subsurface water ocean. But considering the plausible acido-alkaline properties of the ammonia-water ocean, additional species could be dissolved in the ocean and present in the magma. They could also be included in our hydrolysis experiments.

The preliminary results of those experiments will be presented.

[1] Mitri et al. (2008) *Icarus* **196**, 216-224. [2] Poch et al.(2011) *Planetary and Space Science* **61**, 114-123. [3] Beghin et al. (2012) *Icarus* **submitted**. [4] Tobie et al. (2011) EPSC-DPS2011 **6**.

Comparison of methods and results in recent studies of direct groundwater discharge to the Atlantic coast and Great Lakes

JOHN F. BRATTON[1*], KEVIN D. KROEGER[2], STEVEN A. RUBERG[3], HOLLY A. MICHAEL[4], AND DAVID E. KRANTZ[5]

[1]NOAA Great Lakes Environmental Research Lab, Ann Arbor, Michigan, USA, john.bratton@noaa.gov (* presenting author)
[2]USGS, Woods Hole, Mass., USA, kkroeger@usgs.gov
[3]NOAA-GLERL, Ann Arbor, Mich., USA, steve.ruberg@noaa.gov
[4]Univ. of Delaware, Newark, Del., USA, hmichael@udel.edu
[5]Univ. of Toledo, Toledo, Ohio, USA, david.krantz@utoledo.edu

Submarine and Sublacustrine Groundwater Discharge

Groundwater/surface water interaction has been the subject of intense investigation in both marine and freshwater settings in recent years. Although many study methods can be used interchangeably in these systems (e.g., seeepage meters), those that rely on salinity contrasts to distinguish surface water from groundwater (e.g., electrical resistivity profiling) cannot. A schematic spatial framework that was recently developed for dividing submarine groundwater discharge (SGD) phenomena [1] can also be applied to large lakes with some modifications. Some natural radioisotopic tracers of SGD developed in marine systems can be used in freshwater settings [2]. Conversely, a regional approach to examining groundwater occurrence and flow in a watershed containing large lakes, as has been undertaken for the Great Lakes [3], might be productively applied to a coastal ocean region.

In addition to the salinity contrasts, one major geochemical difference between discharge of groundwater to fresh or saline surface water is the influence on eutrophication. Because nitrogen is typically the limiting nutrient in marine systems, whereas phosphorus limits productivity in most freshwater systems [4], SGD plays a much larger role in eutrophication of marine systems than in freshwater systems. Dissolved nitrogen species tend to be concentrated in coastal groundwater, but phosphorus is particle reactive and unlikely to be delivered to surface water in large quantities from groundwater in most lakes. Most phosphorus comes from runoff and sediment recycling in freshwater systems.

Unusual groundwater vent features have been documented in both marine and lake settings, especially along carbonate-dominated coasts. Among the most spectacular are brackish sinkhole springs in Florida and Lake Huron, the latter of which include extensive purple cyanobacterial mat communities [5].

Conclusion

Significant opportunities exist for advancing understanding of elemental cycling and other features of groundwater/surface water interaction in large water bodies with more exchange of methods and results among scientists that work in marine and freshwater settings.

[1] Bratton (2010) *J. Geol.* **210**, 565-575. [2] Moore (2008) *Mar. Chem.* **109**, 188-197. [3] Granneman *et al.* (2000) *USGS WRIR* **00-408**. [4] Howarth and Marino (2006) *Limnol. Oceanogr.* **51**, 364-376. [5] Biddanda *et al.* (2009) *Eos* **90**, 61-62.

Contemporary saprolite production rates and aggressiveness of pore waters: Comparison between Nsimi and Mule Hole small experimental watersheds

JEAN JACQUES BRAUN[1]*, JEAN-CHRISTOPHE MARECHAL[2], JEAN RIOTTE[1,3], MUDDU SEKHAR[1,4]

[1]IFCWS IISc-IRD joint laboratory, Bangalore, India, jjbraun1@gmail.com (* presenting author)
[2]BRGM, Montpellier, France, jc.marechal@brgm.fr
[3]GET, Toulouse, France, jeanriotte1@hotmail.com
[4]Dept. of Civil Engg., IISc., Bangalore, India, sekhar.muddu@gmail.com

Introduction

Thanks to geochemical, mineralogical and hydrological studies and using Chloride Mass Balance approach, we compare two ridge top weathering profiles (WP) developed on granodioritic basement from Mule Hole (South India) and Nsimi (South Cameroon) small experimental watersheds (SEW). The objective is to get deeper insight into (i) the contemporary saprolite production rates and (ii) the combined effect of precipitation and evapotranspiration on the aggressiveness of the draining solutions.

Field settings

The Nsimi SEW presents the contemporary weathering conditions for a 36 meter deep, mature weathering cover under humid climate (Mean Annual Rainfall = 1660 mm/yr, Actual EvapoTranspiration (AET) = 1270 mm/yr) with a Recharge (R) = 332 mm/yr out of which 90% of the solutes are discharged into the springs/brook and 10 % through the groundwater[1][2]. The Mule Hole SEW presents the contemporary weathering conditions for a 17 meter deep, immature weathering cover under sub-humid climate (MAR = 1280 mm/y, AET = 1100 mm/yr) with R = 45 mm/yr out of which 100% of the solutes are discharged through the groundwater as underflow from the watershed[3][4][5]. Moreover, the Nsimi groundwater saturates the entire saprolite whilst the Mule Hole groundwater saturates the fractured bedrock only.

Results and conclusions

Considering (i) Na as representative of the dissolution of plagioclase crystals and conservative during saprolitization processes and (ii) steady state of the inter-annual recharge for a 10 years period, the current saprolite production rates (SPR) are of 22 mm/kyr for Mule Hole and 2 mm/kyr for Nsimi, respectively.

Even with a very low R/MAR ratio (0.04) compared to Nsimi, the chemical weathering at Mule Hole is active and related to the groundwater exports. However, the high Nsimi R/MAR ratio (0.2) allows the solution to be still aggressive with respect to the plagioclase at the bedrock interface leading to their complete breakdown in a few centimeters. For Mule Hole, plagioclase are still present in the saprolite and the soil cover.

[1] Braun (2005) *Geochimica Cosmochimica Acta* **73,** 935-961. [2] Maréchal (2011) *Hydrological Processes* **25**, 2246–2260. [3] Maréchal (2011) *Applied Geochemistry* **26,** S94-S96. [4] Maréchal (2009) *J. of Hydrology* **361,** 272-284 [5] Ruiz (2010) *J. of Hydrology* **380,** 460-472.

The source of carbon in cave air CO_2 under mixed woodland and grassland vegetation

DANIEL O. BREECKER[1*], ASHLEY E. PAYNE[1], JAY QUADE[2], JAY L. BANNER[1], CAROLYN E. BALL[3], AND KYLE W. MEYER[1]

[1]The University of Texas at Austin, Austin, USA, breecker@jsg.utexas.edu (* presenting author)
[2]The University of Arizona, Tucson, USA
[3]The University of Florida, Gainesville, USA

We measured concentrations and stable carbon isotope compositions of CO_2 in the atmospheres of several caves in central Texas and southern Arizona in order to identify the sources of CO_2-carbon. The vegetation above all of the caves studied is a mixture of grasslands (C_3 and C_4 vegetation) and woodlands (dominantly C_3 juniper and oak trees). We tested the hypothesis that the deepest rooting plants have a dominant influence of the $\delta^{13}C$ value of CO_2 in the caves. Within caves, we monitored CO_2 at individual locations on monthly and daily time-scales. We also measured CO_2 in the pore spaces of soils dominated by different vegetation types above each cave. The $\delta^{13}C$ value of respired CO_2 ($\delta^{13}C_r$) was calculated for all gas samples from the measured $\delta^{13}C$ values and CO_2 concentrations by rearranging equations derived by Davidson[1]. The sources of cave CO_2 were then identified by comparing soil and cave air $\delta^{13}C_r$ values. In three of the caves, mean cave air CO_2 $\delta^{13}C_r$ values were within 0.5 ‰ of mean $\delta^{13}C_r$ values in woodland soils (-23 to -24‰ vs VPDB), even when measured $\delta^{13}C$ values of cave and soil CO_2 were different by up to 2.5‰. The $\delta^{13}C_r$ values in grassland soils above these three caves were 3-5 ‰ higher than cave and woodland soil values. In one cave covered primarily by grassland and roads, the cave $\delta^{13}C_r$ values were intermediate between grassland and woodland values. When cave-air CO_2 concentrations were below 1000 ppmV, cave $\delta^{13}C_r$ values were more negative than woodland soil values by 20‰ or more, likely the result of preferential degassing of $^{12}CO_2$ from CO_2-supersatured drip water[2]. The consistent agreement between soil and cave air $\delta^{13}C_r$ values indicate that the same mixing and diffusion equations, which are used to calculate $\delta^{13}C_r$ and have been previously applied to soils, also apply to cave atmospheres. Our results suggest that unless cave CO_2 concentrations are <1000 ppm the majority of CO_2 advects or diffuses into these caves from soils as a gas rather than being transported in aqueous solution. Calculated $\delta^{13}C_r$ values suggest that juniper and/or oak trees supply most of the carbon to CO_2 in the atmospheres of these caves, likely because these trees have deeper roots than the other plants in these ecosystems. A one-dimensional numerical model of CO_2 production and diffusion that uses depth-dependent $\delta^{13}C_r$ values as input supports our empirical results and our hypothesis that deeply rooted trees control the $\delta^{13}C_r$ values of cave air CO_2, even if deep respiration rates are small compared with those in the shallow subsurface. We further suggest that if a vegetation signal is archived in the carbon isotope composition of speleothem calcite, then it may be biased toward deep-rooted plants.

[1] Davidson (1995) *Geochimica et Cosmochimica Acta* **59**, 2485-2489. [2] Spötl et al. (2005) *Geochimica et Cosmochimica Acta* **59**, 2451-2468.

Sulfide-silicate partitioning of PGEs (and Au): Implications for noble metal behaviour in magmatic systems

JAMES M. BRENAN[1*]

[1]University of Toronto, Toronto, Canada, brenan@geology.utoronto.,ca (* presenting author)

There is considerable variation in sulfide-silicate melt partition coefficients for the noble metals (PGEs and Au), with most direct measurements (analysed by bulk methods) yielding values of 10^4 or less [e.g., 1]. More recent estimates, which combine separate metal solubility measurements in sulfide and silicate, have suggested partition coefficients exceeding 10^7 [2,3]. Resolving this discrepancy is essential for developing accurate models of noble metal behaviour during melting, and validating metal concentration mechanisms in magmatic systems.

In this study, sulfide and silicate were equilibrated at known fO2-fS2 conditions, with run-products analysed by LA-ICPMS to ensure exclusion of sulfide contamination from the silicate melt analysis. Experiments were done at 1200 deg. C and 1 atm with fS2 controlled using the Pt-PtS buffer and fO2 estimated to be FMQ-1. Three different synthetic basalts were employed, differing in their FeO content (5-15 wt%), with the added sulfide melt composition having FeS stoichiometry + 1 wt% each of Cu and Ni. Glass + sulfide were packed in crucibles made from natural chromite, then loaded, along with the sulfide buffer, in silica ampoules, which were evacuated, then sealed. Samples were held for 1 to 4 days at temperature, then quenched in cold water. Run-product glasses were free of obvious sulfide contamination, as evidenced by uniform, and low time-resolved signals for the PGE and Au.

Concentrations of Ru and Os in run-product glasses were always below detection (approx 20 and 5 ppb, respectively), yielding minimum sulfide/silicate partition coefficients of >10^5 (Ru) and >10^6 (Os). Measurable, but low, abundances for other PGE and Au were determined, with calculated sulfide/silicate partition coefficients of >10^5 (Pd, Rh, Ir, Pt) and 4000-11000 (Au). Partition coefficients for Pd, Rh, Ir and Pt were found to increase with increasing concentrations of these elements added to the sulfide melt, with little or no change in the silicate melt concentration. This is interpreted to reflect a low level of sulfide contamination in the silicate melt, and argues for even higher partition coefficients for these elements. Thus, results are in line with the large partition coefficients estimated from combined sulfide and silicate PGE solubility data. Application of these data to sulfide-saturated partial melting models yields levels of PGE and Au in calculated melts which are much lower than observed for MORB or OIB; only at the point of near complete sulfide exhaustion are calculated and observed abundances similar. An alternative to residual sulfide, such as a combination of olivine, chromite along with an alloy phase, may be required to account for levels of these elements in oceanic basalts.

[1] Fleet *et al* (1999) Lithos **47**, 127–142. [2] Andrews & Brenan (2002) *Chem Geol* **192**, 163-181. [3] Fonseca et al (2009) *GCA* **73**, 5764–5777.

Concentrations and isotope ratios of He and other noble gases in the atmosphere during 1978–2011

M.S. BRENNWALD[1*], M.K. VOLLMER[2], N. VOGEL[1,3], S. FIGURA[1,4], R.P. NORTH[1,4], R. LANGENFELDS[5], L.P. STEELE[5], R. KIPFER[1,3,4]

[1] Eawag, Swiss Federal Institute of Aquatic Science and Technology, Dübendorf, Switzerland (*matthias.brennwald@eawag.ch)

[2] Laboratory for Air Pollution and Environmental Technology, Empa, Swiss Federal Laboratories for Materials Science and Technology, Dübendorf, Switzerland

[3] Institute of Geochemistry and Petrology, Swiss Federal Institute of Technology, Zurich, Switzerland

[4] Institute of Biogeochemistry and Pollutant Dynamics, Swiss Federal Institute of Technology, Zurich, Switzerland

[5] Centre for Australian Weather and Climate Research/CSIRO Marine and Atmospheric Research, Aspendale, Victoria, Australia

The concentration of He in the atmosphere (residence time ~10^6 years) is governed by the balance between its release from the solid earth and its loss into space. Due to the burning of fossil fuels, which is known to be rich in He, an increase of the atmospheric He concentration over the past decades has been predicted. However, the predicted increase is small, and the precision of currently available measurement techniques is insufficient to verify this potential increase.

An alternative approach to study this possible increase in the atmospheric He concentration is to analyse the $^3He/^4He$ ratio in historic air samples. The $^3He/^4He$ ratio in fossil fuels is commonly one to two orders of magnitude lower than in the atmosphere. An increase of the He concentration in the atmosphere due to burning of fossil fuel would therefore correspond to a decrease of the atmospheric $^3He/^4He$ ratio that might be detectable with currently available measurement techniques. However, while some studies claim to have found evidence for a decrease in the $^3He/^4He$ ratio in the atmosphere during the last few decades, other studies were not able to confirm this observation.

In an attempt to resolve this long-standing controversy, we conducted isotopic analyses of *all* the atmospheric noble gases (He, Ne, Ar, Kr and Xe) in air samples from a well-defined archive of marine boundary layer air in the southern hemisphere (Cape Grim Air Archive, Australian Bureau of Meteorology and CSIRO). In our presentation we will report the results of these analyses and discuss them in terms of a possible change in the atmospheric He concentration. The $^4He/^{20}Ne$ ratio in particular turned out to be a very sensitive proxy for this purpose. Because the $^4He/^{20}Ne$ ratio in fossil fuels is about 8 orders of magnitude lower than in the atmosphere, the addition of noble gases from fossil fuels to the atmosphere has a much stronger effect on the $^4He/^{20}Ne$ ratio than on the $^3He/^4He$ ratio. At the same time, if He and Ne are not separated from each other before analysis in the mass spectrometer, the $^4He/^{20}Ne$ ratio can be quantified with a better precision than the $^3He/^4He$ ratio. Broadening the atmospheric He analysis to include other noble gas isotopes therefore allows us to put much firmer constraints on possible changes in the atmospheric He concentration that may have resulted from the burning of fossil fuels during the last few decades.

Improving ^{182}Hf-^{182}W ages in altered CR chondrites

T. BRETON*, G. QUITTÉ AND F. ALBARÈDE

CNRS UMR 5276, ENS de Lyon, Université Lyon 1, Lyon, France, thomas.breton@ens-lyon.fr (* presenting author)

Introduction

Despite their high content of segregated metal and their diverse degrees of alteration, CR chondrites are considered among the most primitive meteorites in the solar system. Applying the ^{182}Hf-^{182}W chronometer to these samples therefore seems interesting to better constrain the earliest stages of metal segregation. While NWA 721 and NWA 801 yield ^{182}Hf-^{182}W ages of ~5 Ma after CAIs, Renazzo is surprisingly ~50 Ma younger [1], which suggests that the ^{182}Hf-^{182}W chronometer may have been disturbed in this particular sample.

Hf and W behavior in natural processes

Although the ^{182}Hf-^{182}W chronometer may have been reset by thermal metamorphism [2], Renazzo seems free of thermal overprinting. However, this meteorite shows evidence of strong aqueous alteration [3] and Pourbaix (Eh-pH) diagrams indicate that tungsten is affected by this process [4]. $\varepsilon^{182}W$ values, which are corrected for mass dependent fractionation, will not be harmed, whereas the Hf/W (parent/daughter) ratios will. Hafnium is indeed far less mobile than W that, in neutral to high-pH fluids, are most likely lost as tungstate. The internal isochron is thus disturbed and the apparent age is younger.

A simple single-stage model suggests that aqueous alteration rotates the isochron around the y-intercept. Thus, the y-intercept seems suited to determine the timing of metal-silicate segregation, even in altered samples. This model reduces the time interval between NWA 701 / NWA 801 and Renazzo to 14 ± 14 Ma.

Tafassasset: an old unaltered CR chondrite

Tafassasset, an anomalous CR chondrite [5, 6] is metamorphosed but not aqueously altered. If alteration affects the Hf-W isochron, this meteorite is of particular interest to experimentally infer the timing of metal-silicate segregation in the CR parent body(ies). Seven different mineral phases (pure metal, several magnetic phases, silicate phases and two bulks) have been separated and analyzed. The W concentrations are 800 ppb and 15 ppb in metal and silicates, respectively. MC-ICPMS and N-TIMS measurements were performed, depending on the amount of W available in each fraction. Both techniques yield the same results within uncertainties. Data plot on a well defined line in an isochron diagram. Ages calculated from the slope or from the initial of this isochron relative to CAIs [7, 8] are consistent with each other: metal-silicate equilibration in Tafassasset occurred less than 2 Ma after Allende CAIs. This meteorite is thus older than the other CR2 chondrites analyzed so far, and among the oldest known chondrites.

[1] Quitté et al. (2010) *MAPS* **45**, A167. [2] Kleine et al. (2005) *EPSL* **231**, 41-52. [3] Schrader et al. (2008) *GCA* **72**, 6124-6140. [4] Lillard et al. (1998) *J. Electrochem. Soc.* **145**, 2718-2725. [5] Bourot-Denise et al. (2002) *LPSC 33rd* Abstr. #**1611** [6] Göpel et al. (2011) *Mineral. Mag.* **75**, 936. [7] Kleine et al. (2005) *GCA* **69**, 5805-5818. [8] Burkhardt et al. (2008) *GCA* **72**, 6177-6197.

Interaction of selenite with iron sulphide minerals: a new perspective

ERIC BREYNAERT[1,*], DIRK DOM[1], ANDREAS C. SCHEINOST[2], CHRISTINE E.A. KIRSCHHOCK[1], ANDRÉ MAES[1]

[1] KULeuven, Center for Surface Chemistry and Catalysis, kasteelpark arenberg 23, bus 2461, B-3001 Leuven, Belgium eric.breynaert@biw.kuleuven.be (* presenting author)

[2] HZDR, Inst. of Resource Ecology, Bautzener Landstrasse 400, 01314 Dresden, Germany

The geochemistry of selenium, exhibiting valence states from +VI to –II, is of key importance due to its role as a highly toxic essential micronutrient and as a significant component of high level radioactive waste (HLRW). XAS studies conducted at circum-neutral pH have shown that pyrite (FeS_2), the most relevant redox-active mineral in Boom clay, reduces selenite to a solid-state Se(0) phase. This observation raises several questions. First, why does an Fe-free Se(0) phase form in presence of pyrite, while selenite is reduced to $FeSe_x$ by troilite and mackinawite (FeS)?[1-4]. What is the exact identity of this Se(0) phase, which has been observed by several authors? Why is a dissolved, low oxidation-state selenium species encountered in association with the Se(0) phase; and what is its identity? Correlating selenium redox chemistry with sulphide mineral oxidation pathways allowed to link these observations to the different oxidation behaviour of acid-soluble and acid-insoluble metal sulphides [5].

Acid insoluble metal sulphides such as pyrite, molybdenite or tungstenite exhibit oxidative dissolution only. Upon six consequent one-electron oxidation steps, a thiosulphate anion is liberated (thiosulphate pathway). In contrast, acid soluble metal sulphides (troilite, mackinawite, sphalerite, etc.) exhibit also non-oxidative dissolution thereby liberating sulphide species (H_2S, HS^-,S^{2-}). Under oxidative dissolution in presence of Fe^{III}, they release sulphide cations (e.g. H_2S^+). The latter can spontaneously dimerize into disulphide species, which may further react to polysulphide (polysulphide pathway) and finally elemental sulphur.

The end products of Se(IV) reduction by acid-soluble iron sulphur minerals are fairly well known, but the solid and liquid phase species present during interaction of SeO_3^{2-} with pyrite are poorly characterized. The solid phase reaction product could not yet be assigned as a specific phase, but clearly identified as a Se^0 compound. Trigonal (grey) selenium could be excluded as a canditate.[4]

The presence of an unexpected high concentration of reduced, dissolved species in presence of pyrite, led to a new pyrite-centered reduction mechanism. Based on this mechanism, a hypothesis about the identity of the unknown dissolved species was put forward. In addition, the new mechanism explains all current experimental observations, especially the presence of the currently non-identified dissolved species and the unexpected relation between Se(IV) reduction and pH.[6]

[1] Breynaert, *et al.* (2008) ES&T. **42**(10): 3595-3601.

[2] Scheinost and Charlet, L. (2008) ES&T. **42**(6): 1984-1989.

[3] Scheinost, *et al.* (2008) J. Contam. Hydrol. **102**(3-4): 228-245.

[4] Breynaert, *et al.* (2010) ES&T. **44**(17): 6649-6655.

[5] Rohwerder and Sand (2007) in *Microbial Processing of Metal Sulfides.p* 35-58.

[6] Kang, *et al.* (2011) ES&T. **45**: 2704-2710.

Numerical modelling of nano-scale mineral dissolution and simulation of mycelial growth dynamics to couple observations of mycorrhizal weathering at single-hypha and whole-plant scales

JONATHAN W BRIDGE[1*], STEEVE BONNEVILLE[2], LIANE G. BENNING[3], JONATHAN LEAKE[4], LYLA TAYLOR[4], STEVEN A BANWART[1] AND THE WEATHERING SCIENCE CONSORTIUM TEAM

[1] Kroto Research Institute, The University of Sheffield, Sheffield, UK (* presenting author: j.bridge@sheffield.ac.uk)

[2] Université Libre de Bruxelles, Departement de Science de la Terre et d'Environnement, Brussels, Belgium

[3] School of Earth and Environmental Sciences, The University of Leeds, UK

[4] Department of Animal and Plant Sciences, The University of Sheffield, Sheffield, UK.

Soil mycorrhizal fungi act through biochemical interactions at nanometre scale to dissolve minerals and transport weathering products to plant symbionts through metre-scale mycelial networks. This symbiosis has profound consequences for rates of carbon sequestration from the atmosphere to soil, and rates of nutrient mobilisation from soils, that are apparent on global and geological time scales [1]. Previous research within our consortium has shown convincingly the nanoscale weathering of minerals by hyphae in direct contact with minerals [2], and at the same time the transport and redistribution of mineral- and plant-derived nutrients (carbon, phosphorus) within the rhizosphere and the plant itself [3].

A key factor in this biologically-driven weathering system is the relationship between the energy supplied from the plant to the mycorrhiza, and the rate of weathering of minerals. Critically, what is the nature of the feedback between the plant root and the distal hyphae that controls allocation of photosynthate within the mycelial network in response to nutrient uptake? Here, we present the results of numerical modelling and simulation of hypha-mineral weathering and hyphal network growth which couples a mechanistic model of element release from minerals with fluxes of carbon and mineral nutrients between the plant root and the whole mycelium. Our models indicate that the efficiency of mycorrhizal weathering is sensitive to both geochemical and biological parameters and is time-dependent. We hypothesize that pore-scale variations in weathering efficiency as mycorrhizae progressively spread through soil provide a mechanism to drive hyphal growth behaviour (e.g., exploratory vs. exploitative) and direct photosynthate demand.

References

[1] Taylor (2011) *American Journal of Science* **311(5)**, 369-403

[2] Bonneville (2011) *Geochimica et Cosmochimica Acta* **75**, 6988–7005.

[3] Leake (2008) *Mineralogical Magazine*. **72**, 85–89.

Unlocking the Zinc Isotope Systematics of Iron Meteorites

L.J. BRIDGESTOCK[1], M. REHKÄMPER[1,2]*, F. LARNER[1], M. GISCARD[1,2], R. ANDREASEN[1,3], B. COLES[1], G. BENEDIX[2], K.J. THEIS[4], M. SCHÖNBÄCHLER[4], C. SMITH[2]

[1] Dept. of Earth Science & Engineering, Imperial College, London, UK; luke.bridgestock07@imperial.ac.uk (* presenting author)
[2] Dept. of Mineralogy, The Natural History Museum, London, UK
[3] Department of Earth and Atmospheric Science, University of Houston, 312 SR1, Houston TX 77204, USA
[4] School of Earth, Atmospheric and Environmental Sciences, University of Manchester, Manchester M13 9PL, UK

High precision Zn concentration and stable isotope composition data were acquired for 21 metal samples of 15 different iron meteorites of groups IAB, IIAB and IIIAB. Troilite nodules were also analyzed, in addition to leachates and leachate residues of troilites separated from the IAB iron Toluca. All results were obtained by MC-ICP-MS using a Zn double spike technique for correction of instrumental mass bias.

The metal samples of each group display a discrete range of Zn concentrations – about 80 to 250 ppb for IIABs, 1 to 3 ppm for IIIABs and 10 to 35 ppm for IABs – at similar and overlapping $\delta^{66/64}$Zn values. These results are in accord with earlier studies [e.g., 1], which inferred that IAB irons are derived from a volatile rich parent body, whilst IIABs and IIIABs are from more volatile depleted precursors. They furthermore support previous stable isotope work, which concluded that volatile element depletion in the solar nebula was not associated with significant isotope fractionation because it did not involve partial Rayleigh evaporation or condensation [e.g.,2].

The Zn isotope compositions of the metal samples are ubiquitously heavy with $\delta^{66/64}$Zn of between about 0‰ and +2.5‰. In comparison, both the silicate Earth, which contains the bulk of the Earth's Zn budget, and most chondritic meteorites are characterised by $\delta^{66/64}$Zn values of about 0.0±0.5‰ [3,4]. Considered together, this suggests that metal–silicate segregation during planetary differentiation is associated with minor but resolvable Zn isotope fractionation, whereby isotopically heavy Zn is enriched in the metal phase.

Furthermore, distinct negative trends of decreasing $\delta^{66/64}$Zn with increasing Zn content were observed for each meteorite group. Such systematic variations were also seen for four sub-samples of the IIAB iron meteorite Sikhote – Alin. Hence it is likely that the trends are caused by small-scale heterogeneities in the distribution of Zn within the meteorites. Furthermore, our analyses and previous work [e.g., 5] suggest that the correlations reflect the variable occurance of isotopically light and Zn-rich phases, most likely chromite and/or daubreelite associated with troilite inclusions, within a metal matrix characterised by low Zn contents and high $\delta^{66/64}$Zn values.

[1] Palme, H., Larimer, J.W., Lipschutz, M.E. (1988) in: *Meteorites and the early Solar System*, 436-461. [2] Wombacher, F., Rehkämper, M., Mezger, K., Bischoff, A., Münker, C. (2008) *Geochim. Cosmochim. Acta* **72**, 646-667. [3] Luck, J.-M., Ben Othman, D., Albarède, F. (2005) *Geochim. Cosmochim. Acta* **69**, 5351-5363. [4] Moynier, F., Blichert-Toft, J., Telouk, P., Luck, J.-M., Albarède, F., (2007) *Geochim. Cosmochim. Acta* **71**, 4365-4379. [5] Keil, K., (1968) *Amer. Mineral.* **53**, 491-495.

Constraints on seawater sulfate concentrations through examination of temporal trends in δ^{13}C of methane seep carbonates

THOMAS F. BRISTOW[1*], JOHN P. GROTZINGER[2],

[1]NASA Ames Research Center, Moffett Field, USA, (thomas.f.bristow@nasa.gov)
[2]California Institute of Technology, Pasadena, USA, grotz@gps.caltech.edu

Since the relatively recent discovery of ecosystems based on energy derived from anaeorobic methane oxidation (AMO) more than 50 ancient examples have been recognized in the geological record [1]. Ancient methane seeps are recognized by endemic seep fauna and/or lithological, textural evidence of the passage and metabolism of methane bearing fluids. Highly ^{13}C-depleted carbonates (<-30‰ PDB) that precipitate from carbonate alkalinity generated by AMO provide an additional diagnostic indicator of ancient seeps; no other biogeochemical process is known to produce carbonates with such isotopic signatures at Earth-surface conditions.

Examination of the temporal occurance of seep deposits reveals that the majority of examples are reported from the Phanerzoic. Furthermore, δ^{13}C depletion to <-30‰ PDB in seep carbonates is not observed until the Early Carboniferous [2]. Because the main oxidant utlized in AMO at modern methane seeps is sulfate, it has been hypothesized that the temporal and isotopic trends of seep carbonates may reflect the influence of changing oceanic sulfate concentrations on AMO rates [3]. This hypothesis was investigated using 1D reaction-transport model that simulates the δ^{13}C of porewaters and precipitation of carbonates in a porous sedimentary profile where AMO is the main biogeochemical process.

AMO rates and controls on rates at modern methane seeps are well documented [4]. The model was tuned using porewater data collected from cores taken at Hydrate Ridge – a site with one of the highest integrated AMO rates observed in recent seeps. With these parameters we are able to estimate minimum threshold ocean [SO_4^{2-}] required to produce the levels of δ^{13}C depletion in seep carbonates observed in the geological record. Preliminary results show that low ocean [SO_4^{2-}], thought to characteristize much the Proterozoic and Archean, provides a plausible explanation for the absence of geochemical evidence for seeps in this period. Although the Paleozoic record of seeps is sparse, model calculations support S-isotope and fluid inclusion data indicating mM [SO_4^{2-}] in the early Paleozoic oceans, with a rise to >10 mM levels in the Late Devonian/Early Carboniferous, corresponding with the rise of land plants [5,6]. Implications for Ediacaran ocean [SO_4^{2-}] will also be discussed. Our investigation shows that secular variations in ocean [SO_4^{2-}] provide a plausible explanation for the temporal distribution and δ^{13}C of seep carbonates and highlight the need to refine criteria for recognizing ancient methane seep ecosystems.

[1] Campbell (2006) *Palaeogeo. Palaeoclim. Palaeoecol.* **232,** 362-407. [2] Peckmann (2001) *Geology* **29**, 271-274. [3] Bristow (2011) *Nature* **474,** 68-71. [4] Regnier (2011) *Earth Science Reviews* **106,** 105-130. [5] Gill (2007) *Palaeogeo. Palaeoclim. Palaeoecol.* **256,** 156-173. [6] Gill (2011) *Nature* **469,** 80-83.

The unusual nature of the Proterozoic biomarker record and the Mat-Seal hypothesis

JOCHEN J. BROCKS[1*], MARIA M. PAWLOWSKA [2], AND NICHOLAS J. BUTTERFIELD[2]

[1] The Australian National University, Research School of Earth Sciences, jochen.brocks@anu.edu.au

[2] University of Cambridge, Earth Sciences, mmp30@cam.ac.uk and njb1005@cam.ac.uk

Petroleum and bitumens are concentrates of hydrocarbon fossils of biological lipids (biomarkers). These biomarkers often contain significant biological and environmental information and can remain stable over hundreds of millions of years. However, bitumens of pre-Ediacaran age (>635 Ma) are scarce in the geological record and frequently adulterated by younger contaminants [1].

In this study, we re-analysed most known pre-Ediacaran bituminous deposits and determined 10 basins that contain clearly indigenous biomarkers dating back to 1,640 Ma [2, 3]. After exclusion of allochthonous hydrocarbons, the molecular fossils detected in these Precambrian sequences are distinct from their Phanerozoic counterparts. The pre-Ediacaran bitumens show significantly higher concentrations of 'unresolved complex mixture' (UCM), low concentrations or absence of eukaryotic steranes, the presence of putative bacterial aromatic steroids, high relative concentrations of mono- and dimethyl alkanes, and a conspicuous carbon isotopic enrichment of straight-chain lipids relative to acyclic isoprenoids and total organic carbon. Here we propose that these unusual characteristics primarily derive from non-actualistic taphonomic processes based on the pervasive presence of microbial mats in the Precambrian. This 'mat-seal effect' was broken with the onset of bioturbation in the Ediacaran when the primary source of fossil biomarkers switched from the benthos to the plankton.

The disturbance of soft sediments and associated microbial mat cover by infaunal burrowing was one of the most important geobiological innovations in the Neoproterozoic-Phanerozoic transition. This "Cambrian substrate revolution" [3] had profound effects on contemporaneous ecology [4], sedimentology [5] and sulphur geochemistry [6]. We argue that it also fundamentally altered the way in which organic matter was incorporated and preserved in the sedimentary record, giving rise to typical Ediacaran and Phanerozoic petroleum reserves, and potentially contributing to increasing atmospheric oxygen levels.

[1] Brocks (2011) *GCA* **75**, 3196-3213. Brocks *et al.* (2008) *GCA* **72**, 871-888. [2] Brocks *et al.* (2005) *Nature* **437**, 866-870. Summons *et al.* (1988) *GCA* **52**, 1747-1763. [3] Indigenous hydrocarbons occur as far back as ~2,500 Ma (Brocks *et al.* (2003) *Org. Geochem.* **34**, 1161-1175). However, these bitumens exclusively consist of PAH and diamondoids with little biological information. [3] Bottjer *et al.* (2000) *GSA Today* **10**, 1-7. [4] Seilacher (1999) *PALAIOS* **14**, 86-93. [5] Droser *et al.* (2002) *PALAIOS* **17**, 3. [6] Canfield and Farquhar (2009) *PNAS* **106**, 8123-8127.

What cooled the Earth during the last 20 million years?

WALLACE S. BROECKER[1*]

[1]Lamont-Doherty Earth Observatory of Columbia University, Palisades, New York, USA, broecker@ldeo.columbia.edu (*presenting author)

Abstract

During the last 20 million years earth temperature decreased but the CO_2 content of the atmosphere appears to have remained constant. Further, large changes in the Mg to Ca ratio and in the isotopic content of lithium in sea water also took place during this time interval. Explaining the lack of a CO_2 change constitutes a dilemma.

Capabilities of LA-ETV-MC-ICPMS for the measurement of Sr isotope ratios in Rb-rich samples

R. BROGIOLI, L. DORTA, B. HATTENDORF* AND D. GÜNTHER

[1]Laboratory of Inorganic Chemistry, ETH Zurich, Wolfgang-Pauli Strasse 10, 8093, Zürich, Switzerland

The successful use of LA-MC-ICPMS for the determination of Sr isotope ratio in the field of geochronology has been demonstrated for samples with relatively low Rb concentration [1, 2]. Its applicability for samples with higher Rb content is however still a challenge, mainly because mathematical correction of the isobaric interference of ^{87}Rb on ^{87}Sr affects the accuracy of the method [3, 4].

In an earlier study we investigated the effect of heating laser generated aerosols within an Electrothemal Vaporizer (HGA600 MS, Perkin Elmer, CAN) prior to the introduction into the ICPMS. Passing the laser generated aerosol through a commercial electrothermal vaporizer heated to 2000°C before the ICP allowed to attenuate the Rb interference by almost two orders of magnitude [6] for a silicate glass reference standard (NIST SRM610, Rb/Sr ~1). This same approach was now used for the measurement of Sr isotope ratios by LA-MC-ICPMS. To benchmark the Rb removal efficiency and the accuracy of Sr isotope ratio, a wide range of reference standard material were tested: NIST SRM610 (Silicate glass, Rb/Sr = 1), MPI-DING ATHO-G (rhyolite glass, Rb/Sr = 0.54), MPI-DING T1G (diorite glass, Rb/Sr = 0.28), USGS BCR-2G (basalt glass, Rb/Sr = 0.14) and $Li_2B_4O_7$ fused disks of NIST 607 (potassium feldspar, Rb/Sr = 8) . Depending on crater size adopted for the analysis and the ETV heating temperature, Rb signal was decreased by factor ~5 (for NIST SRM 607) to 100 (for NIST 610 and BCR-2G) resulting in an improved accuracy for the measured ^{87}Sr/^{86}Sr ratio.

Rb is not the only element interfering with Sr isotope analysis, doubly charged rare earth elements, metal oxides or calcium polyatomic ions are known to affect results accuracy [3]. For this reason $Li_2B_4O_7$ fused disks of NIST SRM987 (Sr carbonate) were spiked with Er, Yb, Hf, Ca, Fe, Ga, Zn to investigate the formation of potential interferences and the applicability of mathematical corrections. This study will show that he use of electrothermal vaporization coupled to LA sampling has the potential to widen the range of samples suitable for accurate *in-situ* determination of Sr isotope ratio.

[1] Yang Z.P. (2011) *J. Anal. Atom. Spectrom.* **26**, 241-351. [2] Fietzke J. (2009) *J. Anal. Atom. Spectrom.* **23**, 955-961. [3] Ramos F.C. (2004) *Chem. Geol.***211**, 135-158. [4] Jackson M.G. (2006) *Earth Planet. SC Lett.*, **245**, 260-277 [5] Rowlan A. (2008) *J. Anal. Atom . Spectrom* **23**, 167-172. [6] Brogioli R. (2011) *Anal. Bioanal. Chem.* **399**, 2201-2209

Biogeochemistry of mercury in contaminated sediments of East Fork Poplar Creek

SCOTT C. BROOKS[1*], DAVID KOCMAN[2], CARRIE MILLER[1], XIANGPING YIN[1], AMI RISCASSI[1]

[1]Oak Ridge National Laboratory, Oak Ridge, TN, USA, brookssc@ornl.gov (* presenting author)

[2] Jožef Stefan Institute, Ljubljana, Slovenia, david.kocman@ijs.si

Mercury use at the Oak Ridge Y-12 National Security Complex (Y-12 NSC) between 1950 - 1963 resulted in contamination of the East Fork Poplar Creek (EFPC) ecosystem. Hg continues to be released from point sources and diffuse contaminated soil and groundwater sources within the Y-12 NSC and outside the facility boundary. In general, methylmercury (MeHg) concentrations in water and in fish have not declined in response to improvements in water quality and exhibit trends of increasing concentration in some cases.

Therefore, our study focuses on identifying ecosystem compartments and/or characteristics that favor the production, as well as degradation, of MeHg in EFPC. Detailed geochemical characterization of the surface water, interstitial pore water, and creek sediments were performed during quarterly sampling campaigns in 2010 and 2011 at two locations. One site is 3.7 km (NOAA) and the other 20 km (NH) downstream of the headwaters and source of the point discharges. Vertical profiles of interstitial pore water collected from fine-grained deposits at the creek margin showed decreases in nitrate, sulfate, and oxidation-reduction potential (ORP) with depth as well as increases in dissolved manganese, iron, and small increases in sulfide. The results indicate the progression of terminal electron accepting processes with depth in the upper 30 cm of these fine grained sediments. Dissolved (passing 0.2 μm pore) MeHg concentration was positively correlated with depth suggesting these areas served as a source of MeHg. MeHg in the surface water is associated with phases small enough to pass a 3 kiloDalton filter. In contrast, interstitial water collected from the cobbly center channel of the creek did not exhibit these redox gradients. The observed constant or decreasing MeHg concentrations with depth suggest that the interstitial water in the fast flowing sections of the creek is rapidly exchanging with the surface water and these sections do not serve as MeHg sources. Total Hg concentration in sediment cores from the creek margin was variable, 0.057-24 mg/kg and 0.02-155 mg/kg, at NH and NOAA respectively. MeHg measured on a subset of these sectioned cores ranged from 0.71-17.5 μg/kg at NH and 1.08-46.7 μg/kg at NOAA. Large intra- and inter-site variability of Hg distribution in these samples is partly attributed to the very heterogeneous sediment texture that ranged from coarse- to fine-grained. Methylation potential, measured using enriched stable isotopes of Hg on intact sediment cores, was significantly correlated with ambient MeHg concentration at both sites.

Enhanced radionuclide capture by bioreduced biotite and chlorite

DIANA R. BROOKSHAW[1]*, KATHERINE MORRIS[1], JONATHAN R. LLOYD[1], RICHARD A.D. PATTRICK[1] GARETH T. LAW[1/2], AND DAVID J. VAUGHAN[1]

[1]Williamson Research Centre and Research Centre for Radwaste and Decommissioning, SEAES, The University of Manchester, Manchester, M13 9PL. diana.brookshaw@postgrad.manchester.ac.uk (*presenting author)

[2]Centre for Radiochemistry Research The University of Manchester, Manchester, M13 9PL. gareth.law@manchester.ac.uk

Background and methodology

Management and geological disposal of our nuclear waste legacy requires an in-depth understanding of biogeochemical processes that occur in the subsurface and their influence on radionuclide speciation and mobility. Here, we explore molecular-scale processes involved in radionuclide immobilisation at the solution-mineral interface and the indirect, but potentially crucial role which microorganisms play in such reactions. The research focuses on two common rock-forming minerals, biotite and chlorite that contain both ferric (Fe(III)) and ferrous (Fe(II)) iron within their octahedral layers. The experimental systems were focussed around "unaltered" or as-sampled biotite and chlorite, and "bioreduced" biotite and chlorite. For the bioreduced minerals, biotite and chlorite were exposed to the model Fe(III)-reducing subsurface microorganism *Geobacter sulfurreducens* in the presence of an electron shuttle (AQDS) to promote reduction of bioavailable Fe(III) within the mineral moeity to Fe(II). After this, unaltered or bioreduced biotite and chlorite were suspended in solutions containing undersaturated Tc(VII), U(VI) or Np(V). The solubility of the redox active radionuclides was then monitored and the variations in the solid phase speciation of the radionuclides was characterised by X-ray absorption spectroscopy (XAS).

Results and implications

G. sulfurreducens was able to reduce Fe(III) associated with biotite and chlorite thus priming the minerals with Fe(II) for "indirect" reductive transformations. However, the interactions of the different radionuclides with the mineral systems differed. There was evidence for reductive transformation of Tc(VII) to Tc(IV) in the bioreduced biotite and chlorite, presumably mediated by labile Fe(II) associated with the bioreduced minerals [1,2]. By contrast, there was poor reactivity towards Tc(VII) in the unaltered samples. Ongoing work with the actinides shows some selectivity for the different mineral surfaces with both sorption and potentially reductive precipitation pathways possible.

Overall, these results show that relatively small increases in Fe(II) content (up to 0.12 mmoles per gram) in the bioreduced minerals can have a profound effect on mineral reactivity and radionuclide behaviour compared to bacterial-free systems. This suggests that indirect reduction of microbially reduced minerals may be an important pathway to immobilisation in rock environments typical of geological disposal sites for radioactive wastes.

[1] Lloyd et al (2000) *Appl. Environ. Microbiol* **66,** 3740-3749, [2] Morris et al (2008) *App. Geochem.* **23**, 603-617.

Effects of pore fluid chemistry on diagenesis.

J. BROUWER*, A. PUTNIS

Institut für Mineralogie, Westf. Wilhelms Univ. Münster, Germany, brouwer.janneke@gmail.com

Sediment compaction by dissolution – precipitation creep

Sediment compaction occurs largely through dissolution-precipitation creep, also called pressure solution, a process that is driven by gradients in stress. Grains dissolve at grain contacts that support the load of overlying sediments, and solutes precipitate at pore walls, leading to a decrease in permeability. Pore fluid chemistry can be expected to significantly affect sediment compaction behavior and therefore how permeability changes with time. However, not much research has been done to study such chemical effects. Recently, [1] studied the effect of additives on calcite compaction. We investigate the influence of trace elements in solution that affect dissolution and precipitation rates, and the effect of mineral replacement on compaction behavior.

Experiments

We present results of uniaxial compaction experiments on cylindrical (10 mm. length, ø 2.3 mm.) aggregates of various alkali halides. A stress of 1.2 MPa is applied and compaction monitored using a simple set-up after [2]. We show that certain trace metals in solution may affect compaction rates of NaCl, but not of KCl. We investigate the effect of mineral replacement during compaction in the solid-solution system $K(Br_xCl_{1-x})$. A reservoir containing a saturated solution of KCl or KBr is placed on top of the cylindrical aggregate of KBr resp. KCl. The results show that reaction leads to enhancement and localization of compaction, leading to fast reduction in permeability. The change in permeability with time, and therefore fluid infiltration and reaction progress, is not only influenced by the compaction rate, but also by solid volume changes related to the reaction.

Conclusion

Mineral and pore fluid chemistry is an important factor in sediment compaction behavior. Chemical disequilibrium leading to mineral reaction during compaction leads to enhancement and localization of compaction.

[1] Zhang et al. (2011) *Geofluids* **11**, 108-122. [2] De Meer and Spiers (1997) *J. Geophys. Res.* **102**, B1 875-891.

Impact of radiation on the microbial reduction of iron oxides

ASHLEY R. BROWN[1*], PAUL WINCOTT[1], DAVID J. VAUGHAN[1], SIMON M. PIMBLOTT[2], ROYSTON GOODACRE[3] AND JONATHAN R. LLOYD[1]

[1]Williamson Research Centre for Molecular Environmental Science, School of Earth, Atmospheric and Environmental Sciences, University of Manchester, Manchester, UK, ashley.r.brown@postgrad.manchester.ac.uk (* presenting author)

[2]Dalton Nuclear Institute and School of Chemistry, University of Manchester, Manchester, UK

[3]Manchester Interdiscplinary Biocentre and School of Chemistry, University of Manchester, Manchester, UK

The microbial reduction of Fe(III) in geodisposed nuclear waste or radwaste contaminated land can play a significant role in controlling the mobility of a range of long-lived radionuclides, including U(VI), Np(V) and Tc(VII). As such environments are likely to receive large radiation doses, radiation induced changes to the iron mineralogy may impact upon microbial respiration and subsequently alter the stability of the radionuclide inventory. Hence, characterization of radiation damage to Fe(III) mineralogy and the resultant impact upon microbial respiratory processes is essential in the preparation of a geological waste disposal safety case. In this study aerobic irradiation (1 MGy gamma) of hematite and ferrihydrite led to an increase in the rate of Fe(III) reduction by the Fe(III)-reducing bacterium *Shewanella oneidensis* MR-1 in the presence of an electron shuttle, riboflavin. Sequential extractions of iron in microbial cultures containing irradiated ferrihydrite suggested a 10% increase in ferrous iron partitioned into an operationally defined iron carbonate phase. A 15% increase in microbially reduced iron in irradiated hematite systems was incorporated into a combination of a putative carbonate phase, an easily reducible fraction and also increased dissolved Fe(II). Mossbauer spectroscopy of irradiated ferrihydrite suggests conversion to a more crystalline phase similar to akaganeite, whilst anoxically irradiated hematite appears to show a decrease in Fe coordination. This study suggests that structural changes in the mineralogy by irradiation lead to an increase in bioavailabilty of ferric iron. This may have positive implications to the geological disposal of nuclear waste, as reducing conditions may be accelerated by radiation-induced microbial iron reduction, potentially mediating the enhanced stability of key radionuclides.

Geochemical insights from accessory phases in a sanukitoid-like suite: Towards understanding temporal changes in subduction style

E. BRUAND[1*], C. STOREY[1], M. FOWLER[1]

[1]School of Earth and Environmental Sciences, Portsmouth, United Kingdom, emilie.bruand@port.ac.uk (* presenting author)

Crustal evolution is governed by plate tectonics and it has been shown that between the Archean and the Phanerozoic major changes in subduction style occured. Among others, the chemistry of different plutonic rocks through time and the understanding of their petrogeneses have helped to define different stages in the evolution of plate tectonics on Earth. Although TTG, the direct product of melted oceanic lithosphere, were the main plutonic rocks generated during the Archean, an important change around 2.7 Ga led to the genesis of rocks that are the result of melting of a metasomatized mantle wedge: the sanukitoids. This observation is often interpreted as the result of a change from shallow to steep subduction. Modern plate tectonics generally generates calc-alkaline suites but exceptions can occur such as the Caledonian (Paleozoic) high Ba-Sr plutons in Northern Scotland. The latter have been interpreted as a "modern" analogue of sanukitoids [1].

In this contribution, we present a study of accessory minerals from this Caledonian sanukitoid-like suite (ultrabasic to acidic). Whole-rock chemistry (trace elements, radiogenic and stable isotopes) is well constrained [1] but the study of accessory phases reveals additional petrogenetic constraints [2]. Indeed, accessory phases are important beyond their modal proportion because they commonly contain elements that are not incorporated easily into major rock forming minerals. The incorporation of trace elements and more particularly rare earth element (REE) in their structures make them ideal to delineate petrogenetic processes. In particular, the study of apatite, titanite and zircon will test the ability of accessory phases to retain the signature of their tectonic affinity. We present a detailed petrographic study and the systematic analysis of trace elements and O isotopes of these phases in a range of fractionated plutonic rocks from appinitic (ultrabasic) to granitoid composition. These results have an important impact in the understanding of accessory phases saturation during the magma genesis and thus offer another way to study the petrogenesis of these sanukitoid-like rocks. This approach will be extended to other magma compositions to further our insight into petrogenetic processes and tectonic affinity that may be available from accessory phase studies.

[1] Fowler et al. (2008) *Lithos* **105**, 129-148. [2] Hoskin et al. (2000) *Journal of Petrology* **41**, 1365-1396.

Mineralogical and geochemical evidence for syngenetic precious metal enrichment in a deformed volcanogenic massive sulfide (VMS) system

STEFANIE M. BRUCKNER[1*], STEPHEN J. PIERCEY[1], PAUL J. SYLVESTER[1], STEPHANIE MALONEY[2], LARRY PILGRIM[2]

[1]Memorial University, Dept. of Earth Sciences
s.brueckner@mun.ca (* presenting author)
[2]Rambler Metals & Mining Canada Ltd., Baie Verte, NL, Canada

Introduction

The early Ordovician Ming Mine (487 Ma; total resource 12.5 Mt ore @ 1.52 wt% Cu, 1.69 ppm Au, 8.11 ppm Ag, and 0.45 wt% Zn), NW Newfoundland, Canada, is a type example of a precious metal-enriched VMS deposit. Moderate deformation and metamorphism makes deciphering the origin of Au-Ag-enrichment (e.g., syngenetic vs. epigenetic) difficult. However, mineralogic and geochemical evidence support a syngenetic origin with Au-Ag coming via a magmtic contribution to the primary VMS hydrothermal fluid [1, 2, 3]. Mineralogical observations show a complex sulfide mineral assemblage in stringer and massive sulfide mineralization. Besides base metal sulfides (e.g., pyrite, chalcopyrite, sphalerite, galena, pyrrhotite), sulfosalts rich in magmatic suite elements (e.g., arsenopyrite, tetrahedrite-tennantite, stannite, boulangerite, loellingite), Te-bearing phases (e.g., BiTe, coloradoite), Ag-phases (e.g., miargyrite, unnamed AgCuFeS phase, argentotetrahedrite, AgHg alloy), and electrum occur throughout the deposit, but are slightly more enriched in the upper part of the deposit. Main, minor and trace element analysis by electron microprobe (EPMA) show the emrichment of magmatic suite elements (e.g., As, Bi, Hg, Sb, Sn, Te) as major, minor and trace constituent in base metal and other sulfides phases.

Results and Conclusions

Electrum and Ag-phases occur as: (1) free phases in gangue or on pyrite/chalcopyrite margins; (2) as inclusions in pyrite, arsenopyrite, pyrrhotite, and galena; (3) along veinlets in and on grain boundaries of pyrite and arsenopyrite; (4) in odd myrmekitic-like textures; and (5) in close proximity to each other and tetrahedrite-tennantite. EPMA data on 17 elements in sulfide and precious metal phases reveal: (1) no invisible gold in any phase; (2) a high Hg-content (12 – 17 wt%) in electrum; and (3) sphalerite with a varying Fe-content (2 – 9 wt%). The mineralogical and geochemical features of the ores favor a syngenetic, magmatic origin for precious metal enrichment. However, later deformation remobilized some metals, especially Au and Ag, as evidenced by textural relationships and the absence of invisible gold.

[1] Sillitoe et al. (1996) *Economic Geology* **91**, 204-212. [2] Hannington et al. (1999) *Reviews in Economic Geology* **8**, 325-351. [3] Huston (2000) *Reviews in Economic Geology* **13**, 401-426.

From aqueous to solid solutions: A process understanding of trace metal incorporation into solid structures

JORDI BRUNO[1,2*]

[1]Amphos 21 Group Barcelona, Catalunya,
jordi.bruno@amphos21.com (* presenting author)
[2]UPC BarcelonaTech, Barcelona, Catalunya, jordi.bruno@upc.edu

Introduction

Aqueous-solid solution systems are ubiquitous in natural and anthropogenic systems and they influence the fate and mobility of heavy metals and radionuclides.

The process understanding of the structural incorporation of trace components into existing or forming solid phases is essential to the assessment of the potential environmental consequences.

Objective of the presentation

In my presentation I will introduce some of the key concepts involved in the suite of processes that are involved in the transition of a trace component from the aqueous to the solid solution both from the kinetic and thermodynamic points of view.

I will devote particular attention to recent solution chemical and spectroscopic data that has been recently acquired in the frame of the EC Funmig project[1] and I will frame it to the conceptual developments presented in [2]

I will also propose some ways forward to integrate the experimental information on the structural incorporation of trace elements into the current models used in current environmental assessments.

[1] Bruno, J. and Montoya, V. (2012 *Applied Geochemistry*, **27, 444–452**
[2] Bruno, J., Bosbach, D., Kulik, D. Navrotsky, A., (2007) *Chemical Thermodynamics of Solid Solutions of Interest in Nuclear Waste Management* **Chemical Thermodynamics Volume 10. OCDE-NEA**.

On the use of hydrochemical mixing models to conceptualize hydrogeology in fractured rocks

JORGE MOLINERO[1], JORDI BRUNO[1] (*)PAOLO TRINCHERO[1], AND LUIS MANUEL DE VRIES[1]

[1]Amphos 21 Consulting SL, Barcelona, Spain, jordi.bruno@amphos21.com (* presenting author)

Abstract

Mixing models are broadly used in hydrogeology as a tool to understand groundwater systems. Simple mixing models are based on inferring the relative abundance of assumed end-member waters from measured concentrations of conservative species in the mixture. However, simple mixing methodologies present clear limitations for complex systems with the influence of several initial and boundary waters. For these cases, more sophisticated mixing models have to be used by using statistical multivariate techniques such as Principal Component Analysis.

On the other hand it is also known that mixing modeling presents practical limitations, basically derived from the uncertainties in the definition of the end-members, as well as mixing artifacts associated to groundwater sampling procedures by drilling and pumping, that use to magnify the apparent mixing in the system.

In addition to the abovementioned practical limitations, we claim in this work that mixing models are also subjected to conceptual limitations that can lead to serious misuses, especially when applied to fractured rocks. This is due to the fact that matrix diffusion phenomena introduce a "memory" effect in the system previously affected by the influence of different waters. This fact could make mixing modelers to misunderstand the real groundwater behavior.

We present a series of synthetic numerical simulations to illustrate that hydrogeological models based on computed mixing models, of known end-member waters, are unable to properly conceptualize the real hydrogeological behavior of a fractured rock aquifer.

Mechanisms governing nanoparticle transport in porous media

STEVEN BRYANT*,[1], HAIYANG YU[2], MICHAEL MURPHY[2], TIANTIAN ZHANG[2], ANDREW WORTHEN[3], KI YOUL YOON[3], KEITH JOHNSTON[3], CHUN HUH[2]

[1]Dept. of Petroleum and Geosystems Engineering, The University of Texas at Austin, Austin, USA, steven_bryant@mail.utexas.edu (* presenting author)

[2] Dept. of Petroleum and Geosystems Engineering, The University of Texas at Austin, Austin, USA

[3] Dept. of Chemical Engineering, The University of Texas at Austin, Austin, USA

Abstract

The prospect of using engineered nanoparticles for subsurface applications raises practical questions. How far can nanoparticles be transported through porous media? If multiple fluid phases are present, does this affect the transport distance? Do the nanoparticles travel at their injected concentration and at the velocity of the carrier phase? The science needed to answer these questions raises its own set of interesting problems. Can nanoparticle transport be treated like solute transport, or must the nanoparticles be treated like colloids? If the latter, what forces govern the interaction between nanoparticle and the solid surface of the porous medium? If nanoparticles attach or adhere to the solid, can they detach? Is the nanoparticles/solid interaction reversible? In this talk we review a large set of transport experiments conducted in our laboratory. The data provide some insight into key mechanisms of nanoparticle transport and retention. For example, we typically observe small amounts (much less than a monolayer) of irreversible adsorption, and even smaller amounts of reversible adsorption. Experiments with variable flow velocities indicate that nanoparticle adsorption capacity is a dynamic, hysteretic property. For suitably engineered particle coatings, particle adhesion at fluid/fluid interfaces is the same magnitude as adhesion on the solid surface. We discuss a framework for modeling these phenomena.

Progress of weathering reactions in ultramafic rocks

KURT BUCHER

[1]Institute of Geosciences. University of Freiburg. Albertstr. 23b. D-79102 Freiburg. Germany. bucher@uni-freiburg.de

Section 7a: The Art of weathering

Chemical weathering results from a complex interaction between geochemistry, hydrology, biology, and physical erosion and is therefore site specifie [1].

Chemical weathering of dark green massive ultramafic rocks produces a distinct and remarkable yellow weathering rind when exposed to the atmosphere long enough. Crust formation on rocks from three European climates have been studied: a) Ronda Peridotite, Spain, b) Seiland Complex, Norway, c) Zermatt Ophiolite, Switzerland). Rinds from the three areas vary mineralogically and have very different thicknesses. The rind thickness depends on the mineralogy of the bedrock, atmospheric parameters and on the details of transport and kinetics of the chemical reactions.

Fig. Weathering rinds on dunite (Reinfjorden, N Norway)

The fundamental reaction "peridotite (serpentinite) + rainwater = weathering rind + runoff water" describes the crust forming process. This hydration reaction depends on the water supply from the rock surface to the reaction front. The transport mechanism is grain boundary diffusion. At the reaction front, kinetics controls the progress of the weathering reactions. The competing kinetics-diffusion control determines the rate of rind growth. The alteration zone must be wetted after a dry period and the reaction resumed at the front. The wetting-drying cycles may contribute significantly to the hydraulic properties of the weathering rind. Reaction details of the rind forming process are saved in the subtle structures of the crusts.

The propagation of the reaction front and the internal structure of the rinds have strong similarities to hydrothermal reaction veins [2]. It is evident that rind thickness development is not related to pervasive advective fluid flow.

[1] White A. F. 2008, Quantitative Approaches to Characterizing Natural Chemical Weathering Rates. In *Kinetics of Water-Rock Interaction* (ed. S. L. Brantley, J. D. Kubicki, and A. F. White), pp. 151-210. Springer.
[2] Bucher K. 1998, Growth mechanisms of metasomatic reaction veins in dolomite marbles from the Bergell Alps. Mineralogy and Petrology, 63, 151-171.

Biomineralization of selenium: proteins as the reason for altered colloidal stability of nanoparticle suspensions

BENJAMIN BUCHS[1], MICHAEL W.H. EVANGELOU[2], PHILIPPE F.X CORVINI[1,3], MARKUS LENZ[1,4*]

[1] University of Applied Sciences and Arts Northwestern Switzerland (FHNW), Institute for Ecopreneurship
[2] ETH Zürich , Institute of Terrestrial Ecosystems
[3] School of the Environment, Nanjing University, 22# Hankou Rd., Nanjing, 210093, P.R.China com
[4] Wageningen University, Sub-Department of Environmental Technology, markus.lenz@fhnw.ch (* presenting author)

Although biomineralization of selenium has been investigated in the frame of bioremediation for decades, the molecular principles behind it remain largely unknown. Despite of its microbial origin, biogenic elemental selenium typically consists of nanosized spherical particles (Figure 1), stabilized against gravitational settling. These particular properties were suspected to be mediated by organic molecules associated to the selenium particles. In this study, organic molecules associated with high-affinity to selenium bionanominerals were isolated from such molecules with low-affinity by density-based centrifugation. The proteic fraction was characterized via capillary liquid chromatography-electrospray ionization-tandem mass spectrometry (LC-ESI-MS/MS). A plenitude of proteins was found to strongly associate to biomineralized selenium formed by physiologically different microorganisms [1]. Interestingly, one protein - a metalloid reductase - did associate strongly to both biogenic nanoselenium and synthetically produced selenium surfaces, indicating some specific recognition properties. By means of electrophoretic measurements (zeta –potential) and settling experiments it was demonstrated that, indeed, the proteic fraction considerably alters the colloidal stability of selenium bionanominerals. Furthermore, it could be demonstrated that the aqueous transport will be considerably influenced by the environmental media composition (i.e. acidic vs. neutral waters; sea vs. surface waters; waters differing in dissolved organic matter content, etc.).

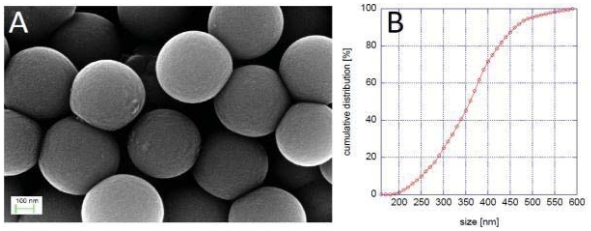

Figure 1: SEM images of purified biomineralized selenium produced by *Bacillus selenatarsenatis* (A) and corresponding cummulative particle size distribution (B)

[1] Lenz, M. et al. (2011). *Applied and Environmental Microbiology*, **77 (13)**, 4676-4680.

Buoyant asthenosphere affects mid-ocean ridge depths and melt patterns

W. ROGER BUCK[1*], CHRISTOPHER SMALL[2], AND WILLIAN B. F. RYAN[3]

[1]Lamont-Doherty Earth Observatory, buck@ldeo.columbia.edu (*presenting author)
[2]Lamont-Doherty Earth Observatory, small@ldeo.columbia.edu
[3]Lamont-Doherty Earth Observatory, ryan@ldeo.columbia.edu

The East Pacific Rise (EPR) is the fastest spreading ridge yet it is deeper that most other spreading centers. Along the 5000 km of the EPR the depth averages 400 m greater than the adjacent Pacific-Antarctic Ridge [1]. The other very deep section of ridge is the Australian-Antarctic Discordance (AAD). Analytic and numerical models show that dynamic thinning of asthenosphere with a lower density than the underlying mantle can explain the magnitude and wavelength of the depth anomalies along the EPR and the AAD [2]. At the EPR, fast plate divergence thins the asthenosphere by both sequestering it into diverging lithosphere and dragging it with the plates in contrast to the slower spreading, but faster migrating PAR [1]. The AAD asthenosphere is greatly thinned because of the restriction of asthenospheric flow due to nearby thick continental lithospheric roots combined with a moderately fast spreading rate [2]. The ADD is a major isotopic boundary. This can be explained if there is efficient mixing within the low-viscosity asthenosphere of the Indian and Pacific Ocean basins. Low-viscosity, low-density asthenosphere that is thinned beneath a spreading center should accentuate the asymmetry in melting related to migration of a spreading center as illustrated in Figure 1. This may help explain the observed pattern of oceanic crustal thickness variations as a function of ridge offsets and spreading directions [3].

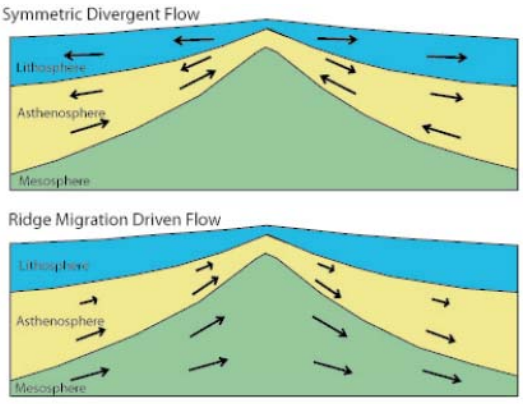

Figure 1: Flow under a migrating ridge should combine the effect of divergent and migration driven flow, but the asymmetry of upwelling and melting is accentuated due to relief on the base of the buoyant asthenosphere.

[1] Small, and Danyushevsky (2003) *Geology* **31**, 399-402. [2] Buck, Small and Ryan (2009) *Geochemistry, Geophysics, Geosystems* **10**, doi:10.1029/2009GC002373. [3] Carbotte, Small and Donnelly (2004), The influence of ridge migration on the magmatic segmentation of mid-ocean ridges, *Nature* **429**, 743-746.

Using automated mineralogy to evaluate bioaccessibility of Pb-bearing mine waste

MARTHA BUCKWALTER-DAVIS[1*], HEATHER JAGGARD[1], SUZETTE MORMAN[2], GEOFFREY PLUMLEE[2], AND HEATHER JAMIESON[1]

[1]Queen's University, Kingston Ontario, Canada mbuckwalterdavis@gmail.com (*presenting author)
[2]U. S. Geological Survey, gplumlee@usgs.gov, smorman@usgs.gov

The toxic effects of Pb, especially on children, are well known. The concentration of Pb in waters draining mine tailings tends to be low due to the relative insolubility of galena (PbS) and weathering products such as anglesite ($PbSO_4$). A more hazardous route of exposure is the direct ingestion of windblown dust or contaminated soil, particularly if the ingested material contains the Pb carbonate mineral cerussite ($PbCO_3$), a highly bioaccessible form of Pb.

Detailed mineralogical examination of mine tailings from the New Calumet Pb-Zn mine in Quebec has shown that after decades of subaerial exposure, almost all Pb is hosted in primary galena and secondary cerussite ($PbCO_3$), with only trace amounts of anglesite and massicot (PbO). Some of the goethite formed from alteration of pyrrhotite contains detectable Pb.

Simulated gastric fluids (pH=1.5) were used to evaluate Pb bioaccessibility in the <250 micron fraction of six near-surface tailings samples (Pb_{total} =1740-4730 $mgkg^{-1}$). The percent of Pb that is bioaccessible ranges from 23% to 69% and is not correlated with total Pb. The bioaccessible Pb for some samples is below industrial soil clean-up criteria.

Automated SEM-based mineralogy provides the opportunity to rapidly characterize thousands of Pb-bearing particles in terms of mineralogy, grain size and degree of liberation from armouring silicates, all features which control bioaccessibility. We have used a FEG-SEM instrument with the Mineral Liberation Analyzer (MLA) software suite to characterize and quantify the Calumet tailings samples. MLA was developed for the metallurgical industry but has increasing environmental applications due to its ability to characterize fine grained sediments including tailings. Some difficulties were presented in distinguishing galena (low bioaccessibility) and cerussite (high bioaccessibility), due to overlapping peaks between S and Pb but these issues have been largely resolved with careful development of a standard reference library within the MLA software and use of X-ray mapping of Pb-bearing grains.

Sample GD-nonVEG (bioaccessibility = 38% Pb) is more fine grained with respect to all particles than sample MS-nonVEG (bioaccessibility = 23% Pb). The ratio (by analyzed area) of cerussite to galena is higher in MS-nonVEG than sample GD-nonVEG, which is contrary to what is expected based on the relative bioaccessibilites of these two minerals, but particle size analysis indicates that cerussite grains are larger in sample MS-nonVEG. Smaller particles have a larger surface area and are more leachable and bioaccessible, which may explain why GD-nonVEG is more bioaccessible while having relatively less cerussite. Research is continuing with efforts to improve the distinction of galena and cerussite and to better characterize very fine grained material.

Reconstructing the Toba magmatic system: insights from stable isotope geochemistry

DAVID A. BUDD[1*], VALENTIN R. TROLL[1,5], ESTER M. JOLIS[1], FRANCES M. DEEGAN[1,3], VICTORIA C. SMITH[2], MARTIN J. WHITEHOUSE[3], CHRIS HARRIS[4], CARMELA FREDA[5], DAVID R. HILTON[6] AND SAEMUNDUR A. HALLDORSSON[6]

[1]CEMPEG, Uppsala University, Sweden
david.budd@geo.uu.se (* presenting author)
[2]Research Lab. for Archaeology, University of Oxford, UK
[3]Swedish Museum of Natural History, Sweden
[4]Dept. Geological Sciences, University of Cape Town, South Africa
[5]Istituto Nazionale di Geofisica e Vulcanologia, Italy
[6]Scripps Institution of Oceanography, UCSD, USA

The Toba caldera located in Sumatra (Indonesia) is the result of the four successive eruptions at 1.2, 0.84, 0.5 and 0.074 Ma [1]. This study presents oxygen isotope data for a suite of whole rocks and quartz crystals erupted as part of the Young Toba Tuff (YTT), an eruption event producing 2,800 km^3 of material some 74 ka ago [1, 2]. Oxygen isotope data have been obtained from whole rock (conventional fluorination), single mineral grains (laser fluorination-LF) and *in-situ* (SIMS) in combination with cathodoluminescence (CL) imaging in order to establish the relative roles of magmatic fractionation, magma-crust interaction and crystal recycling occurring in the Toba magmatic system. The CL images of quartz crystals exhibit defined patterns of zoning that often coincide with fluctuations in $\delta^{18}O$ values, allowing correlation of textural and compositional information. Measured $\delta^{18}O_{quartz}$ values from SIMS and LF range from 6.7 to 9.4 ‰, independent of their position on the crystal. Whole rock values, in turn, range from 8.2 to 9.9 ‰. The $\delta^{18}O_{magma}$ values calculated from quartz (assuming $\delta^{18}O_{quartz\text{-}magma}$ = 0.7 ‰), suggest a minimum value of 6.0 ‰, similar to that expected from a mantle derived magma [3], and a maximum value of 8.7 ‰. Several quartz crystals, however, have rims with lower $\delta^{18}O$ values, suggesting a late, low-$\delta^{18}O$ contaminant. This indicates multiple sources to the Toba system, including at least two crustal components, one with high- and one with low-$\delta^{18}O$. Helium isotope data obtained from pyroxenes from the oldest Toba eruption (R/R_A = 0.7 and 1.8) are consistent with a significant crustal contribution.

Barometry calculations from feldspar and amphibole suggest the magma chamber system resided at similar depth (~ 10 km) for all four Toba eruptions. The system probably persisted as a crystal mush, which was repeatedly re-mobilised by fresh magma injections. Crystal recycling, consistent with compositional and textural features in most of the YTT quartz crystals, seems an integral part of how super-eruptions are assembled. Therefore, large volumes of isotopically heterogeneous sources were mixed to make the final YTT cocktail, including a late low-$\delta^{18}O$ contaminant, substantial high-$\delta^{18}O$ crustal contributions, and considerable amounts of recycled antecrysts from the three previous eruptive episodes of the Toba system.

[1] Rose & Chesner (1987) *Geology* **15**, 913-917. [2] Aldiss & Ghazali (1984) *J Geol. Soc. London* **141,** 487-500. [3] Taylor & Sheppard (1986) *Rev. Min.* **16,** 227-271.

A mesocosm study of fate and effects of CuO nanoparticles on endobenthic species (*Scrobicularia plana*, *Nereis diversicolor*)

PIERRE EMMANUEL BUFFET[1], MARION RICHARD[2], FANNY CAUPOS[2], AURORE VERGNOUX[1*], HANANE PERREIN-ETTAJANI[1], HELENE THOMAS-GUYON[2], ANDREA LUNA-ACOSTA[2], CLAUDE AMIARD-TRIQUET[1], JEAN-CLAUDE AMIARD[1], CHRISTINE RISSO[3], MARIELLE GUIBBOLINI[3], PAUL REIP[4], EUGENIA VALSAMI-JONES[5], AND CATHERINE MOUNEYRAC[1]

[1] Groupe Mer, Molécules, Santé (MMS), Université de Nantes et Université Catholique de l'Ouest (Angers), France, aurore.vergnoux@univ-nantes.fr (* presenting author)
[2] Littoral Environnement et Sociétés (LIENSs), Université de La Rochelle, France, helene.thomas@univ-lr.fr
[3] ECOMERS, Université de Nice Sophia-Antipolis, France, christine.risso@unice.fr
[4] Intrinsiq Materials Ltd., Hants, UK, paulreip@intrinsiqmaterials.com
[5] Department of Mineralogy, Natural History Museum London, UK, e.valsami-jones@nhm.ac.uk

Introduction. To investigate the transfer of CuO nanoparticles (CuONPs) from the medium to endobenthic species (*S. plana*, *N. diversicolor*), under environmentally realistic conditions, animals were exposed in field mesocosms to Cu (10 µg.L^{-1}) added either as CuONPs or as soluble Cu in comparison with controls for 21 days. The fraction of Cu under labile form was determined in water and sediment by using Diffusive Gradient in Thin film (DGT). Bioaccumulation of Cu was measured in the whole soft tissues of both species. Behavioural and biochemical biomarkers were determined in organisms.

Figure 1: Experimental intertidal mesocosms deployed in natural environment.

Results. No release of labile Cu from CuONPs was observed at days 7, 14 and 21. Cu bioaccumulation was shown in both species with CuONPs and with soluble Cu for clams. Impairments of behaviour (feeding and burrowing) were observed in both species. Antioxidant activities (CAT, GST) increased in both species for both chemical forms except for GST in worms exposed to soluble Cu. In clams exposed to both Cu forms, detoxification protein (MT) induction was observed and an apoptosis effect only under CuONP exposure. Concerning other biomarkers of defense (SOD, LDH, Laccase) and damage (TBARS, AChE, acid phosphatase) no significant effects were detected.

Conclusion. This experiment shows the suitability of mesocosms for studying the environmental effects of nanoparticles. Behavioral biomarkers and antioxidant defenses are the most sensitive tools to highlight the effect of soluble or nanoparticulate Cu forms.

Soil salinity: a driver in macroevolutionary processes?

ELISABETH BUI[1*], JOE MILLER[2]

[1]CSIRO Land and Water, GPO Box 1666, Canberra ACT 2601, Australia, elisabeth.bui@csiro.au (* presenting author)

[2]Centre for Australian National Biodiversity Research, GPO Box 1600, CSIRO Plant Industry, Canberra, ACT 2601, Australia

Recent evidence from Australia, one of the most biologically diverse areas of the world, with one of the most extensive arid zones and widespread natural salinity, suggests a role for soil salinity in biogeography and ecology. The distribution of plant species in Queensland responds strongly to a geochemical gradient as expressed by soil salinity and pH, starting at levels of salinity much lower than those for saline soil [1]. Statistical modelling shows that adding soil salinity to climatic and other soil variables in a Generalized Additive Model to account for site scores from a correspondence analysis of site by species data improved the results dramatically (Mean Squared Error decreased from 0.89 to 0.65 and R^2 improved from 0.41 to 0.57) [1]. Three *Acacia* species (*Acacia harpophylla* (commonly called 'brigalow'), *A. cambagei and A. argyrodendron)* that exhibit high salt tolerance are closely related species of microneurous *Plurinerves* as indicated by *Acacia* systematics [2].

Parallel investigations of thrips systematics and their behavioral ecology have shown that: 1) there are specific host-plant relationships of elongate and round gall thrips (*Kladothrips* spp.) on the *A. harpophylla* clade of Plurinerves; 2) phyllode-glueing thrips also show host specificity; and 3) thrips on *A. harpophylla* and *A. cambagei* display high species richness [2, 3]. Chronological phylogenetic analyses indicate that the approximate age of origin of gall thrips (*Kladothrips* spp.) is Miocene and that their subsequent diversification is closely linked to host-plant evolution [3]. Host affiliation with *Plurinerves* has been estimated to date from 7.5 My with a pronounced diversification episode for gall-thrips lineages affiliated with *Plurinerves* hosts between 3 and 6 My [3]. Aridity developed across Australia in the late Miocene [4]. The *A. harpophylla* clade of Plurinerves with host-specific gall-inducing *Kladothrips* occurs on alkaline and/or saline substrate throughout Australia. Other *Plurinerves* occur in a range of different habitats. Thus congruence between plant and insect phylogenies and co-speciation are apparent. While adaptive radiation may be a response to climatic change, more proximal environmental drivers include aridity, alkalinity, and salinity.

Independent lines of evidence—phytogeography, plant and insect systematics, and insect behavioral ecology—point to a potentially important role for soil salinity in macroevolutionary processes for the genus *Acacia*. The potential role of substrate chemistry in macroevolutionary processes should be investigated for other genera found in arid environments.

[1] Bui & Henderson (2003) *Austral Ecology* **28**, 539-552. [2] Crespi, Morris & Mound (2004) *Evolution of ecological and behavioural diversity: Australian Acacia thrips as model organisms*. CSIRO, Canberra. [3] McLeish et al. (2007) *BMC Biology* **5**, 3. doi:10.1186/1741-7007-5-3. [4] Martin (2006) *Journal of Arid Environments* **66**, 533–563.

Sulphur and carbon isotope records across the terrestrial Permian-Triassic (P-T) boundary

THI HAO BUI[1*], JEAN-FRANCOIS HELIE[2], AND BOSWELL WING[1]

[1] McGill University, Earth and Planetary Sciences, thi.h.bui@mail.mcgill.ca (* presenting author)

boswell.wing@mcgill.ca

[2] Département des sciences de la Terre et de l'atmosphère, UQAM, PK-7720

helie.jean-francois@uqam.ca

The end Permian mass extinction (~ 252 Ma [1]) is known as the greatest biotic crisis in earth history with the disappearance of more than 90% of marine species and 70% of terrestrial vertebrate families [2]. To better understand the interaction of the carbon and sulphur cycles across the terrestrial P-T boundary, we collected 27 sedimentary rock samples at average resolution of 35 cm and 9 carbonate nodules along a section of ~10 meters in Karoo Basin, South Africa. We determined carbon and sulphur contents as well as carbon and sulphur isotope records of above samples.

The organic carbon contents of sedimentary rocks are quite low, less than 0.04 wt %. The average $\delta^{13}C$ value of organic carbon is around -25‰ throughout the section, but at 59 cm before the P-T boundary, this value increases to -23.8‰ and drops sharply to -26.5‰ over a distance of 110 cm. The background value of -25‰ is recovered within 19 cm. The $\delta^{13}C$ values of carbonate nodules in the ≈3 m preceding the boundary are around -8.5‰, while those found n the ≈5 m after the boundary are around -11.5‰. Total sulphur contents of sedimentary rocks are generally less than 0.01 wt%, with the exception of a sharp peak of ≈0.45 wt % at 5 cm above the boundary. Although their full pattern is noisier than that seen in the $\delta^{13}C$ record, the $\delta^{34}S$ values of Cr(II)-reducible sulphides and different sulphate species (water-soluble, acid-soluble, and acid-insoluble sulphates) all decrease by at least 8‰ within the 100 cm after the boundary.

The negative shifts of both $\delta^{13}C_{carbonate}$ and $\delta^{13}C_{organic}$ (≈ -3‰) at the boundary indicate a decrease in the ^{13}C content of carbon input into the P-T terrestrial system. Likewise, the sharp peak of total sulphur content coinciding with the boundary suggests a rapid addition of sulphur into the terrestrial environment. The shared initial decreases in $\delta^{34}S$ values suggest that this sulphur was depleted in ^{34}S. Multiple sulphur isotope compositions ($\delta^{34}S$ and $\Delta^{33}S$) of the different sulphate species are generally equivalent, indicating a shared sulphate source throughout the section. While the $\delta^{34}S$ values of the Cr(II)-reducible sulphides are compatible with bacterial sulphate reduction, the associated $\Delta^{33}S$ values are more negative than those typically associated with this process. Although the $\delta^{13}C$ and $\delta^{34}S$ records imply the coherent transfer of ^{13}C- and ^{34}S-depleted material to the PT terrestrial environment, the $\Delta^{33}S$ values complicate a straightforward identification of the source of this material.

[1] Shen *et al.* (2011) *Science* **334**, 1367-1372.
[2] Erwin (1994) *Nature* **367**, 231-235.

Determining solute sources and water flowpaths in catchments using the Ca-Sr-Ba multi-tracer

THOMAS BULLEN[1*], SCOTT BAILEY[2] AND KEVIN MCGUIRE[3]

[1]U.S. Geological Survey, Menlo Park, CA, USA, tdbullen@usgs.gov (* presenting author)
[2]U.S.Forest Service, N. Woodstock, NH, USA, swbailey@fs.fed.us
[3]Virginia Tech, Blacksburg, VA, USA, kevin09@vt.edu

Determining solute sources and water flowpaths in catchments is essential for understanding how catchments function. For example, stream water chemistry is determined by multiple factors including delivery of water from different portions of the catchment and from different depths along hillslopes and processes such as mineral weathering, ion exchange and biological cycling. As part of a larger study aimed at understanding the inter-relationships of these factors, we are using a hydropedologic approach to interpret concentration and isotope ratios of the alkaline earth elements Ca, Sr and Ba in stream water, groundwater, the soil exchange pool and plants from a catchment at the Hubbard Brook Experimental Forest, New Hampshire, USA. This 41 hectare forested headwater catchment supports a beech-birch-maple-spruce forest growing on vertically- and laterally-developed Spodosols and Inceptisols formed on granitoid glacial till that mantles Paleozoic metamorphic bedrock. Across the watershed in terms of the soil exchange pool, the forest floor has high Sr/Ba and Ca/Sr ratios, weathered mineral soil has intermediate Sr/Ba and low Ca/Sr ratios, and relatively unweathered till has low Sr/Ba and high Ca/Sr ratios. Waters moving through these various soil compartments obtain Sr/Ba and Ca/Sr ratios reflecting these characteristics, and thus variations of Sr/Ba and Ca/Sr ratios of streamwater provide evidence of the depth of water flowpaths feeding the streams. $^{87}Sr/^{86}Sr$ of soil exchangeable Sr spans a broad range from 0.715 to 0.725, with highest values along the mid- to upper flanks of the catchment and lowest values in a broad zone along the central axis of the catchment associated with groundwater seeps. Thus, variations of $^{87}Sr/^{86}Sr$ in streamwater provide evidence of the spatial distribution of water flowpaths feeding the streams. In addition, we are using Ca, Sr and Ba stable isotope ratios ($^{44}Ca/^{40}Ca$, $^{88}Sr/^{86}Sr$, $^{138}Ba/^{134}Ba$) as novel tracers of Ca, Sr and Ba sources and transport pathways in catchments. Initial results indicate that: 1) Sr and Ba stable isotopes are fractionated by plants similarly to patterns observed globally for Ca stable isotopes; 2) organic soils have the lightest values and weathered mineral soils have the heaviest values of exchangeable Ca, Sr and Ba, with particularly heavy Sr and Ba associated with accumulation of humic materials (i.e., in Bh horizons); and 3) the total range of isotope ratios observed for the exchange pool on a mass percent basis increases unexpectedly in the order Ca<Sr<Ba, suggesting an important role for Ca-oxalate that contains lighter Ca than that sampled in the exchange pool. We hypothesize that while biologically-cycled Ca is efficiently retained in the organic soil-plant system (e.g. as Ca-oxalate), biologically-cycled Sr and especially Ba will be more easily leached by soil waters and delivered to the streams and thus their stable isotope ratios may provide an additional means to distinguish between shallow and deep water flowpaths.

XRF archaeometry for lithic characterization and provenance.

ADRIAN L. BURKE[1*], GILLES GAUTHIER[2]

[1]Université de Montréal, Anthropologie, Montréal, Canada, adrian.burke@umontreal.ca (* presenting author)
[2]Université de Montréal, Chimie, Montréal, Canada, gilles.gauthier@umontreal.ca

The use of XRF over the last forty years to determine whole-rock geochemistry and establish an internationally approved chemical nomenclature for igneous rocks [1] has proven to be vital for the geological community. Its use as an archeometric tool specifically for lithic materials has been limited and historically overshadowed by INAA. This is in part due to the lower amount of material required to perform the latter, which is more in line with archaeological conservation guidelines.

If one considers the silicate nature of lithic materials used in the fabrication of sharp-edged tools one is immediately confronted by the inability of INAA to determine the major component of such materials: silica. This precludes the use of rock type based chemical classifications which for aphanitic materials have proven to be crucial, and unbiased, when compared to macroscopic ones (mineralogy based). A complete set of major element oxide determinations, compatible with data found in geological publications, is essential to determine the rock type and in turn narrow possible geological sources . Most importantly, for igneous types, it permits the use of an internationally approved and established chemical rock nomenclature (basalt, andesite, rhyolite, etc.) [1].

Non-destructive methods were developed [2, 3] in order to comply fully with archaeological conservation rules, and in order to profit from the many advantages of XRF when characterizing archaeological lithic materials, such as relative cost, throughput, and the immediate reuse of samples (non-radioactive) for other specific archaeological and geochemical assays.

Concentration data for major and trace elements produced with a specific non-destructive method using long counting times, calibrations using certified rock reference materials, and a geochemical data treatment approach [4] – notwithstanding the caveats imposed by unprocessed samples (slabs versus fused beads and powder pellets) such as surface irregularities, inhomogeneities and varying thicknesses – will be shown here to be quite useful for 1) the correction of macroscopic misclassifications in archaeological collections, 2) the assessment of chemical variations among chert types (nodular, bedded, chemically precipitated, etc.), 3) the determination of specific chemical markers, 4) the evaluation of the geochemical effects of weathering, and finally 5) the determination of provenance.

[1] Le Maître (2002) Second ed., *Cambridge University Press, New York*, 236p. [2] Hermes (1997) *Geoarchaeology* **12**, 31-40. [3] Lundblad & Mills (2008) *Archaeometry* **50**, 1-11. [4] Gauthier & Burke (2011) *Geoarchaeology* **26**, 269-291.

Modern and deglacial radiocarbon depth profiles from the Southern Ocean

ANDREA BURKE[1*] AND LAURA F. ROBINSON[1,2]

[1]Dept. of Marine Chemistry and Geochemistry, Woods Hole Oceanographic Institution, Woods Hole, USA, aburke@whoi.edu (* presenting author)

[2]Dept. Earth Sciences, University of Bristol, Bristol, UK, laura.robinson@bristol.ac.uk

Mixing and upwelling in the Southern Ocean is thought to be an important driver of glacial-interglacial atmospheric CO_2 change, but paleoceanographic records from this region are sparse. Radiocarbon is a useful tool for reconstructing past circulation change because it is produced in the atmopshere, enters the ocean through air-sea gas exchange at the surface, and then decays away as it is isolated from the atmosphere. Here we present twenty-two new radiocarbon measurements of U-Th dated deep-sea corals from the Drake Passage and combine them with forty previously published deep-sea coral radiocarbon data from this region [1]. Measured $\delta^{234}U$ values from these corals are within error of modern seawater values, consistent with closed-system behavior of the uranium series isotopes. These new corals come from twelve new dredge sites ranging from 328 to 1710 m water depth, and grew between 9.9 and 27.2 thousand years ago. These additional corals provide an increased depth resolution which allows us to reconstruct radiocarbon depth profiles within the Drake Passage at important time intervals during the deglaciation, such as the Younger Dryas, Antarctic Cold Reversal, and Heinrich Stadial 1. We compare these depth profiles to modern radiocarbon profiles from seawater dissolved inorganic carbon. Millenial scale changes in the vertical structure of radiocarbon in the Drake Passage suggest variation in the mixing and exchange of carbon between different water masses and the atmosphere over the deglaciation.

[1] Burke, A. and Robinson, L. F. (2011) *Science Express* 10.1126/science.1208163.

"Bubble-less" degassing of MORB magmas

PETE BURNARD[1*], AURELIA COLIN[2]

[1]CRPG-CNRS, Vandoeuvre-lès-Nancy, France, peteb@crpg.cnrs-nancy.fr

[2]Faculty of Earth and Life Sciences, VU University, Amsterdam, The Netherlands

Noble gas and major volatile systematics indicate that MOR magmas lose volatiles via open system distillation. However, given the low Stokes velocity of bubbles within basaltic magmas (~10 cm h^{-1} for a 300 μm vesicle), it is not possible to efficiently separate bubbles from their enclosing liquids and hence it is difficult to see how open system degassing can physically occur. However, if the magma – crust interface is sufficiently permeable, then volatile loss could be achieved via degassing directly into the crust, without necessarily passing through the vesicle phase. This "bubble-less" degassing could potentially be efficient because the partial pressure of volatiles in the enclosing crust should be very low in contrast to the partial pressure of volatiles within vesicles which is limited by their solubility at the pressure of the degassing magma.

In order that degassing directly into the crust can be efficient, three conditions need to be met: 1) the surface area of the magma-crust interface needs to be similar to or greater than the surface area of the sum of the vesicles; 2) the magma crust interface needs to be permeable; 3) the magma needs to be sufficiently convective to ensure that a significant fraction of the magma passes within the characteristic diffusion distance of the magma-crust interface.

We asses here condition #1. The surface area of bubbles in a magma depends on the bubble size distribution, the total vesicularity and magma pressure during degassing; typically specifc surface areas of magmas will be in the range 1 – 10 $mm^2\ g^{-1}$ for most MORBs (up to a maximum of ~50 $mm^2\ g^{-1}$ for the "popping rock"). Sill-like magmas have surface/volume ratios of between $1x10^{-2}$ and $1x10^{-5}$ (corresponding approximately to sills between 0.15 and 150 m) thick. Figure 1 shows that the total vesicle surface area of a magma is the same as or slightly higher than the surface area of the magma/crust interface. Given the uncertainties involved, it is possible that "bubble-less" degassing may be a potential mechanism through which magmas lose their volatiles. Further modelling will investigate conditions 2) and 3).

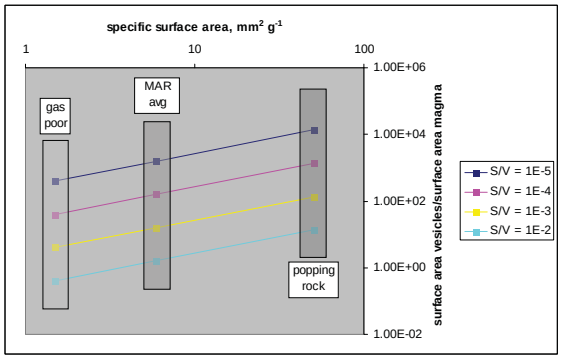

Figure 1: Variation of (vesicle surface area)/(magma-crust interface area) as a function of vesicle specific surface area ($mm^2\ g^{-1}$) for different magma geometries (different Surface/Volume ratios).

Diffusion compensation and application of Graham's law to noble gas diffusivities

PETE BURNARD[1*]

[1]CRPG-CNRS, Vandoeuvre-lès-Nancy, France, *peteb@crpg.cnrs-nancy.fr (* presenting author)

Diffusion Compensation

The temperature dependence (E_a) of slow-diffusing species tends to be greater than that of faster diffusing species, resulting in an interdependence between D_0 and E_a [1, 2, 3]. The net result is that the difference in diffusivity between two species in a given matrix will reduce with temperature, converging at a particular "compensation" or "isokinetic" temperature where the two (or more) species have the same diffusivities.

Graham's Law of effusion on the other hand states that, as far as gases are concerned, the relative diffusivity of two species is equal to the inverse of the square root of their masses:

$D_1/D_2 = \sqrt{(M_2/M_1)}$

In situations where experimental data are lacking, this relationship is often used to calculate the relative diffusivities of noble gas pairs. However, Graham's Law and "Compensation Temperature" relationships are mutually exclusive: according to Graham's Law, two noble gases should have the same Ea and differ only in D_0 (which should be constrained by $\sqrt{(M_2/M_1)}$). There cannot be compensation of diffusion with temperature for species following Graham's Law.

Non-Graham's Law behaviour

Recent results (Amalberti et al, this volume) show that He and Ar diffusivities in silicate glasses do infact differ in Ea: Graham's Law does not apply to diffusion of noble gases in silicate glasses (i.e. it is not possible to assume that $D_{He}/D_{Ar} = \sqrt{(M_{Ar}/M_{He})}$). The predicted isokinetic temperature for He and Ar diffusion in basaltic glasses is ~1000 K. The lack of conformity to Graham's law is easily understood: The Graham's Law relation is based on the two gas species of interest having the same kinetic energy (for example, for gases diffusing through a pinhole in the classic experiments by Graham in the 19th century). Volatile species diffusing through solid matrices are not expected to be isokinetic (they are not free gases) and Graham's law likely does not apply to diffusion of gases dissolved in solid matrices.

Implications

As a result, kinetic fractionation of different noble gases will only occur at "low" temperatures (the lower the temperature, the greater the potential for kinetic fractionation). Thus it does not appear likely that diffusion during magmatic processes (mantle melting or degassing of magmas) will be able to kinetically fractionate the noble gases. However, post-deposition (low temperature) processes out of equilibrium will create large He-Ar (and by extension, Ne-Ar, Kr-Ar etc) fractionation. The geological implications of these observations will be discussed.

[1] Winchell (1969) *High Temp. Sci.* **1**, 200 - 215. [2] Hart (1980) *Earth Planet Sci. letts* **269**, 507 - 516. [3] Zhao (2007) *Am. Mineral.* **92**, 289-308.

Identification of chromitite and kimberlite occurences in the James Bay lowland using statistical analysis of detrital chromite compositions

MARCUS BURNHAM[1*], DAVE CRABTREE[1] & RIKU METSARANTA[2]

[1]Geoscience Laboratories, Ontario Geological Survey, Sudbury, Canada. marcus.burnham@ontario.ca

[2]Precambrian Geoscience Section, Ontario Geological Survey, Sudbury, Canada. riku.metsaranta@ontario.ca

Introduction

In 2001, under the Operation Treasure Hunt (OTH) program [1], the Ontario Geological Survey carried out a stream sediment sampling program in the James Bay lowland during which over 1000 stream sediment samples were collected and processed for kimberlite and metamorphic/magmatic massive sulphide indicator minerals and gold grains. Because the primary objective of this survey was to evaluate the potential of the region to host additional kimberlite pipes, an emphasis was placed on the compositions of the garnet fraction. However, with the recent discoveries of chromite, Cu-Ni-PGE-sulphide and Ti-V mineralisation in the McFaulds Lake or "Ring of Fire" area, the chemistry of the detrital chromite grains is being re-investigated through statistical analysis of the original OTH dataset (>5500 electron probe microanalyses [2]) supplemented by analyses of chromites from the bed rock (in particular lithologies associated with the McFaulds Lake area mineralisation and Attawapiskat kimberlite diatremes).

Statistical Analysis

Initial statistical analysis of the major and minor element contents of the chromites, using agglomerative hierarchical clustering (AHC) after log-ratio transformation of the data to remove the constant-sum problem [3], suggests that at least nine compositional groups can be recognised. These groups show spatial associations with the bedrock geology, most notably in their Ti, Fe^{3+}, Fe^{2+}, and V contents (Figure 1).

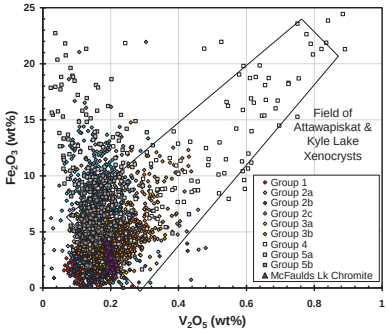

Figure 1: Compositions of detrital chromites from the James Bay lowlands. Field of Attawapiskat and Kyle Lake xenocrysts from [4].

[1] Crabtree (2003) *OGS Open File Report* **6108**, 115p. [2] Crabtree & Felix (2005) *OGS Misc. Release Data* **161**. [3] Aitchison (1986) The Statistical Analysis of Compositional Data, 416 pp. [4] Sage (2000) *OGS Open File Report* **6019**, 341p.

Plastic Deformation in Olivine Polycrystals:In-situ diffraction and EPSC models

PAMELA C. BURNLEY[1*]

[1]University of Nevada Las Vegas, Department of Geoscience, Burnley@physics.unlv.edu

Introduction

An important problem in rock deformation studies is the so-called meso-scale problem; understanding how the behaviour of individual mineral grains deforming via grain-scale processes interact to produce the bulk behaviour of the aggregate. A number of models for thinking about this problem exist, ranging from various averages of isolated grain behaviour to those that are dominated by grain configuration, for example stress percolation (as observed in granular materials). It is likely that the degree to which any given model is useful for a particular material depends on the degree of mechanical heterogeneity and anisotropy of the material. We are investigating the deformation of polycrystalline olivine in this light.

Methods

We report on in-situ synchrotron x-ray diffraction from high pressure deformation experiments conducted using olivine in the D-DIA apparatus at beamline X17b2 at the NSLS. We observe the diffraction behaviour of x-ray reflections for lattice planes oriented nearly perpendicular to compression and at several other orientations including the transverse orientation. Sample strain is measured using radiograph of the sample (which is bounded by metal foils). We used elastic plastic self-consistent (EPSC) modelling[1] to analyse diffract-tion from the sample during deformation. The models assume that rheology of the bulk is controlled by the critical resolved shear stress of the slip systems and the orientation of the grains in the polycrystal.

Results and Discussion

The failure of the known olivine slip systems to meet the von Mesis criteria for arbitrary shape change causes the EPSC models to exhibit very strong work hardening and nearly elastic behaviour for many grain populations. This is in stark contrast to our experimental data which consistently shows little or no work hardening after yield.

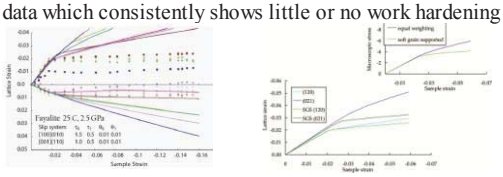

Figure 1: a) (left) Experimental diffraction results (points) for the (021), (010), (120), (002), (131) and (112) lattice planes in compression (above axis) and transverse directions (below axis). EPSC model is shown with matching coloured lines. **b)** (right) Modified EPSC model in which weakest grains dominate.

One possible reason that the deformation behaviour of polycrystalline olivine cannot be predicted with the EPSC model is that grains in the polycrystal that are well oriented for slip (soft grains) dominate the deformation behaviour or the aggregate, with grains that are not well oriented for slip passively "riding along" and not contributing to the aggregate strength. To test this, we assign a weighting factor to each grain depending on the degree of plastic strain that accumulates in the grain during deformation. Using this strategy the EPSC model more closely mimics the lack of work hardening as well as smaller difference in lattice strain between the (120) and (021) reflections.

[1] Turner and Tome (1994) *Acta Metallurgica Materialia* **42**(12) 4143-4153

Integrated 3D multimodal CARS microscopy, Raman spectroscopy, and microthermometry of gas-rich inclusions in the Marcellus shale-gas system

R. C. BURRUSS[1*], M. EVANS[2], A. D. SLEPKOV[3], A. F. PEGORARO[4] AND A. STOLOW[4]

[1]USGS, Reston, USA, burruss@usgs.gov (* presenting author)
[2]Central Connecticut State University, New Britain, USA, evansmaa@mail.ccsu.edu
[3]Trent University, Peterborough, Canada, aaronslepkov@trentu.ca
[4]National Research Council of Canada, Ottawa, Canada Adrian.Pegoraro@nrc-cnrc.gc.ca; Albert.Stolow@nrc-cnrc.gc.ca)

Gas-rich inclusions in fracture filling cements in the Marcellus Shale and younger Devonian age formations in the Appalachian basin record a complex history of gas generation, migration, and alteration during evolution of the Alleghenian orogen[1]. Quartz and calcite cements contain multiple overlapping fluid inclusion assemblages (FIAs) formed during crystal growth and deformation. To resolve the complex sequences of gas generation and migration recorded by FIAs we applied a nonlinear optical microscopy method capable of 3D, molecule-specific imaging with sub-micrometer resolution: multimodal coherent anti-Stokes Raman scattering (CARS) microscopy. Our implementation of CARS microscopy[2] produces molecule-specific images in the range of 2100 to 4000 cm^{-1} (N_2, CH_4, H_2O) and simultaneously creates second harmonic generation (SHG) images of inclusions with associated quartz microstructures, and two-photon excitation fluorescence (TPEF) images of higher hydrocarbons. The CARS images show the distribution of methane-rich and aqueous phases in inclusions and the TPEF images show the distribution of gas-rich inclusions that contain trace levels of higher hydrocarbons. Individual gas-rich inclusions within distinct 3D FIAs identified with multimodal CARS were analyzed by conventional confocal Raman spectroscopy for minor components (C_2H_6, CO_2, H_2S, N_2) and internal pressure[3]. 2D maps of inclusions with microthermometric measurements were correlated with 2D projections of 3D SHG images. Integration of measurements on individual inclusions with 3D images allows identification of FIAs with distinct spatial orientation and differences in composition (C_2H_6, CO_2, higher hydrocarbons) and density. 3D imaging with CARS microscopy is a major advance in our ability to assign FIAs with distinct compositions to distinct orientations of microstructures formed during kinematic evolution of the orogen. These observations provide new insight to the temporal evolution of hydrocarbon gas generation and migration during evolution of the Marcellus shale-gas system.

[1] Evans (2010) *Geol. Soc. Am. Mem.* 206. [2] Pegoraro *et al.* (2010) *App. Phys.* 49, F10–F17. [3] Lu *et al.* (2007) *GCA* 71, 3969–3978.

Pore-water diffusive fluxes of ^{224}Ra and CO_2 in Bedford Basin, Nova Scotia.

WILLIAM BURT[1*], HELMUTH THOMAS[1], KATJA FENNEL[1], JOHN N. SMITH[2], AND EDWARD HORNE[2]

[1]Dalhousie University, Department of Oceanography, Halifax, NS, Canada willburt@dal.ca, helmuth.thomas@dal.ca, katja.fennel@dal.ca, (*presenting author)

[2]Bedford Institute of Oceanography, Fisheries & Oceans Canada, Dartmouth, NS, Canada John.Smith@dfo-mpo.gc.ca, Ed.Horne@dfo-mpo.gc.ca

Introduction and aim of the study

On the seafloor, chemical processes occurring within sediments create pore-waters highly enriched in various chemical constituents. Many of these processes are fuelled by particulate organic matter (POM), generated during primary production in the euphotic zone and settled onto the surface sediments. Biological transformations of POM in the surface sediments, aerobic or anaerobic, eventually increase pore-water concentrations of dissolved inorganic carbon (DIC), and depending on redox conditions, also alkalinity (A_T). Furthermore, the decay of radioactive elements in the sediments constitutes a further source of chemical species enriched in pore-waters, such as the decay of sediment-bound ^{228}Th ($t_{1/2}$=1.91y), which yields high concentrations of its shorter-lived daughter ^{224}Ra ($t_{1/2}$=3.66 d). We investigate the diffusive flux of three such constituents, the short-lived radium isotope ^{224}Ra, DIC and A_T, from pore-waters into the deep waters of Bedford basin (Nova Scotia, Canada), in order to shed light on both the biogeochemical behaviour of ^{224}Ra and on the return flow of DIC and A_T into the water column from POM respiration on the surface sediments.

Results and Discussion

We apply a 1-D diffusive mixing model (Moore, 2000) to near-bottom profiles of excess ^{224}Ra activity. The recurrence of sharp Ra gradients supports the assumption of a diffusion-dominated mixing regime. We yield vertical eddy-diffusion coefficients (K_Z), along with estimates of ^{224}Ra activity at the sediment-water interface, from which we derive ^{224}Ra fluxes per unit area of sediment. Subsequently, we apply K_Z values to the near-bottom gradients of DIC and A_T, in order to estimate benthic DIC and A_T fluxes from Bedford Basin sediments into the overlaying water column.

Integrating our findings over a full annual cycle, the benthic return flux of DIC constitutes as much as 50% of the annual primary production [2], suggesting substantial additional delivery of organic carbon to deep sediments in the basin. Input from nearby sewage outfalls, re-suspension and transport of sediments at shallower depths [3], and high retention levels within the basin [4] may provide the mechanisms required for this enhanced carbon delivery. Finally, we do not observe any significant release of A_T from the surface sediments to the overlaying water column, which can be seen as an indicator of primarily aerobic respiration of the settled POM, fuelled by sufficiently high dissolved oxygen levels. [5]

[1] Moore (2000) *Cont. Shel. Res.* **20**, 1993-2007. [2] Irwin (1981) *Mar. Ecol. Prog. Ser.* **71**, 97-102. [3] Taguchi and Hargrave (1978) *J. Fish. Res. Board. Can* **35**, 1604-1613. [4] Shan et al. (2011) *Ocean Dynamics* **61**, 951-976. [5] Hargrave et al. (1976) *Tech. Rep. Fish. Mar. Serv., Envir. Can.* **608**, 1-129.

Assessing global N cycling in subduction zones from data on metamorphic rocks: Implications for the evolution of N in Earth's reservoirs

VINCENT BUSIGNY*, PIERRE CARTIGNY, PASCAL PHILIPPOT

IPG-Paris and Univ. Paris Diderot, Sorbone Paris Cité, France, busigny@ipgp.fr (* presenting author), cartigny@ipgp.fr, philippot@ipgp.fr

In order to evaluate the budget of nitrogen buried to the mantle in subduction environments, we performed quantitative and N isotopic analyses of Alpine metamorphic rocks subducted to different depths, and on their non-metamorphic analogues. The samples investigated represent a complete section of the oceanic lithosphere including from bottom to top, serpentinized peridotites, metagabbros, metabasalts and overlying metasediments.

A global annual flux of N subducted by metagabbros has been estimated at about 4.2 ($\pm$ 2.0) $\times$ 10^{11} g/yr with an average δ^{15}N-value of 1.8 $\pm$ 0.8 ‰ (1σ). This flux is about half that of sedimentary rocks, which indicates that gabbros carry a significant portion of the subducted nitrogen. The net budget between subducted N and that outgassed at volcanic arcs indicates that ~80% of the subducted N is not recycled to the surface.

On a global scale, the total amount of N buried to the mantle via subduction zones is estimated to be 3 times higher (13.2 $\times$ 10^{11} g/yr) than that released from the mantle via mid-ocean ridges, arc and intraplate volcanoes and back-arc basins. This implies that N contained in Earth surface reservoirs, mainly in the atmosphere, has been progressively transferred and sequestered into the mantle, with a net flux of ~9.6 $\times$ 10^{11} g/yr. Assuming a constant flux of subducted N over the Earth's history suggests that an amount equivalent to the present atmospheric N may have been sequestered into the silicate Earth over a period of 4 billion years.

Considering a present day mantle value of ~ -5‰, an average δ^{15}N value of subducted nitrogen of about 3.4 $\pm$1.4 ‰ implies that the secular evolution of the mantle δ^{15}N value should have increased through time, whereas that of the crust and atmosphere should have decreased.

Probing the deep critical zone beneath the Luquillo Experimental Forest, Puerto Rico

H.L. Buss[1*], S.L. Brantley[2], F.N. Scatena[3], M. Schulz[4], A.F. White[4], A.E. Blum[5], and R. Jiminez[3]

[1]School of Earth Sciences, University of Bristol, Bristol, UK, h.buss@bristol.ac.uk (* presenting author)
[2]Earth and Environmental Systems Institute, The Pennsylvania State University, University Park, PA, USA, brantley@eesi.psu.edu
[3]Department of Earth and Environmental Science, University of Pennsylvania, Philadelphia, PA, USA, fns@sas.upenn.edu
[4]US Geological Survey, Menlo Park, CA, USA, mschulz@usgs.gov, afwhite@usgs.gov
[5]US Geological Survey, Boulder, CO, USA, aeblum@usgs.gov

The interfaces where intact bedrock weathers to disaggregated material, such as saprolite and soil, are often hidden deep within the critical zone. The majority of weathering studies in the field focus on the shallow critical zone: soils, sediments, regolith, saprolite, and outcrops. However, weathering of primary minerals along bedrock fractures located in the groundwater or deep vadose zones may supply significant weathering products to streams and oceans.

We investigated the deep critical zone in the Bisley watershed in the Luquillo Critical Zone Observatory from two 9.6 cm diameter boreholes drilled with a hydraulic rotary drill to 37.2 and 27.0 m depth. Continuous core samples through coherent rock were taken using an HQ-wireline barrel. Bulk solid-state chemical analysis and powdered XRD were performed on rock and saprock samples. Thin sections were examined by optical microscopy and SEM. A history of low- to moderate-grade metamorphism is reflected by the presence of epidote, prehnite, pyrite, and tourmaline. Fresh rock contains abundant plagioclase and chlorite, with lesser quartz, K-spar, and pyroxene.Weathering rinds developed on fracture surfaces are porous and contain abundant secondary Fe(III)-oxides.

Drilled cores revealed repeated zones of highly fractured rock, identified as corestones, embedded within layers of regolith. Some corestones are massive and others are highly fractured. Subsurface corestones are larger and less fractured in the borehole drilled along the spine of a ridge, compared to the borehole drilled near a stream channel. As corestone size is thought to be a function of fracture spacing, the location of the valleys and ridges in the watershed may be controlled by the fracture spacing of the underlying bedrock.

Drilling terminated in coherent rock, thought to be bedrock based on a model that hypothesized a thickness for the corestone zone [1]. The 2 drilled boreholes and a resistivity profile [2] are only 20-50m apart and of similar elevation. However, all 3 have different profiles demonstrating that this is a complex landscape that needs both geophysics and drilling to understand. Even so, all of the profiles indicate that the weathering zone is well below the stream channel; thus weathering depth is not controlled by local base level. Furthermore, weathering rinds on fracture surfaces at depth indicate that water and oxygen are transported below the stream channel; thus not all of the water in the watershed is discharged to the stream.

[1] Fletcher and Brantley (2010) *Amer. J. Sci* **310**, 131-164.
[2] Schellekens et al. (2004) *Hydrological Processes* **18**, 505-530.

Efficiency of covers made of low sulphide tailings to control AMD from surface impoundments

Bruno Bussière[1*], Michel Aubertin[2]

[1]Université du Québec en Abitibi-Témiscamingue, Institut de recherche Mines et Environnement, (*presenting author), Bruno.bussière@uqat.ca
[2]École Polytechnique de Montréal, Département de génie civil, géologique et des mines, Michel.Aubertin@polymtl.ca

Introduction

It is now recognized that one of the best options to reclaim acid-generating tailings impondments is to use an oxygen barrier. Water contamination can be controlled by limiting the oxygen flux reaching the reactive tailings. Different types of oxygen barriers can be used, including engineered covers that rely on a high moisture content in one of its layers to prevent oxygen migration [1,2]. The authors work has shown that when appropriate soils are not available close to the mine site, low sulphide tailings can advantageously be used as a component of layered covers.

Main results

Different laboratory and *in situ* tests were performed over the last 20 years or so by the authors and collaborators to evaluate the response and performance of covers made with low sulphide tailings to limit water contamination. The initial series of tests used «naturally» low sulphide tailings as the moisture retaining layer in covers with capillary barrier effects (CCBE). Results showed that it was possible to maintain the water quality below the regulation criteria with such type of CCBE placed over reactive tailings. The control tests on exposed acid-generating tailings (without the cover) showed that the pH of the leachates droped below 3, with concentrations in dissolved metals in the hundreds of mg/l [3]. Another series of tests were performed in the laboratory to evaluate the feasibility of artificially producing the low sulphide tailings by a flotation process, and to use the desulphurized tailings as moisture-retaining layer in a CCBE. When the tailings are properly desulphurized, testing results showed that water contamination was effectively prevented, producing a leachate that meets water quality criteria [4]. An additional series of experiments were performed to evaluate the performance of monolayer covers made of low sulphide tailings, in combination with the elevated water table technique [5]. These column tests results show that the water table level is the most important parameter affecting the monolayer cover performance to control acid generation. The water table must be located at a minimum depth below the cover to prevent water contamination.

Conclusion

Results from different experiments at different scales showed that low sulphide tailings can be an efficient material to be used in engineered covers designed to control acid production from reactive tailings. In adddition, the use of low sulphide tailings valorises a mining waste and reduces the borrowing of natural soils and the related pertubations.

[1] Nicholson et al. (1989), *Can.Geot.J.* **26**, 1-8. [2] Bussière et al. (2003), *Can.Geot.J.* **40**, 512-535. [3] Molson et al. (2008), *Appl. Geochem.* **23**, 1-24. [4] Bussière et al. (2004), *Env. Geol.* **45**, 609-622. [5] Ouangrawa et al. (2009) *Appl. Geochem.* **24**, 1312-1323.

Shear-Induced Melt Bands with Anisotropic Viscosity and Implications for Melt Extraction at Mid-Ocean Ridges

SAMUEL BUTLER[1*]

[1]University of Saskatchewan, Department of Geological Sciences, Saskatoon, Canada, sam.butler@usask.ca (* presenting author)

Introduction

Melt at mid-ocean ridges is produced over a broad lateral area but is mostly extracted in a narrow region in the vicinity of the ridge crest. Geochemical evidence also indicates that it is extracted rapidly, necessitating a mechanism to focus melt towards the ridge axis. When systems of partial melt are subjected to an externally driven strain-rate, melt segregates into bands of low and high porosity provided that the viscosity of the solid matrix decreases with increasing porosity and that the system is larger than the material compaction length. These bands have been suggested as candidates for focusing melt flow towards the ridge axis[1]. Experimental investigations of these systems have shown that the bands form at roughly 25° to the direction of maximum compression, regardless of the degree of strain-rate dependence of the matrix viscosity. In contrast, numerical and theoretical investigations show that bands should grow fastest if they are oriented parallel to the direction of maximum compression of the background flow if the viscosity is strain-rate independent and isotropic. Recently, it has been suggested that the matrix viscosity should be anisotropic because of the anisotropic arangement of melt at the grain scale caused by stress and that this anisotropy could result in low angle bands as observed in the experiments[2]. In this contribution, I will present numerical simulations of melt bands with anisotropic viscosity.

Results

When matrix viscosity is anisotropic with orientation appropriate for the orientation of grain-scale melt seen in experiments at low strain, the bands do form at angles that are consistent with those seen in experiments. However, in experiments at high strain, the melt in seen to reorient and the resulting viscosity anisotropy results in simulated bands that are not consistent with those seen in experiments.

The effects of buoyant interstitial fluid are also investigated and it is found that a large degree of buoyancy results in two sets of band orientations and short wavelength bands.

[1] Katz R.F., Spiegelman M., Holtzman B., (2006) , *Nature*, 442, 676-679.
[2] Takei Y, Holtzman B., (2009), *J. Geophys. Res.*, 114, doi:10.1029 /2008JB005852.